



University of HUDDERSFIELD

University of Huddersfield Repository

Algadi, Abdualmagid

Computational Fluid Dynamics (CFD) Based Investigations on the Flow of Capsules in Vertical Hydraulic Pipelines

Original Citation

Algadi, Abdualmagid (2017) Computational Fluid Dynamics (CFD) Based Investigations on the Flow of Capsules in Vertical Hydraulic Pipelines. Doctoral thesis, University of Huddersfield.

This version is available at <http://eprints.hud.ac.uk/id/eprint/34669/>

The University Repository is a digital collection of the research output of the University, available on Open Access. Copyright and Moral Rights for the items on this site are retained by the individual author and/or other copyright owners. Users may access full items free of charge; copies of full text items generally can be reproduced, displayed or performed and given to third parties in any format or medium for personal research or study, educational or not-for-profit purposes without prior permission or charge, provided:

- The authors, title and full bibliographic details is credited in any copy;
- A hyperlink and/or URL is included for the original metadata page; and
- The content is not changed in any way.

For more information, including our policy and submission procedure, please contact the Repository Team at: E.mailbox@hud.ac.uk.

<http://eprints.hud.ac.uk/>

Computational Fluid Dynamics (CFD) Based Investigations on the Flow of Capsules in Vertical Hydraulic Pipelines

Abdualmagid Algadi

A Thesis Submitted in Partial Fulfilment of the Requirements for the Degree of Doctor of
Philosophy at the University of Huddersfield

In

School of Computing and Engineering

University of Huddersfield

UK

October 2017

Abstract

The rapid depletion of power sources has remarkably impacted the transport sector, where the costs of the freight transportation are rising dramatically every year. Significant endeavours have been made to develop innovative means of transport that can be adopted for economic and environmental friendly operating systems. Transport pipelines consider one such alternative mode that can be used to transfer goods. Although the flow behaviour of a solid-liquid mixture in hydraulic capsule pipeline is quite complicated, due to its dependence on a large number of geometrical and dynamic parameters, it is still a subject of active research. In addition, published literature is extremely limited in terms of identifying the impacts of the capsules shape on the flow characteristics of pipelines. The shape of these capsules has a significant effect on the hydrodynamic behaviour within such pipelines.

This thesis presents a computational investigation employing advanced Computational Fluid Dynamics (CFD) based tool to simulate the capsules flow of varied shapes quantified in form of a novel shape factor in a vertical hydraulic capsule pipeline. The 3-D Dynamic Meshing technique with Six Degrees of Freedom approach is applied for numerical simulation of unsteady flow fields in vertical capsule pipelines. Variations in flow related parameters within the pipeline have been discussed in detail for geometrical parameters associated with the capsules and flow conditions within Hydraulic Capsule Pipelines (HCPs).

Detailed quantitative and qualitative analyse has been conducted in the current research. The qualitative analysis of the field of the flow comprises descriptions of the pressure and velocity distribution within the pipeline. The investigations have been conducted on the flow of spherical, cylindrical and rectangular shaped capsules each one separately for offshore applications. As it can be notice that the flow behaviour inside HCP relies on the flow conditions and geometric parameters. The development of novel predictive models for pressure drop and capsule velocity is considered as one of the goals that have been achieved in this research. Moreover, the flow of a variety of different shaped capsules, in combination, has also been investigated based on the impact of the order of the capsule shape within the

vertical pipeline. It has been found that the motion of mixed capsules along the pipeline shows a significant variation comparing to the basic capsules shapes for the same shape being transported across the pipelines.

Capsule pipeline designers need accurate data regarding the pressure drop, holdup and the shape of the capsules etc., at early design phases. The methodology of optimisation is developed based on the least cost principle for vertical HCPs. The inputs to the predictive models are the shape factor of the capsule and solid throughput demanded of the system, while the outcomes represent the pumping power demanded for the capsule transportation process and the optimal diameter of the HCP.

In the present study, a complete visualisation of capsules flow and design of vertical hydraulic capsule pipelines has been reported. Sophisticated computational tools have allowed the possibility to analyse and map the flow structure in an HCP, which resulted to a deeper comprehension of the flow behaviour and trajectory of the capsules in vertical pipes.

Declaration

- The author of this thesis (including any appendices and/or schedules to this thesis) owns any copyright in it (the “Copyright”) and he has given The University of Huddersfield the right to use such Copyright for any administrative, promotional, educational and/or teaching purposes.

- Copies of this thesis, either in full or in extracts, may be made only in accordance with the regulations of the University Library. Details of these regulations may be obtained from the Librarian. This page must form part of any such copies made.

- The ownership of any patents, designs, trademarks and any and all other intellectual property rights except for the Copyright (the “Intellectual Property Rights”) and any reproductions of copyright works, for example graphs and tables (“Reproductions”), which may be described in this thesis, may not be owned by the author and may be owned by third parties. Such Intellectual Property Rights and Reproductions cannot and must not be made available for use without the prior written permission of the owner(s) of the relevant Intellectual Property Rights and/or Reproductions.

Acknowledgments

First of all, praise and thank Allah Almighty for His blessings on me, which enabled me to complete this thesis. I would like to express my deep and sincere gratitude to my supervisor Prof. Rakesh Mishra for his valuable guidance, inspiration and constant encouragement.

My deep thanks to my co-supervisor Dr Taimoor Asim, who helped me to learn the different aspects of science and technology as well support provided throughout. A special thanks to all my colleagues at the Energy, Emissions and Environment Research group at the University of Huddersfield.

Last, but not the least, my greatest appreciation goes to my parents who always motivated me to go for the best. Heartiest thanks to my wife and my sweet sons, whose patience, understanding and constant encouragement enabled me to complete this work.

List of Contents

Abstract	i
Declaration	iii
Acknowledgments	iv
List of Contents	v
List of Figures	x
List of Tables	xviii
Nomenclature	xix
Greek Symbols	xxi
Chapter 1 - Introduction	1
1.1 Transporting Capsules in Pipelines.....	2
1.2 Historical Background of Capsule Transport Pipelines	3
1.3 Components of the Hydraulic Capsule Transportation System	4
1.4 Characteristics of Capsule Flow in Pipelines.....	5
1.5 Design Considerations for Transporting Capsules in Pipelines	6
1.5.1 The Carrier Fluid in the Pipe.....	7
1.5.2 The Shape and Size of Capsule.....	7
1.5.3 The Concentration of Capsules within Pipeline.....	7
1.5.5 Diameter of the Pipe	7
1.5.6 Pressure Drop in the Pipeline.....	7
1.6 Mechanisms of Capsule Flow in Pipelines	8
1.7 Motivation for this Study	9
1.8 Research Aims	10
1.9 Structure of the Thesis	10
Chapter 2 - Literature Review	13
2.1 Introduction.....	14

2.2 Flow Characteristics in Hydraulic Capsules Pipelines.....	14
2.2.1 Summary	24
2.3 Optimisation of Capsule Pipeline Systems	24
2.3.1 Summary	27
2.4 Research Scope	28
2.5 Research Objectives.....	28
Chapter 3 - CFD Modelling of HCPs	30
3.1 Overview of CFD Modelling.....	31
3.2 Basic Principles of CFD Methodology	31
3.3 Pre- Processing of the HCP.....	33
3.3.1 Construction of Pipe Geometry.....	33
3.3.2 Construction of Capsule Geometries	34
3.3.3 Meshing of the Flow Domain	34
3.3.4 Near Wall Treatment.....	35
3.4 Solver Settings	36
3.4.1 Turbulence Modelling.....	36
3.4.2 Material Properties	37
3.4.3 Boundary Conditions	37
3.4.4 Introduction to Dynamic Meshing	38
3.4.5 User Defined Functions and Six Degrees of Freedom Properties.....	39
3.4.6 Dynamic Mesh Setup	40
3.4.7 Mesh Independency Test	42
3.4.8 Time Step Size and Solution Initialisation.....	43
3.5 Scope of Numerical Investigations	44
Chapter 4 - Flow Diagnostics in HCPs Transporting Basic Capsule Shapes	46
4.1 Validation of CFD Predictions.....	47
4.2 Single Phase Flow Analysis in a Vertical Pipeline	48
4.3 Flow Diagnostics in HCPs Transporting Spherical Capsules	49
4.3.1 Effect of Average Flow Velocity	54
4.3.2 Effect of Capsule Density	56
4.3.3 Effect of Capsule Diameter	58
4.3.4 Effect of the Capsules Concentration.....	60
4.4 Flow Diagnostics in HCPs Transporting Cylindrical Capsules	62

4.4.1 Effect of Average Flow Velocity	63
4.4.2 Effect of Capsule Length	65
4.4.3 Capsule Density Effects	67
4.4.4 Effect of Capsule Diameter	69
4.4.5 Effect of the Capsules Concentration.....	71
4.5 Flow Diagnostics in HCPs Transporting Rectangular Capsules	73
4.5.1 Effect of Average Flow Velocity	75
4.5.2 Effect of Rectangular Capsule Length	77
4.5.3 Capsule Density Effects	79
4.5.4 Effect of Capsule Diameter	81
4.5.5 Effect of Capsules Concentration.....	83
4.6 Development of a Mathematical Relation for a Shape Factor	85
4.7 Development of Prediction Models	85
4.7.1 Capsule Velocity Prediction Model	86
4.7.2 Friction Coefficient Prediction Model	87
4.8 Summary	88
Chapter 5 - Flow Diagnostics in HCPs Transporting Mixed Capsules Shapes.....	90
5.1 Simple Combination Analysis of an Equi-Density Capsules Flow.....	91
5.1.1 Effect of the Position of the Capsule Shape in the (SC) order	91
5.1.2 Effect of the Position of the Capsule Shape in the (CS) order	94
5.1.3 Effect of the Position of the Capsule Shape in the (RS) order	95
5.1.4 Effect of the Position of the Capsule Shape in the (SR) order	96
5.1.5 Effect of the Position of the Capsule Shape in the CR order	98
5.1.6 Effect of the Position of the Capsule Shape in the RC order	100
5.2 Simple Combination Analysis of Heavy Density Capsules Flow.....	101
5.2.1 Effect of the Position of the Capsule Shape in the SC order.....	101
5.2.2 Effect of the Position of the Capsule Shape in the CS order.....	103
5.2.3 Effect of the Position of the Capsule Shape in the RS order.....	105
5.2.4 Effect of the Position of the Capsule Shape in the SR order.....	106
5.2.5 Effect of the Position of the Capsule Shape in the CR order	108
5.2.6 Effect of the Position of the Capsule Shape in the RC order	109
5.3 Complex Combination Analysis of an Equal Density Capsules Flow.....	111
5.3.1 Effect of the Position of the Capsule Shape in the SCR order	111
5.3.2 Effect of the Position of the Capsule Shape in the SRC order	112

5.3.3 Effect of the Position of the Capsule Shape in the RSC order	114
5.3.4 Effect of the Position of the Capsule Shape in the RCS order	115
5.3.5 Effect of the Position of the Capsule Shape in the CRS order	117
5.3.6 Effect of the Position of the Capsule Shape in the CSR order	118
5.4 Complex Combination Analysis of Heavy Density Capsules Flow	120
5.4.1 Effect of the Position of the Capsule Shape in the SCR order	120
5.4.2 Effect of the Position of the Capsule Shape in the SRC order	121
5.4.3 Effect of the Position of the Capsule Shape in the RSC order	123
5.4.4 Effect of the Position of the Capsule Shape in the RCS order	124
5.4.5 Effect of the Position of the Capsule Shape in the CRS order	126
5.4.6 Effect of the Position of the Capsule Shape in the CSR order	127
5.5 Development of Novel Semi-Empirical Prediction Model	129
5.6 Summary	130
Chapter 6 - Optimisation Modelling	132
6.1 Overview	133
6.2 Optimisation Process Theory	133
6.3 Cost of Piping Material	134
6.4 Cost of the Capsules	134
6.5 Cost of Power Consumption	134
6.6 Solid Throughput	136
6.7 Total Cost of the Optimal Pipeline	136
6.8 The Optimisation Model Implementation	137
6.9 Design Example of Vertical HCP	139
6.9.1 Effect of Cylindrical Capsule Shape	141
6.9.2 Effect of Rectangular Capsule Shape	142
6.10 Effect of Mixed Capsules Shapes	144
6.10.1 Effect of the Capsules order of Mixed Shapes	146
6.11 Summary	148
Chapter 7 - Conclusions	150
7.1 Research Problem Synopsis	151
7.2 Research Aims and Main Achievements	151
7.3 Thesis Conclusions	154
7.4 Thesis Contributions	159

7.5 Future Work	161
References.....	163
Appendices.....	169
A-1: Computational Fluid Dynamics	169
A-2: Mass and Moment of Inertia for a Capsule Shape.....	172
A-3: UDF Used in ANSYS FLUENT.....	174
A-4: Capsule Velocities.....	182
A-5: Pressure Drop in Vertical HCPs	185
A-6: Pressure Drop for Capsules Combination	188
A-7: Expressions for Capsule Velocities, Friction Coefficient and Correction Factor in Vertical HCPs	189

List of Figures

Figure 1.1 Vertical Capsule Pipeline [7].....	4
Figure 1.2 Hydraulic capsule pipeline system [9].....	5
Figure 2.1 Variation of V_c / V_{av} with Re for capsules of different shapes [19]	15
Figure 2.2 The elliptic capsule flow in a two-dimensional channel [21].....	16
Figure 2.3 The Time histories of capsule and water velocities at an inlet head [22]	17
Figure 2.4 Relation between the pressure gradient and the mixture's Re number according to the experimental data [25]	18
Figure 2.5 Effect of inclination angle and capsule specific gravity on capsule lift-off velocity [28]... 19	
Figure 2.6 The relation between the balance velocity and the inclination angle (a) $k = 0.664$ (b) $k = 0.507$ (c) $k = 0.403$ [29]	20
Figure 2.7 The schematic diagram of the experimental set-up [30].....	21
Figure 2.8 The pressure distributions along cylindrical capsule of $k = 0.8$ and $Re = 143398$ by different turbulence models and experimental data [35]	22
Figure 2.9 The friction factor for equi-density spherical capsules [36]	23
Figure 2.10 Hoist description [34]	25
Figure 2.11 Variation of costs in pipelines transporting zinc tailings [45].....	27
Figure 3.1 Summary of CFD Modelling	32
Figure 3.2 Schematic of the pipe geometry	33
Figure 3.3 Schematic of the geometry of spherical, cylindrical and rectangular capsules	34
Figure 3.4 Meshing of the flow domain.....	35

Figure 3.5 Dynamic mesh for the cylindrical capsule motion	41
Figure 3.6 Time histories of the pressure drop	42
Figure 3.7 Time histories of the capsule velocity	43
Figure 4.1 Validation of the CFD results with the experimental results for the capsule velocity in a vertical pipe that transporting an equi-density cylindrical capsule	48
Figure 4.2 Distribution of (a) Static gauge pressure and (b) Flow velocity magnitude	49
Figure 4.3 (a) Static gauge pressure and (b) Flow velocity magnitude variations for an equi-density spherical capsule of $k = 0.5$ and $V_{av} = 2\text{m/sec}$ at different flow times	51
Figure 4.4 (a) Variations in the mixture pressure drop and (b) the capsule pressure drop, for a single equi-density spherical capsule of $k = 0.5$ at $V_{av} = 2\text{m/sec}$	52
Figure 4.5 Time history of an equi-density spherical capsule velocity for $k = 0.5$ at	53
Figure 4.6 Time history of the acceleration of an equi-density spherical capsule for $k = 0.5$ at $V_{av} = 2\text{m/sec}$	53
Figure 4.7 (a) Static gauge pressure and (b) Flow velocity magnitude variations for an equi-density spherical capsule of $k = 0.5$ and $V_{av} = 4\text{m/sec}$ at different flow times	54
Figure 4.8 The effect of average flow velocity on the pressure drop variation for an equi-density spherical capsule of $k = 0.5$	55
Figure 4.9 The effect of average flow velocity on the capsule velocity for an equi-density spherical capsule of $k = 0.5$	55
Figure 4.10 (a) Static gauge pressure and (b) Flow velocity magnitude variations for a heavy density spherical capsule of $k = 0.5$ and $V_{av} = 2\text{m/sec}$ at different flow times	56
Figure 4.11 The effect of capsule density on the pressure drop variation for a spherical capsule of $k = 0.5$ at $V_{av} = 2\text{m/sec}$	57
Figure 4.12 The effect of specific gravity ratio on capsule velocity history for a spherical capsule of $k = 0.5$ at $V_{av} = 2\text{m/sec}$	57
Figure 4.13 (a) Static gauge pressure and (b) Flow velocity magnitude variations for a heavy density spherical capsule of $k = 0.6$ and $V_{av} = 2\text{m/sec}$ at different flow times	58
Figure 4.14 The effect of capsule diameter on the pressure drop variation for a heavy density spherical capsule at $V_{av} = 2\text{m/sec}$	59

Figure 4.15 The effect of capsule diameter on capsule velocity history for a heavy density spherical capsule at $V_{av} = 2\text{m/sec}$	59
Figure 4.16 (a) Static gauge pressure and (b) Flow velocity magnitude variations for two equi-density spherical capsules of $k = 0.5$ and $V_{av} = 2\text{m/sec}$ at different flow times.....	60
Figure 4.17 The effect of capsule concentration on the pressure drop variation for two equi-density spherical capsule of $k = 0.5$ at $V_{av} = 2\text{m/sec}$	61
Figure 4.18 The effect of capsule concentration on capsule velocity history for two equi-density spherical capsule of $k = 0.5$ at $V_{av} = 2\text{m/sec}$	61
Figure 4.19 (a) Static gauge pressure and (b) Flow velocity magnitude variations for an equi-density cylindrical capsule of $k = 0.5$, $L_c = 1d$ and $V_{av} = 2\text{m/sec}$ at different flow times	62
Figure 4.20 The capsule velocity history for an equi-density cylindrical capsule of $k = 0.5$ and $L_c = 1d$	63
Figure 4.21 (a) Static gauge pressure and (b) Flow velocity magnitude variations for an equi-density cylindrical capsule of $k = 0.5$, $L_c = 1d$ and $V_{av} = 4\text{m/sec}$ at different flow times	64
Figure 4.22 The effect of average flow velocity on the pressure drop variation for an equi-density cylindrical capsule for $k = 0.5$ and $L_c = 1d$	64
Figure 4.23 The effect of average flow velocity on capsule velocity history for an equi-density cylindrical capsule for $k = 0.5$ and $L_c = 1d$	65
Figure 4.24 (a) Static gauge pressure and (b) Flow velocity magnitude variations for an equi-density cylindrical capsule of $k = 0.5$, $L_c = 1.5d$ and $V_{av} = 2\text{m/sec}$ at different flow times	66
Figure 4.25 The effect of a capsule length on the pressure drop variation for an equi-density cylindrical capsule for $k = 0.5$ and $V_{av} = 2\text{m/sec}$	66
Figure 4.26 The effect of a capsule length on capsule velocity history for an equi-density cylindrical capsule for $k = 0.5$ and $V_{av} = 2\text{m/sec}$	67
Figure 4.27 (a) Static gauge pressure and (b) Flow velocity magnitude variations for a heavy density cylindrical capsule of $k = 0.5$, $L_c = 1d$ and $V_{av} = 2\text{m/sec}$ at different flow times	68
Figure 4.28 The effect of capsule density on the pressure drop variation for a heavy density cylindrical capsule of $k = 0.5$ and $L_c = 1d$ at $V_{av} = 2\text{m/sec}$	68
Figure 4.29 The effect of capsule density on capsule velocity history for a heavy density cylindrical capsule of $k = 0.5$ and $L_c = 1d$ at $V_{av} = 2\text{m/sec}$	69
Figure 4.30 (a) static gauge pressure and (b) Flow velocity magnitude variations for a heavy density cylindrical capsule of $k = 0.6$, $L_c = 1d$ and $V_{av} = 2\text{m/sec}$ at different flow times	70

Figure 4.31 the effect of capsule diameter on the pressure drop variation for a heavy density cylindrical capsule at $V_{av} = 2\text{m/sec}$ and $L_c = 1d$	70
Figure 4.32 The effect of capsule diameter on capsule velocity history for a heavy density cylindrical capsule at $V_{av} = 2\text{m/sec}$ and $L_c = 1d$	71
Figure 4.33 (a) Static gauge pressure and (b) Flow velocity magnitude variations for two equi-density cylindrical capsules of $k = 0.5$, $L_c = 1d$ and $V_{av} = 2\text{m/sec}$ at different flow times.....	72
Figure 4.34 The effect of capsule concentration on the pressure drop variation for two equi-density cylindrical capsules of $k = 0.5$ and $L_c = 1d$ at $V_{av} = 2\text{m/sec}$	72
Figure 4.35 The effect of capsule concentration on capsule velocity history for two equi- density cylindrical capsules of $k = 0.5$ and $L_c = 1d$ at $V_{av} = 2\text{m/sec}$	73
Figure 4.36 (a) Static gauge pressure and (b) Flow velocity magnitude variations for an equi-density rectangular capsule of $k = 0.5$, $L_c = 1d$ and $V_{av} = 2\text{m/sec}$ at different flow times	74
Figure 4.37 The capsule velocity history for an equi-density rectangular capsule of $k = 0.5$ and $L_c = 1d$	74
Figure 4.38 (a) Static gauge pressure and (b) Flow velocity magnitude variations for an equi-density rectangular capsule of $k = 0.5$, $L_c = 1d$ and $V_{av} = 4\text{m/sec}$ at different flow times	75
Figure 4.39 The effect of average flow velocity on the pressure drop variation for an equi-density rectangular capsule for $k = 0.5$ and $L_c = 1d$	76
Figure 4.40 The effect of average flow velocity on capsule velocity history for an equi-density rectangular capsule of $k = 0.5$ and $L_c = 1d$	76
Figure 4.41 (a) Static gauge pressure and (b) Flow velocity magnitude variations for an equi-density rectangular capsule of $k = 0.5$, $L_c = 1.5d$ and $V_{av} = 2\text{m/sec}$ at different flow times	77
Figure 4.42 The effect of a capsule length on the pressure drop variation for an equi-density rectangular capsule for $k = 0.5$ and $V_{av} = 2\text{m/sec}$	78
Figure 4.43 The effect of a capsule length on capsule velocity history for an equi-density rectangular capsule for $k = 0.5$ and $V_{av} = 2\text{m/sec}$	78
Figure 4.44 (a) Static gauge pressure and (b) Flow velocity magnitude variations for a heavy density rectangular capsule of $k = 0.5$, $L_c = 1d$ and $V_{av} = 4\text{m/sec}$ at different flow times	79
Figure 4.45 The effect of capsule density on the pressure drop variation for a heavy density rectangular capsule of $k = 0.5$ and $L_c = 1d$ at $V_{av} = 4\text{m/sec}$	80

Figure 4.46 The effect of capsule density on capsule velocity history for a heavy density rectangular capsule of $k = 0.5$ and $L_c = 1d$ at $V_{av} = 4m/sec$	80
Figure 4.47 (a) Static gauge pressure and (b) Flow velocity magnitude variations for a heavy density rectangular capsule of $k = 0.6$, $L_c = 1d$ and $V_{av} = 4m/sec$ at different flow times	81
Figure 4.48 The effect of capsule diameter on the pressure drop variation for a heavy density rectangular capsule at $V_{av} = 4m/sec$ and $L_c = 1d$	82
Figure 4.49 The effect of capsule diameter on capsule velocity history for a heavy density rectangular capsule at $V_{av} = 4m/sec$ and $L_c = 1d$	82
Figure 4.50 (a) Static gauge pressure and (b) Flow velocity magnitude variations for two equi-density rectangular capsules of $k = 0.5$, $L_c = 1d$ and $V_{av} = 2m/sec$ at different flow times.....	83
Figure 4.51 The effect of capsule concentration on the pressure drop variation for two equi-density rectangular capsules of $k = 0.5$ and $L_c = 1d$ at $V_{av} = 2m/sec$	84
Figure 4.52 The effect of capsule concentration on capsule velocity history for two equi- density rectangular capsules of $k = 0.5$ and $L_c = 1d$ at $V_{av} = 2m/sec$	84
Figure 4.53 The holdup for any shape of capsules.....	86
Figure 4.54 Friction coefficient for any shape of capsules	88
Figure 5.1(a) Static gauge pressure and (b) Flow velocity magnitude variations for capsules in the (SC) order of $k = 0.5$, $L_c = 1.5d$ and $V_{av} = 2m/sec$ at different flow times	92
Figure 5.2 Variations in mixture pressure drop and capsules pressure drop, for two capsule flow in the (SC) order of $k = 0.5$, $L_c = 1.5d$ and $V_{av} = 2m/sec$	93
Figure 5.3 The effect of capsules in the (SC) order on the capsules velocity history	93
Figure 5.4 (a) Static gauge pressure and (b) Flow velocity magnitude variations for capsules in the (CS) order of $k = 0.5$, $L_c = 1.5d$ and $V_{av} = 2m/sec$ at different flow times	94
Figure 5.5 The effect of capsules in the (CS) order on the capsule velocity history	95
Figure 5.6 (a) Static gauge pressure and (b) Flow velocity magnitude variations for capsules in the (RS) order of $k = 0.5$, $L_c = 1.5d$ and $V_{av} = 2m/sec$ at different flow times	95
Figure 5.7 The effect of capsules in an (RS) order on capsule velocity history	96
Figure 5.8 (a) Static gauge pressure and (b) Flow velocity magnitude variations for capsules in the (SR) order of $k = 0.5$, $L_c = 1.5d$ and $V_{av} = 2m/sec$ at different flow times	97

Figure 5.9 The effect of capsules in the (SR) order on the capsule velocity history	98
Figure 5.10 (a) Static gauge pressure and (b) Flow velocity magnitude variations for capsules in the (CR) order of $k = 0.5$, $L_c = 1.5d$ and $V_{av} = 2m/sec$ at different flow times.....	99
Figure 5.11 The effect of capsules in the (CR) order on the capsule velocity history	99
Figure 5.12 (a) Static gauge pressure and (b) Flow velocity magnitude variations for capsules in the (RC) order of $k = 0.5$, $L_c = 1.5d$ and $V_{av} = 2m/sec$ at different flow times.....	100
Figure 5.13 The effect of capsules in the (RC) order on the capsule velocity history	101
Figure 5.14 (a) Static gauge pressure and (b) Flow velocity magnitude variations for capsules in the (SC) order of $k = 0.5$, $L_c = 1.5d$ and $V_{av} = 2m/sec$ at different flow times	102
Figure 5.15 Variations in pressure drop, for two heavy density capsule flow in the (SC) order of $k = 0.5$, $L_c=1.5d$ and $V_{av} = 2m/sec$	102
Figure 5.16 The effect of capsules in the (SC) order on the capsules velocities history	103
Figure 5.17 (a) Static gauge pressure and (b) Flow velocity magnitude variations for capsules in the (CS) order of $k = 0.5$, $L_c = 1.5d$ and $V_{av} = 2m/sec$ at different flow times	104
Figure 5.18 The effect of capsules in the (CS) order on the capsule velocity history	104
Figure 5.19 (a) Static gauge pressure and (b) Flow velocity magnitude variations for capsules in the (RS) order of $k = 0.5$, $L_c = 1.5d$ and $V_{av} = 2m/sec$ at different flow times	105
Figure 5.20 The effect of capsules in the (RS) order on capsule velocity history	106
Figure 5.21 (a) Static gauge pressure and (b) Flow velocity magnitude variations for capsules in the (SR) order of $k = 0.5$, $L_c = 1.5d$ and $V_{av} = 2m/sec$ at different flow times	107
Figure 5.22 The effect of capsules in the (SR) order on the capsule velocity history	107
Figure 5.23 (a) Static gauge pressure and (b) Flow velocity magnitude variations for capsules in the (CR) order of $k = 0.5$, $L_c = 1.5d$ and $V_{av} = 2m/sec$ at different flow times.....	108
Figure 5.24 The effect of capsules in the (CR) order on the capsule velocity history	109
Figure 5.25 (a) Static gauge pressure and (b) Flow velocity magnitude variations for capsules in the (RC) order of $k = 0.5$, $L_c = 1.5d$ and $V_{av} = 2m/sec$ at different flow times.....	110
Figure 5.26 The effect of capsules in the (RC) order on the capsule velocity history	110

Figure 5.27 (a) Static gauge pressure and (b) Flow velocity magnitude variations for capsules in the (SCR) order of $k = 0.5$, $L_c = 1.5d$ and $V_{av} = 2\text{m/sec}$ at different flow times	111
Figure 5.28 The effect of capsules in the (SCR) order on the capsule velocity history.....	112
Figure 5.29 (a) Static gauge pressure and (b) Flow velocity magnitude variations for capsules in the (SRC) order of $k = 0.5$, $L_c = 1.5d$ and $V_{av} = 2\text{m/sec}$ at different flow times	113
Figure 5.30 The effect of capsules in the (SRC) order on the capsules velocity history	113
Figure 5.31 (a) Static gauge pressure and (b) Flow velocity magnitude variations for capsules in the (RSC) order of $k = 0.5$, $L_c = 1.5d$ and $V_{av} = 2\text{m/sec}$ at different flow times	114
Figure 5.32 The effect of capsules in the (RSC) order on the capsule velocity history.....	115
Figure 5.33 (a) Static gauge pressure and (b) Flow velocity magnitude variations for capsules in the (RCS) order of $k = 0.5$, $L_c = 1.5d$ and $V_{av} = 2\text{m/sec}$ at different flow times	116
Figure 5.34 The effect of capsules in the (RCS) order on the capsule velocity history.....	116
Figure 5.35 (a) Static gauge pressure and (b) Flow velocity magnitude variations for capsules in the (CRS) order of $k = 0.5$, $L_c = 1.5d$ and $V_{av} = 2\text{m/sec}$ at different flow times	117
Figure 5.36 The effect of capsules in the (CRS) order on the capsule velocity history.....	118
Figure 5.37 (a) Static gauge pressure and (b) Flow velocity magnitude variations for capsules in the (CSR) order of $k = 0.5$, $L_c = 1.5d$ and $V_{av} = 2\text{m/sec}$ at different flow times	119
Figure 5.38 The effect of capsules in the (CSR) order on the capsule velocity history.....	119
Figure 5.39 (a) Static gauge pressure and (b) Flow velocity magnitude variations for capsules in the (SCR) order of $k = 0.5$, $L_c = 1.5d$ and $V_{av} = 2\text{m/sec}$ at different flow times	120
Figure 5.40 The effect of capsules in the (SCR) order on the capsule velocity history.....	121
Figure 5.41 (a) Static gauge pressure and (b) Flow velocity magnitude variations for capsules in the (SRC) order of $k = 0.5$, $L_c = 1.5d$ and $V_{av} = 2\text{m/sec}$ at different flow times	122
Figure 5.42 The effect of capsules in the (SRC) order on the capsule velocity history.....	122
Figure 5.43 (a) Static gauge pressure and (b) Flow velocity magnitude variations for capsules in the (RSC) order of $k = 0.5$, $L_c = 1.5d$ and $V_{av} = 2\text{m/sec}$ at different flow times	123
Figure 5.44 The effect of capsules in the (RSC) order on the capsule velocity history.....	124

Figure 5.45 (a) Static gauge pressure and (b) Flow velocity magnitude variations for capsules in the (RCS) order of $k = 0.5$, $L_c = 1.5d$ and $V_{av} = 2\text{m/sec}$ at different flow times	125
Figure 5.46 The effect of capsules in the (RCS) order on the capsule velocity history.....	125
Figure 5.47 (a) Static gauge pressure and (b) Flow velocity magnitude variations for capsules in the (CRS) order of $k = 0.5$, $L_c = 1.5d$ and $V_{av} = 2\text{m/sec}$ at different flow times	126
Figure 5.48 The effect of capsules in the (CRS) order on the capsule velocity history.....	127
Figure 5.49 (a) Static gauge pressure and (b) Flow velocity magnitude variations for capsules in the (CSR) order of $k = 0.5$, $L_c = 1.5d$ and $V_{av} = 2\text{m/sec}$ at different flow times	128
Figure 5.50 The effect of capsules in the (CSR) order on the capsule velocity history.....	128
Figure 5.51 Correction factor for a mixed shapes flow of capsules.....	130
Figure 6.1 Flow chart of the optimisation model.....	138
Figure 6.2 Variations in manufacturing and operating costs versus pipeline diameter	140
Figure 6.3 The total cost and pumping power versus pipeline diameter.....	141
Figure 6.4 Effect of the solid throughput required and the shape factor of the capsules on the optimal diameter	144
Figure 6.5 Variations in the different costs of the pipeline versus pipeline diameter for the transport of capsules in a CS order.....	146
Figure 6.6 Comparison of different costs of the pipeline for the SC and CS order	148

List of Tables

Table 3-1 Boundary Conditions.....	38
Table 3-2 Mesh Independence based on Pressure Drop across the HCP.....	42
Table 3-3 Mesh Independence based on Capsule Velocity in HCP.....	43
Table 3-4 Factors and levels of Taguchi's method for an HCP.....	44
Table 4-1 Validation Tests.....	47
Table 6-1 Variations in Various Costs versus Pipeline Diameter.....	139
Table 6-2 Variations in Various Costs versus Pipeline Diameter.....	141
Table 6-3 Variations in Various Costs Variations versus Pipeline Diameter.....	142
Table 6-4 Effect of the Shape Factor of the Capsules on the Optimal Pipeline Diameter and the Total Cost of the Pipeline.....	143
Table 6-5 Variations in Transportation Costs versus Pipeline Diameter in the CS order.....	145
Table 6-6 Variations in Transportation Costs versus Pipeline Diameter in the SC order.....	147

Nomenclature

A	Cross-sectional Area of the Pipe (m^2)
C_1	Power Consumption Costs per unit Watt (£/W)
C_2	Pipe Cost per unit Weight of Pipe Material (£/N)
C_3	Capsules Cost per unit Weight of the Capsule Material (£/N)
C_c	Proportionality Constant of (-)
C_f	Correction Factor (-)
C_g	Centre of Gravity for Capsule (-)
c	Solid Phase Concentration (-)
d	Capsule Diameter (m)
D	Pipe Diameter (m)
f	Darcy Friction coefficient (-)
g	Gravity Acceleration due (m/sec^2)
h	Elevation (m)
h_l	Head Loss (m)
H	Holdup (-)
k	Capsule to Pipe diameter ratio (-)
L	Pipe Length (m)
L_c	Capsule Length (m)
N	Number of Capsules (-)
P	Pressure (Pa)
ΔP_c	Capsule Pressure Drop (Pa)

ΔP_m	Mixture Pressure Drop (Pa)
ΔP_{comb}	Pressure drop for mixed shapes of a capsules combination (Pa)
ΔP_{single}	Pressure drop for a single capsule shape flow (Pa)
Q	Flow Rate (m^3/sec)
Q_c	Solid Throughput (m^3/sec)
Re	Reynolds Number (-)
R_v	Velocity Ratio (-)
s	Specific Gravity (-)
Sc	Spacing between the Capsules (m)
t	Thickness of the Pipe Wall (m)
τ_w	Wall Shear Stress (Pa)
u	Local Flow Velocity (m/sec)
u_*	Frictional Velocity (m/sec)
V	Flow Velocity (m/sec)
V_{av}	Average Flow Velocity (bulk velocity) (m/sec)
V_c	Capsule Velocity (m/sec)
Vol_c	Volume of the Capsule (m^3)
Vol_p	Volume of the Pipe (m^3)
x	Radial Distance (m)
y	Axial Distance (m)
y^+	Dimensionless Wall Distance (-)
Z	Coordinates of Capsule (-)

Greek Symbols

ρ	Density (kg/m ³)
μ	Dynamic Viscosity (Pa-sec)
Υ	Specific Weight (N/m ³)
η	Efficiency of the Pump (%)
ε	Roughness Height of the Pipe (m)
π	Pi (-)
\emptyset	Shape Factor (-)
ζ	Loss Coefficient of Abrupt Contraction (-)

Chapter 1 - Introduction

Capsule flow in vertical pipelines has a vast range of applications in areas such as deep sea or underground mining and chemical processes in general. It is expected that the capsule flow in a vertical pipeline behaves considerably differently from that in a horizontal pipeline. Therefore, in order to supplement the existing knowledge of capsule pipeline transport and provide necessary information for the design of future capsule pipeline systems, extensive research on vertical capsule pipeline flows is needed. Thereby, this chapter presents a precursory debate concerning the flow of water and capsule across the pipeline. Moreover, the existing chapter presents an overview of the capsule pipeline design requirements and motivation of the work. At the end, a roadmap is given regarding how this thesis is structured.

1.1 Transporting Capsules in Pipelines

The last two decades have witnessed an increasing interest in efficient transport of cargo in pipelines through alternative methods, better than the conventional methods. Pipelines used for transportation purposes can be in general categorised into three generations. The first generation consist of a single-phase transportation. The second generation of pipelines comprises of multi-phase flow pipelines. The third type of these generations consists of the transport of capsules, where capsule pipelines are generally utilised to transport solids with water or any other fluid as the carrying medium. Transport of goods within capsules across pipes is a comparatively novel method of cargo convey, which is earning considerable significance globally due to rise in the fossil fuels prices [1] [2]. The transport of capsules has some attractive features in that a specific material can be easily separated from the transporting fluid.

As a matter of fact, the economic surveys that have been carried out by several universities and companies have presented that the capsules transport is more economic than traditional manners of transporting cargo such as lorries and trains etc. [3]. For instance, Mole Solutions Ltd. [4] did an economic analysis comparing different transportation systems and found that the capsule pipelines for the long distances are considered economically desirable. Moreover, the pipelines transporting capsules provide additional advantages such as [5]:

- Low cost for freight transport as compared to conventional transportation modes;
- Fluid is not contaminated and can be recycled;
- No manpower needed for the transport mechanisms unless at the insertion and ejection of the capsules from the pipe;
- No traffic incidents or some delay because of the congestion, and thus it is safer and faster for the cargo being transferred;
- Capsule pipelines have been found to be relatively friendly to the environment as compared to conventional transporting methods.

These attractive features of the capsule transport system provide a vast field of future applications for the transfer of materials from unreachable regions such as high hills and mountains across water bodies and deep-sea recapture of minerals. Thus, extensive research

is needed to generate an adequate knowledge base enabling the development of optimal design methodologies for capsule transport pipelines.

The pipelines transporting capsules are predominantly comprised of two forms, one of which is referred to as Pneumatic Capsule Pipelines (PCPs). The transportation medium in PCPs is conventionally comprised of an air or gas.

The second form is referred to as Hydraulic Capsule Pipelines (HCPs), in which water is utilised as the means of transportation rather than gas or air. The contrast in pressure between each end of the pipeline results in the capsules transforming to be waterborne and subsequently the capsules are spread to the evacuation of the capsule end of the pipe.

1.2 Historical Background of Capsule Transport Pipelines

Capsule pipelines, as a mode of freight transport, convey hollow containers, also called capsules, of different shapes. These capsules are loaded with the goods to be transported within the pipeline. Sometimes, as in the state of coal log pipes, the material to be transported is itself given the shape of the capsules as stipulated by Carter and Troyano-Cuturi [6]. The idea of pipeline transportation of goods was initially put in operation close to two centuries of operation. A proposal for transporting supplies via pipelines, utilizing capsules, was initially set up in 1810 by George Midhurst. Around 160 years later, a fresh era of wheeled capsules was embraced. This led to the establishment of two pipe systems incorporating wheeled capsules. A US-based firm, Tubexpress Systems Inc, came up with pipelines with an average diameter of 36 inches, and a length of 1400 feet, having 7 feet capsules impelled by compressed air.

Later on, in 1980, a Japanese firm, Sumitomo Metal Industries, attained the most flourished utilization of this technology, hence thereafter constructing a pipeline of 3.2 km in length and a diameter of 1 meter for the purposes of transporting limestone to cement plant [7]. Another exhibition project by Magplane Technology Inc was enacted by the Florida Institute of Phosphate Research for pipeline capsule system, typically impelled by linear synchronous

motors. The system's length and diameter were 270m and 0.61m respectively. Capsules attained a speed of 18m/s, plus the capacity to bear 300 kilograms of load [8].

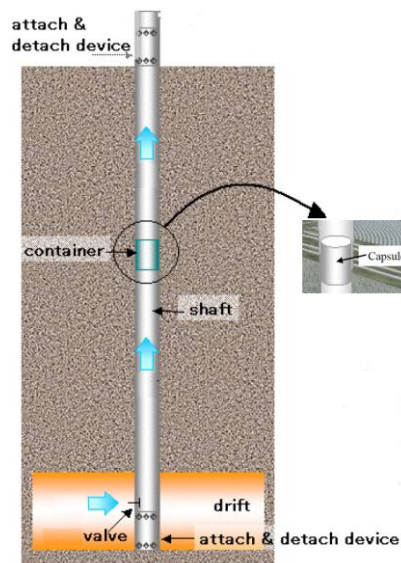


Figure 1.1 Vertical Capsule Pipeline [7]

1.3 Components of the Hydraulic Capsule Transportation System

In generally, any HCP system has the following main components:

- Pump
- Capsules
- Capsule Injection System
- Capsule Evacuation System

This system of capsule transportation used conveyor belts to inject the capsules into the pipeline. The capsules evacuation is carried out in a reverse way as that of injection, except that no pumps are required, and only a transporter is needed.

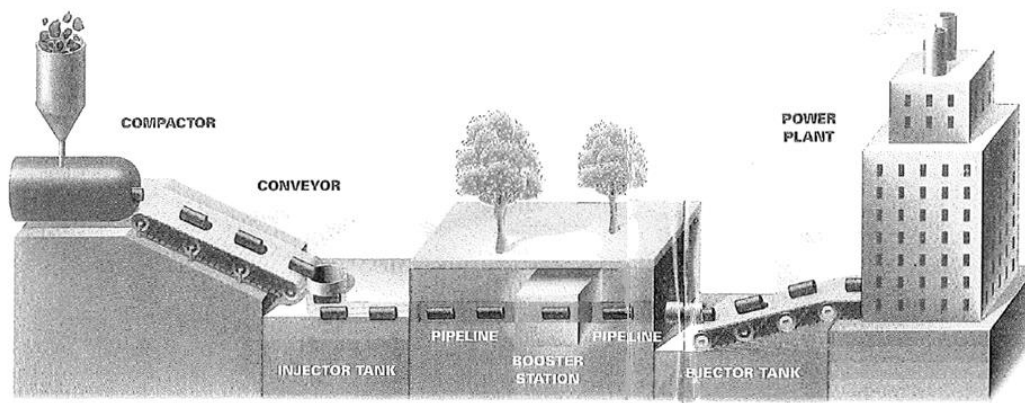


Figure 1.2 Hydraulic capsule pipeline system [9]

1.4 Characteristics of Capsule Flow in Pipelines

There is a body of research globally which explores pipeline flows. Bernoulli first characterised this in the principle named after him, that pressure in a fluid is a manifestation of kinetic energy. This can be expressed by the following equation [10]:

$$P + \frac{1}{2} \rho u^2 = \text{constant} \quad (1-1)$$

The first term of the equation on the left side, P refers to the fluid static pressure, whereas ρ represents the fluid density and u is the fluid velocity. The second part refers to the dynamic pressure. Consideration of the head loss and the elevation of the pipeline lead to a generalisation of this equation as following:

$$P_1 + \frac{1}{2} \rho_1 u_1^2 + \rho_1 g_1 h_1 = P_2 + \frac{1}{2} \rho_2 u_2^2 + \rho_2 g_2 h_2 + \rho_2 g_2 h_l \quad (1-2)$$

where h is the vertical elevation of the water column, h_l is the head loss experienced by the fluid and g is the gravitational acceleration (generally constant). The first part of the equation is known as the static head, whereas the second part is known as dynamic head and the final part is known as the potential head.

Since the flow is incompressible and the acceleration due to gravity is constant in a vertical pipe, this can be rewritten Equation (1-2) as:

$$\Delta P = f \frac{L}{D} \frac{\rho V^2}{2} + \rho g \Delta h \quad (1-3)$$

A relationship for the mixture pressure drop in a vertical hydraulic capsule pipeline can be developed, based on equation 1-3, where the impacts of capsules and water on the pressure drops across the pipeline can be distinguished. For the flow of capsules in upward direction (Δh positive) within a vertical pipeline, the mixture pressure drop can be expressed as:

$$\Delta P_m = (\Delta P_w + \Delta P_c) + \rho_w g \Delta h_w \quad (1-4)$$

where ΔP_w is the pressure drop due to water flow, ΔP_c the pressure drop due to the capsule flow and $\rho_w g \Delta h_w$ is the pressure drop due to the elevation increase (applicable in vertical or inclined pipelines).

Therefore, the pressure drop within a vertical HCP can be expressed as:

$$\Delta P_m = f_w \frac{L}{D} \frac{\rho_w V_{av}^2}{2} + f_c \frac{L}{D} \frac{\rho_w V_{av}^2}{2} + \rho_w g \Delta h_w \quad (1-5)$$

1.5 Design Considerations for Transporting Capsules in Pipelines

In designing capsule pipelines, a predictive model is required to calculate the pressure drop. The pipeline design transferring capsules is quite complicated owing to a large number of parameters involved. The designers require different parameter categories such as the hydraulic, mechanical and operational parameters. The current study addresses the optimum design of a vertical pipeline transporting capsules depended on hydraulic capsule parameters, such as the capsule specific gravity, diameter, shape and length, excepting the influences of the additives necessary to reduce the pressure drop.

1.5.1 The Carrier Fluid in the Pipe

The selection of the carrier fluid depends significantly on the fluids' availability in the nearby areas. This study offers a detailed analysis on the capsules transportation relying on the final employ of the capsules.

1.5.2 The Shape and Size of Capsule

The capsule velocity is a major factor affecting pressure drop, which is a function of the size and the shape of the capsules. The design process of HCPs is a function of the capsule shape and size [11]. This work provides a detailed analysis of the effects of capsule size and shape on transporting capsules within pipes.

1.5.3 The Concentration of Capsules within Pipeline

The capsules concentration in a pipeline is generally regulated by the throughput demands of the system. The maximum limit of the capsules concentration within pipelines is regulated by the reality that the pressure drops within the pipe grow notably at high concentration. The generally ideal concentration for transporting hydraulic capsules is determined by the lowest level of energy consumption [11]. This research provides extensive analysis of the impacts of the capsule concentration in a vertical pipeline.

1.5.5 Diameter of the Pipe

The pipeline should be built with an appropriate diameter to transport the required throughput at acceptable capsule concentration as well as capsules velocity. Practically, the capsule concentration, capsule velocities and pipeline diameters are interrelated, and hence it has become requisite for designers to improve all these parameters, taking into account power consumption constraints. This study provides a methodology of an optimisation that gives the optimum diameter of the pipeline for transporting capsules.

1.5.6 Pressure Drop in the Pipeline

In this study, the pressure drop across the HCP is considered as the primary parameter for analysis. The pressure drop data has been obtained from the numerical simulations under various geometric and flow conditions. In order to better comprehend the complicated flow

phenomena, the range of variations in pressure and velocity must be accurately measured. A visualisation can be created where appropriate to best understand the character of the flow. Thereby, the velocity profile and pressure can be visualised. Using pressure gradient data can develop semi-empirical correlations of predicting the pressure drop at specific points within the pipeline.

1.6 Mechanisms of Capsule Flow in Pipelines

The force is being applied on the capsules by the carrier fluid so that it can push them forwards in the stream of flow. The driving force in transporting these capsules through the stream of flow is the drag of fluid, affected by the flow velocity of the capsules, its density, shape and size of the capsules. The flow in a capsule pipeline is asymmetric in nature, owing to the fact that the velocities of the capsule and the flow are different. This variation in the capsules velocities and the flow is usually known as the Slip, and as such is a function of flow velocity, size, density and capsule shapes under various flow conditions. In instances of heavy density capsules flows, whenever the velocity of the flow reduces to a quite low limit, the capsules will tend to stop travelling along the pipeline's flow. The minimum flow velocity that retains the capsule motion in the pipeline is known as incipient velocity. This minimum velocity is indeed a function of several parameters e.g. size, shape and capsule density. This velocity for the capsules flow is considerably higher within vertical pipelines when compared to horizontal pipelines [11-14].

There are four flow regimes in hydraulic capsule pipelines. In the first flow regime, the capsule is stationary and water flows around the capsule, while in the other three flow regimes, the capsule move with the water flow. The second flow regime corresponds to initial capsule motion (lift-off). The third flow regime corresponds to when capsule velocity exceeds the fluid velocity. The fourth regime corresponds to the steady flying state of the capsules [15].

1.7 Motivation for this Study

The design of capsules transporting pipelines requires study of the flow parameters that are interdependent. As the power demands of vertical pipelines are considerably higher compared with horizontal pipelines, the design process is significantly impacted because of the further pressure drop within the vertical pipeline owing to the change in the pipe elevation. Thereby, requisite modifications regarding the friction coefficient and the pressure drop considerations have to be conducted for precisely design a vertical HCP with acceptable precision.

The existing literature on the capsule flow in pipelines reveals that most of the numerical research is based on steady-state flow analysis, which corresponds to the fourth flow regime mentioned earlier. The main issue with this approach is the fact that these studies specify the capsule motion characteristics (like capsule velocity etc.) rather than computing them. Hence, the energy is being imparted to the flow, which is physically unrealistic. The present study investigates a novel area of research of numerically simulating the capsule motion, with the ability to predict capsule trajectory and velocity in vertical pipelines. Thereby, the present study uses a more accurate modeling approach for capsule flow in vertical pipelines.

It is important to study the basic capsule shapes such as spherical, cylindrical and rectangular as these shapes can be combined in a number of ways to develop any complicated shape of the capsule. A thorough understanding of the velocity and pressure variations within a vertical HCP is fundamental to its design. Consequently, the flow field variables in conjunction with geometrical parameters are the basis of the formulation of the prediction models for pressure drops and capsule velocity. Furthermore, the flow field of mixed capsules shapes (i.e. capsules of different basic shapes flowing together in a train) is significantly complex as compared to the capsule train of just one particular shape. The flow of mixed capsules shapes has a significant effect on the motion of capsules, and hence, on the capsules' velocity and pressure drop. It is desirable to know the effects of the mixed capsules flow in a vertical pipeline in industrial applications as it is expected to have a wide variety of capsule of different shapes.

The designers must apply an efficient design methodology, which represents the hydraulic design of capsule transport within vertical pipes. Although there are several design

methodologies being reported in the literature for this purpose, as mentioned earlier, they use rather simplified approaches for predicting of the pressure drop across HCPs. This leads to inaccuracies in the design and optimisation process for HCPs. Hence, in the present study, an efficient optimisation model was developed, based on the Principle of Least-Cost, which takes into account the dynamic behavior of capsule flow in vertical pipelines. The developed optimisation model is both robust and user-friendly.

1.8 Research Aims

The key aims of this study will be presented in this section, while the research objectives are debated beyond conducting a comprehensive review of the literature in the following chapter. According to the study motivations that have been shown, the aims of this research have been divided as follows:

- Flow diagnostics in off-shore HCPs transporting basic capsule shapes under different operating conditions.
- Flow diagnostics in off-shore HCPs transporting a combination of basic capsule shapes under different operating conditions.
- Development of an efficient optimisation model for predicting the optimal size of off-shore HCPs.

These research aims encompass a number of practical problems faced in the real world for transporting capsules through a vertical pipeline. The next chapter presents a detailed literature review on the aforementioned research aims.

1.9 Structure of the Thesis

This section which provides a brief summary of the contents of the different chapters of this thesis is presented.

Chapter 1, presents the general introduction to the research topic, providing details of the capsules transportation mechanism in pipelines. From this overview, the motivation behind this work is presented, which determines main fields to be reviewed in the next chapter.

Chapter 2, presents an extensive insight into literature published in relation to capsule transport in hydraulic pipelines. It incorporates an analysis of literature concerning transport characteristics of capsules in hydraulic pipelines, whilst also emphasising varying methods and parametric research that has previously been utilised. Additionally, the chapter reviews the literature relating to optimisation strategies that were utilised for an HCP. Details regarding the research area are presented within the particular objectives based on the essential research aims.

Chapter 3, presents the basic conceptions of Computational Fluid Dynamics (CFD). It comprises of the CFD modelling of vertical capsules pipes, comprising the boundary conditions and solver settings determined in the solver. This is followed by his is followed by an extensive debates on Dynamic Meshing technique utilised for capsules motion. Moreover, the mesh independency tests for the capsules velocities and pressure gradient across the pipeline are investigated.

Chapter 4, provides an insight regarding the flow structure in basic capsules shapes and how this affects transportation for off-shore applications. An extensive scrutiny of the pressure and the velocity fields has been undertaken to be analysed with more depth to examine the impacts of the solid body existence on the pressure gradient inside the pipe. In relation to an extensive array of flow conditions, the flow of spherical, cylindrical and rectangular capsules have been reviewed within the context of contrasting geometric configurations and specific gravities. Semi-empirical models relating to the anticipation of capsule velocity and pressure drops in vertical pipelines were established to ease the design of HCPs systems.

Chapter 5, is comprised of extensive investigations relating to the flow of mixed capsule shapes for off-shore applications. Extensive analysis has been conducted in relation to the pressure and the velocity fields. It is hoped that this will illuminate the influence of a combination of capsule shapes flowing in the pipeline. Additionally, this chapter explores the influence of the ordering of the capsules within the train on the pressure drop. To help with

developing the pipeline design method, a semi-empirical correlation that predicts the pipeline's pressure drop for the flow of mixed capsule shapes has been devised.

Chapter 6, illustrates the development of the vertical HCPs design methodology. The optimisation concept for HCPs relates to Least-Cost Conception. The optimisation method is stringent and easy for users to use. The throughput of solid considers as the inputs to the models needed from the HCP, whereas its outputs are the optimum diameter of pipeline and the corresponding pumping needs. This model is relatively easy to be used and can be implemented at a wide commercial range.

Chapter 7, presents main conclusions drawn from the results of the current study and the suggested recommendations for future work.

Chapter 2 - Literature Review

This chapter provides an insight regarding the current state of knowledge about the capsule flow characteristics in pipes by detecting the published literature. A vast range of sources has been investigated in an attempt to obtain a full comprehension of the problem and how different researches addressed these issues. The existing literature includes the published works regarding transport characteristics of hydraulic capsules in pipelines and optimisation of a capsule pipeline design. This has also assisted in deciding the scope of the current work and research objectives of this study.

2.1 Introduction

Hydraulic capsule pipelines in recent decades were undergone intense investigations activities. The first significant investigative research in this domain dates back to the early 1960s when Charles [16] investigated the flow of an one cylindrical capsule having a density such as water. From this work, Charles devised an analytical expression representing the pressure drop and capsule velocity inside the pipeline, in relation to capsule-to-pipe hydraulic diameter ratios. Following this work, further studies were carried out almost exclusively at the Research Council of Alberta to define the characteristics of a flow system in which the observed slugs of oil in water were replaced by capsules of cylindrical or spherical shape. The HCP systems are presently under effective investigations for application into the cargo industry for loading and unloading processes. This calls for a deeper analysis of HCPs in a bid to extend the knowledge in this area of research.

2.2 Flow Characteristics in Hydraulic Capsules Pipelines

Round and Bolt [17] conducted experimental investigations with a particular focus on spherical capsules with heavy density. The work addressed dimensional analysis where it has been established that the capsule velocity is affected by the average flow velocity (V_{av}) and (k) capsule diameter ratio. The investigations scope covered values of $V_{av} = 1$ to 3.7m/sec and $k = 0.39$ to 0.89 for a single capsule. The debate on the findings that have been obtained for the capsule's velocities, was restricted to the impacts on capsule velocity (V_c) respect to V_{av} and k . The pressure drop analysis, and the flow distribution across the pipeline, was not discussed in the investigation. No formulation has been developed for the velocity of the capsule.

Mishra et. al [18] experiments were performed on a train of an equal density spherical capsules within a hydraulic pipeline. The experimental investigation range was for the average flow velocity from 1 to 2.2m/sec and $k = 0.44$ to 0.67 . Using statistical algorithms such as multiple regression analysis, an expression for hold (ratio of capsule to average flow velocities) has been developed. On the other hand, the variation in the pressure gradient in the pipeline was not computed. Moreover, no analysis was performed on the flow parameters in the pipeline.

Agarwal et. al [19] performed experimental studies in a hydraulic pipeline on the flow of spherical, cylindrical and rectangular capsules with heavy densities. The investigations range was $V_{av} = 1.4$ to 2.9 m/sec and $k = 0.5$ to 0.9 . The debates concentrates on the effect of the shape of the capsule on the holdup (figure 2.1). The capsule shape has the most dominant effect on the velocity ratio and the investigation mainly concentrated on determining the capsule velocity. It however falls short in describing the flow and capsule behaviour in HCPs, plus the flow of combination of capsule shapes was not studied. Moreover, the pressure drop inside the pipeline was not recorded.

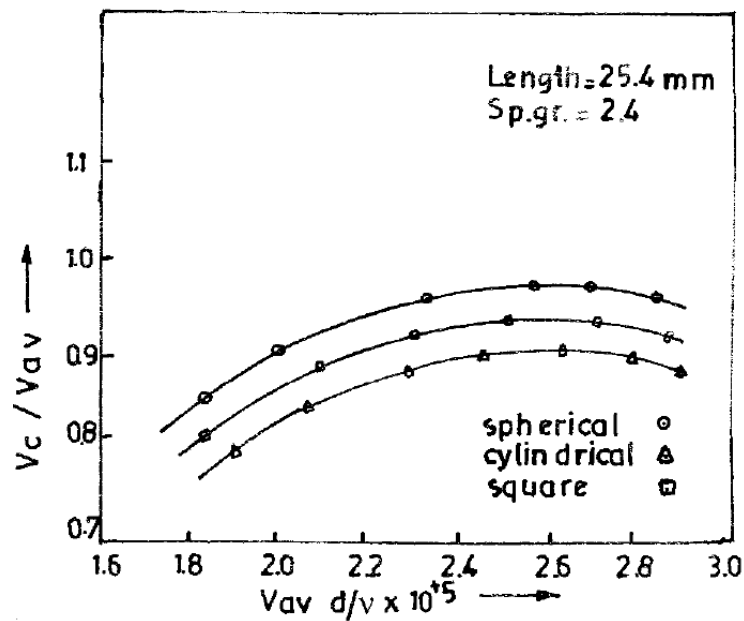


Figure 2.1 Variation of V_c/V_{av} with Re for capsules of different shapes [19]

Mathur and Agarwal [20] and Agarwal et. al [19] have performed experimental investigations on the capsules flow of shape factor (ψ) of 1 in HCPs, where the shape factor has been defined as:

$$\psi = \left(\frac{\text{Volume of Capsule}}{\text{Volume of Circumscribing Sphere}} \right)^{\frac{1}{3}} \quad (2-1)$$

The investigation focused on developing relationships for capsules' velocity.

Feng et. al [21] used a dynamic method to compute the motion of an elliptic heavy density capsule in a 2D horizontal channel. The numerical model allowed the computation of the capsule motion and the fluid around it. A two-dimensional model has been used in the study to simulate the flow of an elliptical capsule as shown in the figure 2.2. The investigation mainly focused on the mechanisms of the lift force and shear stress acting on the capsule. The results revealed that the motion could be decomposed into three stages: initial lift-off, transient oscillations and steady flying. The effects of geometry and the capsule velocity variations were not studied. In addition, the analysis of the pressure variations inside the pipeline has not been investigated.



Figure 2.2 The elliptic capsule flow in a two-dimensional channel [21]

Tomita et. al [22, 23] performed a set of analytical examinations on the cylindrical capsules flows, concentrating only on the velocity and the trajectory of the capsules, within a hydraulic pipeline. As it can be noted in figure 2.3, the time histories of water (V) and capsule (Z) velocities were analysed. Nevertheless, the capsules have been considered as point masses, and a restricted debate on the flow velocity and pressure variation in the vicinity of the capsules was recorded. The capsules were all equipped with wheels in order to maintain its position in the pipe axis, and thereby, no investigation of a freely flowing cylindrical capsule was carried out. Moreover, the impact of the capsule length was not considered through this study.

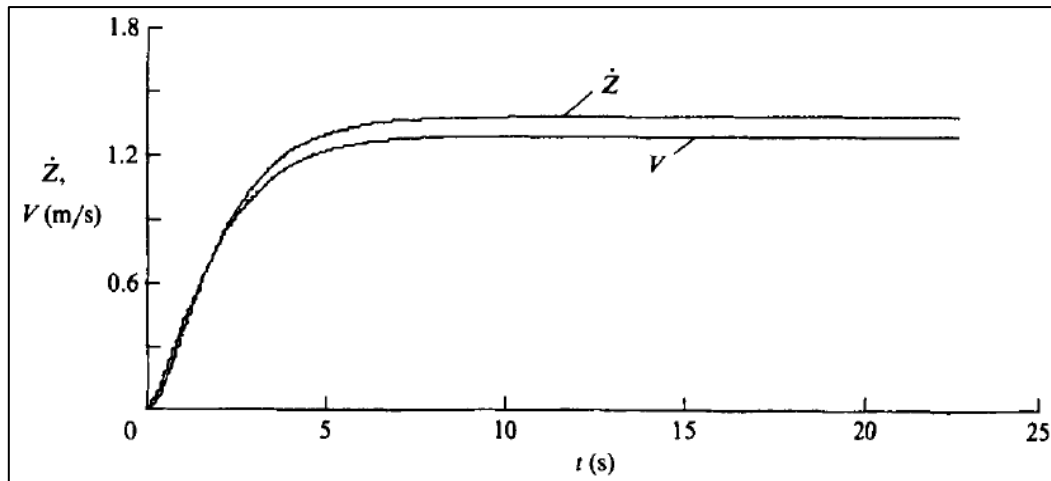


Figure 2.3 The Time histories of capsule and water velocities at an inlet head [22]

Lenau and El-Bayya [24] extended Tomita et. al [22] work and developed two mathematical models to analyse the transient flow of a one cylindrical capsule. The capsule has been considered both a rigid body and elastic. They numerically solved the mathematical models using the method of characteristics. The trajectory and capsule velocity were found out at node points, but an incomplete debate on the flow domain distribution was presented. In addition, the study is restricted on the flow of a one cylindrical capsule.

Ulusarslan [25] undertaken the experimental investigation to examine the flow characteristics of a spherical capsules train. The investigation was performed in the Reynolds number range of $1.2 \times 10^4 < Re < 1.5 \times 10^5$ and a capsule concentration of 5 to 30% by volume. The capsules were made from polypropylene having density slightly less than water. The results depicted that the pressure gradient increases as the solid concentration increases as shown in figure 2.4. Based on the experimental findings, mathematical models were developed for establishing relationships between the pressure drop and the Reynolds number of the flow.

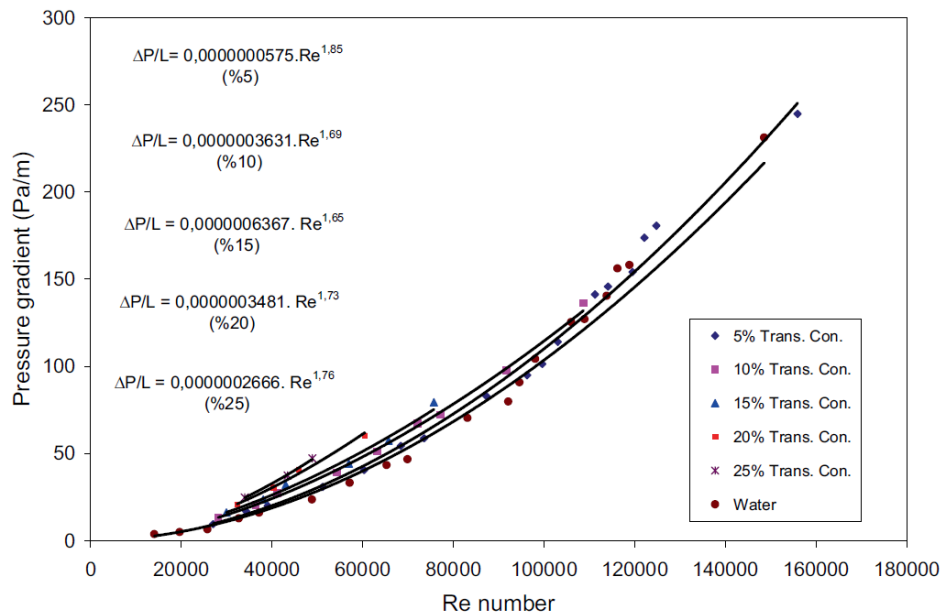


Figure 2.4 Relation between the pressure gradient and the mixture's Re number according to the experimental data [25]

Extensive experimental investigations were conducted by Chow [26] on the flow of spherical and cylindrical capsules with an equi-density inside a vertical pipeline. The scope of values under this investigation were $V_{av} = 1$ to 4m/sec , $k = 0.5$ to 0.9 , and capsule length (L_c) of 1 to 14 times the capsule diameters. This work presents an analysis of the velocity of capsules and the pressure drop across the pipe. Equations for both these parameters were developed; however, the range in which these equations are valid is severely limited.

Tsuji et. al [27] have carried out an experimental investigation on stationary capsules within vertical pipelines. The detailed investigation on the flow structure with respect to the wake region downstream of the capsules, and its impact on the trailing capsules in the train has been recorded in respect to the drag coefficient of the capsules. The study depicted how the capsules presence within the pipelines impacts the velocity profile at various cross sections of the pipeline. Nevertheless, the study is extremely restricted by the fact that the capsules are stationary within the pipe.

Hwang et. al [15] performed a blend of experimental and analytical investigation in a vertical pipeline on the flow of cylindrical capsules with a heavy-density. Investigations in this work were in the range of $k = 0.5$ to 0.9 , with the concentration of the study on finding out the total

efficiency of capsule conveying systems, in relation to the pressure drop and energy loss. From the experiments, it was found that the best value of k that attains maximum value in efficiency is $2/3$ or 0.66 . Moreover, it was found that the capsule length has small effect on the system efficiency. The structure of the flow in the pipe was not studied in these investigations.

Hammoud and Khalil [28] have implemented experiments regarding the cylindrical capsules flow with a heavy-density. The main concentration of this study is on the effects of capsule propagation in both upward and downward directions within the pipeline. The range of investigation covers flow velocities from 0.5 to 4m/s and capsule's specific gravity between 1.5 and 3.5 . The results show that the capsule lift-off velocity increases as the capsule specific gravity and the pipe's inclination angle increases (figure 2.5). The pressure drop in upward flows was generally higher than in horizontal flows and downward flows. However, the investigations scope is restricted to one cylindrical capsule without taking into consideration the effect of the capsule length on the capsule velocity and low pressure. In addition, no expressions for the velocity and pressure drop of the capsule have been developed.

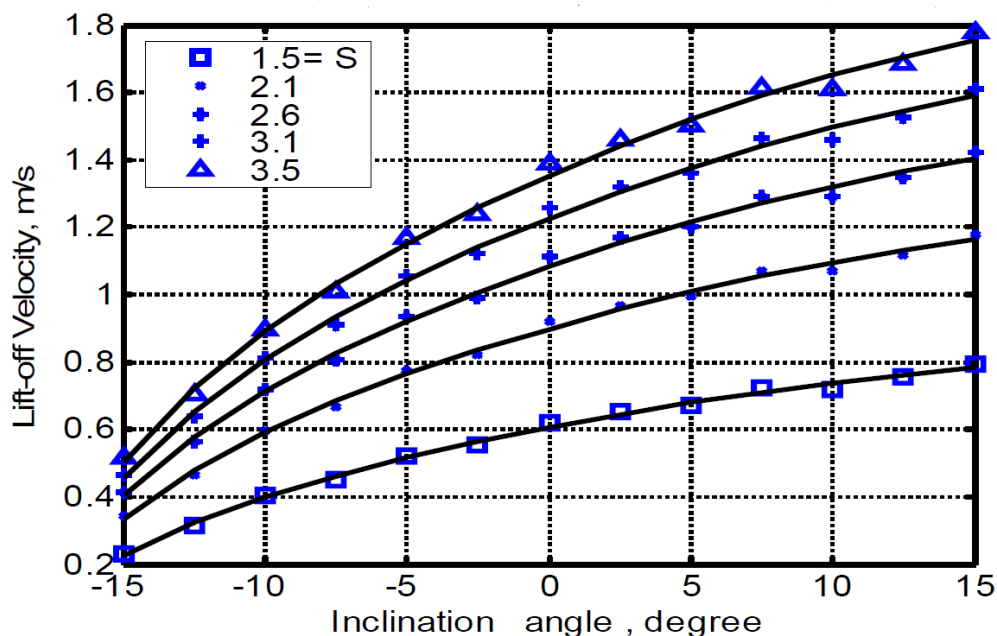


Figure 2.5 Effect of inclination angle and capsule specific gravity on capsule lift-off velocity [28]

Govier and Aziz [5] stated that the analysis of Zuber and Findlay (1965) is directly applicable for predicting the capsule velocity, as there were no relations available at that time. The equation revealed that the capsule velocity is linearly proportional to the average bulk velocity. The authors have used a distribution coefficient (C_0) to relate the capsule velocity and the average bulk velocity. This coefficient depends on both the fluid velocity profile and the capsule diameter ratio. At slightly higher diameter ratios (0.8 to 0.9), the distribution coefficient is suggested to be 1.2 for capsule flow in vertical pipelines at normal velocities. For higher velocities, the authors suggested a range of 1.10 to 1.15 for this coefficient, and this approach is thought to be practical for bulk velocities equal to or greater than the lift-off capsule velocity, but not at considerably higher bulk velocities.

Tachibana [29] carried out experiments pertaining the flow of cylindrical capsules with a heavy-density within vertical and inclined pipes. The investigation range is $k = 0.5-0.9$ and $l/d = 2-10$, where l and d are the length and diameter of the capsules. The study was particularly interested in looking at the power loss in capsule transporting processes (figure 2.6). It can be observed that capsules with lower l/d have lower power loss associated with them. No details relating to the flow structure in the pipeline has been provided. Moreover, the changes in power loss are non-linear in relation to the angle of inclination of the pipeline.

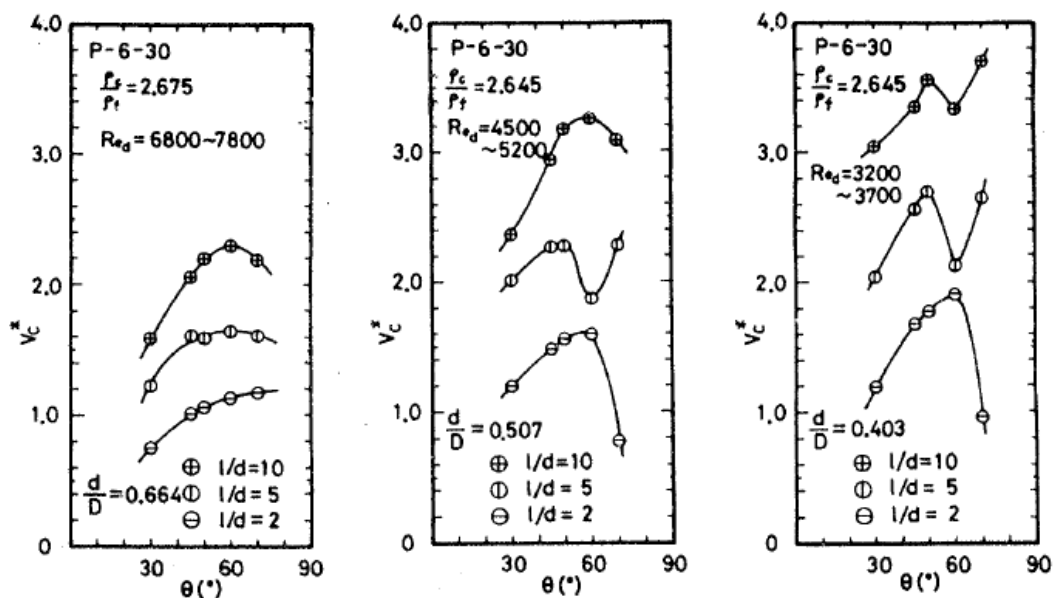


Figure 2.6 The relation between the balance velocity and the inclination angle (a) $k = 0.664$ (b) $k = 0.507$ (c) $k = 0.403$ [29]

Latto and Chow [30] have undertaken experimental investigations on the cylindrical capsules flow within vertical pipelines. The values range used in this investigation were $V_{av} = 1$ to 4m/sec , $L_c = 4$ to 15 times the capsule diameters and $k = 0.5$ to 0.82 . The test set up used in the study is shown in figure 2.7 below. This study also included a detailed analysis of the pressure drop and the capsule velocities in pipelines. Nevertheless, no data concerning the structure of the flow in the pipeline was provided. In addition, the capsule shape effects on the flow characteristics within the vertical pipeline have not been studied.

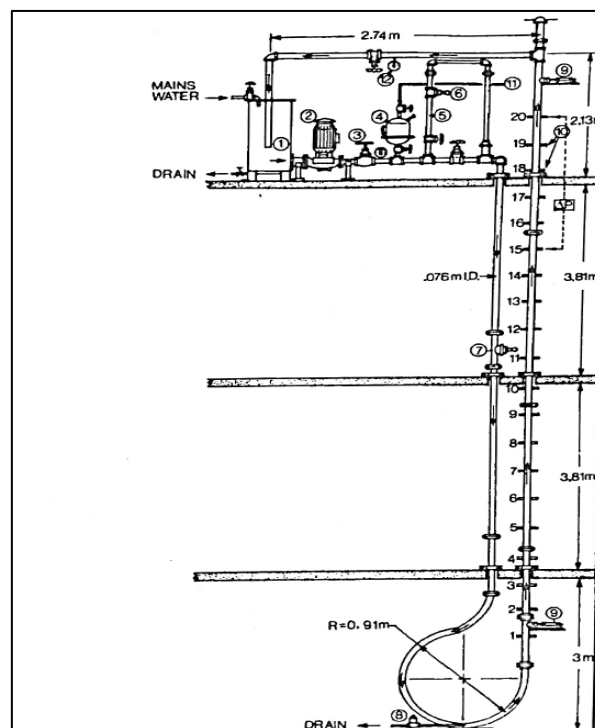


Figure 2.7 The schematic diagram of the experimental set-up [30]

Ohashi and Yanaida [31] conducted experimental and analytical studies on the cylindrical capsules flow across vertical pipelines. The investigations range was $k = 0.78$ to 0.96 , specific gravity (s) of 1.39 to 7.84 and $L_c/d = 1.5$ to 5 . The other key aspect of this study is the prediction model presented to find the pressure drop in the pipeline with respect to the Froude number of the capsules. This work has not presented information on the flow structure in the capsule pipelines. Similarly, the work by Yanaida and Tanaka [32] also leaned towards experiments and analytical investigations about the flows of cylindrical capsules in vertical pipes. In this regards, this work discussed the flow development in these

kinds of pipelines coupled with doing an analysis of the drag coefficient of capsules in different geometric and flow conditions. On the other hand, the pressure drop analysis has not been performed in the pipeline.

Bartosik and Shook [33] have undertaken a range of numerical investigations regarding the flow of solid-water mixtures within vertical pipes. Their investigations have scrutinised the velocity flow field and the impacts that the concentration has on the solid medium on the pressure gradient in the pipeline. Yet no references have been made to the pressure distribution and pressure gradient within the pipeline. Swamee [34] carried out design studies in the field of flow of cylindrical capsules carrying a range of densities (heavy and equal) within vertical pipelines. Yet the study is restricted significantly as no data regarding the pipeline's flow structure has been given.

Khalil et. al [35] performed numerical investigations about the steady flow of a single cylindrical capsule with diameters ratio between 0.8 and 0.9 within a hydraulic pipeline. A contrast of a range of turbulence models has been provided. Figure 2.8 illustrates that the pressure gradient predicted from the different turbulence models show reasonable agreement with those obtained from experiments. Moreover, the velocity profiles and pressure gradients computations were extensively studied. Nevertheless, the capsule length has been regarded identically for every instance in this study. An incomplete analysis has been presented to the flow field in the pipeline.

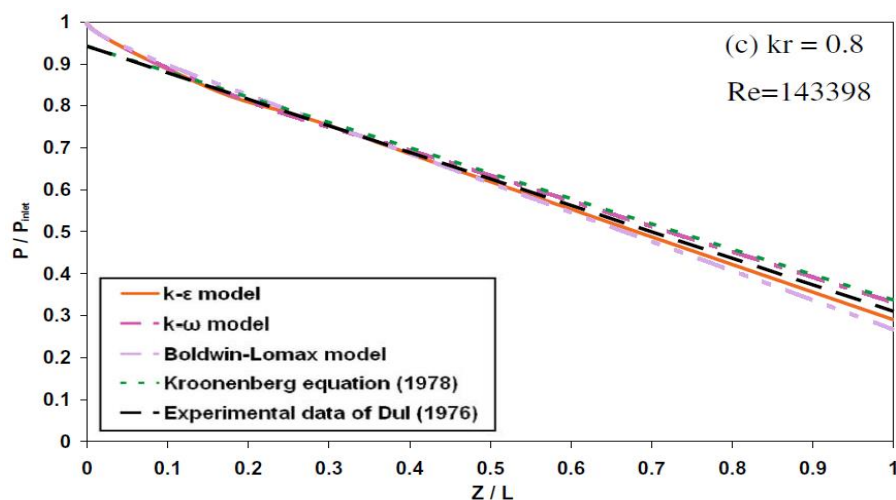


Figure 2.8 The pressure distributions along cylindrical capsule of $k = 0.8$ and $Re = 143398$ by different turbulence models and experimental data [35]

Asim and Mishra [36] conducted a numerical investigation of the flow in hydraulic pipelines transporting spherical capsules at different capsule densities, capsule concentrations and capsule sizes in order to determine the behaviour of the flow in such systems under steady state conditions. The study used CFD to simulate the flow conditions. A depth analysis of the pressure drop has been given in pipelines. Semi-empirical correlations were established for the friction factor of the capsules. Figure 2.9 shows the validity of one of these relationships for the capsule friction factor. Nevertheless, the flow of a combination of basic capsule shapes has not been studied.

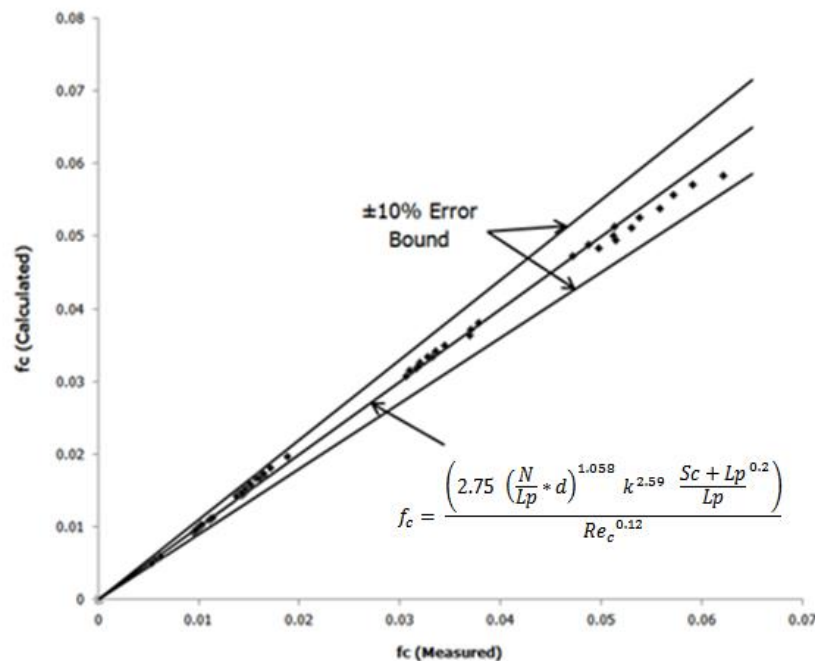


Figure 2.9 The friction factor for equi-density spherical capsules [36]

Asim et. al [37] conducted a numerical investigation of the rectangular capsules flow in hydraulic pipelines with different design considerations. The pressure and velocity distribution inside the pipeline were investigated. Semi-empirical correlations were developed for the pressure drop across the pipeline, however, only rectangular shaped capsules were considered for the analysis. Furthermore no expression for the capsule velocity was developed.

2.2.1 Summary

It can be summed up that the published literature is significantly limited in terms of the capsule flow behaviour within HCPs, and severely lacks local flow field analysis, such as the pressure drop and velocity variations within HCPs. Moreover, most of these studies lack in investigating the flow of a combination of different capsule shapes. In order to efficiently design hydraulic capsule pipelines, this information is critical as most of the industries use a combination of basic capsule shapes for transportation purposes. Thereby, a detailed investigation is needed to better understand the complex flow phenomena within HCPs.

2.3 Optimisation of Capsule Pipeline Systems

Swamee [38] established an optimisation model to be leveraged in sediment transport pipelines based on the least-cost principle. This developed model assumes the value of the friction factor as the input to the model, strictly reducing its use in the case of commercial applications. Swamee [34] also used the least cost principle to optimise the hydraulic pipeline for transporting cylindrical capsules (figure 2.10). The solid throughput considers the input to the needed model of the pipeline systems. However, the friction factor which was considered not to represent the flow of the capsule in the pipeline, thus limiting the practical nature of the model. The form depends on the iterative process. This model has strict limitations in terms of assuming a friction factor and thus can't be adopted in transporting capsules within pipelines.

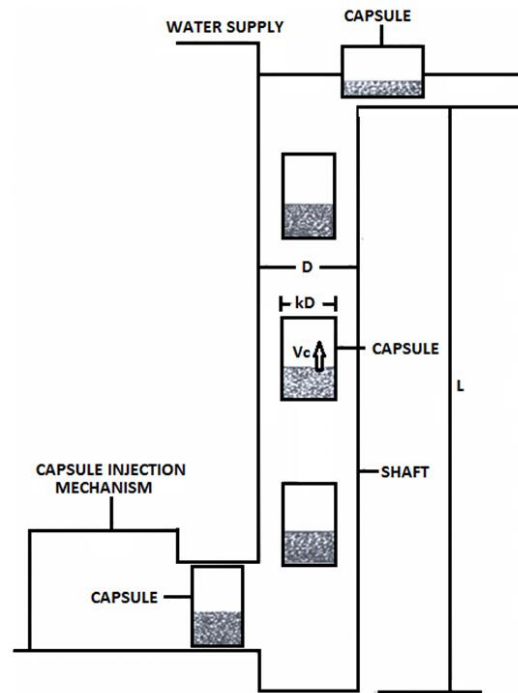


Figure 2.10 Hoist description [34]

The study conducted by Polderman [39] expounded on the design models in the case of offshore and onshore applications. The design models presented are based on some variables such as Reynolds Number and the pipeline's pressure drop etc. In this regards, the study showed the parameters that could be used to create and optimisation model. On the other, optimal models have not been developed, which can be to transport capsules across a pipeline.

Assadollahbaik and Liu [40] have established an optimisation model for hydraulic pipelines that transporting capsules based on the extreme efficiency of pumping. The design costs involved of such pipelines are, however, not included in this model.

Agarwal and Mishra [41] have developed a model for the optimisation of a multi-stage pipeline that transport capsules using the solid throughput as an input to the model, which is depend upon the least-cost conception. However, this model only applies to contact with spherical capsules that occupy the entire length of the pipeline. This optimal model is a simplified model for pressure variation prediction and limited parameters can be used to analyse pipelines that transport capsules. The friction coefficient utilised in the model is the

Colebrook - White's formulation for hydraulic pipelines [42], Significantly restricting the model benefit in respect of precise representation of the pressure reduction in the pipe conveying capsules. Sha and Zhao [43] has also established an another model for a hydraulic pipeline based on power saving. Nevertheless, the model cannot be applied for multi-stage flow.

Asim et. al [44] have conducted a study using a robust approach to predict the optimal size of a hydraulic capsule pipeline based on the findings from the numerical analysis. The pressure drops were predicted for the flow of a spherical capsules train. The pressure drops were used to quantify the pumping requirements in order to use them for the designing of such systems. The study revealed that at lower pipeline diameters, the total initial cost was high that decreases with the increase in the pipeline diameter. At a particular pipe diameter, i.e. the optimal diameter, the overall cost was a minimum, which was the least cost of the system.

A methodology has been developed by Asim et. al [45] to determine the optimal pipeline size for transporting multi-sized solid-liquid mixtures for the life-cycle time of the pipeline. The model adopted in this methodology can predict the life-cycle cost for the flow of multi-sized particulate mixtures of the solid-liquid in a pipeline (figure 2.11). The model provides a closed form solution to expect the optimal diameter of pipe corresponding to the least total cost for given solid characteristics. These solutions are acquired for different life-cycle costs, one of which is associated to minimum annual total cost. The parametric study reveals the interrelationship among different flow parameters including the optimal diameter of pipe and the corresponding minimum overall cost.

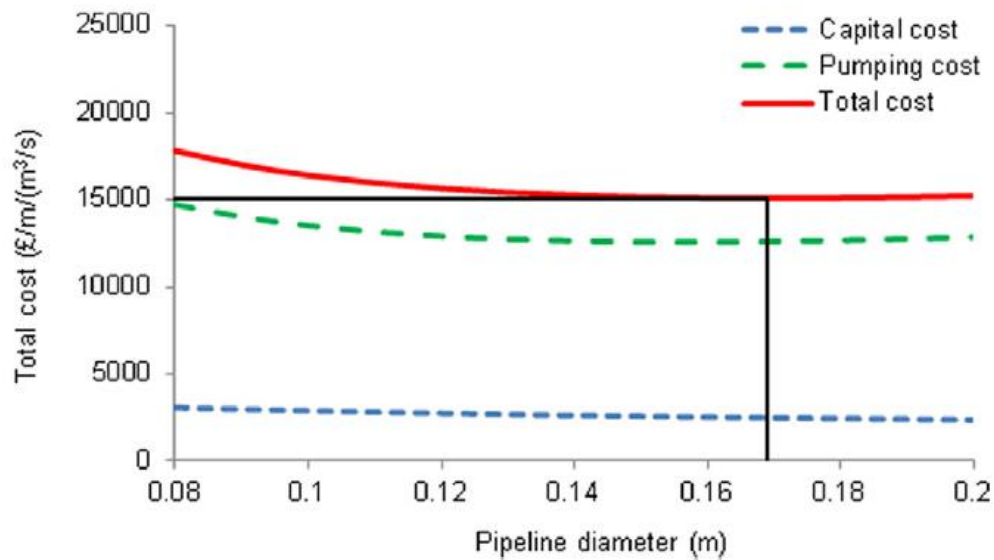


Figure 2.11 Variation of costs in pipelines transporting zinc tailings [45]

Asim and Mishra [46] have developed an optimisation model for transporting equal density cylindrical capsules across a hydraulic pipeline. This model depends on least cost standard, where the total cost was presented as a two-termed equation. Inputs to the model are the throughput of solid demanded of the process. The friction coefficients are considered in the model but the optimisation model addresses cylindrical capsules only. Moreover, the shape factor of the capsule is not taken into consideration.

2.3.1 Summary

In summary, the optimisation techniques discussed in the review of literature studied in this chapter have mainly consisted of estimated prediction models. In other cases, the models presented are ones used in analysing the flow of water in pipelines. According to the review of literature mentioned earlier, in order to optimise pipelines carrying capsule, precise expectation models can be summed up to some extent for the calculations of the pressure drop are required for the sake to optimise and design these types of pipelines. The outcomes of the pressure drop computations obtained from the capsules transport can be utilised to establish some correlations represented in prediction models for the capsules transportation in vertical pipes.

2.4 Research Scope

Most of the research studies previously conducted are centered on experimental tests, in which it is particularly problematic to identify and interpret the flow variables whilst capsules are flowing through the pipelines. The development of contemporary computational software and capacity of advanced software to model and simulate fluid flow in pipelines has made it possible to study and analysis the complicated flow structure and trajectory of the capsule that is located inside pipelines transporting capsules.

Through the reviewed studies, it can be noted that the transport of capsules in pipelines is dependent on a range of different parameters. The flow analysis of different forms of capsules is one of the key research area for this study, where each basic capsule shape is investigated, both separately and in combination with other basic shapes, under various flow and geometric parameters in a vertical pipeline. The capsule shape effect on the capsule motion, especially in a vertical pipeline, needs to be analysed in considerable detail, for off-shore applications. The diagnostics study of the capsule motion in vertical hydraulic pipes under transient conditions is based on advanced CFD based techniques, for analysing the capsule flow behaviour.

The second main area in this research is the flow analysis of a combination of basic capsule shapes in a vertical pipeline. The effect of mixed shapes of capsules on the capsules motion in vertical HCPs requires to be analysed in detail.

The third main area that has been considered throughout this research is the optimisation of the vertical capsules pipelines. The optimisation is as fundamental as it is to the vitality of these commercial pipelines.

2.5 Research Objectives

The research objectives of this study are based on the aims of research formulated in the earlier chapter. In order to achieve those aims, and after carrying out an exhaustive literature review, the following objectives have been defined:

1. Analyse the effect of the spherical capsule on flow characteristics of HCPs. This will include the effect of average flow velocity, capsule size, capsule density and capsule concentration on the flow characteristics.
2. Investigate the effect of the cylindrical capsule on flow characteristics of HCPs. This will include the effect of average flow velocity, capsule size, capsule length, capsule density and capsule concentration on the flow characteristics.
3. Evaluate the effect of the rectangular capsule on flow characteristics of HCPs. This will include the effect of average flow velocity, capsule size, capsule length, capsule density and capsule concentration on the flow characteristics.
4. Develop of a novel mathematical formulation to determine the shape factor for any capsule shape.
5. Develop of prediction models for the capsule velocity and friction coefficient in vertical hydraulic capsule pipes.
6. Investigate the impact of the simple combination of capsules of basic shapes on the flow characteristics under transient conditions.
7. Investigate the effect of the complex combination of capsules of various shapes on the flow characteristics under transient conditions.
8. Estimate the order effect of mixed shapes of capsules on flow characteristics under transient conditions.
9. Develop an optimisation model for vertical pipelines that transporting capsules based on the Least-Cost Principles.

For sake to achieve all the above-mentioned objectives, Computational Fluid Dynamics has been used in this study to simulate the capsules motion inside vertical pipelines.

The underlying numerical techniques being incorporated in this work will be debated in the following chapter.

Chapter 3 - CFD Modelling of HCPs

Computational Fluid Dynamics (CFD) offers a cost-effective solution to many fluid flow problems. In order to achieve the research objectives, sophisticated modelling techniques were utilised to simulate the capsules flow in hydraulic pipelines. Application of these techniques has been provided in this chapter, combined with a novel methodology for the anticipation of capsule velocity, trajectory, orientation as well as position. Hence, the model developed in this study has the advantage of not requiring any inputs in respect of the velocity of the capsule or direction as compared to other numerical studies. The solver settings and the boundary conditions are also debated through this chapter. The Dynamic Mesh technique employed for simulation of the capsule motion is the highlight of this chapter.

3.1 Overview of CFD Modelling

Computational Fluid Dynamics (CFD) is an application of fluid mechanics that uses computational methods and algorithms to find solutions for engineering problems. The application of CFD started in 1960's when the aerospace industry integrated CFD techniques into the design and manufacturing of aircraft and jet engines. Due to the advancements in computer software and hardware in recent years, the computational fluid dynamics based techniques have become a powerful and effective tool to understand the complex hydrodynamics of solid-liquid flows. In this study, CFD has been used to understand the flow characteristics in vertical hydraulic capsule pipelines. The application of CFD in analysing various aspects regarding fluid behaviour is wide. Furthermore, the preference of CFD simulations over experimentation is the capability to predict design verifications or modifications without the expense of requiring physical modifications, hence saving time and cost. In addition, due to the high level of detail generated by the results, the technology has been widely implemented to various engineering applications.

The fundamental governing equations of the fluid flow in a continuum are the basis of CFD applications. It can be found these equations in all CFD books and therefore were not compromised into the primary content of the research. Nevertheless, for reader's interest, more information can be found in Appendix A-1. For interested readers, some textbooks are suggested here for CFD [47-50].

3.2 Basic Principles of CFD Methodology

The CFD codes contain three main steps for numerical analysis [51]:

- Pre – Processing
- Solver Settings
- Post – Processing

Pre- processing: this step involves the definition of the geometry of the computational domain. It also includes the mesh generation, which is the sub division of the domain into several small discrete elements. The process of dividing the domain is called meshing.

Solver Settings: this is where the equations governing the fluid flow are solved by discretization and a series of iterations. This step also involves the definition of fluid properties and the selection of flow models. The convergence is judged when a change in solution variables between two iterations is nearly negligible. In addition, the accuracy of the converged solution relies on the problem setup, grid resolution and accuracy of the physical model being used.

Post-processing: in this phase, the data obtained from the solver is being analysed. This consists of the analysis of the data acquired and the model being revised according to these findings. The major data extracting tools in post-processors are vector plots, 2D or 3D surface plots, contour plots, view manipulations, particle tracking, colour post – script output to display the patterns of pressure, velocity, kinetic energy and other flow properties. A main component of post-processing is being capable to visualising complicated flows[52, 53]. Latterly, these applications might also incorporate animation for dynamic outcome presentation, and as well as graphics, each code generates reliable alphanumeric output and possess data export tools allowing additional manipulation external to the codes. Figure 3.1 depicts the summary of implementing CFD modelling.

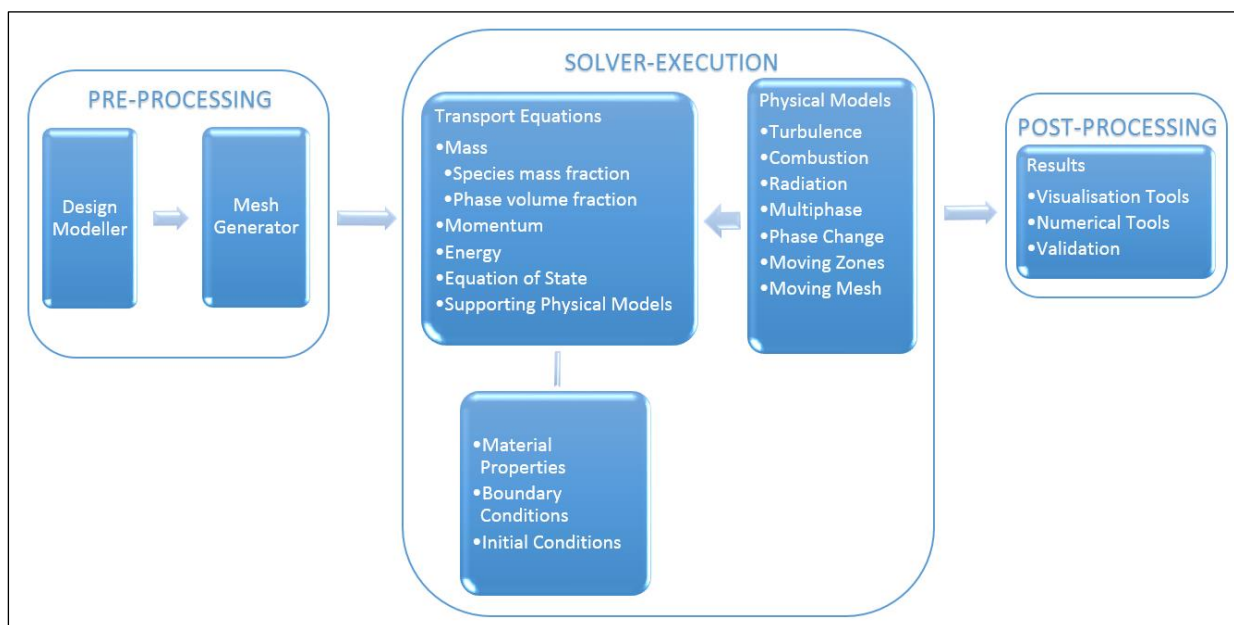


Figure 3.1 Summary of CFD Modelling

3.3 Pre- Processing of the HCP

The pre-processing can be divided into two main stages as creating the geometrical model and flow domain mesh [54, 55]. This part gives detailed information on the meshing of vertical HCPs and the geometric modelling.

3.3.1 Construction of Pipe Geometry

The three-dimensional geometry of the pipe has been numerically created, with pipe diameter of 0.1m and pipe length of 1.5 m. The first 1m of the pipe is considered as the Test Section and the later 0.5m represents the outlet, as shown in figure 3.2. According to Munson [56], the minimum length of the pipe required to obtain a fully developed flow is fifty times the pipe diameter. Therefore, an entrance pipe of length 5m was initially created and the velocity profiles at different cross-sections recorded. The fully-developed velocity profile was recorded, and a User Defined Function (UDF) was created to express this profile. The 5m long entrance section of the pipe was then removed, and the UDF for the velocity profile was specified at the inlet of the test section, mimicing the real-world conditions. The pipe is assumed to be hydro-dynamically smooth, This denotes that the constant of the absolute roughness (ϵ) of the pipe's wall is zero.

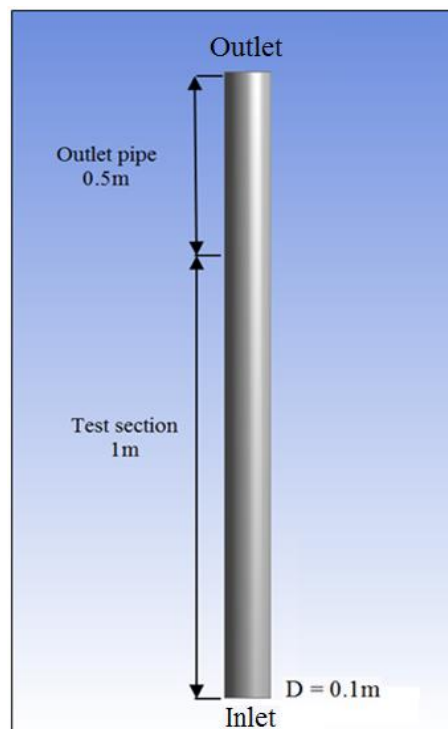


Figure 3.2 Schematic of the pipe geometry

3.3.2 Construction of Capsule Geometries

In this study, a range of capsule shapes and sizes have been considered for analysis within a vertical hydraulic pipeline. Figure 3.3 shows three basic capsule shapes within the test section i.e. spherical, cylindrical and rectangular, of diameter ratios of 0.5 and lengths of $1d$ for cylindrical and $1.5d$ for rectangular capsule, where d is the capsules diameter. The capsule is positioned near the entrance of the test section.

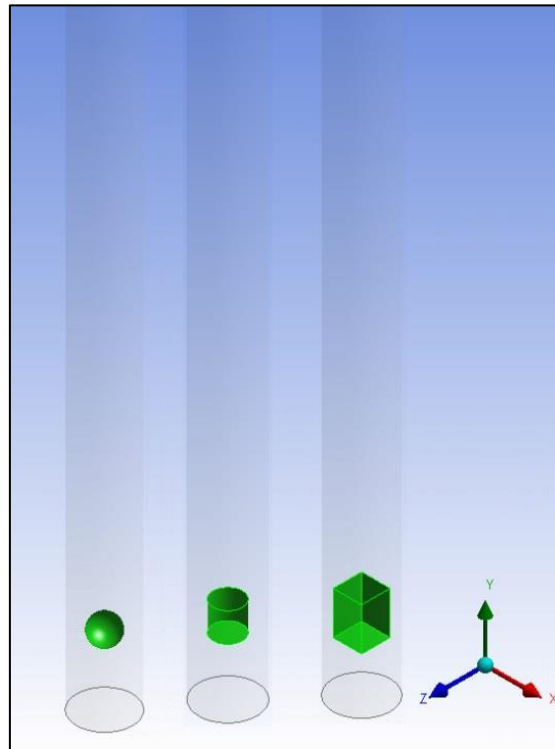


Figure 3.3 Schematic of the geometry of spherical, cylindrical and rectangular capsules

3.3.3 Meshing of the Flow Domain

The flow domain was created using unstructured mesh of tetrahedral elements. The primary reason for using of this type of meshing is the fact that capsules of different shapes are present within the pipe, which adds geometric complexities, which adds geometric complexities. The meshing within the flow domain is shown in figure 3.4.

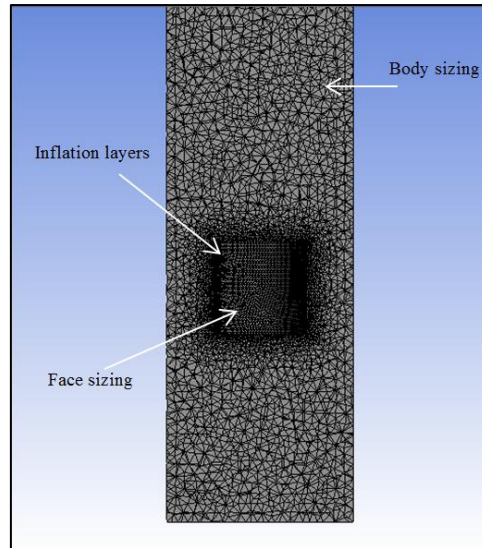


Figure 3.4 Meshing of the flow domain

Two different types of meshes have been selected to test the meshing independence. It has been found that the first type consists of one million elements, while another type has two million elements. The findings of the mesh independence will be debated in section 3.4.7.

3.3.4 Near Wall Treatment

Near-wall regions have large gradients in the solution variables and momentum transfer occur significantly [57]. Therefore, appropriate treatment of the wall boundary layer is necessary to provide a realistic solution of the capsule flow in pipes. The wall boundary layer is a viscosity-affected region, and is made up of three zones (with their corresponding wall y^+ values) [58]. These zones are the viscous sublayer ($y^+ < 5$), the buffer layer ($5 < y^+ < 12$) and the log-law region ($y^+ > 12$). The parameter y^+ represents the dimensionless distance of the wall-adjacent mesh node, from the wall. This ensures resolving the boundary layer around the capsule with reasonable accuracy. The y^+ values can be calculated as follows:

$$y^+ = \frac{\rho_w u_* y}{\mu_w} \quad (3-1)$$

where u_* the friction velocity in the near-wall region and y refers to the distance from the wall. The friction velocity can be calculated as follows:

$$u_* = \sqrt{\frac{\tau_{wall}}{\rho_w}} \quad (3-2)$$

where τ_{wall} is the shear stress acting on the capsule wall/s. The first cell height of 0.001406mm has been calculated based on the wall shear stress acting on the capsule wall/s, with taking in consideration the capsule geometry and the flow velocity. In total, five layers of concentrated mesh elements have been used to encompass the capsule wall/s.

3.4 Solver Settings

A time dependent solver was chosen in the current study to numerically simulate the transport of capsules in hydraulic pipes. The turbulent flow of water in the pipe has been considered, as expected in real-world scenarios, while a pressure-based solver has been specified as the flow velocities are in the range of $200k < Re > 400k$. Green-Gauss Node Based gradient discretisation method has been used to minimise diffusion, since it is more appropriate for unstructured tetrahedral cells. For momentum equations, a second-order upwinding scheme is desirable due to the unstructured nature of the mesh around the capsule. The other solver settings utilised in this research were described in the next subsections.

3.4.1 Turbulence Modelling

Many turbulence models can be used to predict the turbulence in the flows, where every one of these turbulence models has its own advantages. As for the transport of capsules in the pipeline, given the formation of a wake area downstream of the capsule, and the possible flow separation on capsule wall/s, realizable k- ϵ turbulence model has been used in the present study [59]. The main reason for selecting k- ϵ model is its superiority in precisely modelling the wake regions and extreme pressure drop, which are anticipated to occur between the pipe wall and the capsule.

The realizable $k-\epsilon$ model is more appropriate for use in flows with high strain rates than the standard $k-\epsilon$ model due to the inserted changes. The realizable $k-\epsilon$ model has shown better performance than the standard models in flows involving rotation, separation with strong reverse pressure gradients [60]. In this study, the enhanced wall treatment has been used to accurately resolve the boundary layer associated with the capsule wall/s. Enhanced wall treatment is appropriate for low Reynolds number flows, as in case of boundary layers, with complex near-wall phenomena [61]. However, it requires a fine near-wall mesh capable of resolving the viscous sublayer, which has been handled by adding inflation layers and face sizing around the capsule.

3.4.2 Material Properties

The fluid medium that has been used in the present study is liquid-water with a dynamic viscosity of 0.001003kg/m-sec and density of 998.2kg/m^3 . The capsules were utilised in the present study have a density similar to water, i.e. 998.2kg/m^3 , and another set with a density greater than water, having a density of 1700kg/m^3 . operating conditions being identified to the solver are the operating pressure of 101.325kPa (atmospheric pressure) and the gravitational acceleration of 9.81m/sec^2 is activated in such applications.

3.4.3 Boundary Conditions

The wall/s of the capsules undergoes rigid body motion and hence, have been specified as moving walls. The capsule interacts with the carrying fluid when the flow takes place. Practical inlet velocities of 2 and 4m/sec have been used in the current study. The pipe outlet has been treated as a pressure outlet and it has been preserved at atmospheric pressure. The internal pipe wall was considered to be hydro-dynamically smooth, which denotes that the constant of wall roughness is zero. Moreover, all the walls in the flow domain have been modelled as no-slip boundaries, meaning that the flow has the same velocity as that of the wall surface i.e. stationary in case of pipe wall. The intensity of turbulence is 5% at inflow boundaries for 0.1m diameter of the pipe. The boundary conditions are summarised in table 3-1.

Table 3-1 Boundary Conditions

Boundary Name	Boundary Type
Inlet to the Pipe	Velocity Inlet
Outlet of the Pipe	Pressure Outlet
Wall of the Pipe	Stationary Wall
Capsules	Moving walls

The capsule specifications have been identified by using UDF, where depending on on many factors such as capsule diameter, shape, density and length.

3.4.4 Introduction to Dynamic Meshing

The dynamic mesh capability in CFD is utilised in the current study to model the capsule motion. The model of dynamic mesh enables users to move the boundaries of a cell zone relative to other boundaries of the zone, and to adjust the mesh accordingly [62]. The motion of the boundaries can be rigid, such as pistons moving inside an engine cylinder or deforming, such as the elastic wall of a balloon during inflation or a capsule moving in a pipe filled with water. In either case, the nodes that define the cells in the domain must be updated as a function of time, and hence the dynamic mesh solutions are inherently unsteady.

The motion could be termed as prescribed motion or un-prescribed motion where the subsequent motion is determined based on the solution at the current time (e.g., the linear and angular velocities are calculated from the force balance on a solid body, as is done by the (6DOF) solver [62]. The volume mesh update is handled automatically at each time step based on the new positions of the boundaries.

To use the dynamic mesh model needs to provide a primary volume mesh and the description of the motion of any moving zones in the model. CFD allows describing the motion using either boundary profiles, user-defined functions (UDFs), or the Six Degrees of Freedom (6DOF) solver. The 6DOF solver uses the object's forces and moments in order to compute the translational and angular motion of the centre of gravity of an object. The governing equation for the translational motion of the centre of gravity is solved for in the inertial coordinate system.

3.4.5 User Defined Functions and Six Degrees of Freedom Properties

User Defined Functions (UDFs) are utilised to enhance certain advantages of CFD, such as custom boundary conditions. UDFs have been used in the existing study with the six-degrees of freedom (6DOF) solver. The 6DOF works by providing the desired properties via UDFs. These properties comprise mass, moments and products of inertia, external forces and moments, translational and rotational matrices, and the body constraints. UDFs are written in the C programming language, with the addition of a UDF header file for the macros. Three different UDFs have been used in this work, which contains the macros; `DEFINE_USER_INPUT`, `DEFINE_SDOF_PROPERTIES`, and `DEFINE_CONTACT`.

The `DEFINE_USER_INPUT` macro is used to specify the body properties of setting mass and moments of inertia properties for a moving object. This UDF is typical for applications in which a body is dropped, and the 6DOF solver computes the body's motion in the flow field. The `DEFINE_SDOF_PROPERTIES` macro is used to define different properties of a body for the 6DOF solver. These are typical body properties: mass, moment of inertia, product of inertias and external forces. This macro is best used for simulating how a body interacts with a flow field. The 6DOF solver uses the flow around the body, and the body properties, to move the dynamic zone to the next time step. Essentially the flow defines the motion that the dynamic zone will take [63].

The `DEFINE_CONTACT` macro is used to specify the response to a contact detection event in CFD. Contact detection is used to detect if the computed mesh motion will result in contact of a moving surface with other surrounding surfaces. If there is contact within specified tolerances, then the mesh motion of the moving zone can be constrained using nodal contact information within UDFs.

This UDF is typical for applications in which a capsule is conveyed in a flow stream and the 6DOF solver computes capsule motion depending on the momentum exchange between the capsule and the fluid. The capsule is to move freely in the flow field without any restrictions. The general procedure for compiling a UDF source file is first building a shared library for the resulting objects, and then loading the compiled UDF library.

3.4.6 Dynamic Mesh Setup

CFD contains three main options to update interior volume meshes when there is a dynamic boundary. These are smoothing methods, dynamic layering and re-meshing methods. Appropriate dynamic mesh modelling can help avoid negative cell volume errors. Dynamic layering adds or removes layers of cells next to a moving boundary based on the height of the cell layer adjacent to the boundary. This method is only usable with either wedge or hexahedral cells adjacent to the face [64]. In the present study, the mesh around the capsule is tetrahedral; therefore the dynamic layering methods are not applicable and are not used in this study.

Smoothing methods allow the mesh to stretch and contract. This is achieved via various models available, such as spring-based, diffusion-based and linearly elastic solid method. The spring-based smoothing treats the edges between the two nodes as springs. The movement of the boundary nodes creates a force that, using Hook's Law, is used to calculate displacement of all the interior nodes in the deforming boundary. It is applicable to all deforming zones with dynamic boundaries and best used with tetrahedral cells. This method was deemed most applicable to the capsule motion application. The spring stiffness can be controlled by adjusting the value of the Spring Constant Factor from 0 to 1 in the Dynamic Mesh settings where a value of 0 indicates no damping with smoothing progress. The boundary node displacements have a dominant influence on the motion of the interior nodes. The value of 1 represents the default level of damping on the interior node, which can be used for many applications [65]. In this study, a Spring Constant Factor of 0.5 has been considered to allow better chances for re-meshing.

Re-meshing methods are used when the dynamic zone displacement is large compared to the cell size at the boundary. In these cases, when the mesh moves, the cell quality around the boundary can deteriorate, creating negative cell volumes. To avoid this, CFD identifies problematic cells that violate a desired level of skewness or size criteria, and locally re-meshes the problematic cells by interpolating the solution in the new cells from the old cells. If the new cells also fail the skewness or size criteria, they are discarded instead of integrating into the mesh [66].

There are five main methods for re-meshing i.e. local cell, local face, face region, Cut Cell zone, and 2.5D. Like the smoothing techniques, some of these are applicable only to certain cell shapes and can be discarded based on how the mesh was created. Local cell and local face re-meshing are the two techniques used for the capsule motion in the present study. CFD uses the dynamic mesh settings in conjunction with each other to optimise the mesh at every time step. CFD decides, based on the enabled models, which mesh is the most appropriate one for the required deforming zone, and then applies the smoothing techniques. Finally, CFD uses the re-meshing as necessary. The motion of the moving object is accommodated within the computational domain by stretching and squeezing the mesh. Figure 3.5 shows the resulting deformation in the mesh region due to the capsule motion based on the dynamic mesh setup used. As could be seen from the figure, the capsule moves upward in the y-direction to make the mesh to stretch and contract within the flow domain. Hence, the mesh deformation zones are adapted for re-generating the mesh around the field of capsule motion to keep the solution continuing while the motion is taking place. Appendix A-4 provides a complete list of capsule velocities for the present study.

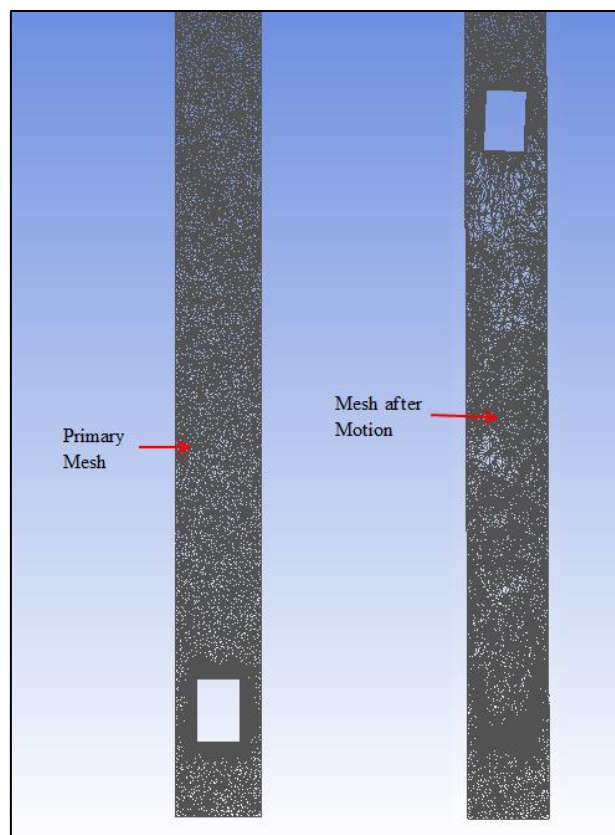


Figure 3.5 Dynamic mesh for the cylindrical capsule motion

3.4.7 Mesh Independency Test

A mesh independency test is important to confirm that the changes in mesh will not affect the numerical solutions significantly. In order to establish the mesh requirements for the simulations, two various meshes, have been used to ensure the numerical results quality. The flow field variables have been used for comparison purposes; pressure drop across the HCP and the capsule velocity, in this case.

The results obtained, as shown in table 3.2 and figure 3.6, depict that the variation is less than 0.1% in the pressure drop between one million mesh elements and two million under study. Whereas, table 3.3 and figure 3.7 depict that the variation in the capsule velocity is less than 4% between the two meshes under consideration. Thereby, one can be deduced that the 1M grids are able to accurately predict the complicated flow characteristics within HCPs and has therefore been selected for more analysis.

Table 3-2 Mesh Independence based on Pressure Drop inside the HCP

Number of mesh elements (Millions)	Average pressure drop per unit length (Pa/m)	Difference ratio (%)
1	10932	
2	10939	0.06

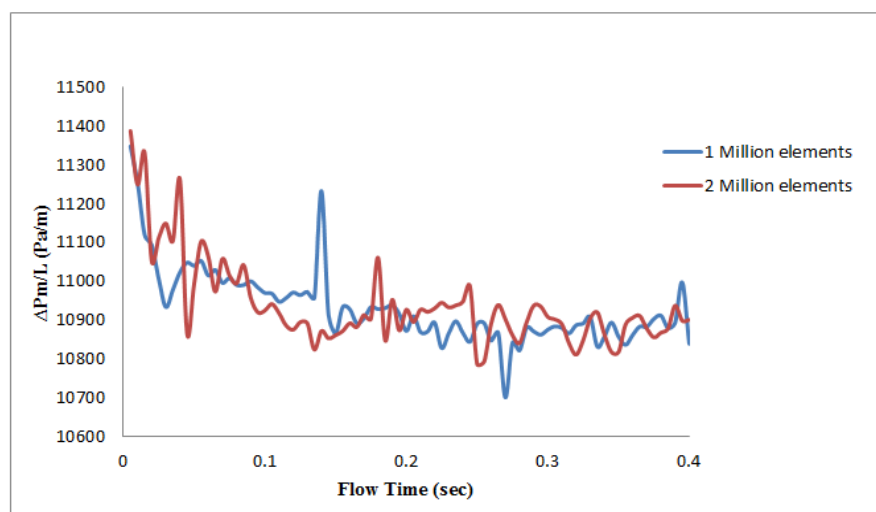


Figure 3.6 Time histories of the pressure drop

It can be observed that the pressure drop values markedly fluctuate due to the capsule motion within the pipeline.

Table 3-3 Mesh Independence based on Capsule Velocity in HCP

Number of mesh elements (Millions)	Capsule velocity (m/sec)	Difference ratio (%)
1	1.513	
2	1.457	3.82

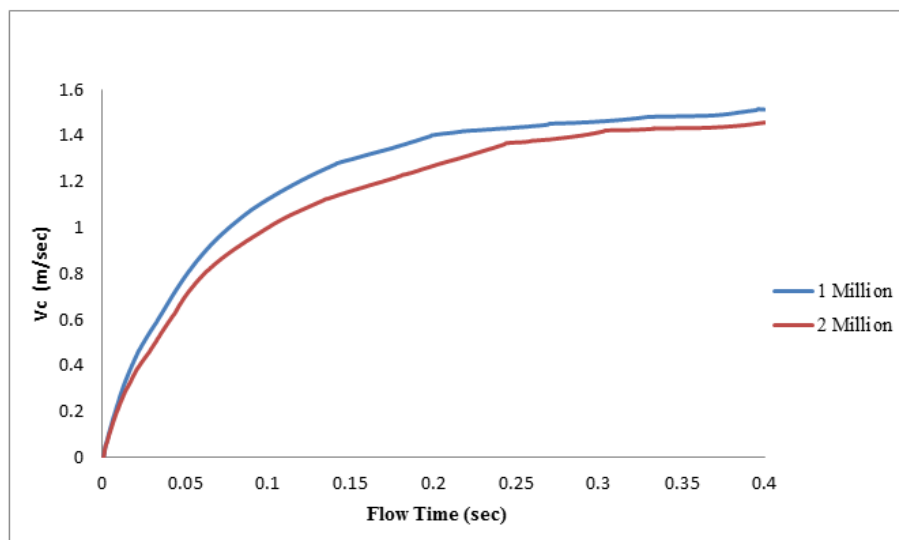


Figure 3.7 Time histories of the capsule velocity

3.4.8 Time Step Size and Solution Initialisation

The time step size used for the calculations has major implications on the solution. The determination of an appropriate time step size is based on the needs of the calculations. There are two competing goals for this decision: re-meshing and computation time. From a standpoint of re-meshing, it is desirable to have a smaller time step to make the re-meshing calculations simpler and to avoid negative cell volumes (i.e. when a cell flips directions and points the wrong way, giving the cell a negative volume). However, from a standpoint of computation time, a larger time step is desirable. Larger steps lead to fewer calculations,

which means significant decrease in simulation time. Various time step sizes have been tested, and finally, the time step size of 0.0005sec is found to be sufficient enough for the time dependent solution. The estimation was made depending on the minimum mesh size and the average flow velocity. The computations begin from an initial flow field obtained from a well converged steady state computation, where the capsule is placed near the test section entrance. The time-independent solution has been achieved by monitoring the time history of the capsule motion and the pressure drop across the test section. The appropriateness of the time-step is established if the continuity residual drops about two orders of magnitude from the beginning of the simulation. To obtain a meaningful solution for time averaging a periodical behaviour of the flow field has to show.

3.5 Scope of Numerical Investigations

There are a large number of geometric and flow related variables associated with the flow of various capsules shapes in pipelines, a Taguchi Method for Design of Experiments (DoE) has been adopted in the current study to identify the possible practical combinations of these parameters. Taguchi's method makes use of orthogonal arrays to estimate the minimum number of numerical simulations to be performed that gives the same amount of information (response) as a full factorial design. Taguchi contended that traditional sampling is insufficient here as there is no method of obtaining a random sample of future conditions. A statistical software (Minitab 17) has been used for this purpose, where a practical range of various parameters has been determined. The factors considered for the flow of different capsules in vertical HCPs, alongside their levels, have been summed up in table 3-4.

Table 3-4 Factors and levels of Taguchi's method for an HCP

Factor	Level 1	Level 2	Level 3
N	1	2	N/A
Lc	1d	1.5d	N/A
k	0.4	0.5	0.6
Vav	2	4	N/A
\emptyset	Sphere	Cylinder	Rectangle
s	1	1.7	N/A

After numerically simulating the capsules flow inside vertical hydraulic pipelines, different performance parameters have been recorded for further analysis. Detailed debates on these findings are given in the following chapters, where the following chapter focuses on the basic capsule shapes, flowing separately in vertical pipes.

Chapter 4 - Flow Diagnostics in HCPs Transporting Basic Capsule Shapes

The results obtained from the numerical models that are debated in the earlier chapter, concerning the transportation of basic capsules shapes across pipelines, provided in this chapter. Detailed quantitative and qualitative unsteady analyses have been performed to understand the complex flow behaviour for capsule motion. The impact of different geometrical parameters and flow conditions on the transport of basic capsule shapes in a vertical pipe was studied. Moreover, semi empirical correlations for capsule velocity and pressure drop have been developed.

4.1 Validation of CFD Predictions

It is essential to validate the numerical model to predict flow fields of capsules within the vertical pipeline before the data analysis. This to ensure that the findings of the numerical model obtained through the computational investigations are compatible with experiments results to allow this predictive model to be such as the physical model used in the practical applications.

The predictive model based on the numerical simulations have been compared with the experiments results for the capsule velocity in the vertical pipe presented by Latto [30]. The accuracy of the experimental data was estimated for some major parameters, based on measurement accuracy and reproducibility, were $V_{av} \pm 4.5\%$ and $V_c \pm 3\%$. The numerical model for the used conditions in table 4-1 has been determined.

Table 4-1 Validation Tests

Name / Property	Value / Range / Comment	Units
s	1	N/A
k	0.5	N/A
Lc	0.05	m
Vav	1 – 4	m/sec
Capsule Shape	Cylindrical	N/A

Figure 4.1 indicates the variations in the capsule velocity with the flow velocity across the pipe, through different average flow velocities for Computational Fluid dynamics (CFD) and practical tests. It is found that a good agreement between the CFD results in comparison with the experimental findings, the maximum difference between them is 5%. It is therefore possible to conclude that the numerical model of a pipeline transporting capsules that considered in this investigation simulates the physical model.

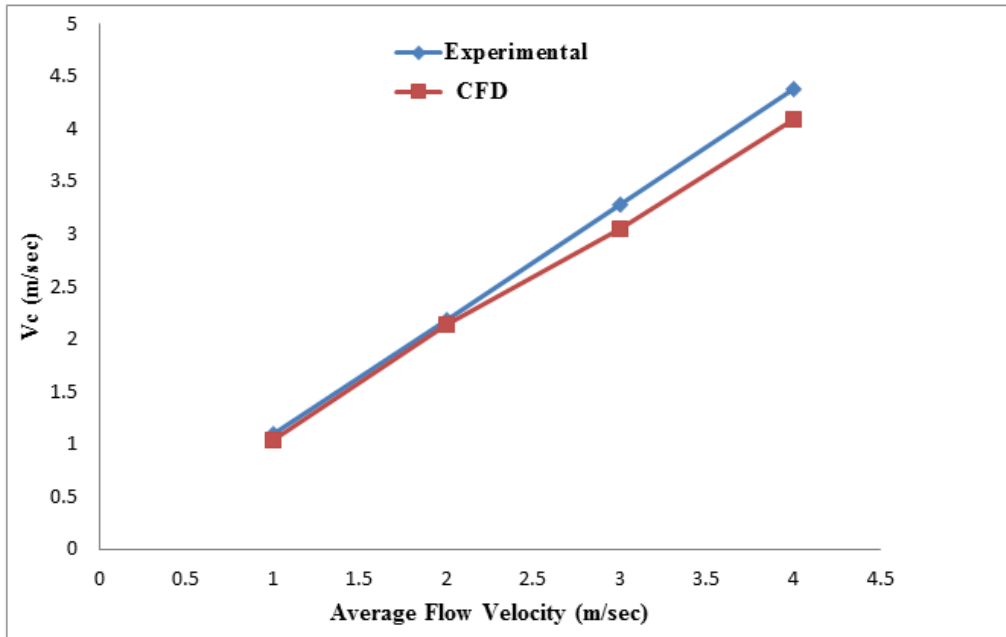


Figure 4.1 Validation of the CFD results with the experimental results for the capsule velocity in a vertical pipe that transporting an equi-density cylindrical capsule

4.2 Single Phase Flow Analysis in a Vertical Pipeline

The structure of single-phase flow needs to be examined in depth before going to study the capsules flow across vertical pipelines. The distribution of static gauge pressure within the pipe is depicted in figure 4.2, at a flow velocity of 2m/sec. It is observed that the static gauge pressure of water has reduced from 15294Pa to 4581Pa along the test section, which corresponds to 70% decrease in the static gauge pressure. Where corresponds to a 70% drop in static gauge pressure. The Darcy friction coefficient (f) has been estimated to be 0.0165, through Moody's chart for a hydrodynamically smooth pipe, at an average flow velocity of 2m/sec. This value of friction coefficient has been used in equation (1.3) to get the pressure drop across the test section (ΔP) to be 10140Pa. The pressure drop predicted by CFD is 10146Pa. Hence, the difference between the analytical and CFD predicted pressure drop values is 0.059%. Consequently, it can be concluded that CFD predicts the pressure reduction of a single-phase flow inside these pipes with acceptable precision.

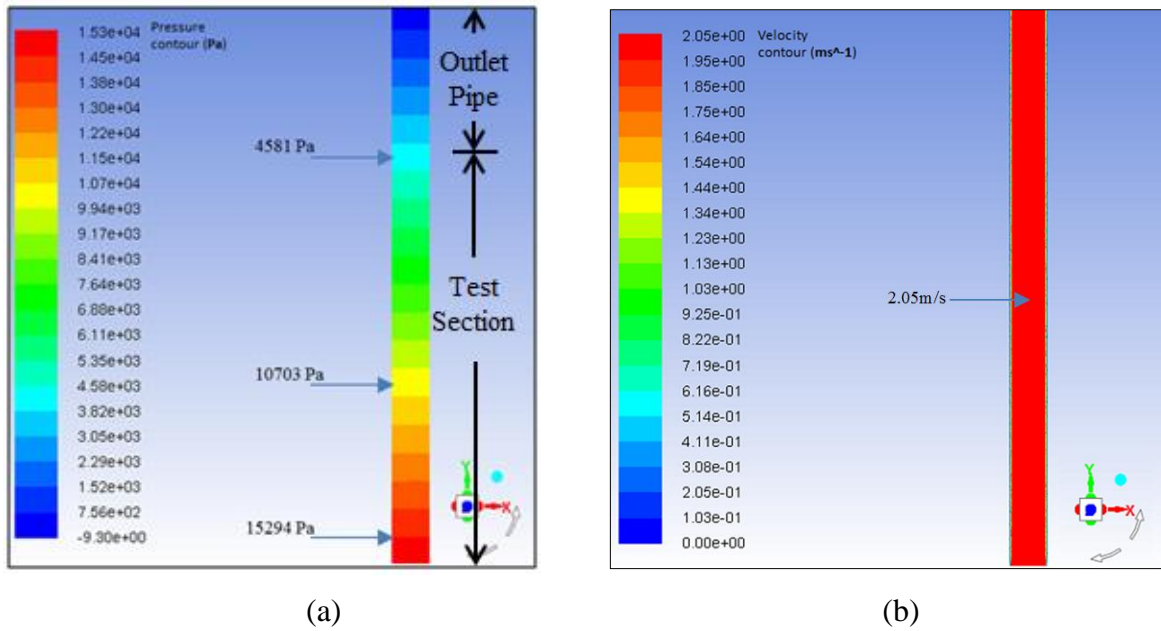


Figure 4.2 Distribution of (a) Static gauge pressure and (b) Flow velocity magnitude

Figure 4.2 (b) depicts the flow velocity magnitude distribution inside the pipeline. One can notice that the velocity of the flow at the pipe's walls is zero because of the no-slip boundary condition; in contrast, the value of the flow velocity is higher at the pipe's centre. The flow velocity at the pipe's centre, in a fully developed flow, exceeds the average flow velocity rate. Thereby, the flow velocity at the pipe's centre is 2.05m/sec compared to an average measure of the velocity is 2m/sec.

4.3 Flow Diagnostics in HCPs Transporting Spherical Capsules

As discussed earlier in Chapter 3, the dynamic mesh technique has been used to numerically simulate the motion of capsules in a hydro-dynamically smooth pipeline. The capsules have been considered to be rigid bodies. The capsules are allowed to move fully freely and interacting with the carrier fluid. Many studies have previously been conducted giving a detailed review of hydraulic capsule transport in general. However, most of these studies consider steady state flow. In the present study however, the author pursues the motion of capsules in a vertical hydraulic pipeline throughout the test section. It has been conducted on various shapes of capsules, and its position in the pipe is always changing. In most of the simulations, the first capsule is released from an initial position $(x_0, y_0, z_0) = (0, 0, 0)$ with the major vertical axis. After the release of the capsule, the centre of the capsule begins to move

upward. Then, there is a transient stage when the orientation of the capsule changes. Finally, the capsule attains an equilibrium position and flows steadily. In the case of multiple capsules, the spacing between the capsules is initially considered to be equal to two diameter of the capsule.

Figure 4.3 (a) presents the variations in the distribution of the static gauge pressure across the test section of the pipeline, which carries a spherical shape for an equi-density capsule of $k = 0.5$ and $V_{av} = 2\text{m/sec}$. It is clearly noticed that the capsule existence changes the pressure variations within a pipeline, in comparison with single-phase water flow. The pressure reduces in the pipeline from the inlet to the outlet continuously, as expected in real life. There are two major reasons for the pressure drop in the present case. The primary reason for the pressure drop through the pipe is the elevation effect of the pipe. It can be noticed from equation (1.3) that as the elevation (or Δh) increases, the pressure drop across the pipeline increases. The second reason for the pressure drop across the pipe is due to the friction forces acting on the flow. These frictional forces arise from the interaction between the flow and the different walls within the flow domain i.e. the pipe wall and the capsule. Although the dominant parameter for the pressure drop in the present case is the elevation of the pipe, it however, does not include the impact of the existence of the capsule/s in the pipe. The pressure gradient contribution from the capsule is represented in the frictional pressure gradient. One can observe in figure 4.3 (a) that the pressure upstream the capsule, at a flow time of 0.05sec, is 14920Pa, however, after 0.75sec, the pressure upstream the capsule decreases by 8828Pa. Hence, the difference in the pressure upstream the capsule is 69% for the two flow times considered. In order to evaluate the pressure drop contribution from the capsule alone, the friction factor for the capsule has been computed. In the present case, the average mixture and capsule pressure drops, and the average capsule friction factor (f_c) are 10720Pa, 556Pa and 0.02790 respectively.

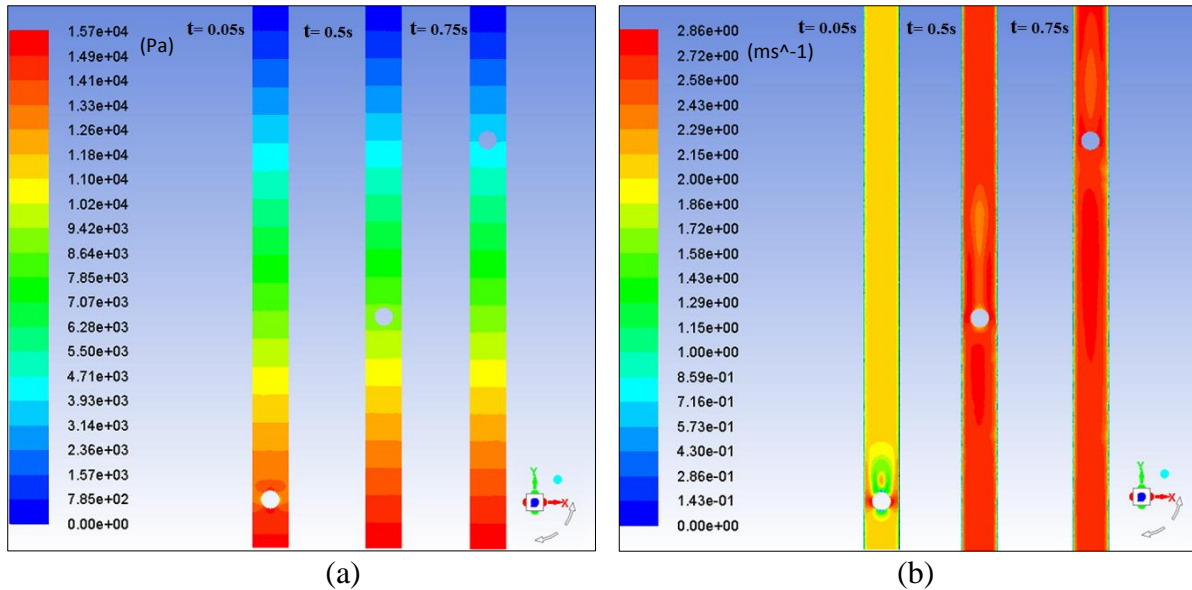


Figure 4.3 (a) Static gauge pressure and (b) Flow velocity magnitude variations for an equi-density spherical capsule of $k = 0.5$ and $V_{av} = 2\text{m/sec}$ at different flow times

The flow velocity in the test section varies according to the capsule position throughout its motion. Figure 4.3 (b) presents flow velocity magnitude distributions in the pipe for the flow of a single equi-density spherical capsule of $k = 0.5$ and $V_{av} = 2\text{m/sec}$. It is observed that the flow velocity magnitude distribution is significantly affected by the capsule existence in the pipe. There are two areas of interest associated with the capsule, in the context of flow velocity variations. The first being the annulus region (between the capsule and pipe wall) and the other being the wake region (downstream of the capsule). It is observed that the flow velocity magnitude is highest in the annulus area. The reason for this increase in the flow velocity magnitude is due to the restriction to the flow by the capsule. The cross sectional area available for the flow to take place decreases, increasing the velocity of the flow. As far as the wake area downstream the capsule is concerned, the flow velocity magnitude variations are highly non-uniform in this region. The reason for reduced flow velocity magnitude in the wake region is the flow separation and the resulting highly three dimensional flow field downstream the capsule..

Figure 4.4 depicts the time history of the variations in the mixture pressure drop ($\Delta P_m/L$) and the pressure drop due to the capsule alone ($\Delta P_c/L$) along the test section for the case under search. The findings exhibit that the mixture pressure drop is greater than the pressure drop caused by the capsule. In spite of the trend of pressure drop for both cases is the same

behaviour. Comparison with the pressure drop owing the flow of capsules only. The increase in pipeline's pressure drop as a result of the capsule existence is 5.3% in comparison with the pressure drop in the flow of single phase.

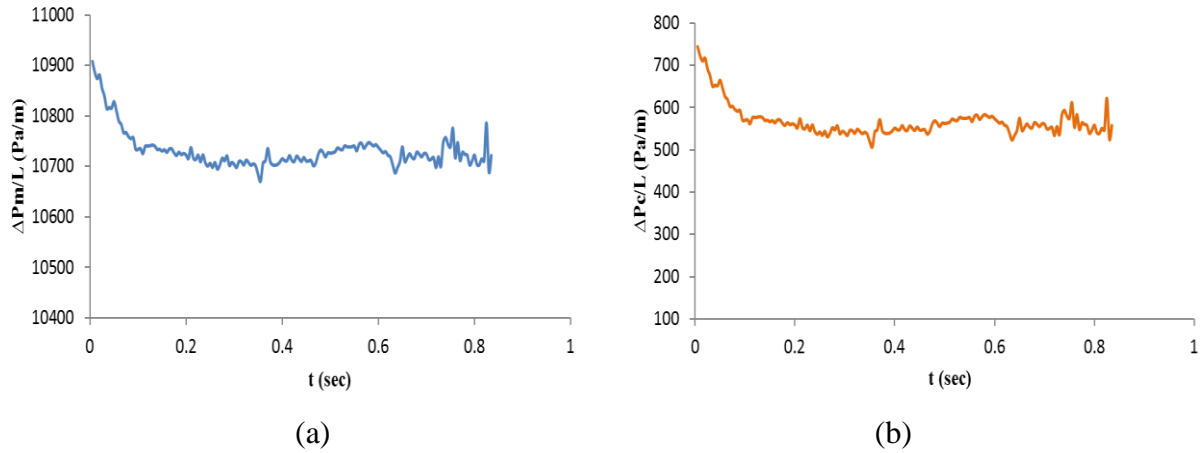


Figure 4.4 (a) Variations in the mixture pressure drop and (b) the capsule pressure drop, for a single equi-density spherical capsule of $k = 0.5$ at $V_{av} = 2\text{m/sec}$

Figure 4.5 shows the time history of the variations in the capsule velocity for the case under consideration. The results depict that the capsule velocity increases almost linearly up to 0.75sec. After that, the capsule reaches the steady flying state, having a capsule velocity of 2.15m/sec, which is 7.2% higher than the average flow velocity of 2m/sec. The reason for higher capsule velocity, as compared to the average flow velocity, is the fact that the capsule diameter is less than the pipe diameter; thereby, the capsule propagates along the centre-line of the pipe (because the capsule is equi-density in this case). As it is an established fact that the centre-line flow velocity in a pipe is considered higher than the average flow velocity, the resulting capsule velocity is higher than the average flow velocity.

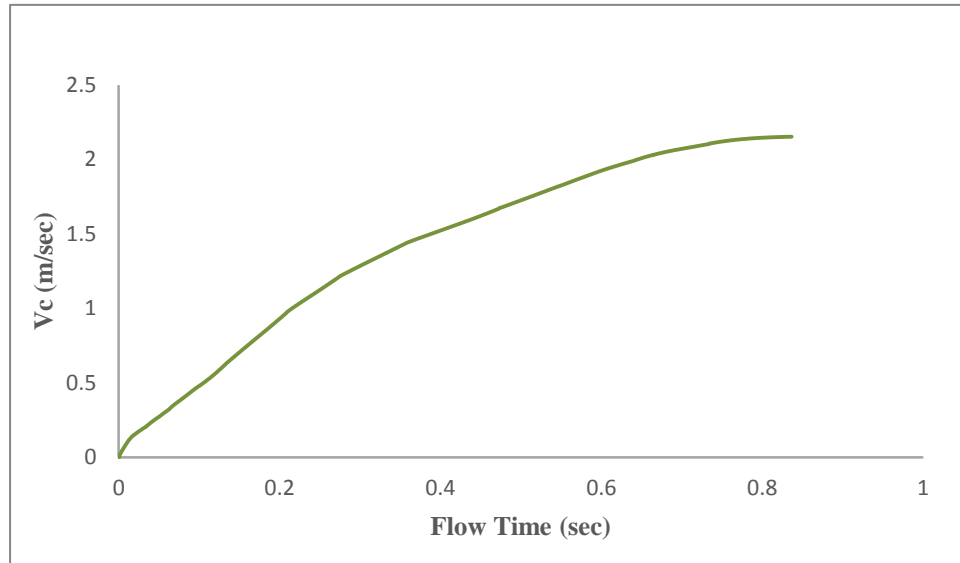


Figure 4.5 Time history of an equi-density spherical capsule velocity for $k = 0.5$ at $V_{av} = 2\text{m/sec}$

Figure 4.6 depicts the time history of the acceleration rate of an equi-density spherical capsule of $k = 0.5$ at the average flow velocity 2m/sec . It is observed that the capsule rapidly accelerates just after the loading, and then decelerates dramatically until reaches the steady velocity, due to the reduction in the driving forces of the capsule flow. The forces acting on the capsule are the pressure, shear and Coulomb forces [22]. These forces have obtained from the numerical model.

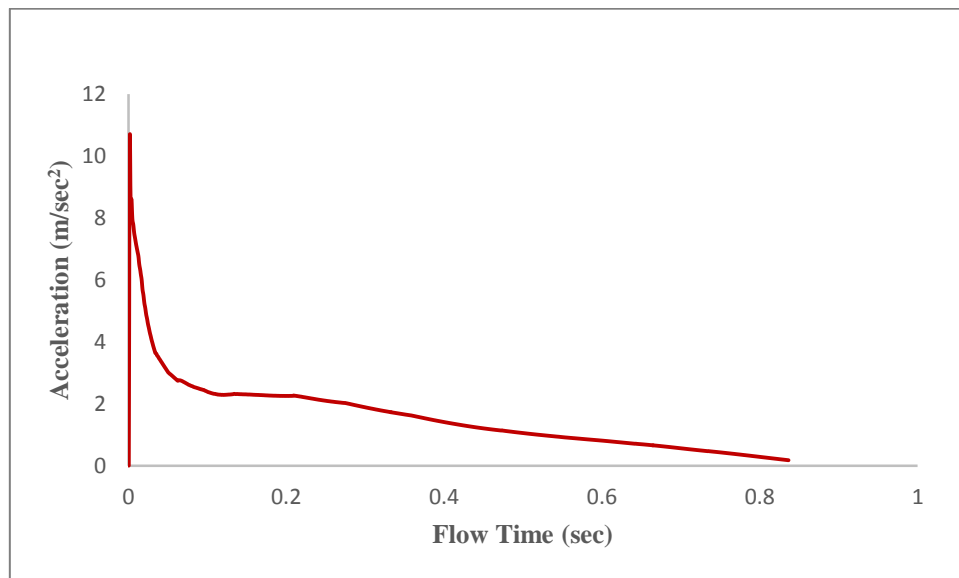


Figure 4.6 Time history of the acceleration of an equi-density spherical capsule for $k = 0.5$ at $V_{av} = 2\text{m/sec}$

4.3.1 Effect of Average Flow Velocity

In order to analyse the flow velocity effect of the carrier fluid on the flow structure, an average fluid velocity of 4m/sec has been considered for investigation. CFD predicted results have then been compared against the previous case i.e. $V_{av} = 2\text{m/sec}$, while the capsule's parameters remain the same in both cases. Figure 4.7 depicts the static gauge pressure and flow velocity magnitude distribution in a pipe transporting the capsule at an average flow velocity of 4m/sec at different flow times during the capsule motion. The pressure drop across the test section of the pipe is 11584Pa, which is 8% higher than the pressure drop at $V_{av} = 2\text{m/sec}$. Moreover, it is noted in figure 4.7 (b) that the velocity field resembles the one seen in the case of $V_{av} = 2\text{m/sec}$ such as a greater velocity in the annulus regions. This is owing to the reduction in the flow cross-sectional area, where the extreme velocity present in the annulus regions gives rise to shear forces acting on the capsule.

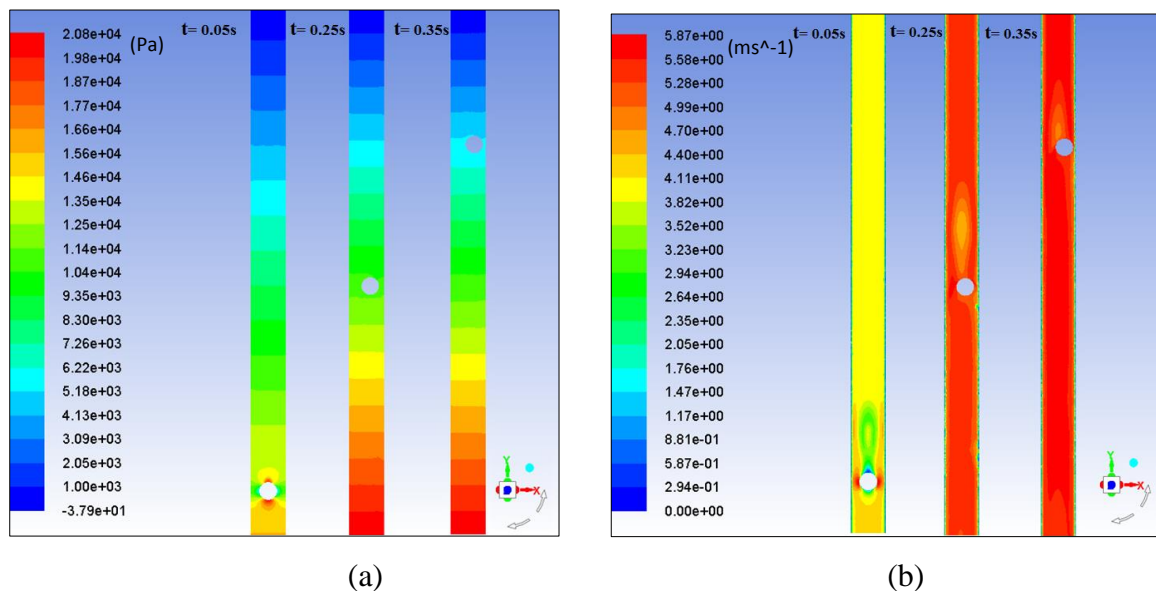


Figure 4.7 (a) Static gauge pressure and (b) Flow velocity magnitude variations for an equi-density spherical capsule of $k = 0.5$ and $V_{av} = 4\text{m/sec}$ at different flow times

the pressure drop variations throughout the test section of the pipe have been depicted in figure 4.8. From this figure is observed that the pressure drop markedly fluctuates during the spherical capsule motion in the pipe. The pressure drop as indicated in the results due to the capsule flow at an average flow velocity of 4m/sec is considerably higher than 2m/sec. The reason for the increase in the pressure drops is the decrease in head losses within the pipeline owing to the increase the flow velocity. More detailed results are provided in Appendix A-5.

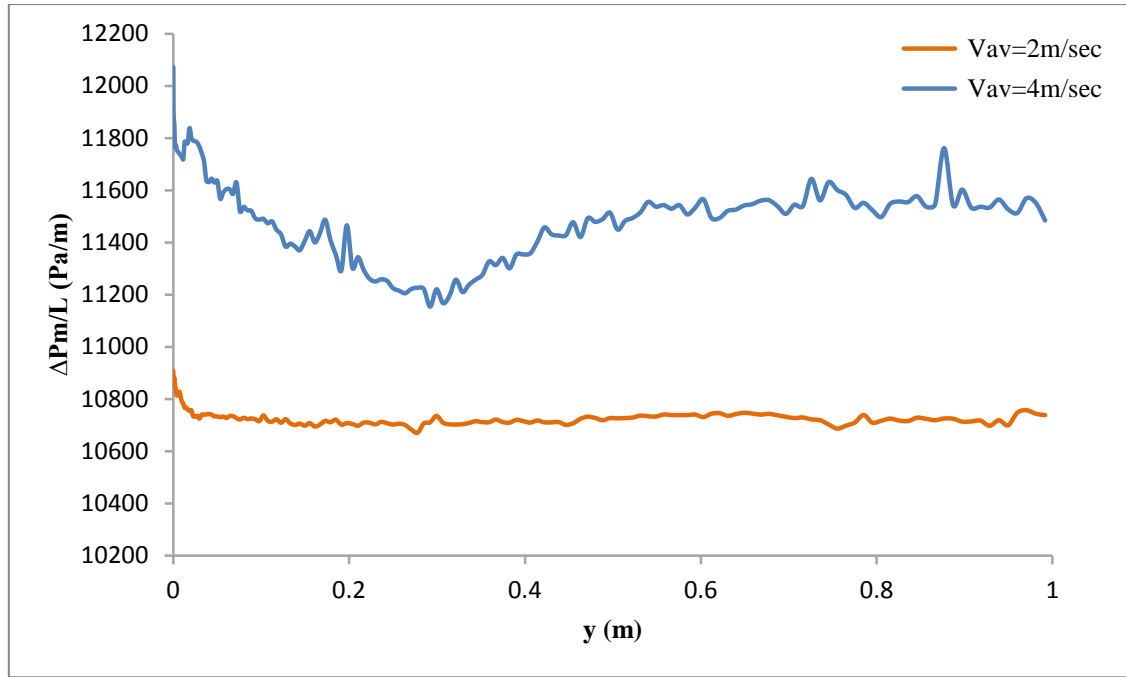


Figure 4.8 The effect of average flow velocity on the pressure drop variation for an equi-density spherical capsule of $k = 0.5$

Figure 4.9 shows time histories of the capsule velocities for an equi density spherical capsule of $k = 0.5$ at different flow velocities considered. The results depict that the capsule velocity increases gradually with the increase in the flow velocity. The capsule velocity in case of $V_{av} = 4\text{m/s}$ attains a stabilised velocity in a shorter time than in the case of $V_{av} = 2\text{m/sec}$.

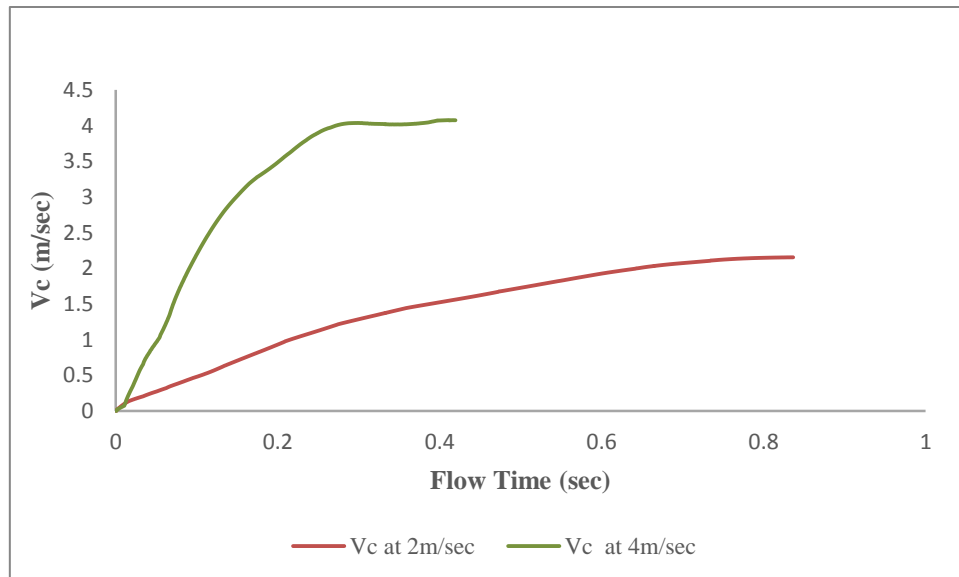


Figure 4.9 The effect of average flow velocity on the capsule velocity for an equi-density spherical capsule of $k = 0.5$

4.3.2 Effect of Capsule Density

Figure 4.10 indicates the differences in the distribution of pressure and velocity within the test section of the pipeline which carries a heavy density spherical capsule for $k = 0.5$ at $V_{av} = 2\text{ m/sec}$. The pressure at the upstream entrance is about 15450 Pa , which is 3.5% greater than the upstream pressure for an equi-density capsule at the same flow velocity as in figure 4.3 (a). The pressure distribution trends are the same as noticed for an equi-density capsules. Moreover, it is obviously observed in figure 4.10(b) the capsule velocity is slower than the equi-density capsule. The reason being the weight of the capsule becomes higher than the equi-density capsule. Hence, The time it takes to cross the test section of the pipe is 1.2 sec , as compared to an equi-density capsule that crosses the test section in 0.75 sec .

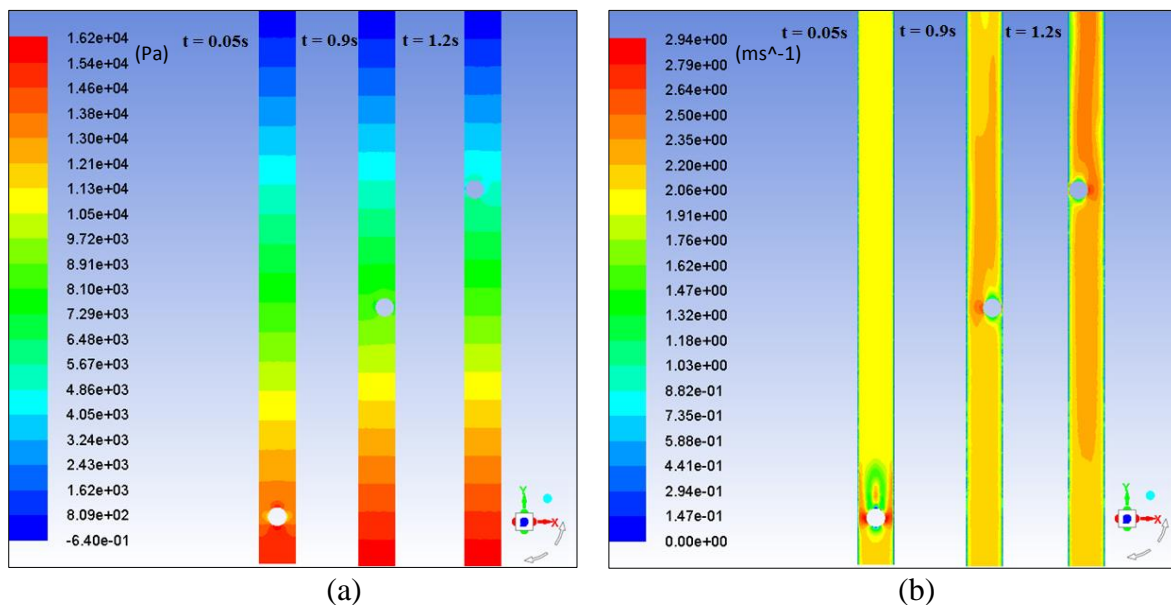


Figure 4.10 (a) Static gauge pressure and (b) Flow velocity magnitude variations for a heavy density spherical capsule of $k = 0.5$ and $V_{av} = 2\text{ m/sec}$ at different flow times

Figure 4.11 shows the variations in the pressure drop along the test section of the pipe. It can be observed that the pressure gradient markedly fluctuates during the capsule motion in the pipe. The results indicate that the pressure drop for a heavy density capsule ($s = 1.7$) is considerably higher than for an equi-density capsule ($s = 1$). However, the pressure drop distribution in the pipeline is similar for both the cases. The pressure drop increases due to increase in the force required to transport the capsule.

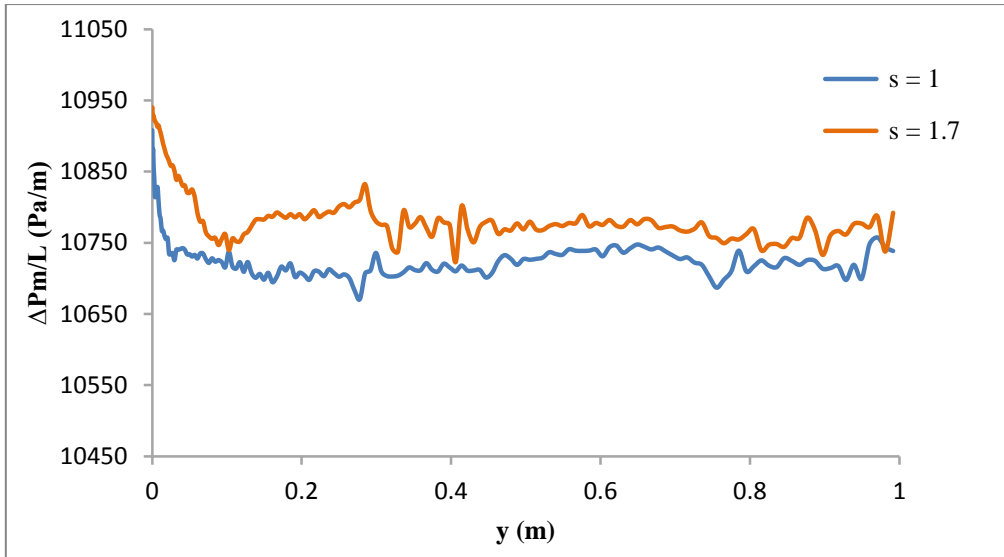


Figure 4.11 The effect of capsule density on the pressure drop variation for a spherical capsule of $k = 0.5$ at $V_{av} = 2\text{m/sec}$

Figure 4.12 depicts time histories of the capsule velocities for a spherical capsule at an average velocity of 2m/sec for two different capsule densities. It is noted that the capsule velocity for a heavy density capsule is less than for the equi-density capsule. The velocity of the equi-density capsule exceeds the average flow velocity when reaches a steady flying state, whereas the velocity of heavy density capsule is less than the average flow velocity. Due to the the increase the weight of the capsule.

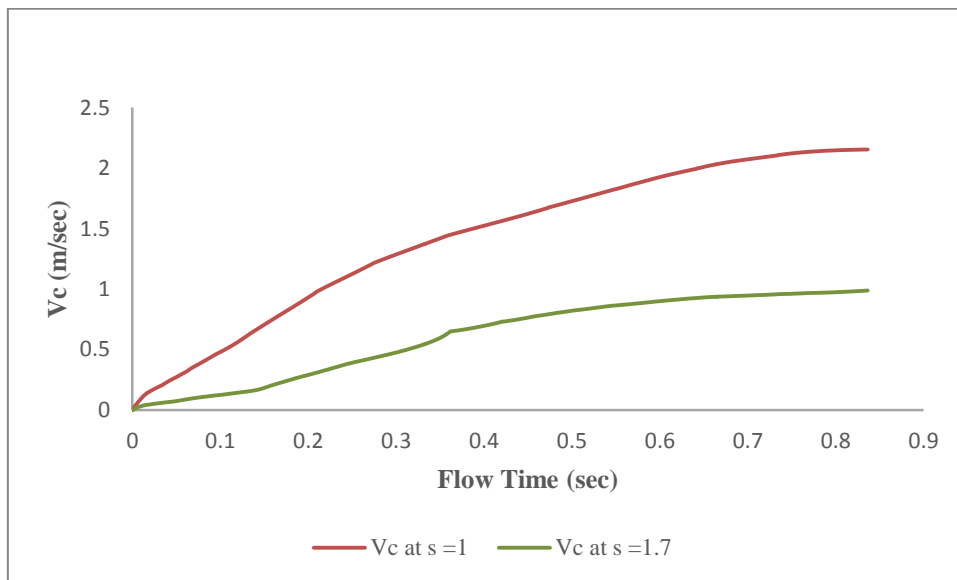


Figure 4.12 The effect of specific gravity ratio on capsule velocity history for a spherical capsule of $k = 0.5$ at $V_{av} = 2\text{m/sec}$

4.3.3 Effect of Capsule Diameter

Figure 4.13 depicts the distribution in a heavy density spherical capsule transporting pipe for both the static gauge pressure and flow velocity magnitude for $k = 0.6$ and $V_{av} = 2\text{m/sec}$. It can observe that in spite of the distribution of the total pressure appears to be similar to the field of pressure for $k = 0.5$ at the same average flow rate, the pressure at the upstream position of the capsule increased by 6%. Moreover, it can be noticed in figure 4.13 (b) at $t = 0.05\text{sec}$ that the flow velocity in the annulus region has increased to 3.34m/sec , owing to decrease in the flow cross-sectional region. While the flow velocity is low at a wake region downstream of the capsule in a pipeline.

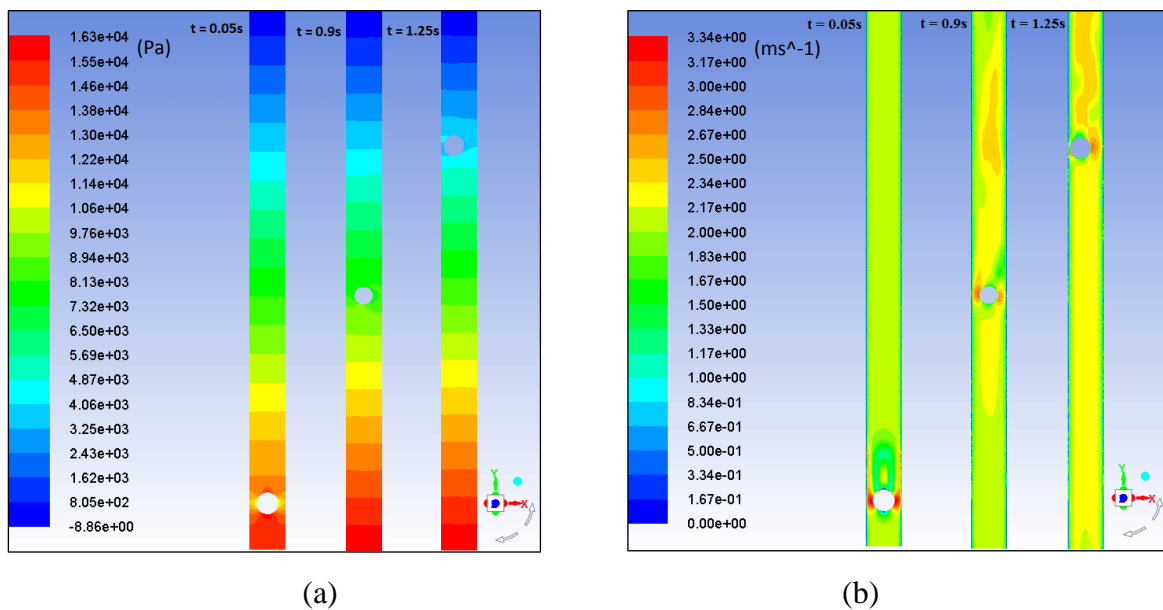


Figure 4.13 (a) Static gauge pressure and (b) Flow velocity magnitude variations for a heavy density spherical capsule of $k = 0.6$ and $V_{av} = 2\text{m/sec}$ at different flow times

Figure 4.14 illustrates the variations in the pressure drop along the pipe test section at an average flow velocity of 2m/sec . It can be observed that the pressure drop markedly fluctuates during the capsule motion in the pipe. The results indicate that the pressure drop recorded during a capsule motion of $k = 0.6$ is considerably higher than the pressure drop for $k = 0.5$.

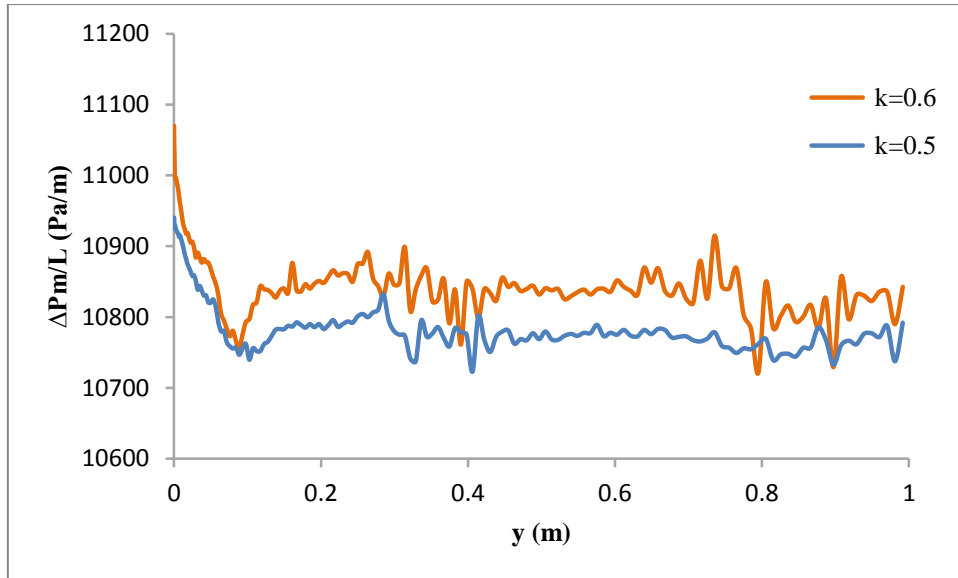


Figure 4.14 The effect of capsule diameter on the pressure drop variation for a heavy density spherical capsule at $V_{av} = 2\text{m/sec}$

Figure 4.15 indicates time histories of the capsule velocities for a heavy density spherical capsule at an average velocity of 2m/sec for different ratios of capsule diameter. It can be seen that the capsule velocity of $k = 0.5$ is slightly higher as compared to $k = 0.6$ during a particular time, and then the capsule velocity of $k = 0.6$ starts increasing till exceed the capsule velocity for $k = 0.5$. Hence, it can be observed that the capsule velocity increases as the capsule diameter increases.

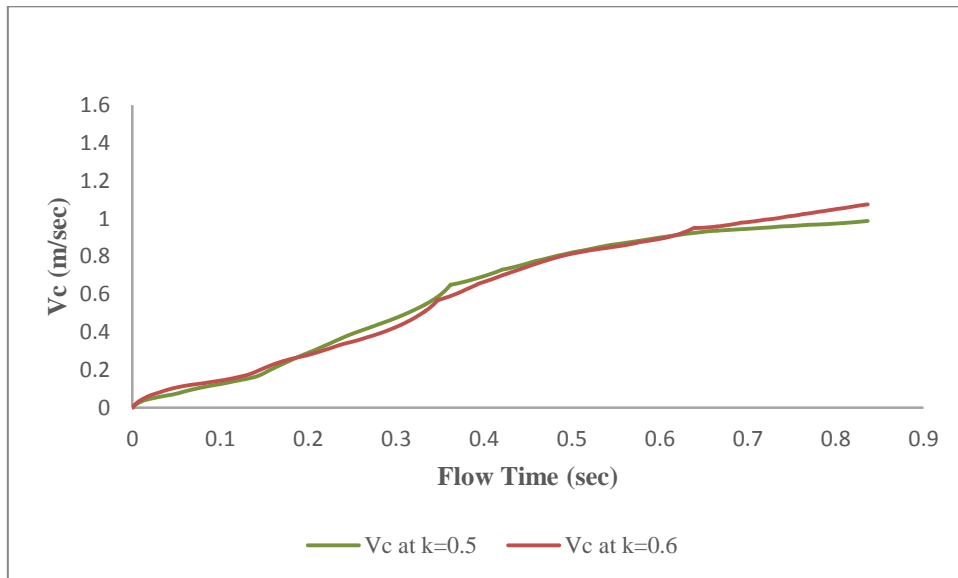


Figure 4.15 The effect of capsule diameter on capsule velocity history for a heavy density spherical capsule at $V_{av} = 2\text{m/sec}$

4.3.4 Effect of the Capsules Concentration

Figure 4.13 depicts the variations within pipelines carrying two equi-density spherical capsules for the static gauge pressure and the flow velocity magnitude for $V_{av} = 2\text{m/sec}$ and $k = 0.6$ at different flow times. The initial distance between capsules is equal to two diameters of the capsule. The pressure distribution trends are the same as noticed for a single equi-density spherical capsule. The pressure at the upstream position has increased to 17145Pa (13%), in comparison to a one equi-density spherical capsule. Thereby, a decrease in total pressure of 0.32% was seen for $N = 2$ compared to $N = 1$. Moreover, in comparison with one spherical capsule, it is observed that increased concentration of the solid medium in the pipeline provides higher flow resistance and increased pressure drops. When a capsule train moves in a pipe, the upstream capsule bears the greatest pressure while the pressure on the second capsule decreases in turn. The difference in the capsules velocities makes the spacing between the capsules changes gradually after the capsule train starts in the motion.

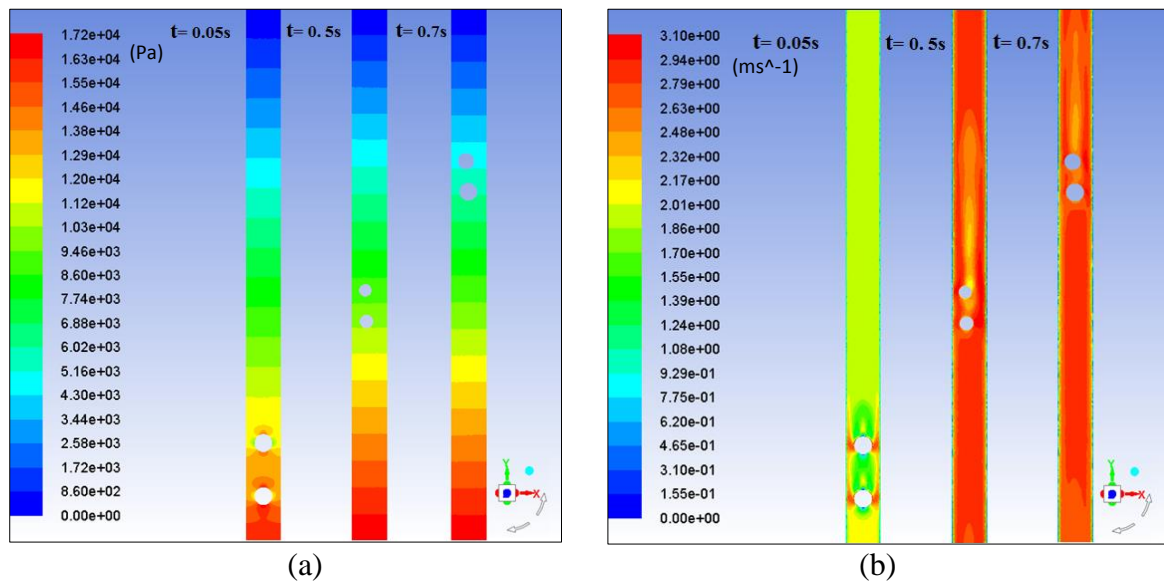


Figure 4.16 (a) Static gauge pressure and (b) Flow velocity magnitude variations for two equi-density spherical capsules of $k = 0.5$ and $V_{av} = 2\text{m/sec}$ at different flow times

Figure 4.17 shows the variations in the pressure drop along the test section of the pipe. It can be observed that the pressure drop markedly fluctuates during the capsule motion in the pipe. The results indicate that the pressure drop recorded through the motion of two equi-density capsules are slightly higher than the pressure drop for a single spherical capsule. This is because the concentration of the solid medium within the pipe is more in the case of $N = 2$ as compared to $N = 1$.

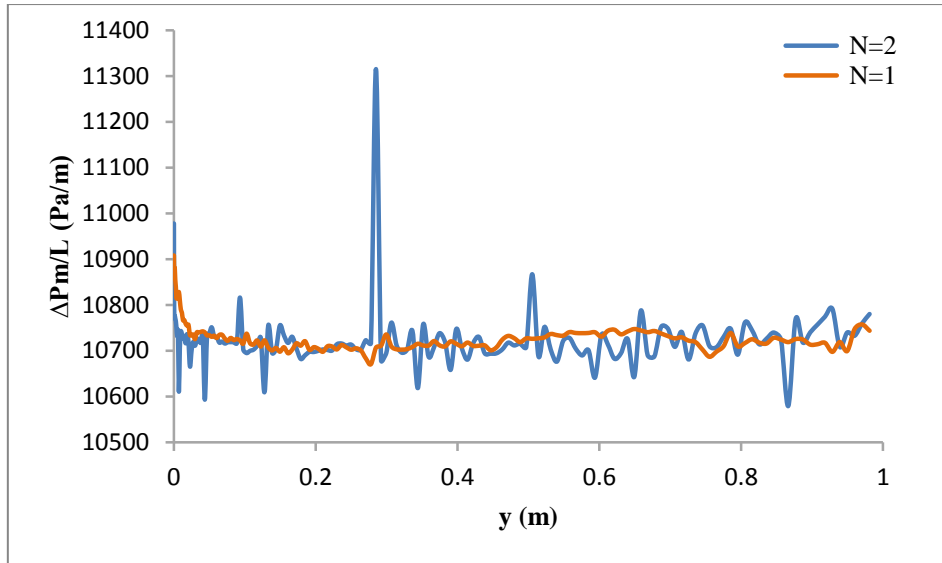


Figure 4.17 The effect of capsule concentration on the pressure drop variation for two equi-density spherical capsule of $k = 0.5$ at $V_{av} = 2\text{m/sec}$

Figure 4.18 depicts time histories of the capsule velocities of two equi-density spherical capsules at an average velocity of 2m/sec. It can obviously notice that the velocity of the first capsule is greater than the second capsule during a period due to the first capsule is subject to the maximum forces from the water, and its hydraulic characteristics are more complex than for the second capsule. Afterwards, the second capsule velocity starts increasing till exceed the first capsule velocity. The velocity distribution is quite similar for both the capsules.

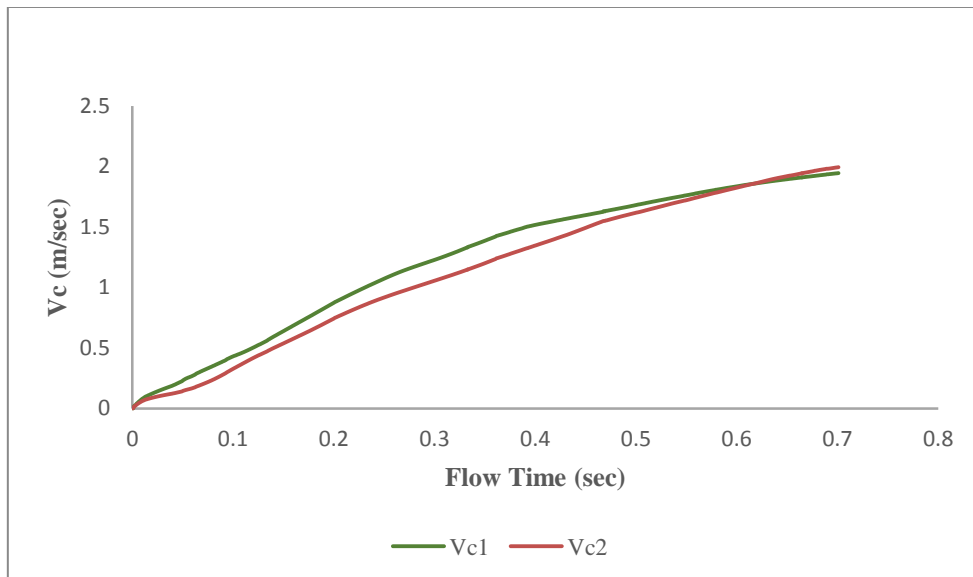


Figure 4.18 The effect of capsule concentration on capsule velocity history for two equi-density spherical capsule of $k = 0.5$ at $V_{av} = 2\text{m/sec}$

4.4 Flow Diagnostics in HCPs Transporting Cylindrical Capsules

Figure 4.19 illustrates the static gauge pressure and flow velocity distribution around an equi-density cylindrical capsule of $k = 0.5$ at a flow velocity of 2m/sec for a capsule length $L_c = 1d$. The pressure in the pipeline decreases continuously from the inlet to the outlet of the pipe. The pressure field around a cylindrical capsule resembles the pressure field around a spherical capsule. It can be noted that the pressure upstream the capsule, at a flow time of 0.05sec, is 14465Pa, however, after 0.55sec, the pressure upstream the capsule decreases by 68.7% for the two flow times considered. It can be observed that the flow velocity in the test section varies according to the capsule position throughout its motion. Moreover, the velocity distribution trend is the same as observed in the flow of a one spherical capsule.

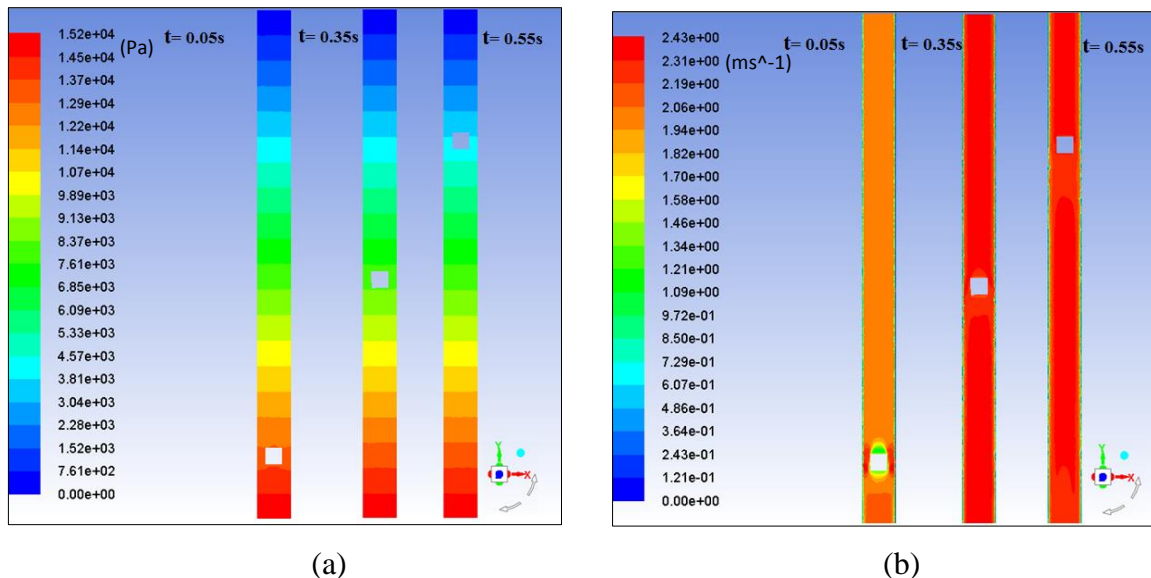


Figure 4.19 (a) Static gauge pressure and (b) Flow velocity magnitude variations for an equi-density cylindrical capsule of $k = 0.5$, $L_c = 1d$ and $V_{av} = 2m/sec$ at different flow times

Figure 4.20 depicts the time histories of equi-density cylindrical and spherical capsules at the flow velocity of 2m/sec. Therefore, it can be obviously noticed that the cylindrical capsules velocity is higher than the spherical capsule. This is due to that the cross section area of the cylindrical capsule is greater than the cross section area of the spherical capsule. Where the cross section area of the cylindrical capsule is subjected to the maximum forces from the water is greater than the spherical capsule. Hence, the time that takes the cylindrical capsule to reach steady velocity is shorter than the spherical capsule.

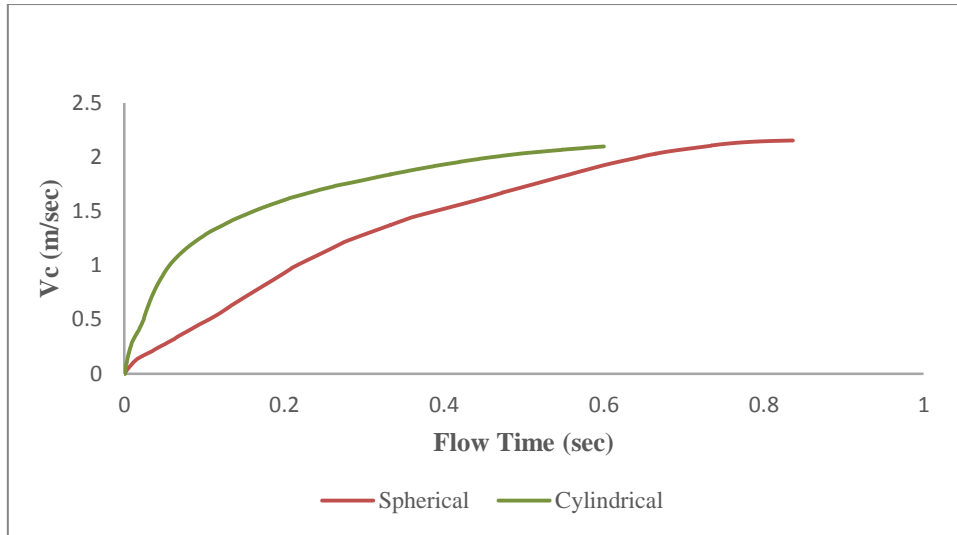


Figure 4.20 The capsule velocity history for an equi-density cylindrical capsule of $k = 0.5$ and $L_c = 1d$

4.4.1 Effect of Average Flow Velocity

Figure 4.21 illustrates the static gauge pressure and flow velocity magnitude distribution for transporting equi-density cylindrical capsules across pipelines of $k = 0.5$ and $L_c = 1d$ at an average velocity of 4 m/sec during different flow times. The pressure drop through the pipeline test section is 11521 Pa , which is 7% higher in compared with the pressure drop of the same capsule at $V_{av} = 2\text{ m/sec}$. Moreover, it can observe as seen in the figure 4.12 (b) that the field of velocity is similar to the field noticed in the case of $V_{av} = 2\text{ m/sec}$, i.e. greater velocity through in the annulus area always be at the beginning of the capsule motion at $t = 0.05\text{ sec}$. Behind a capsule, a wake region has become larger as compared with a wake region when average velocity was 2 m/sec due to increase in the flow velocity.

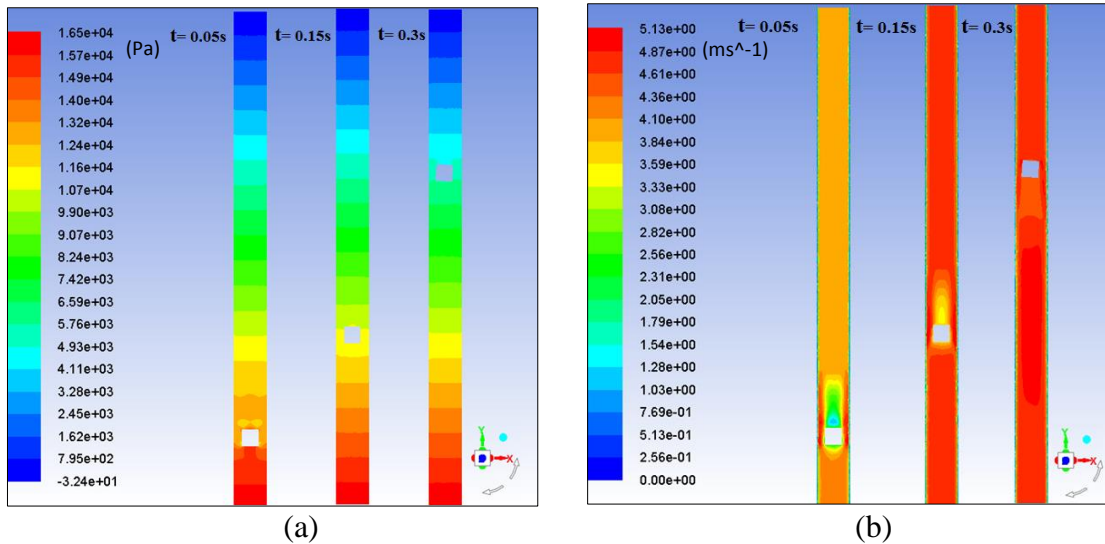


Figure 4.21 (a) Static gauge pressure and (b) Flow velocity magnitude variations for an equi-density cylindrical capsule of $k = 0.5$, $L_c = 1d$ and $V_{av} = 4m/sec$ at different flow times

Figure 4.22 shows the pressure drop variations throughout the pipeline test section. The results indicate that the pressure gradient at an average velocity of a flow of $4m/sec$ is considerably higher than the pressure gradient for a flow velocity $2m/sec$. It can be observed that the pressure gradient markedly fluctuates through the equi-density cylindrical capsule motion in the pipe. Nonetheless, the pressure drop trends in the pipeline are nearly the same as seen in both cases. The Appendix A-5 gives more detailed results.

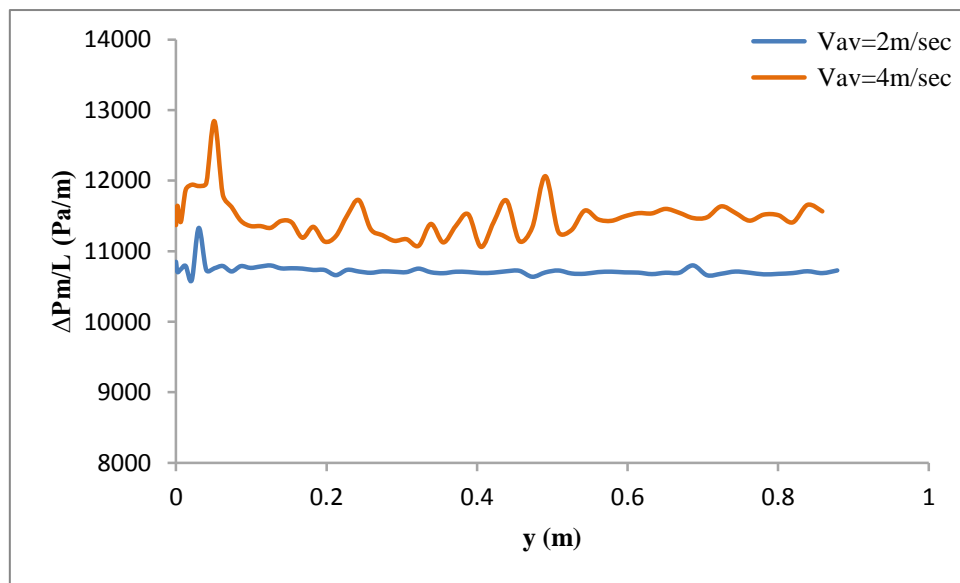


Figure 4.22 The effect of average flow velocity on the pressure drop variation for an equi-density cylindrical capsule for $k=0.5$ and $L_c=1d$

Figure 4.23 shows time histories of the capsule velocities for an equi-density cylindrical capsule of $k = 0.5$ at different flow velocities. It can be noted that the capsule velocity is increased gradually with the increase of the flow velocity. Thereby, the capsule velocity with a flow velocity of 4m/s attains a constant velocity in a shorter time than in the case of $V_{av} = 2\text{m/sec}$. It can be concluded that the capsule velocity is slightly higher than the flow velocity of fluid regardless the fluid velocity value.

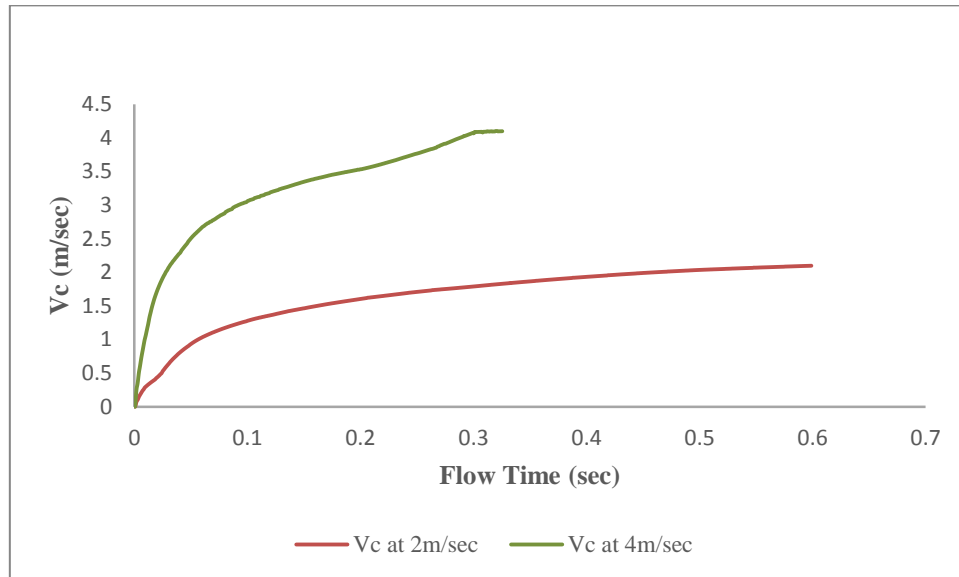


Figure 4.23 The effect of average flow velocity on capsule velocity history for an equi-density cylindrical capsule for $k = 0.5$ and $L_c = 1d$

4.4.2 Effect of Capsule Length

Figure 4.24 illustrates the static gauge pressure and flow velocity distributions of the pipe carrying cylindrical capsule with an equi-density for $k = 0.5$, $L_c = 1.5d$ and $V_{av} = 2\text{m/s}$ during different flow times. It can be noticed that the distributions in the total pressure and velocity appear to be the same in comparison with $L_c = 1d$ at the same capsule diameter and flow velocity. However, the time that the capsule has taken it to reach the end of the test section considers slightly longer as compared with capsule $L_c = 1d$ due to the increase in a capsule length. The pressure drop across the pipe is 10728Pa which is 0.18% greater than the pressure drop for capsule $L_c = 1d$. Moreover, the velocity distribution field remains as similar as one observed in $L_c = 1d$.

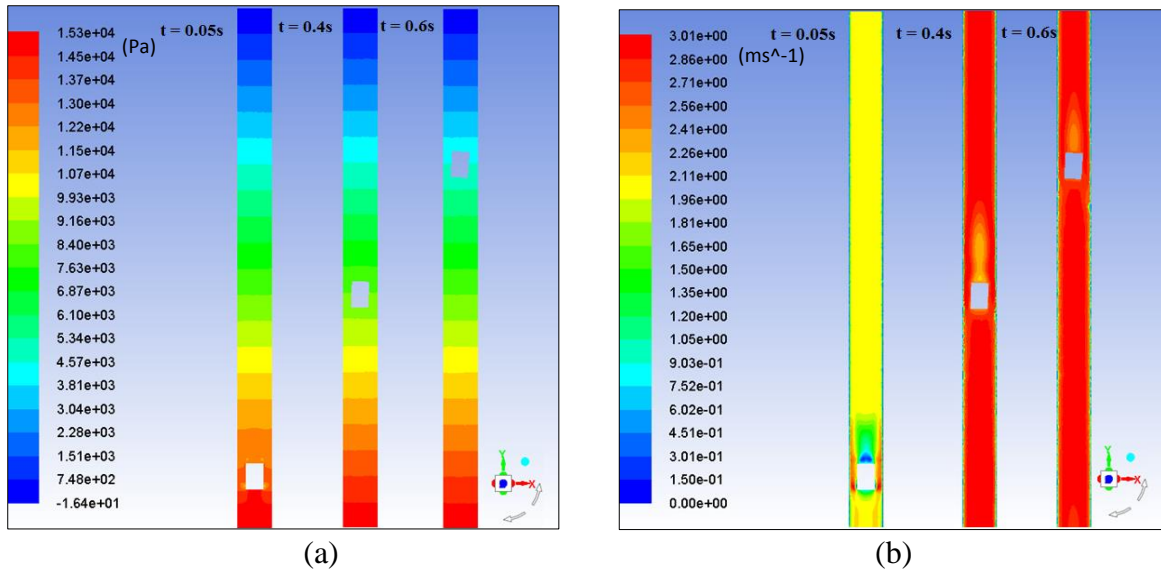


Figure 4.24 (a) Static gauge pressure and (b) Flow velocity magnitude variations for an equi-density cylindrical capsule of $k = 0.5$, $L_c = 1.5d$ and $V_{av} = 2m/sec$ at different flow times

Figure 4.25 shows the pressure drop variations throughout the pipe test section. It can be observed that the pressure gradient markedly fluctuates through an equi-density cylindrical capsule motion in the pipe. The results indicate that the pressure gradient for capsule length $1.5d$ is considerably slightly higher than the pressure gradient for the capsule of $L_c = 1d$.

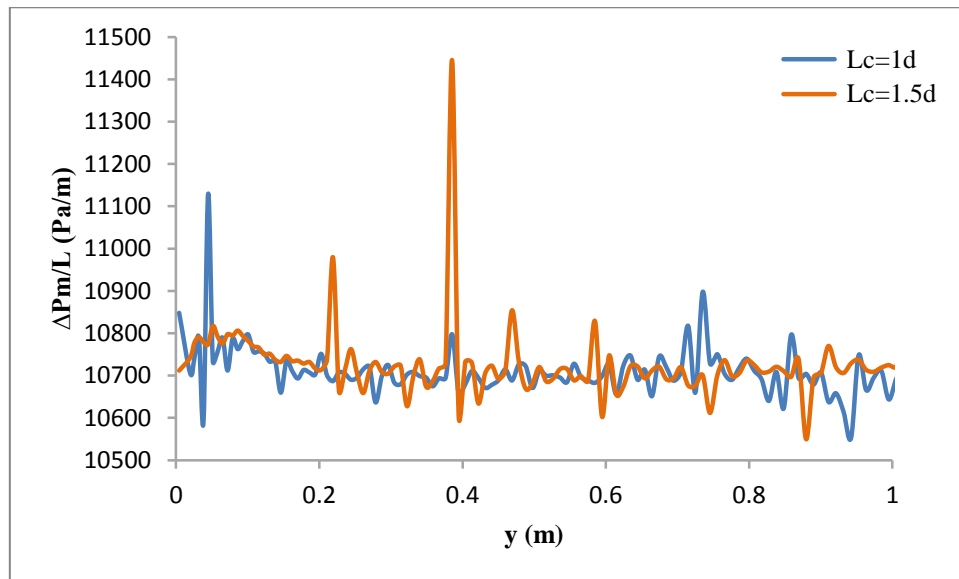


Figure 4.25 The effect of a capsule length on the pressure drop variation for an equi-density cylindrical capsule for $k = 0.5$ and $V_{av} = 2m/sec$

Figure 4.26 depicts the time histories of an equi-density cylindrical capsule at an average flow velocity of 2m/s with different lengths. It can be clearly noticed that the cylindrical capsule velocity with the length of 1.5d is less than the capsule velocity with the length of 1d. This is due to the increase of the capsule length. Hence, the time that takes the cylindrical capsule with the length of 1.5d to reach steady velocity is longer than the time with the length of 1d.

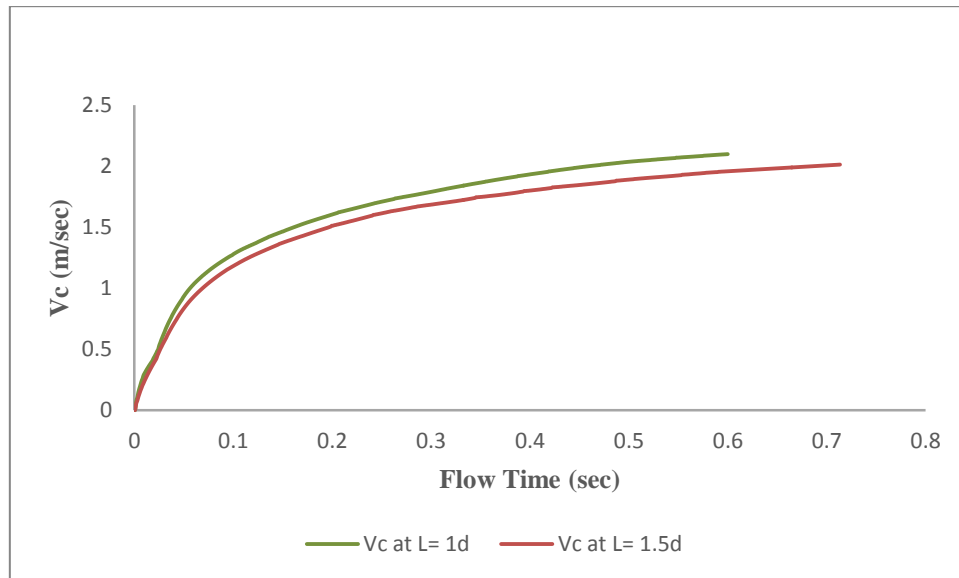


Figure 4.26 The effect of a capsule length on capsule velocity history for an equi-density cylindrical capsule for $k = 0.5$ and $V_{av} = 2\text{m/sec}$

4.4.3 Capsule Density Effects

Figure 4.27 depicts the static gauge pressure and flow velocity magnitude variations in transporting of a cylindrical capsule with a heavy-density for $L_c = 1d$, $k = 0.5$ at $V_{av} = 2\text{m/sec}$ at different times. The pressure at the upstream is about 15436Pa during $t = 0.05\text{sec}$, which is 6.3% higher than the upstream pressure for an equi-density capsule with the same parameters. The trend of pressure distribution is the same as noted for an equi-density cylindrical capsule. Moreover, this can be obviously observed in figure 4.27 (b) the capsule velocity has become slower than the equi-density capsule owing to the capsule weight. In addition to that, the time that takes it to cross the test section of the pipe is $t = 0.65\text{sec}$, as compared to the cylindrical capsule with equi-density that takes less time at $t = 0.55\text{sec}$.

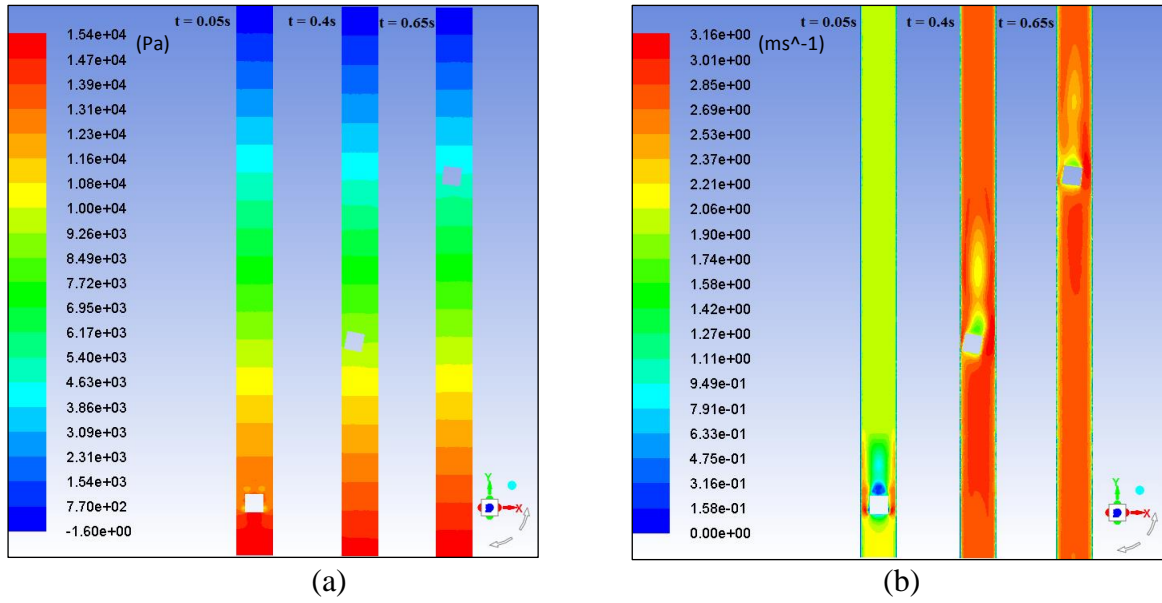


Figure 4.27 (a) Static gauge pressure and (b) Flow velocity magnitude variations for a heavy density cylindrical capsule of $k = 0.5$, $L_c = 1d$ and $V_{av} = 2m/sec$ at different flow times

Figure 4.28 shows the variations in the pressure drop along the test section of the pipe. It can be observed that the pressure drop markedly fluctuates through the capsule motion in the pipe. As in the results indicated that the pressure gradient for a heavy density capsule ($s = 1.7$) is significantly higher than the pressure gradient of an equi-density capsule ($s = 1$). Moreover, the pressure drop variation within the pipe is similar for two cases.

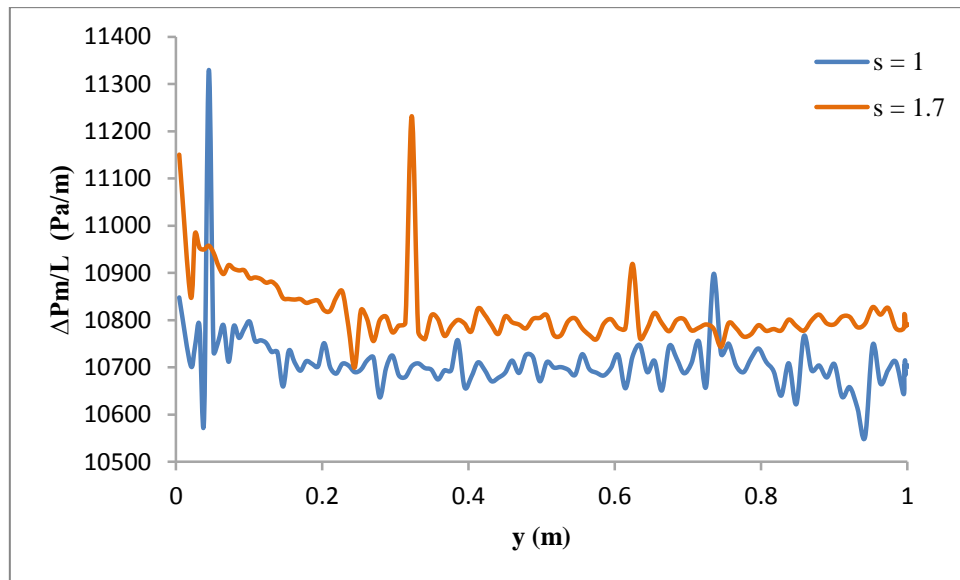


Figure 4.28 The effect of capsule density on the pressure drop variation for a heavy density cylindrical capsule of $k = 0.5$ and $L_c = 1d$ at $V_{av} = 2m/sec$

Figure 4.29 depicts time history of the capsule velocity for cylindrical capsule at an average velocity of 2m/sec for different densities. It can be obviously noticed that the capsule velocity for a heavy density capsule ($s = 1.7$) is less than the capsule velocity for an equi-density capsule ($s = 1$). The velocity of the equi-density cylindrical capsule is exceeded the flow velocity, whereas the velocity of heavy density capsule is less than the flow velocity when reaches to a steady velocity.

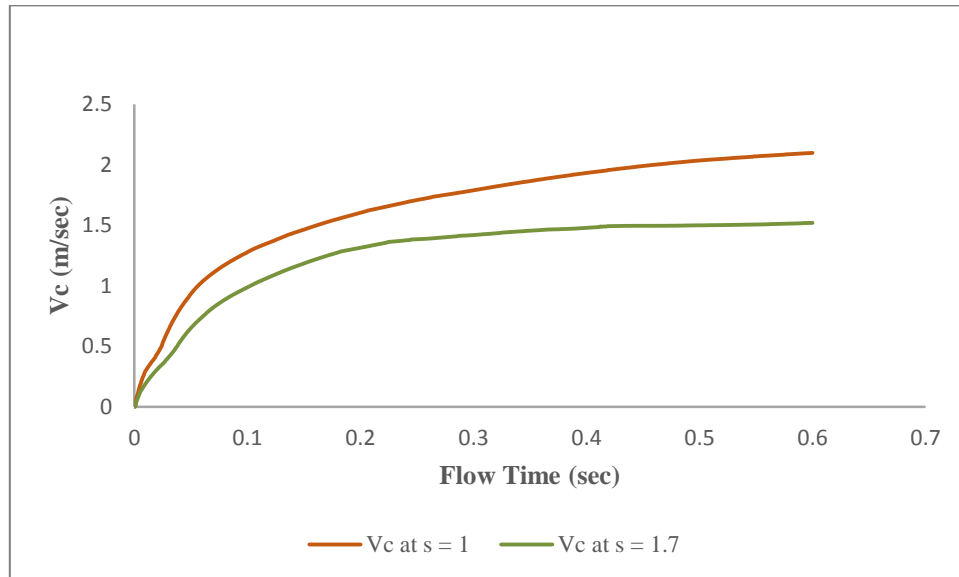


Figure 4.29 The effect of capsule density on capsule velocity history for a heavy density cylindrical capsule of $k = 0.5$ and $L_c = 1d$ at $V_{av} = 2m/sec$

4.4.4 Effect of Capsule Diameter

Figure 4.30 depicts the distribution in a heavy density cylindrical capsule transporting pipe for the static gauge pressure and flow velocity magnitude of $L_c = 1 d$, $k = 0.6$ at $V_{av} = 2m/sec$ during different flow times. The distribution of the total pressure appears to be similar to the field of pressure for $k = 0.5$ at the same average flow rate and the same capsule length. The pressure on the capsule front area during $t = 0.7sec$ has decreased by 65.5% as compared to the pressure on the front area of the capsule during $t = 0.05 sec$. Moreover, the distribution of the flow velocity is the same as seen in the case of $k = 0.5$ at the same capsule length and the same flow velocity. In addition to that, the velocity distribution within the pipe after the initial motion of the capsule at $t = 0.45sec$ becomes more regular distribution.

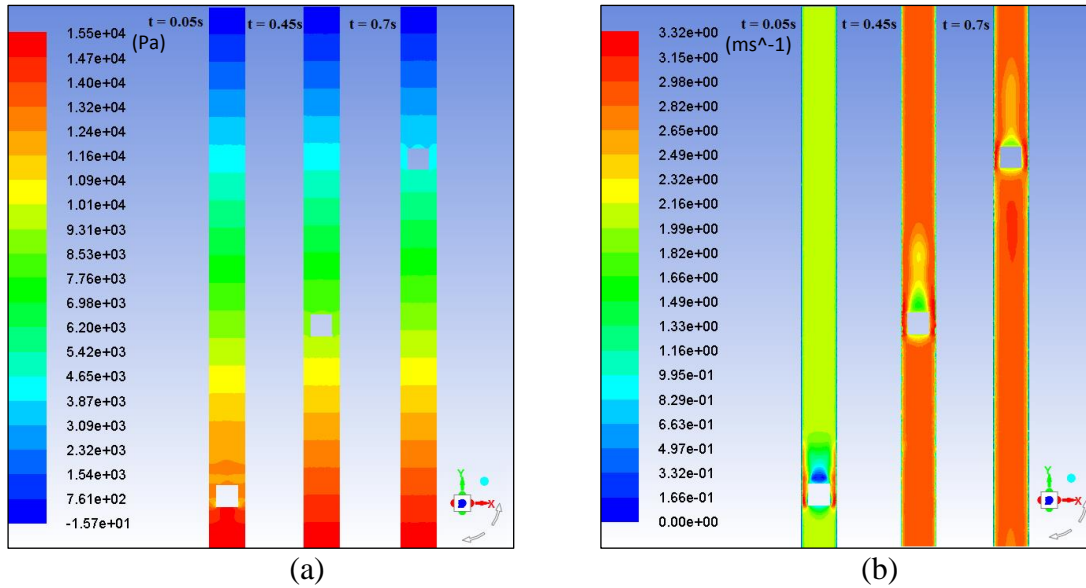


Figure 4.30 (a) static gauge pressure and (b) Flow velocity magnitude variations for a heavy density cylindrical capsule of $k = 0.6$, $L_c = 1d$ and $V_{av} = 2m/sec$ at different flow times

Figure 4.31 illustrates the pressure drop variations throughout the pipe test section at the same average velocity of the flow 2m/sec. It can be observed that the pressure drop markedly fluctuates through the capsule motion in the pipe. The results indicate that the pressure gradients recorded through a capsule motion of $k = 0.6$ remarkable change as compared to the pressure drop as seen in the case of $k = 0.5$.

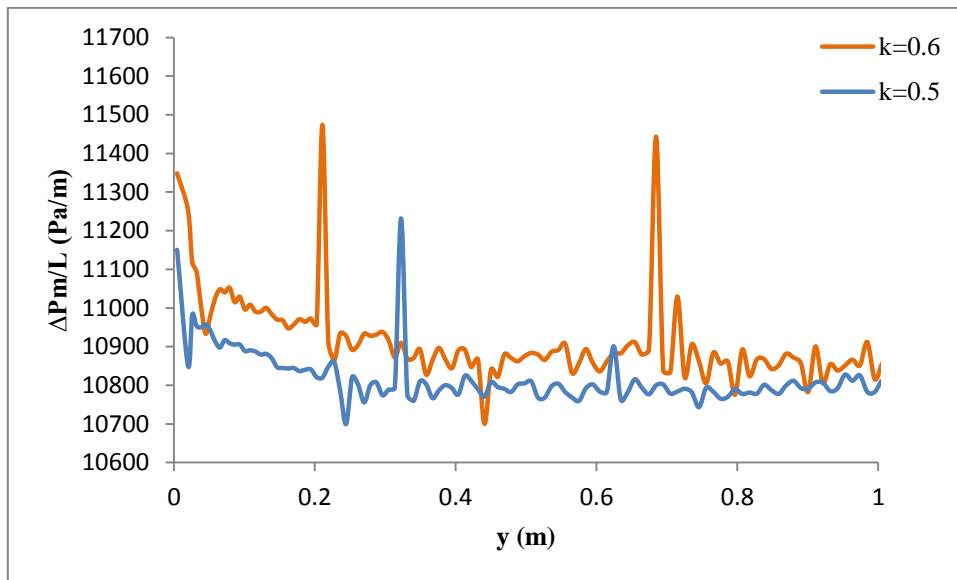


Figure 4.31 the effect of capsule diameter on the pressure drop variation for a heavy density cylindrical capsule at $V_{av} = 2m/sec$ and $L_c = 1d$

Figure 4.32 shows a time history of cylindrical capsule velocity starting from rest until the capsule reaches nearly the steady velocity for different capsule diameters at an average velocity of 2m/sec. It can be clearly seen that the capsule velocity for $k = 0.6$ is slightly higher than of $k = 0.5$ during a particular time, and then the capsule velocity of $k = 0.6$ becomes approaching from the capsule velocity of $k = 0.5$. Afterwards, the capsule velocity tends to be steady.

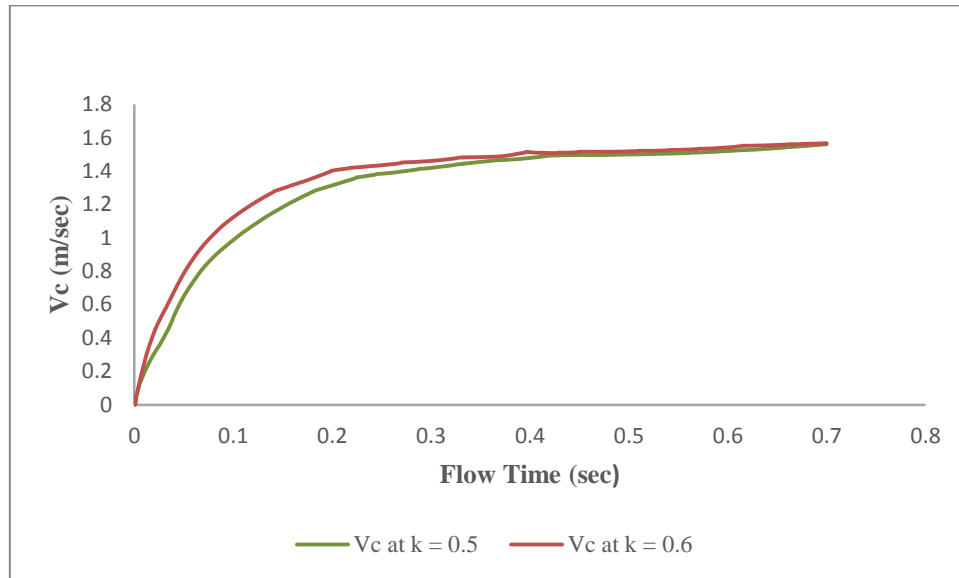


Figure 4.32 The effect of capsule diameter on capsule velocity history for a heavy density cylindrical capsule at $V_{av} = 2\text{m/sec}$ and $L_c = 1d$

4.4.5 Effect of the Capsules Concentration

Figure 4.33 presents the static gauge pressure and flow velocity magnitude variations inside a pipe conveying two equi-density cylindrical capsules of $k = 0.5$, $L_c = 1d$ and $V_{av} = 2\text{m/sec}$ at different times. The distribution trend of the pressure is nearly identical as noticed for a single equi-density cylindrical capsule. The upstream location pressure at $t = 0.05\text{sec}$ has increased to 15135Pa (0.7 %) in contrast to a single equi-density cylindrical capsule at the same flow time. Hence, the overall pressure drop has increased by 0.2% for $N = 2$ in contrast to $N = 1$. Moreover, as compared to a single cylindrical capsule, it can be observed that the flow velocity upstream of the capsules at $t = 0.05\text{sec}$ is 2.15m/sec, but the flow velocity downstream of the capsules at the same time dropped by 21% to 1.7m/sec. Thereby, increasing the concentration of the solid phase in the pipeline provides further resistance to the flow and results in a decline in the flow velocity.

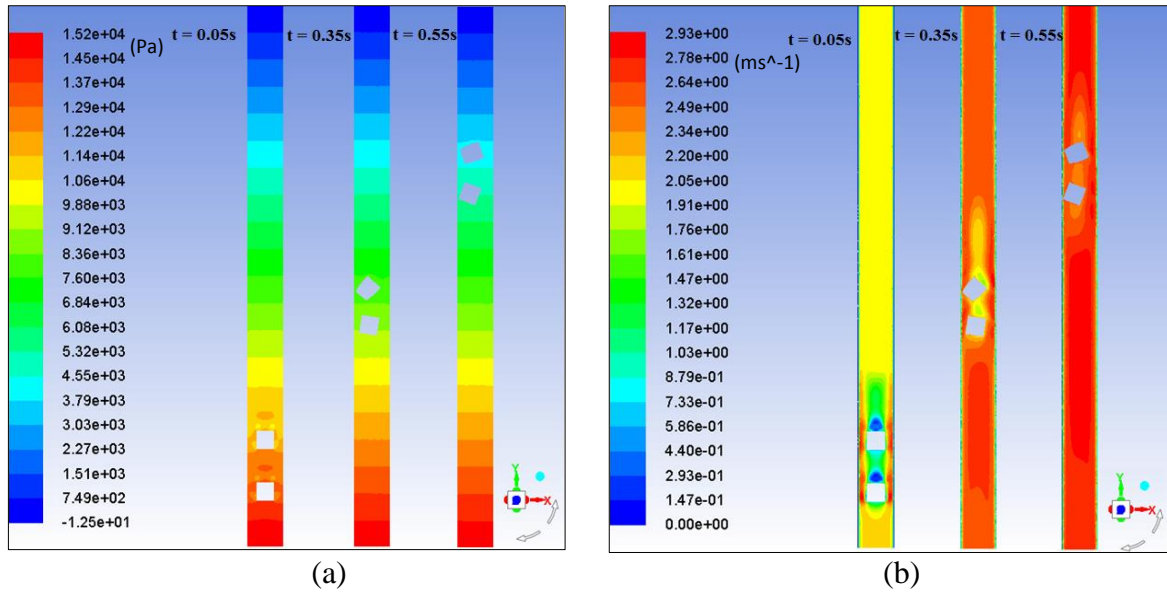


Figure 4.33 (a) Static gauge pressure and (b) Flow velocity magnitude variations for two equi-density cylindrical capsules of $k = 0.5$, $Lc = 1d$ and $V_{av} = 2m/sec$ at different flow times

Figure 4.34 shows the pressure drop variations along the pipe test section. It is noticed that the pressure reduction markedly fluctuates through the capsule motion in the pipe. This can be clearly observed through the change of the capsules position that resulted from the rotational and transient motion of the capsules flow. The results indicate that the pressure drops recorded through the motion of two equi-density cylindrical capsules are slightly higher than the pressure drop for a single cylindrical capsule. This is due to the solid phase concentration inside the pipeline which is more for $N = 2$ as compared to $N = 1$.

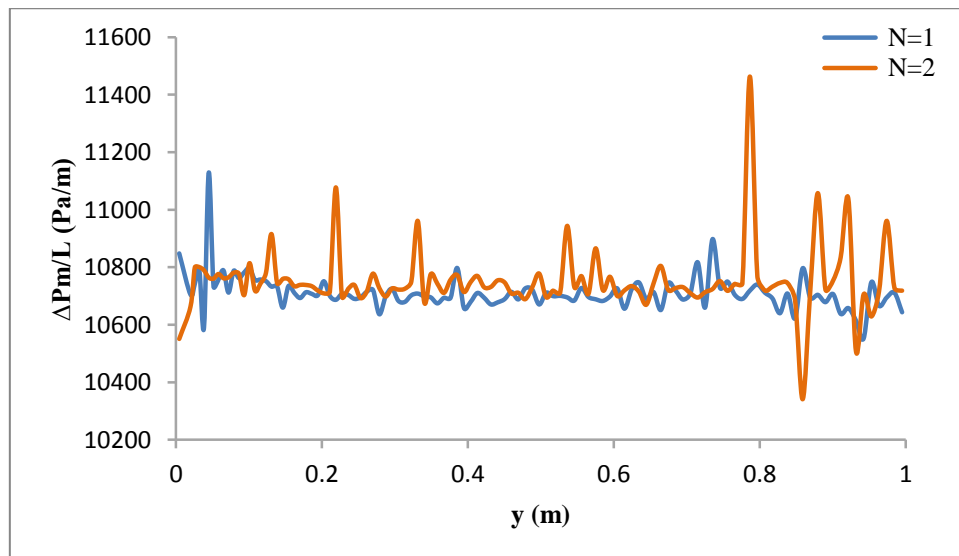


Figure 4.34 The effect of capsule concentration on the pressure drop variation for two equi-density cylindrical capsules of $k = 0.5$ and $Lc = 1d$ at $V_{av} = 2m/sec$

Figure 4.35 depicts time histories of the capsule velocity for two equi-density cylindrical capsules at an average velocity of 2m/sec. It can be obviously seen that the first capsule velocity is greater than the second capsule during a period due to the first capsule is subject to the maximum forces from the water, and its hydraulic characteristics are more complex than for the second capsule. Afterwards, the second capsule velocity starts increasing till exceed the first capsule velocity. The velocity profile is quite similar for both the capsules.

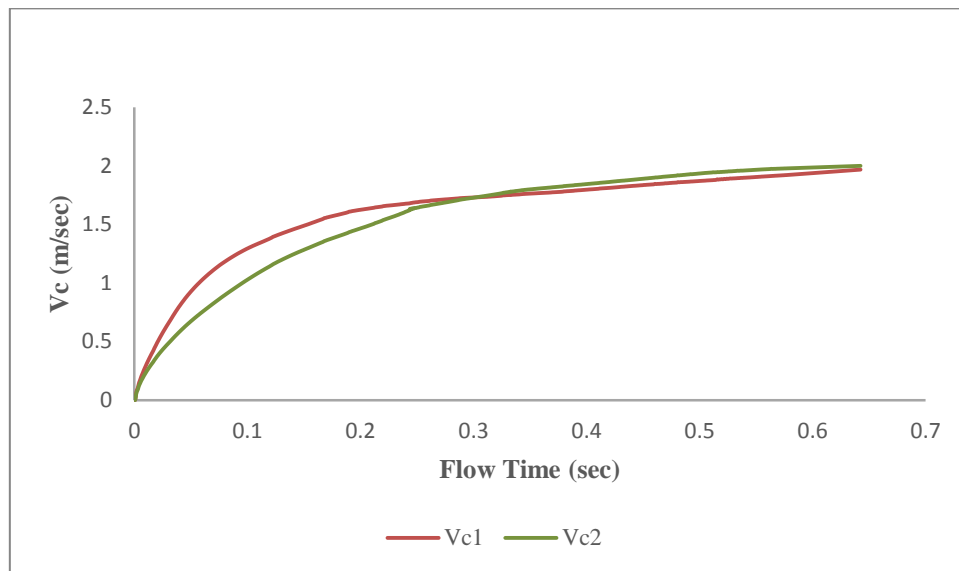


Figure 4.35 The effect of capsule concentration on capsule velocity history for two equi-density cylindrical capsules of $k=0.5$ and $L_c=1d$ at $V_{av}=2\text{m/sec}$

4.5 Flow Diagnostics in HCPs Transporting Rectangular Capsules

Figure 4.36 illustrates the static gauge pressure and flow velocity distribution around a one rectangular capsule for a capsule length $L_c = 1d$, $k = 0.5$ as well as a flow velocity of 2m/sec. The pressure in the pipelines reduces continuously from the inlet to the outlet of the pipe. The pressure scope around a rectangular capsule similar to the pressure scope around a cylindrical capsule. It can be noted that the pressure upstream the capsule, at a flow time of 0.05sec, is 14965Pa, however, after 0.6sec, the pressure upstream the capsule decreases by 72% for the two flow times considered. Moreover, the flow velocity distribution trend is the same as observed in a one cylindrical capsule case. The velocity flow distribution within the pipe after the initial motion of the capsule during time 0.4sec becomes more regular due to the capsule motion.

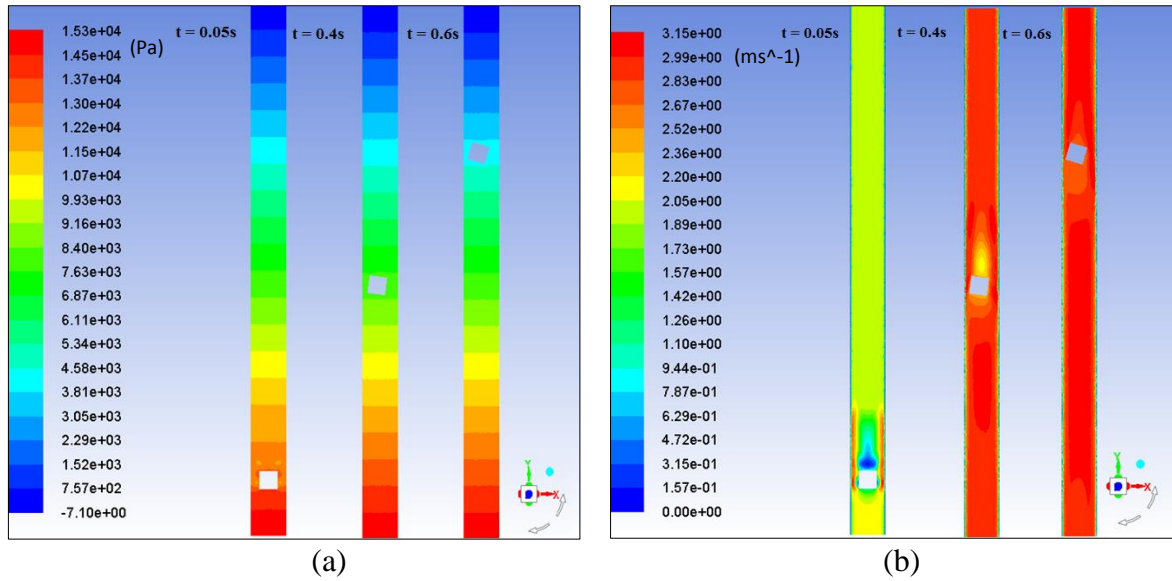


Figure 4.36 (a) Static gauge pressure and (b) Flow velocity magnitude variations for an equi-density rectangular capsule of $k = 0.5$, $L_c = 1d$ and $V_{av} = 2m/sec$ at different flow times

Figure 4.37 depicts the time histories of equi-density rectangular and cylindrical capsules at a flow velocity of $2m/sec$. It can be obviously noticed that the rectangular capsule velocity is higher than the cylindrical capsule during a particular time of the motion. This is due to that the cross section area of the rectangular capsule is greater than the cross section area of the cylindrical capsule. Where the cross section area of the cylindrical capsule is subjected to the maximum forces from the water is greater than the spherical capsule. Then the cylindrical capsule velocity starts in an increase until exceeding the rectangular capsule velocity.

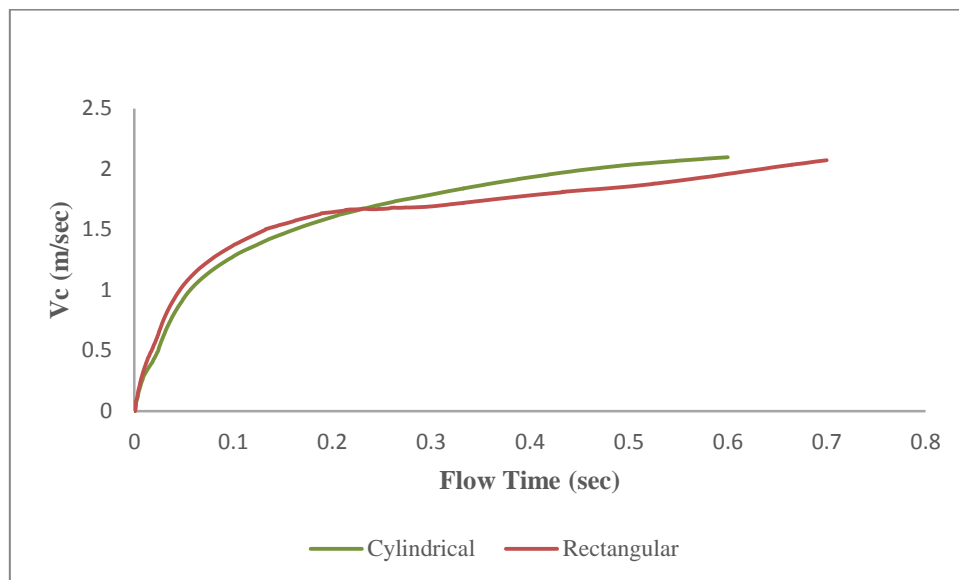


Figure 4.37 The capsule velocity history for an equi-density rectangular capsule of $k 0.5$ and $L_c = 1d$

4.5.1. Effect of Average Flow Velocity

In order to investigate the impact of the velocity of flow on the flow structure, an average flow velocity of 4m/sec has been selected for an equi-density rectangular capsule of $k = 0.5$ and $L_c = 1d$. Figure 4.38 illustrates the static gauge pressure and flow velocity distribution at different flow times during the capsule motion. It can be noted that the pressure in front of the capsule at an initial motion during 0.05sec is 16450Pa as compared to the pressure in front of the capsule in case of $V_{av} = 2m/sec$ at 0.05sec is 14965Pa, which increased by 9%.

Moreover, it can be seen in figure 4.38 (b) that the trend of velocity field resembles the one noticed in case of $V_{av} = 2m/sec$, and $t = 0.05sec$ i.e. a wake region had become larger as compared to the wake region when the average velocity was 2m/sec due to increase in the velocity of flow.

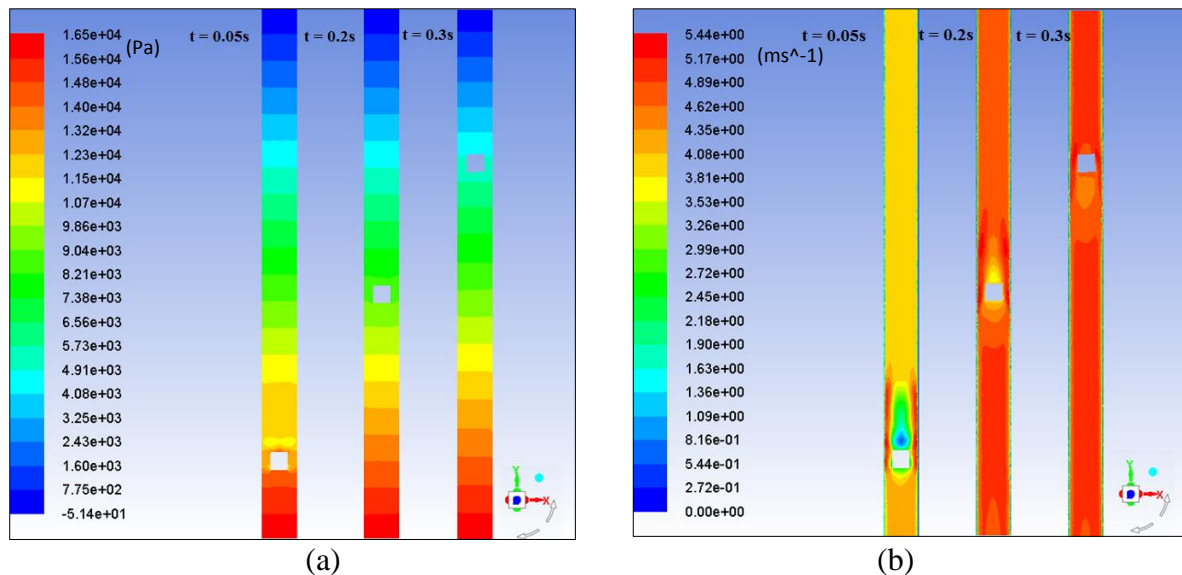


Figure 4.38 (a) Static gauge pressure and (b) Flow velocity magnitude variations for an equi-density rectangular capsule of $k = 0.5$, $L_c = 1d$ and $V_{av} = 4m/sec$ at different flow times

Figure 4.39 shows the variation in the pressure drop along the test section of the pipe. It can be observed that the pressure drop markedly fluctuates through the Equi-density rectangular capsule motion in the pipe. The results indicate that the pressure gradient at an average flow velocity of 4m/sec is considerably higher than the pressure gradient for a flow velocity 2m/sec. However, the trend of pressure drop in the pipeline is similar for two cases. Further details are provided in Appendix A-5.

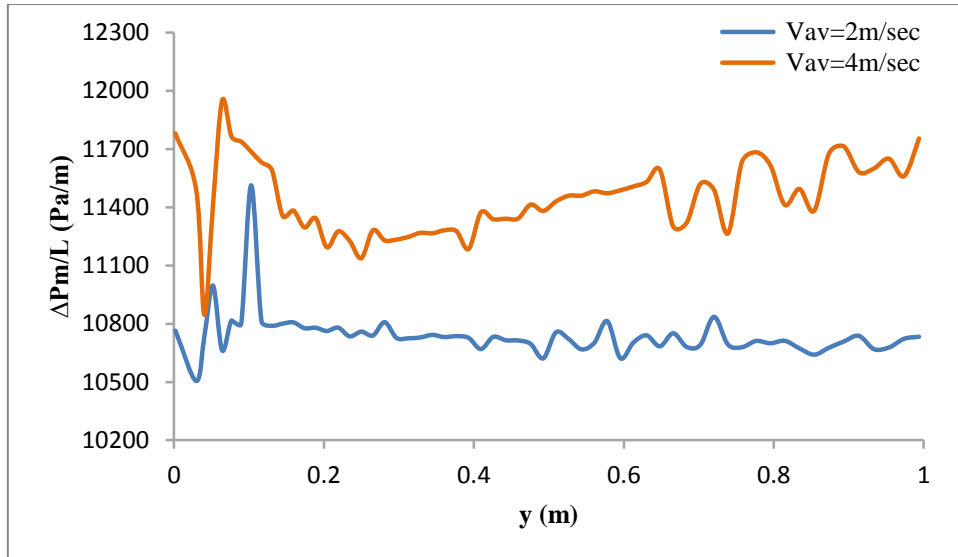


Figure 4.39 The effect of average flow velocity on the pressure drop variation for an equi-density rectangular capsule for $k = 0.5$ and $L_c = 1d$

Figure 4.40 shows time histories of the capsule velocities for an equi-density rectangular capsule of $k = 0.5$ at different flow velocities. It can be obviously seen that when the average flow velocity increases this will lead to that the capsule velocity will increase as well. Thereby, the capsule velocity with a flow velocity of 4m/s attains a constant velocity in a shorter time than in the case of $V_{av} = 2m/sec$. It can be concluded that the capsule velocity is slightly higher than the flow velocity of fluid regardless the fluid velocity value.

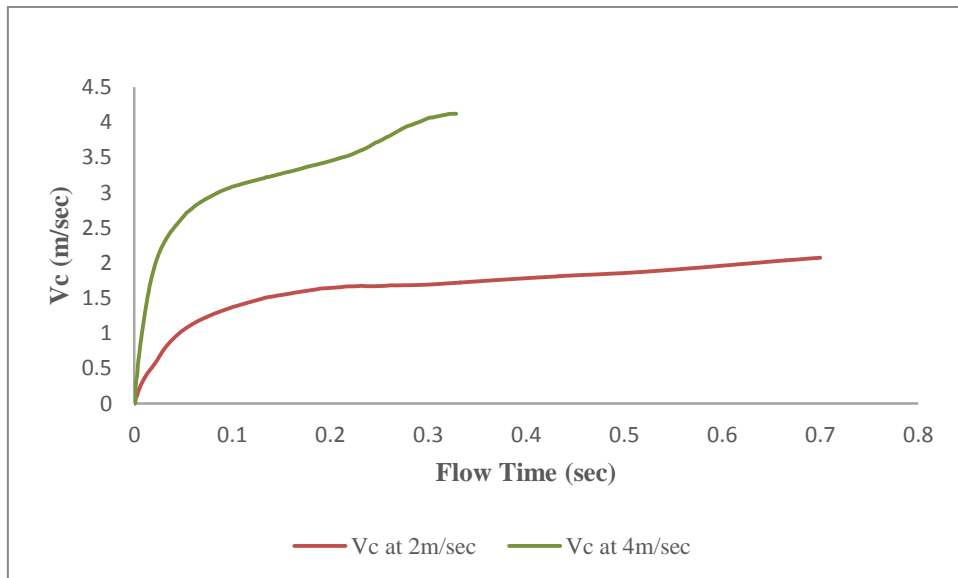


Figure 4.40 The effect of average flow velocity on capsule velocity history for an equi-density rectangular capsule of $k = 0.5$ and $L_c = 1d$

4.5.2. Effect of Rectangular Capsule Length

Figure 4.41 illustrates the static gauge pressure and flow velocity distributions of the pipe carrying an equi-density rectangular capsule for $V_{av} = 2\text{m/sec}$, $L_c = 1.5 d$ and $k = 0.5$, during different flow times. It can be noticed that the velocity distributions and the total pressure seem to be the same in comparison with $L_c = 1d$ at the same flow velocity and capsule diameter. The pressure in front of the capsule at an initial motion during 0.05sec is 15122Pa as compared to the pressure in front of the capsule in case of $L_c = 1d$ at 0.05sec is 14965Pa , which increased by 1% . Moreover, it is observed in figure 4.41 (b) at $t = 0.05\text{sec}$ that the flow velocity in the annulus region has decreased to 2.45m/sec , instead of 2.67m/sec for capsule length of $L_c=1d$.

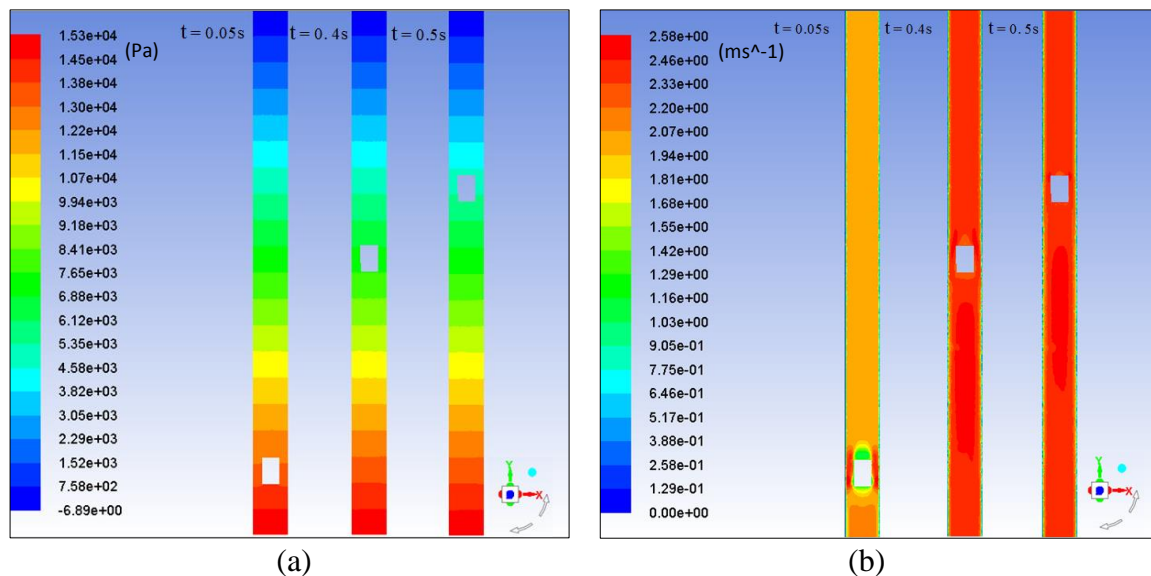


Figure 4.41 (a) Static gauge pressure and (b) Flow velocity magnitude variations for an equi-density rectangular capsule of $k = 0.5$, $L_c = 1.5d$ and $V_{av} = 2\text{m/sec}$ at different flow times

Figure 4.42 shows the pressure drop variations along the test section of the pipe. It can be noticed that the pressure drop markedly fluctuates through an equi-density rectangular capsule motion in the pipe. The results indicate that the pressure gradient for capsule length $1.5d$ is considerably slightly higher than the pressure gradient for the capsule for length $1d$. More detailed results are provided in Appendix A-5.

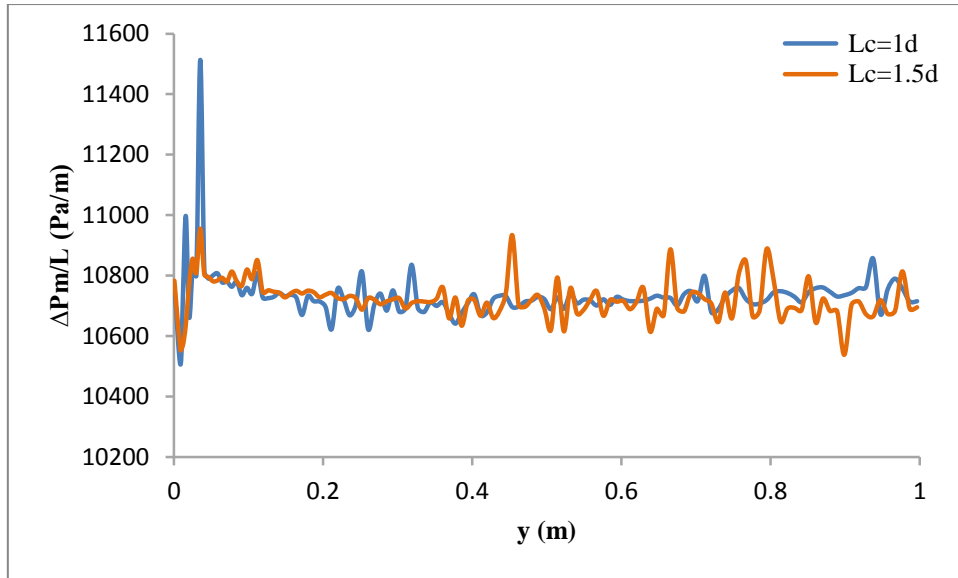


Figure 4.42 The effect of a capsule length on the pressure drop variation for an equi-density rectangular capsule for $k = 0.5$ and $V_{av} = 2\text{m/sec}$

Figure 4.43 depicts the time histories of an equi-density rectangular capsule at an average flow velocity of 2m/sec with different lengths. It can be clearly noticed at the beginning of the motion that the capsule velocity with the length of 1.5d is slightly less than the capsule velocity with the length of 1d. This is due to the increase of the capsule length. Then the capsule velocity with length of $L_c = 1.5d$ starts in an increase until become flying with the capsule velocity of $L_c = 1d$.

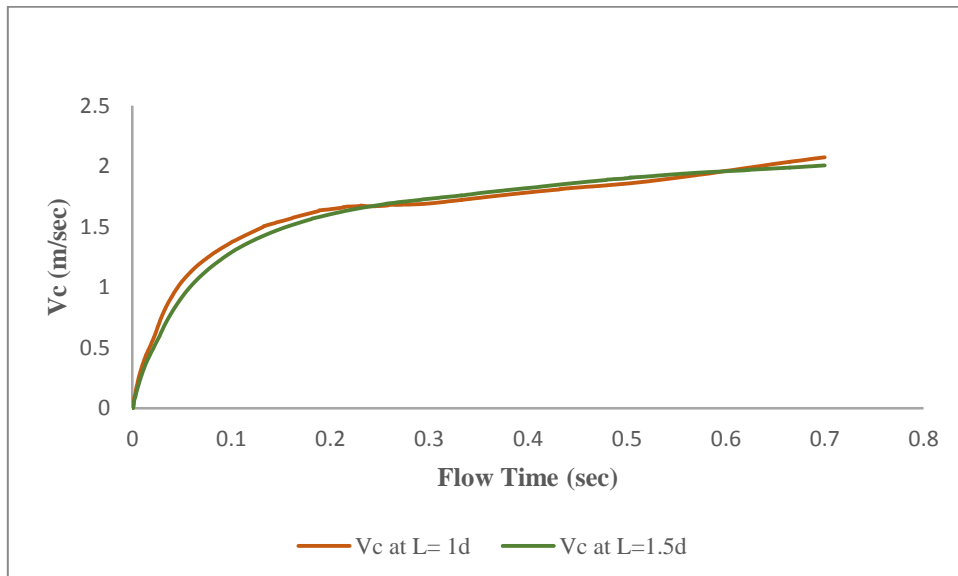


Figure 4.43 The effect of a capsule length on capsule velocity history for an equi-density rectangular capsule for $k = 0.5$ and $V_{av} = 2\text{m/sec}$

4.5.3. Capsule Density Effects

Figure 4.44 displays the static gauge pressure and flow velocity magnitude variations in transporting of a heavy-density rectangular capsule for $k = 0.5$, $L_c = 1d$ at $V_{av} = 4\text{m/sec}$ at different flow times. The pressure at the upstream is 17650Pa during $t = 0.05\text{sec}$, which is 18% higher than the upstream pressure for an equi-density capsule with the same parameters. The trend of pressure distribution is the same as observed for an equi-density cylindrical capsule. The pressure drop has reached to 11775Pa for the case of heavy-density capsule recording an increase of about 3% compared to the case of equi density capsule at the same conditions. This can be explained by the additional resistance of the heavy capsule to the flow. Furthermore, it can be obviously observed in figure 4.44 (b) the capsule velocity has become slower than the equi-density capsule due to the increase in the capsule weight.

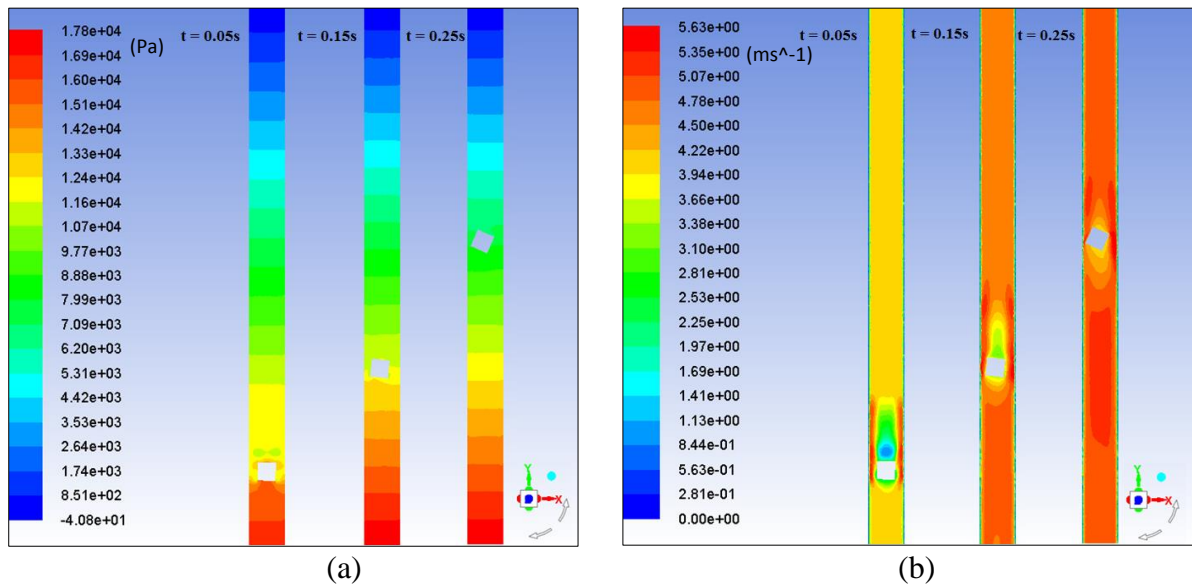


Figure 4.44 (a) Static gauge pressure and (b) Flow velocity magnitude variations for a heavy density rectangular capsule of $k = 0.5$, $L_c = 1d$ and $V_{av} = 4\text{m/sec}$ at different flow times

Figure 4.45 shows the pressure drop variations along the test section of the pipe. It can be observed that the pressure drop markedly fluctuates through the capsule motion in the pipe. The results indicate that the pressure drop for a heavy density capsule ($s = 1.7$) is considerably higher than in the case of an equi-density capsule ($s = 1$). Moreover, the pressure drop distribution in the pipeline is similar for both the cases. More detailed results on the pressure drop across the test section of the pipe are provided in Appendix A-5.

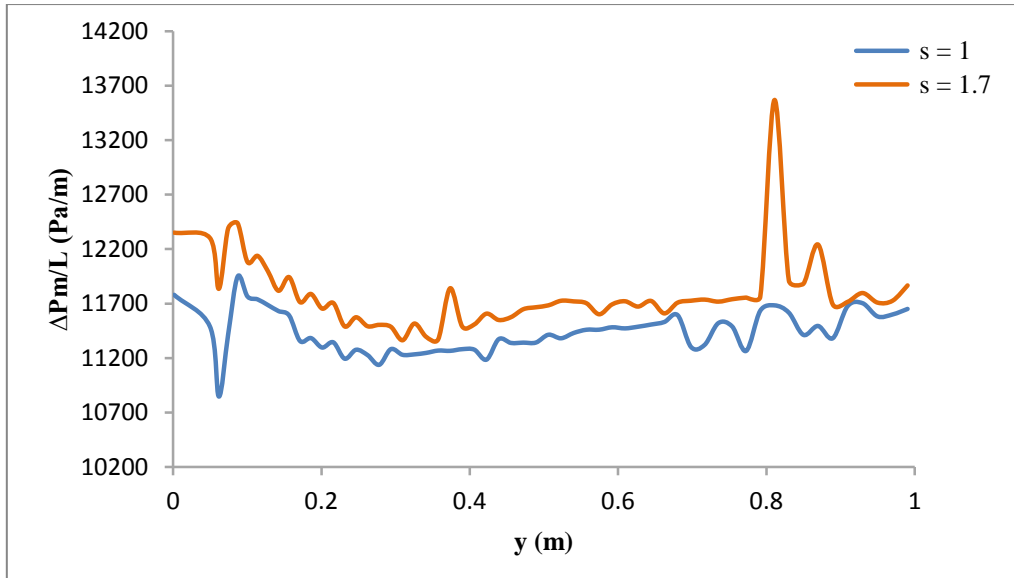


Figure 4.45 The effect of capsule density on the pressure drop variation for a heavy density rectangular capsule of $k = 0.5$ and $L_c = 1d$ at $V_{av} = 4m/sec$

Figure 4.46 depicts time history of the rectangular capsule velocities at an average velocity of 4m/s for different densities. It can be obviously seen that the capsule velocity for a heavy density capsule ($s = 1.7$) is less than the capsule velocity for equi-density capsule ($s = 1$). Moreover, it can be concluded that the capsule velocity decreases as the capsule density increases. The velocity of the equi-density capsule when reaches to a steady flying velocity is exceed the water flow velocity, whereas the velocity of heavy density capsule is less than the water flow velocity.

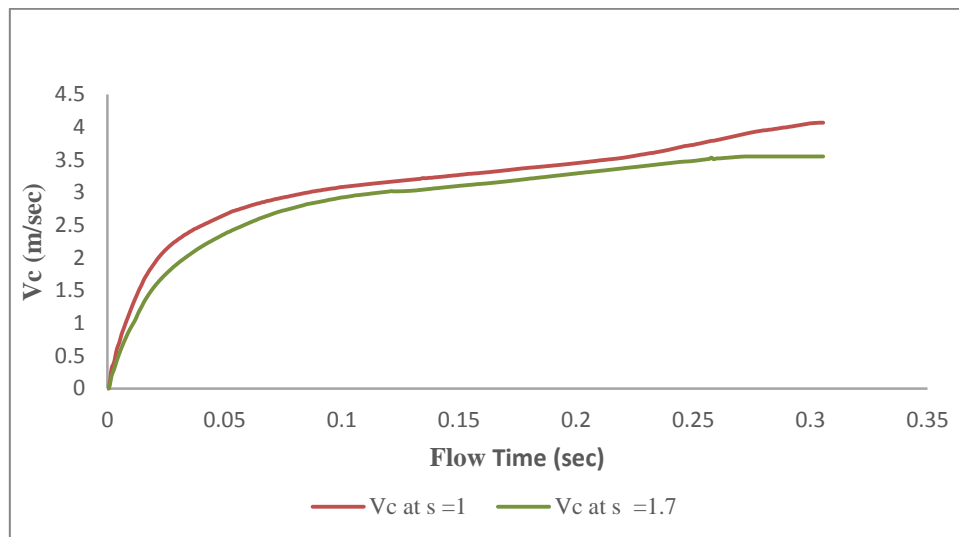


Figure 4.46 The effect of capsule density on capsule velocity history for a heavy density rectangular capsule of $k = 0.5$ and $L_c = 1d$ at $V_{av} = 4m/sec$

4.5.4 Effect of Capsule Diameter

Figure 4.47 depicts the static gauge pressure and flow velocity distribution for a heavy density rectangular capsule of $L_c = 1d$, $k = 0.6$ at $V_{av} = 4\text{m/sec}$ during different flow times. The distribution of the pressure is the same as seen for $k = 0.5$ at same average flow velocity and the same capsule length. However, the pressure upstream of the capsule during 0.05sec of the capsule motion has increased by 2.9% as compared to the pressure upstream in the case of $k = 0.5$ at the same time. Moreover, the distribution of the flow velocity magnitude is the same as shown in the case of $k = 0.5$ at the same flow velocity and for the same length of the capsule. It is observed that the time takes the capsule to cross the test section of the pipe is slightly longer as compared to $k = 0.5$.

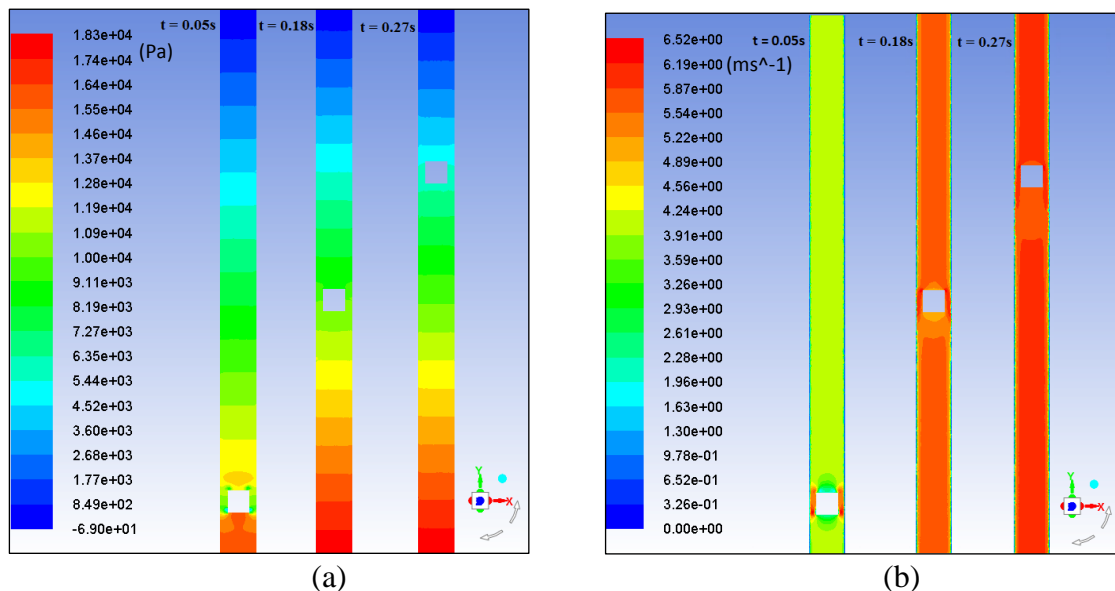


Figure 4.47 (a) Static gauge pressure and (b) Flow velocity magnitude variations for a heavy density rectangular capsule of $k = 0.6$, $L_c = 1d$ and $V_{av} = 4\text{m/sec}$ at different flow times

Figure 4.48 illustrates the pressure drop variations along the test section of the pipe at the same average flow velocity 4m/sec. It can be observed that the pressure drop markedly fluctuates through the capsule motion in the pipe. The results indicate that the pressure gradients recorded through a capsule motion of $k = 0.6$ remarkable change as compared to the pressure drop for $k = 0.5$. Further detailed findings have been provided in appendix A-5.

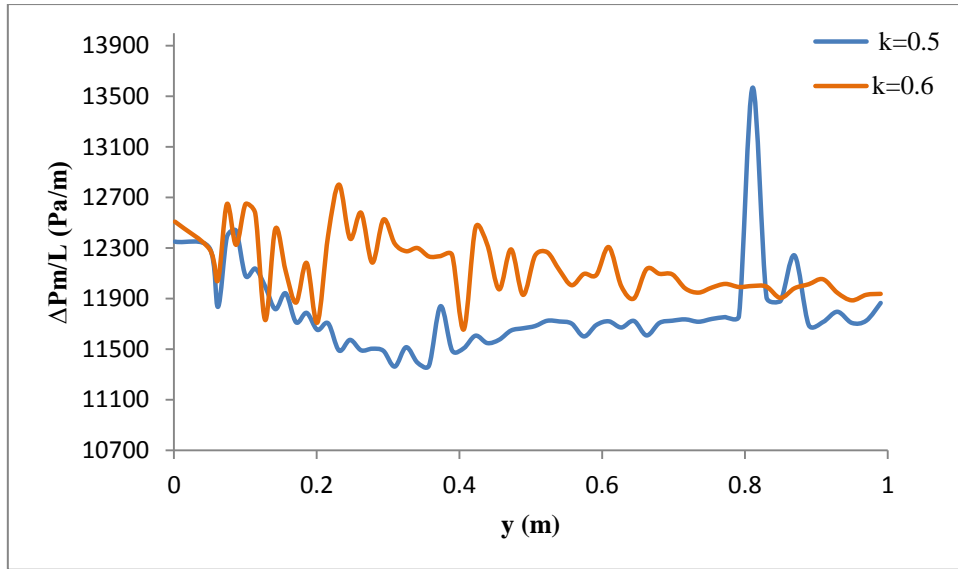


Figure 4.48 The effect of capsule diameter on the pressure drop variation for a heavy density rectangular capsule at $V_{av} = 4\text{m/sec}$ and $L_c = 1d$

Figure 4.49 shows a time history of rectangular capsule velocity starting from rest until the capsule reaches nearly the steady velocity for different capsule diameters at an average velocity of 4m/sec. This can be clearly noticed that the capsule velocity for $k = 0.6$ is slightly higher than of $k=0.5$. Afterwards, the capsule velocity tends to be steady.

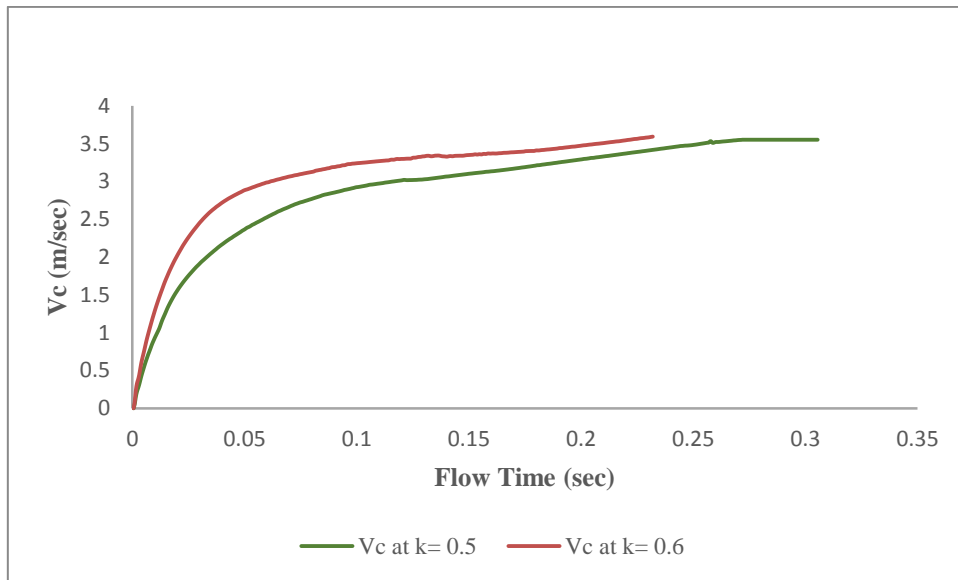


Figure 4.49 The effect of capsule diameter on capsule velocity history for a heavy density rectangular capsule at $V_{av} = 4\text{m/sec}$ and $L_c = 1d$

4.5.5. Effect of Capsules Concentration

Figure 4.50 shows the static gauge pressure and flow velocity magnitude variations in a pipeline carrying two equi-density rectangular capsules of $V_{av} = 2\text{m/sec}$, $L_c = 1d$ and $k = 0.5$, and at different flow times. The pressure variation trend is the same as noticed for a one equi-density rectangular capsule. The pressure at the upstream position during $t = 0.05\text{sec}$ has increased to 15185Pa (1.45 %) as compared to a single equi-density rectangular capsule at the same flow time. Hence, the overall pressure drop has increased by 0.15% for $N = 2$ in comparison with $N = 1$. Moreover, the results show almost the same distribution for the velocity regardless the number of the capsules. Increasing the solid phase concentration within the pipeline provides further resistance to the flow and reducing the flow velocity.

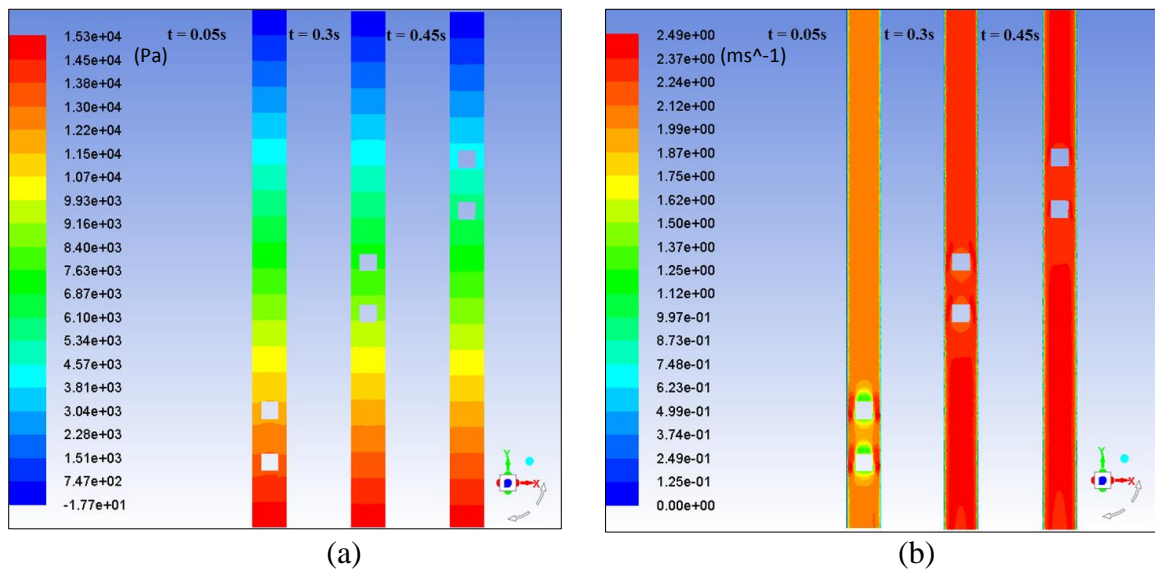


Figure 4.50 (a) Static gauge pressure and (b) Flow velocity magnitude variations for two equi-density rectangular capsules of $k = 0.5$, $L_c = 1d$ and $V_{av} = 2\text{m/sec}$ at different flow times

Figure 4.51 shows the pressure drop variations along the test section of the pipeline. It can be seen that the pressure drop markedly fluctuates through the capsule motion in the pipe. This can be clearly observed through the change of the capsules position that resulted from the rotational and transient motion of the capsules flow. The results indicate that the pressure gradients recorded through the motion of two equi-density rectangular capsules are slightly higher than the pressure drop for a single rectangular capsule. This is because the concentration of the solid phase inside the pipe is more in the case of $N = 2$ as compared to a single capsule.

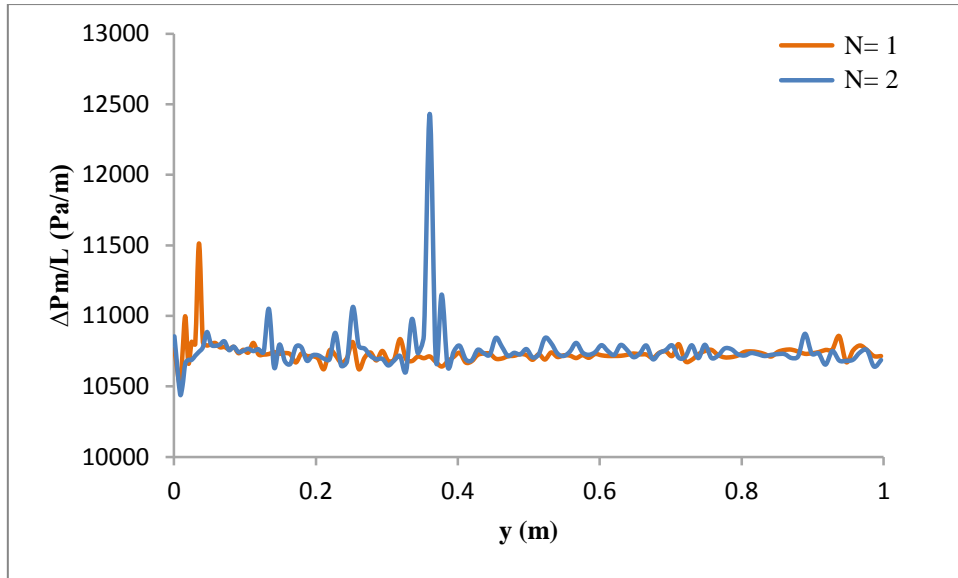


Figure 4.51 The effect of capsule concentration on the pressure drop variation for two equi-density rectangular capsules of $k=0.5$ and $L_c=1d$ at $V_{av}=2\text{m/sec}$

Figure 4.52 depicts time histories of the capsule velocity for two equi-density rectangular capsules at an average velocity of 2m/sec. It can be obviously seen that the first capsule velocity is greater than the second capsule during a period due to the first capsule is subject to the maximum forces from the water, and its hydraulic characteristics are more complex than for the second capsule. Afterwards, the second capsule velocity starts increasing till exceed the first capsule velocity. The velocity profile is very similar to each of the capsules.

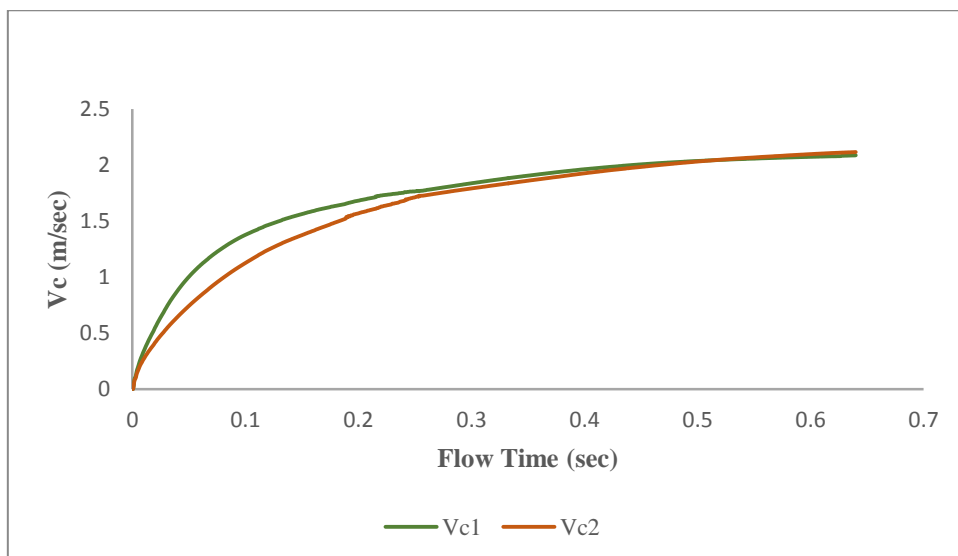


Figure 4.52 The effect of capsule concentration on capsule velocity history for two equi-density rectangular capsules of $k=0.5$ and $L_c=1d$ at $V_{av}=2\text{m/sec}$

4.6. Development of a Mathematical Relation for a Shape Factor

Based on the various shapes of capsules considered in the present study, a shape factor (\emptyset) has been defined to reflect the variations in the shape of the capsules. The shape factor formulation used in the literature is only appropriate for spherical and cylindrical shapes [20], whereas the shape factor for a cylindrical and rectangular shape gives the same value. Therefore, it is necessary to find another formulation to distinguish between the cylindrical and rectangular shapes. Hence, a novel formulation for shape factor in this study has been developed for any capsule shape. The shape factor has been defined as a surface area ratio of the capsule to the mid-plane cross sectional area of a sphere that has the same hydraulic diameter as the capsule.

$$\emptyset = \frac{\text{Surface area of capsule}}{\text{Cross sectional area of a sphere has the same capsule hydraulic diamtere}} \quad (4-1)$$

It can be observed that the shape factor of the spherical capsules is 4. Thereby, for a cylindrical capsule of length equal to its diameter (i.e. $L_c = 1d$), the shape factor is 6. Furthermore, as the shape of the capsule changes to rectangular, the shape factor further increases to 7.63 (for $L_c = 1d$). It can be concluded that the shape factor increases as the capsule's sphericity decrease. From this formulation can compute the shape factor for the capsule shapes, and the effect of this parameter on the development of prediction models that can be used in the design of vertical HCPs.

4.7. Development of Prediction Models

According to the results obtained from dynamic mesh techniques to prediction models for both the capsule velocity and the friction coefficient in vertical HCPs. The capsule shapes included in this investigation have been involved in the formulation of prediction models.

Using analysis of multiple variable regressions, semi-empirical relationships for predicting capsule velocity and friction coefficient owing to capsules, as a function of flow variables and geometric, have been developed.

4.7.1 Capsule Velocity Prediction Model

The capsule velocity for different densities in a vertical pipe can be expressed as:

$$\frac{V_c}{V_{av}} = \frac{(1.76 \phi^{0.0514})}{(s + 1)^{0.9}} \quad (4-2)$$

Then:

$$V_c = \frac{(1.76 \phi^{0.0514} V_{av})}{(s + 1)^{0.9}} \quad (4-3)$$

Equation- 4-3 shows that the velocity of capsule is affected by the average flow velocity, the specific gravity and the shape factor of the capsules. Holdup (V_c/V_{av}) has been plotted in figure (4.53) showing that all data points lying within ± 10 percentage of the present model equation is well capable of predicting holdup. Hence, the prediction model developed here represents the holdup in a vertical pipeline with reasonable accuracy.

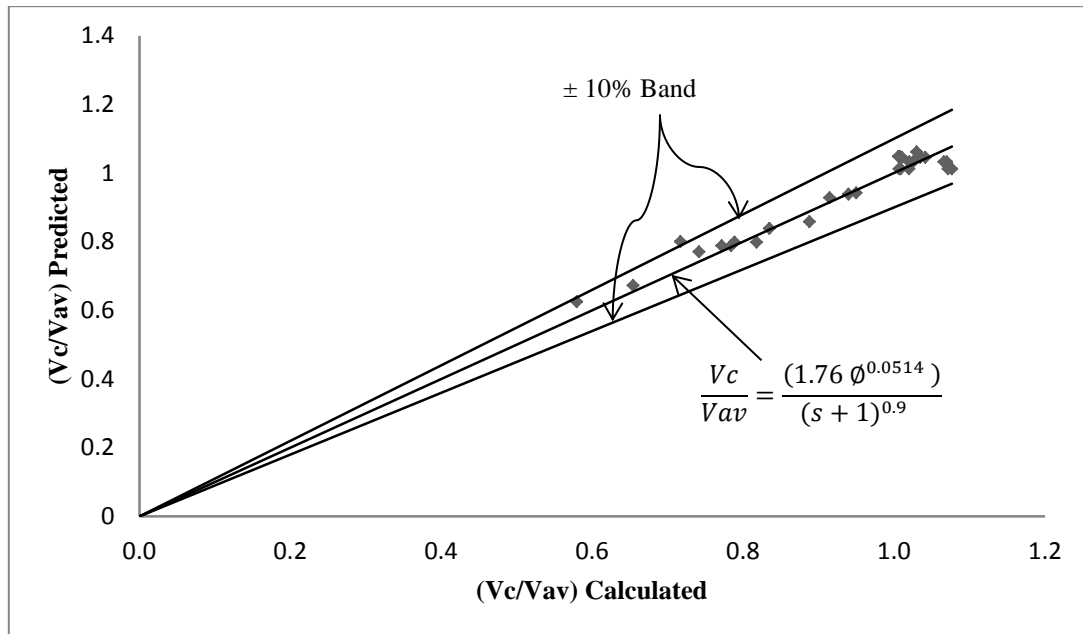


Figure 4.53 The holdup for any shape of capsules

4.7.2 Friction Coefficient Prediction Model

The friction coefficient for fluid flow [67] and the flow of the capsule can be computed via the follows formulations:

$$f_w = 0.0055 + \frac{0.55}{R_w^{\frac{1}{3}}} \quad (4-4)$$

and:

$$f_c = 2D \frac{\left(\frac{\Delta P_m}{L_p} - \frac{\Delta P_w}{L_p}\right)}{\rho_w L_p V_{av}^2} \quad (4-5)$$

The friction coefficient for equal and heavy density capsules in a vertical pipe can be calculated as follows:

$$f_c = \frac{\left(10^{6.17} \phi^{0.567} \left(N * \frac{LC}{L}\right)^{0.43} k^{1.767}\right)}{Re_c^{1.398} (s+1)^{0.5}} \quad (4-6)$$

It can be obviously observed from figure 4.54 that approximately 80% of the data points lying within ± 20 percentage of the best-fit curves, which shows good fitting of the present model equation. While the correlation coefficient shows the strength of the linear relationship between predicted and calculated data. The prediction model that has been developed here represents the friction coefficient because of the capsules presence in vertical pipelines with appropriate precision.

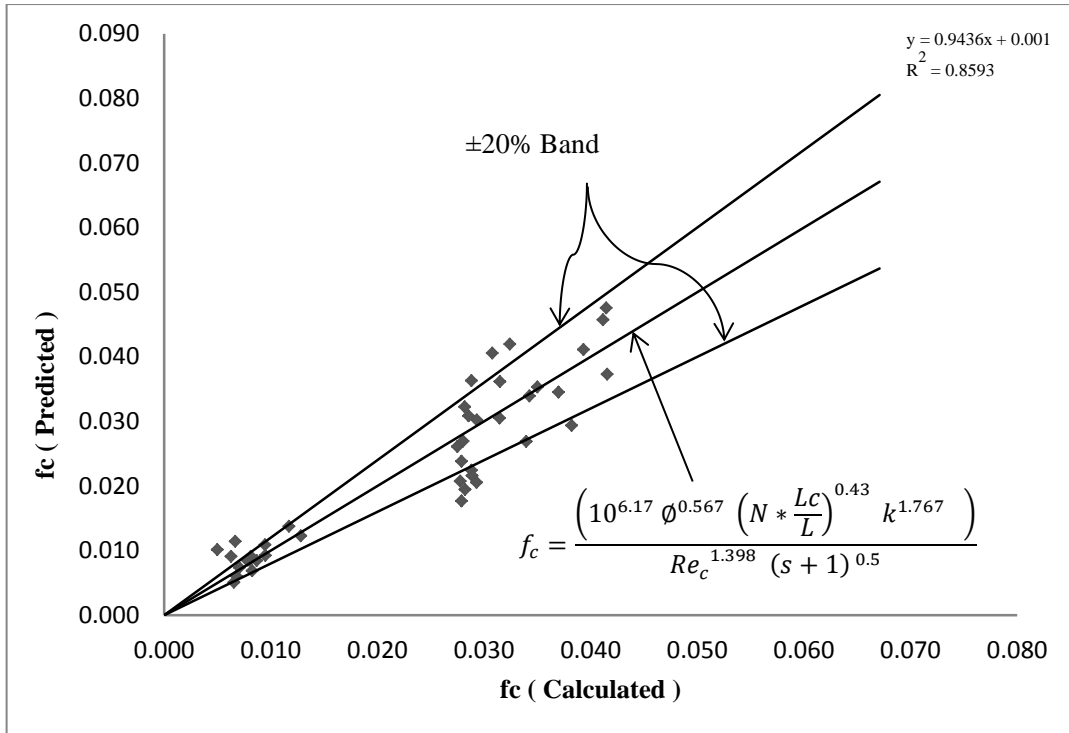


Figure 4.54 Friction coefficient for any shape of capsules

Based on these observations, it can be concluded in this chapter that the prediction model developed can be utilised for different conditions of the flow of capsules across vertical pipes. Moreover, the prediction model developed here will be used in the optimal design of a vertical HCP in Chapter 6.

4.8 Summary

The main aim of this chapter was to study the hydrodynamics of capsule flow in vertical hydraulic pipelines, and to investigate the effects of flow and geometric parameters upon the capsule velocity and pressure drop. A summary of the main findings from the flow analysis of the capsules is:

- There is a reasonable agreement between CFD findings with experimental data. Thereby, the numerical model can be utilised for further investigation with different configurations.
- The general trend was that the capsule velocity and pressure drop increases with an increase in the average velocity of the flow.

- Increasing in the diameter of the capsules leads to increase the pressure drop and capsule velocity in the pipe.
- The square and rectangular capsules travel faster than a cylindrical or spherical capsule.
- The increase in the capsules length leads to increase the pressure drop and decrease the capsule velocity in the pipeline.
- The increase in the density of the capsule leads to increase the pressure drop and decrease the capsule velocity.
- The increase in the capsules concentration leads to increase the pressure drop and decrease the capsule train velocity in the pipeline.

This chapter provides information about the flow of basic capsules shapes, and the prediction models established for both the capsule velocity and the friction coefficient of capsules. For transporting mixed capsules shapes in vertical HCPs, the next chapter will provide more details on the findings obtained from CFD modelling in respect to the flow of mixed capsules shapes in these applications.

Chapter 5 - Flow Diagnostics in HCPs Transporting Mixed Capsules Shapes

The results from CFD simulations have been displayed in this chapter, concerning the transport of mixed shapes of capsules within pipes. Quantitative and qualitative unsteady analyses have been undertaken for sake to understand the flow behaviour of the mixed capsule in vertical HCPs. The effect of the simple and complex combination of the basic capsule shapes, based on the position order of capsules on a flow field in a pipeline has been investigated. Moreover, a semi empirical correlation has been developed to calculate the correction factor as a function of the pressure drop.

5.1 Simple Combination Analysis of an Equi-Density Capsules Flow

Many studies have been conducted giving a detailed review of hydraulic capsule transport in general. However, most of those studies concern steady state flow and very few are known about transient water flow caused by the capsule motion. As we can see from the literature that all the researches have focused on transporting the capsule shapes separately on each other within pipelines.

Furthermore, no studies regarding a combination of capsule shapes flowing within the pipeline have been investigated. It is important to analyse the flow of a capsule train, consisting of mixed capsule shapes, because in real world scenarios, the capsule trains often comprise of mixed shaped capsules. Therefore, this investigation is concerning the combination flow of basic capsule shapes in vertical HCPs. The simple combination consists from two different shapes of the capsules. In addition, the distancing among the capsules was constant i.e. equal to two diameters of the capsule, in order to avoid numerical complications. The order impact of the different shapes of capsules on the flow field with keeping all other parameters constant are considered in this investigation.

5.1.1 Effect of the Position of the Capsule Shape in the (SC) order

Figure 5.1 shows the static gauge pressure and flow velocity magnitude variations within a hydraulic pipe carrying a spherical capsule (S) and another cylindrical capsule (C) of $k = 0.5$, $L_c = 1.5d$ at $V_{av} = 2\text{m/sec}$. It can be seen in order of (SC) that the simple capsule train will collide with each other at 0.18sec. As observed that the trend of the pressure gradient has been changed due to the collision of capsules. Consequently, the system of a mixed capsule shapes impacts on the pipeline's pressure drop.

The pressure at the upstream point has increased at the collision of capsules to 18086Pa (16%) as compared to the pressure at the initial motion of the capsule train at 0.03sec. Furthermore, in figure 5.1(b) shows that the velocity of the flow in the annulus area is 2.87m/sec at 0.03sec, which then increases to 3.20m/s (by 10%) at 0.18sec, which is the instance when the cylindrical capsule collides with the spherical capsule.

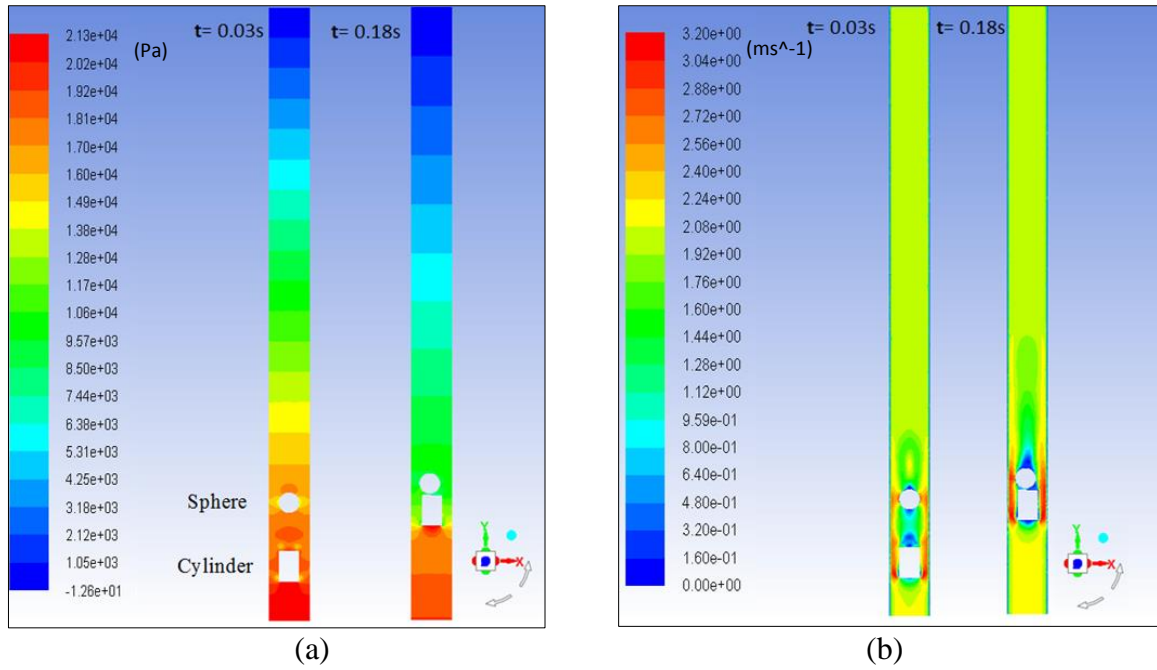


Figure 5.1(a) Static gauge pressure and (b) Flow velocity magnitude variations for capsules in the (SC) order of $k = 0.5$, $L_c = 1.5d$ and $V_{av} = 2\text{m/sec}$ at different flow times

Figure 5.2 presents the variances in $\Delta P_m/L$ and $\Delta P_c/L$ along test section for the case considered. The findings indicate that the mixture pressure drop is greater than the pressure drop due to capsule train only. It is for this reason that the pressure drop for capsules has been plotted on the secondary Y axis of the graph as the scale is in notable contrast for both pressure gradients. Moreover, the trend of the pressure drop for both follows the same behaviour. This can be obviously noticed in the figure that the collision of the capsules significantly enhances the pressure drop throughout the pipe.

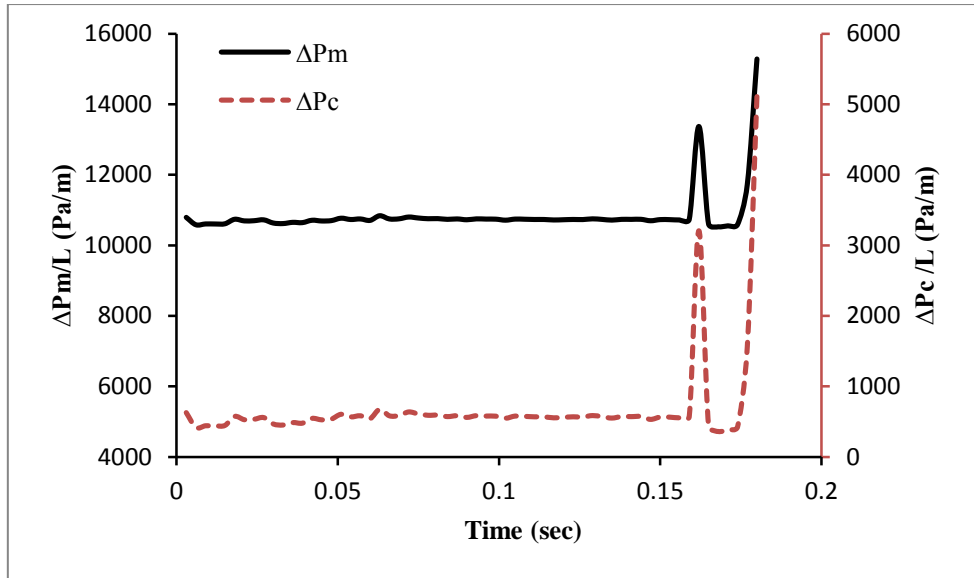


Figure 5.2 Variations in mixture pressure drop and capsules pressure drop, for two capsule flow in the (SC) order of $k = 0.5$, $L_c = 1.5d$ and $V_{av} = 2\text{m/sec}$

Figure 5.3 depicts the time histories of capsules velocities in an (SC) order at flow velocity 2m/sec. It can be clearly noticed that the cylindrical capsule velocity is higher than the spherical capsule velocity. Hence, the cylindrical capsule is travelling faster than the spherical capsule, however, their velocities is less than the water flow velocity.

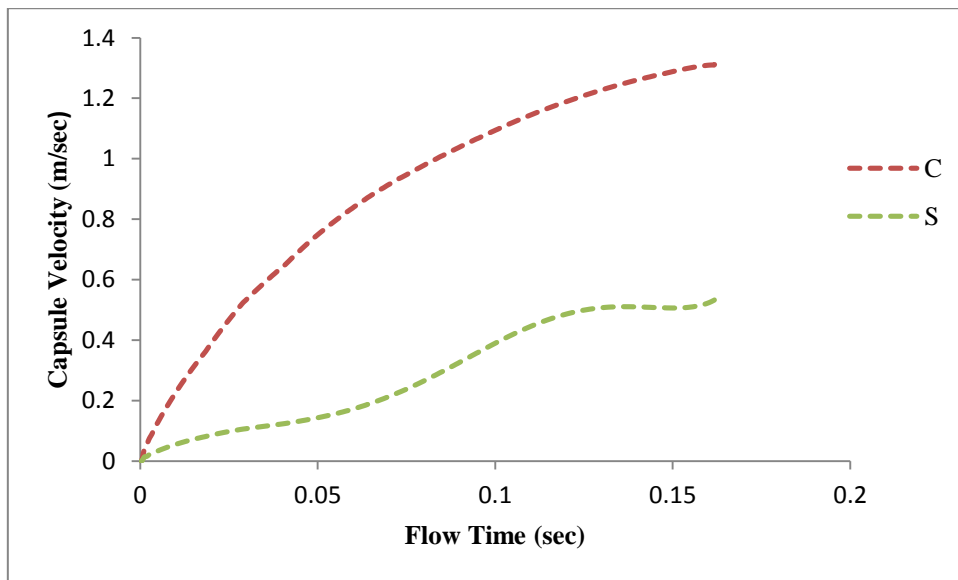


Figure 5.3 The effect of capsules in the (SC) order on the capsules velocity history

5.1.2 Effect of the Position of the Capsule Shape in the (CS) order

Figure 5.4 displays the static gauge pressure and flow velocity distribution within a hydraulic pipe carrying a cylindrical capsule (C) and spherical capsule (S) in an (CS) order of $k = 0.5$, $L_c = 1.5d$ at $V_{av} = 2\text{m/sec}$. It is evident in this order of (CS) that the capsule train does not collide with each other as compared with the (SC) order. Therefore, the trend of the pressure distribution is different with what has observed in the order of (SC). The pressure at the upstream of the capsules is about 15170Pa , which is 0.38% higher than the upstream pressure observed in case of (SC) order. Furthermore, the results show almost the same velocity distribution regardless the order of capsules. However, the only difference observed is the capsule behaviour and its location. It is found that the cylindrical capsule travels faster than the spherical capsule, thus there is no collision in this order of (CS).

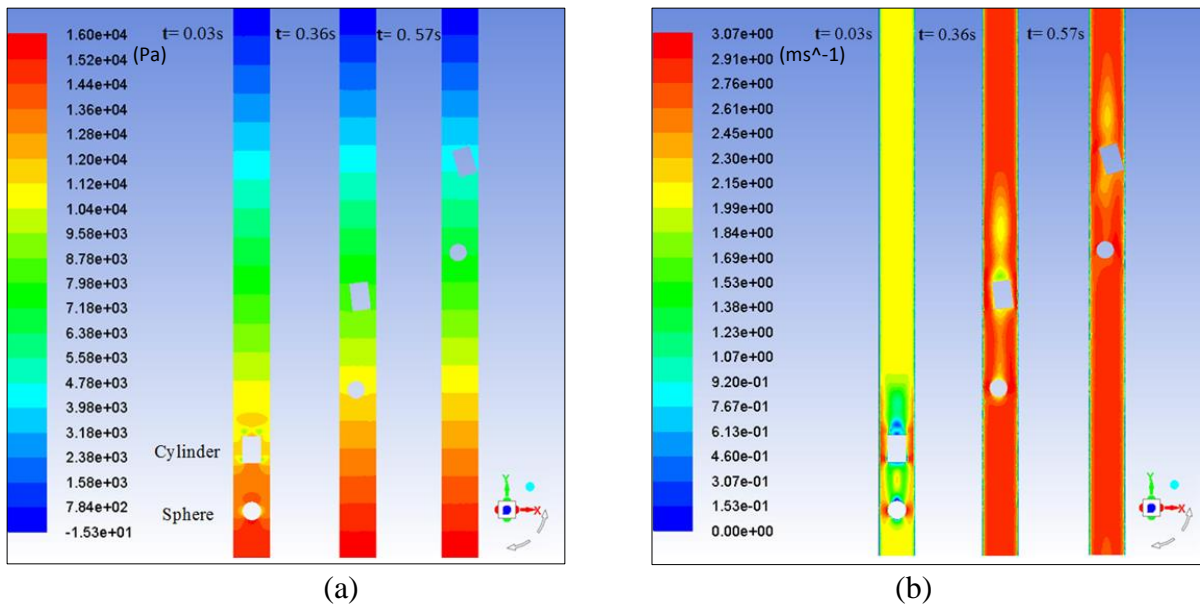


Figure 5.4 (a) Static gauge pressure and (b) Flow velocity magnitude variations for capsules in the (CS) order of $k = 0.5$, $L_c = 1.5d$ and $V_{av} = 2\text{m/sec}$ at different flow times

Figure 5.5 depicts the time histories of capsules velocities in an (CS) order at flow velocity 2m/sec . It has been clearly noticed that the cylindrical capsule velocity is higher than the spherical capsule velocity. However, the cylindrical capsule represents the second capsule in the order in the vertical pipeline. This is due to the surface area of cylindrical capsule that facing the flow direction is larger than the spherical capsule.

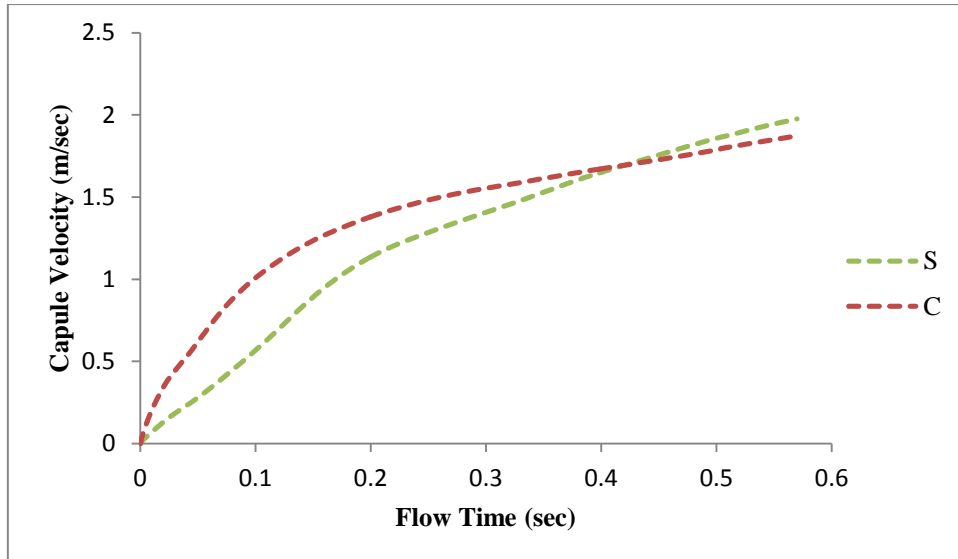


Figure 5.5 The effect of capsules in the (CS) order on the capsule velocity history

5.1.3 Effect of the Position of the Capsule Shape in the (RS) order

Figure 5.6 depicts the static gauge pressure variation and flow velocity distribution in a vertical pipeline conveying a rectangular capsule (R) and spherical capsule (S) in an (RS) order of $k = 0.5$, $L_c = 1.5d$ and $V_{av} = 2\text{m/sec}$. Note that the pressure distribution trend appears to be the same as the field of pressure in the order (CS) in the previous section. Pressure rate has reduced slightly in the upstream location to 15080Pa (0.61 %) at $t = 0.03$ sec as compared to the (CS) order at the same flow time.

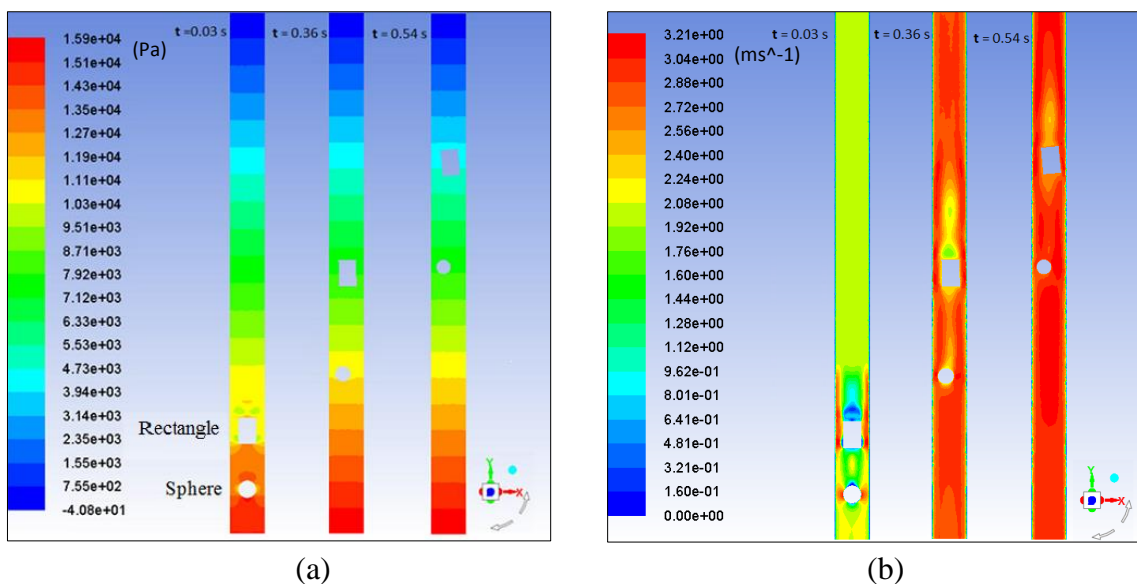


Figure 5.6 (a) Static gauge pressure and (b) Flow velocity magnitude variations for capsules in the (RS) order of $k = 0.5$, $L_c = 1.5d$ and $V_{av} = 2\text{m/sec}$ at different flow times

Furthermore, the results show almost the same velocity distribution regardless the order of capsules between (RS) and (CS). However, the only difference observed is the capsule behaviour and its location. The rectangular capsule travels faster than the spherical capsule, thus there is no collision in this order of (RS).

Figure 5.7 shows the time histories of capsules velocities in an (RS) order at flow velocity 2m/sec. From here can be clearly noticed that the rectangular capsule velocity is higher than the spherical capsule velocity. However, the rectangular capsule represents the second capsule in the order in the vertical pipeline. This due to the surface area of rectangular capsule that facing the flow direction is larger than the spherical capsule. Hence the lift force acting on the rectangular capsule is greater than the lift force on the spherical capsule. The wake region for the rectangular capsule is greater than the spherical capsule due to a higher attack angle, which consequently leads to vortex formation and pressure loss as a result of pressure drag and then increases the capsule velocity.

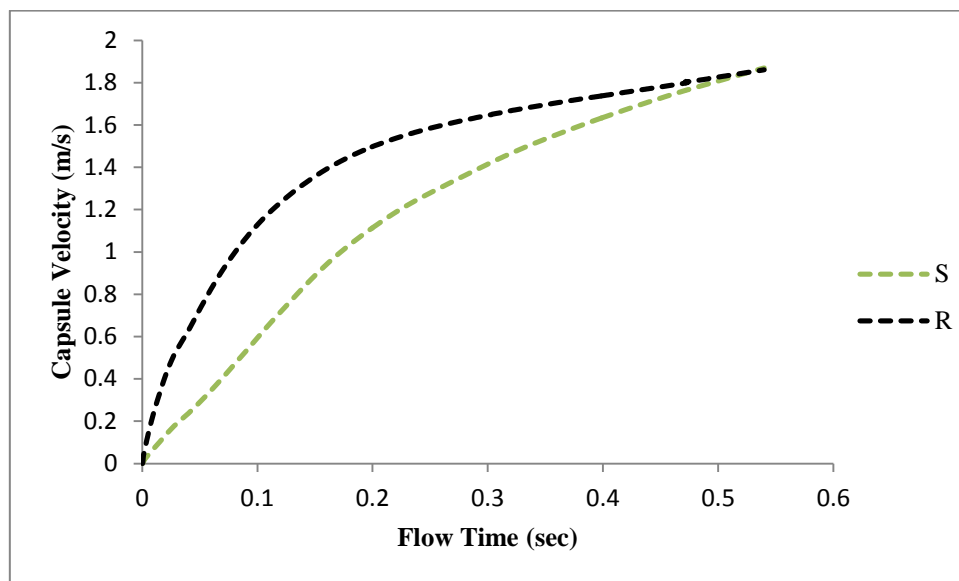


Figure 5.7 The effect of capsules in an (RS) order on capsule velocity history

5.1.4 Effect of the Position of the Capsule Shape in the (SR) order

Figure 5.8 illustrates the static gauge pressure and flow velocity magnitude distribution within a vertical pipeline conveying a spherical capsule (S) and another rectangular capsule (R) of $k = 0.5$, $V_{av} = 2\text{m/sec}$ and $L_c = 1.5d$. From here can be seen in an order of (SR) that

the capsule train will collide with one another at 0.21sec. As observed with the collision of capsules the trend of the pressure distribution has been changed. Consequently, the system of a mixed capsule shapes is unstable without precise position control. Furthermore, in figure 5.8(b) shows the distribution of the velocity field within the pipeline resembles the field of velocity for the capsule train in the (SC) order as shown in figure 5.1b.

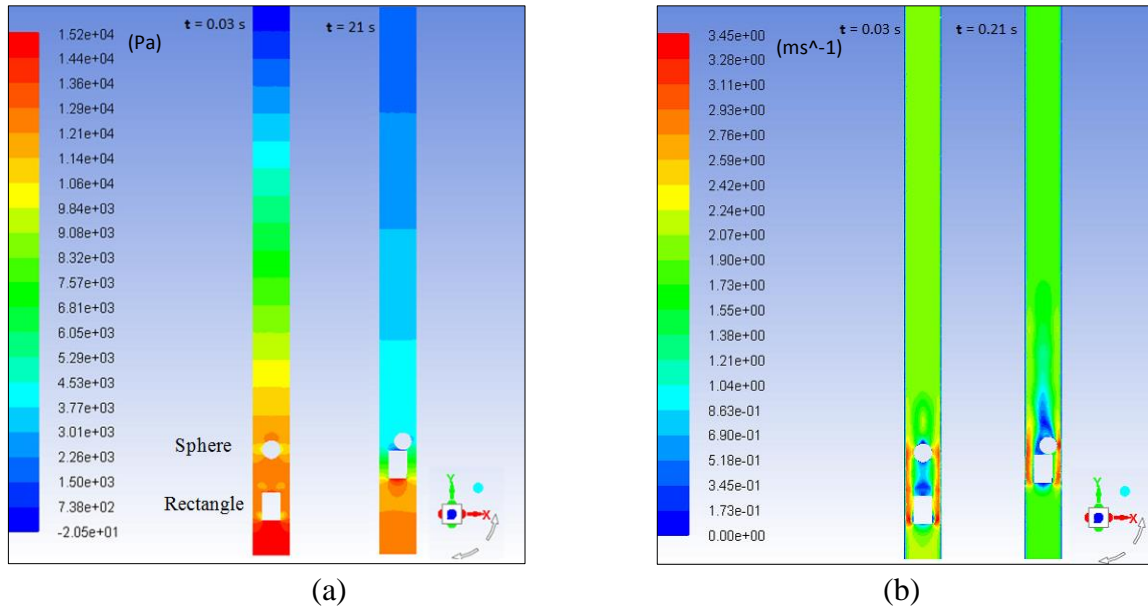


Figure 5.9 illustrates the time histories of capsules velocities in an (SR) order at flow velocity 2m/sec. It has been clearly noticed that the rectangular capsule velocity is higher than the spherical capsule velocity. Hence, the rectangular capsule travelling faster than the spherical capsule. This due to the surface area of rectangular capsule that facing the flow direction is larger than the spherical capsule. However, both of them their velocity is less than the water flow velocity. Moreover, from here it is observed that the velocity profile for the (SR) order resembles the velocity profile observed in case of (SC) order (figure 5.3).

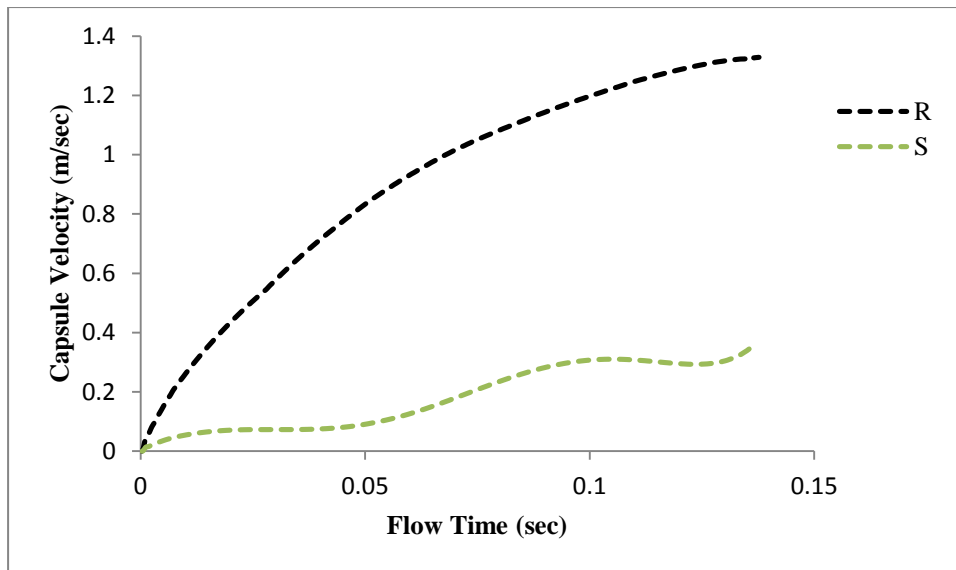


Figure 5.9 The effect of capsules in the (SR) order on the capsule velocity history

5.1.5 Effect of the Position of the Capsule Shape in the CR order

Figure 5.10 shows the static gauge pressure and flow velocity distribution across a hydraulic pipe carrying a cylindrical capsule (C) and another rectangular capsule (R) of $k = 0.5$, $V_{av} = 2\text{m/sec}$ and $L_c = 1.5d$. From here it is observed in this order of (CR) that the capsule train will collide with one another at 0.24sec. As observed with the collision of capsules the trend of the pressure distribution has been changed. Moreover, It can be noticed in figure 5.10 (b) that when the capsules within capsule train collide with each other that the flow velocity in the annulus area is increased significantly, while a large wake area exists downstream of the capsules train.

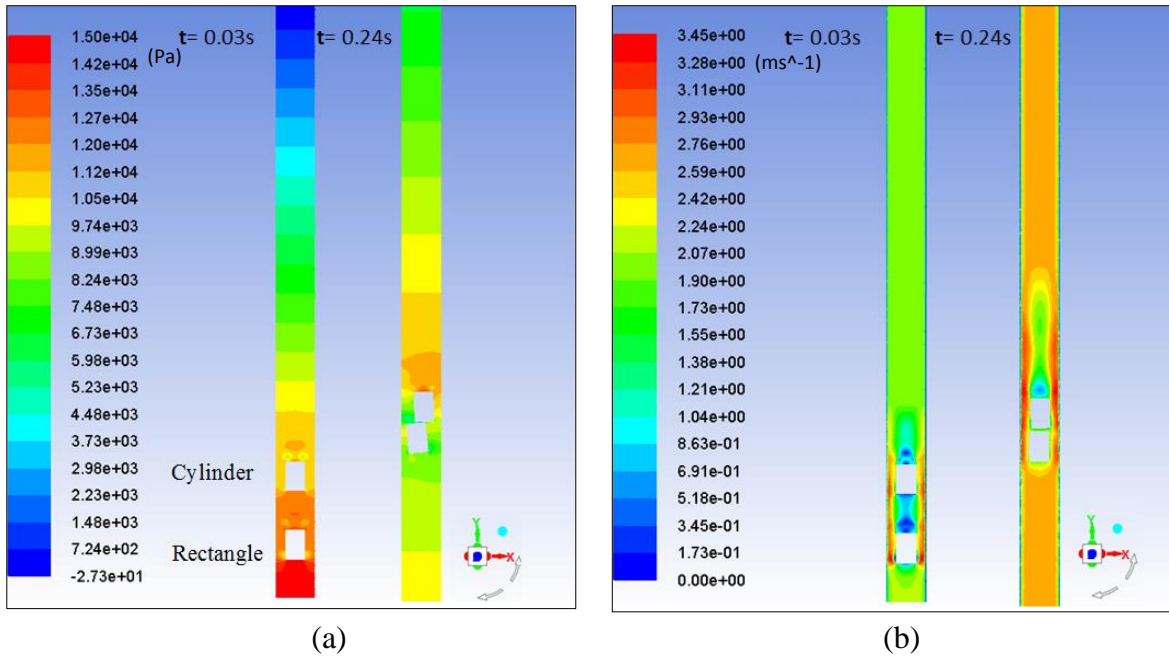


Figure 5.10 (a) Static gauge pressure and (b) Flow velocity magnitude variations for capsules in the (CR) order of $k = 0.5$, $L_c = 1.5d$ and $V_{av} = 2m/sec$ at different flow times

Figure 5.11 illustrates the time histories of capsules velocities in an (CR) order at flow velocity $2m/sec$. One can clearly note that the rectangular capsule velocity is greater than the cylindrical capsule velocity. Hence, the rectangular capsule travelling faster than the cylindrical capsule. This due to the surface area of rectangular capsule that facing the flow direction is larger than the cylindrical capsule. However, both of them their velocity is less than the water flow velocity.

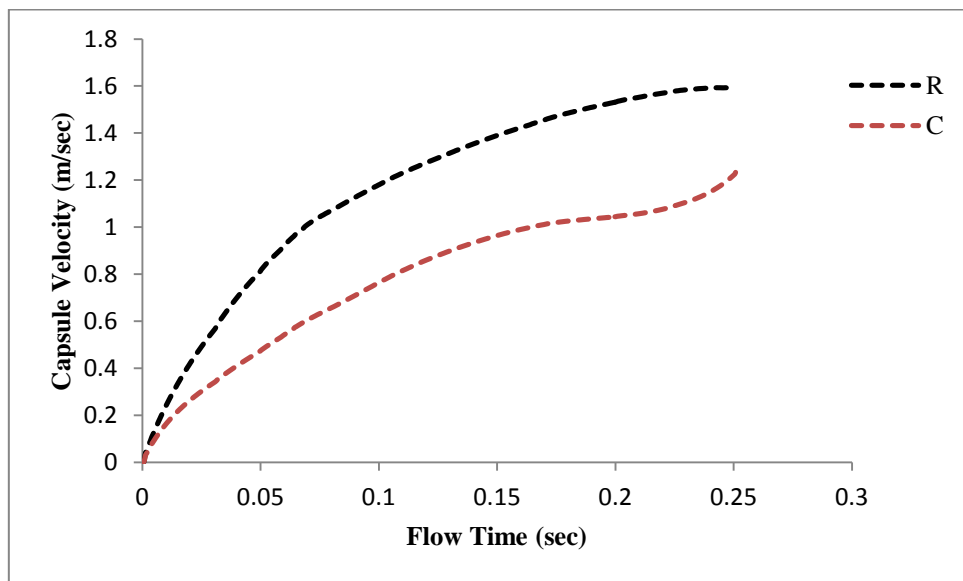


Figure 5.11 The effect of capsules in the (CR) order on the capsule velocity history

5.1.6 Effect of the Position of the Capsule Shape in the RC order

Figure 5.12 shows the static gauge pressure as well as flow velocity distributions inside a pipeline conveying rectangular and cylindrical capsule of $k = 0.5$, $L_c = 1.5d$ and $V_{av} = 2\text{m/sec}$ at different flow times. The trend of the pressure distribution is different as compared to an (CR) order due to the collision that is occurred in the (CR) order. It can be noted that the pressure in front of the capsule train at 0.03sec is 15165Pa, then after the capsule train motion at 0.5sec the in front pressure decreases by 50%. Moreover, the results show almost the same velocity distribution regardless the order of capsules between (RC) and (CR). However, the only difference observed is the capsule behaviour and its location. The rectangular capsule travels faster than the cylindrical capsule, thus there is no collision in this order of (RC).

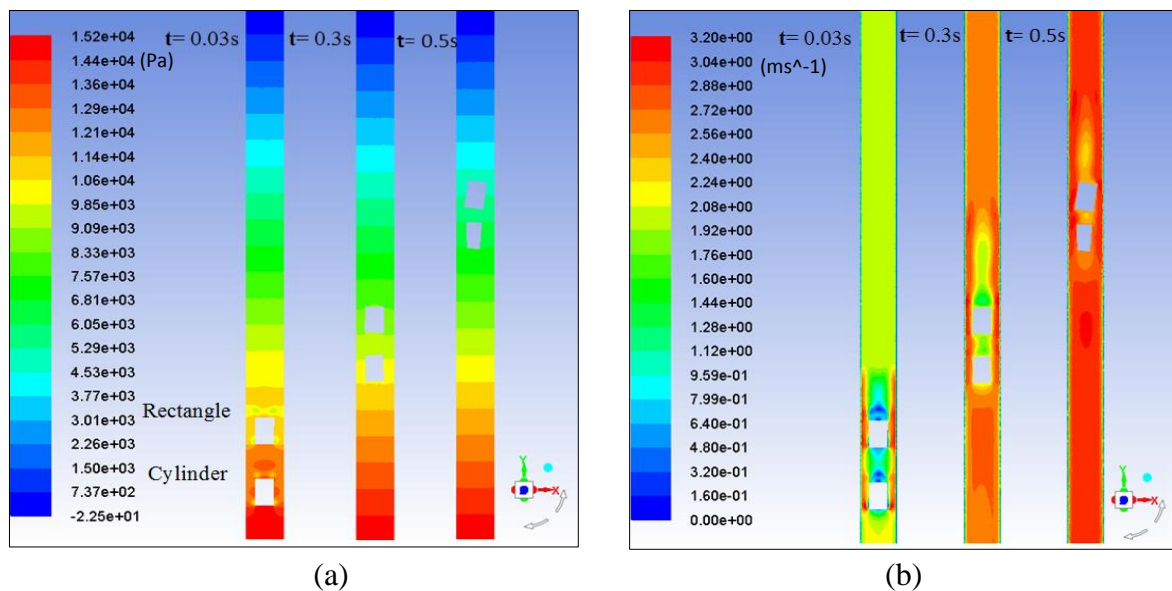


Figure 5.12 (a) Static gauge pressure and (b) Flow velocity magnitude variations for capsules in the (RC) order of $k = 0.5$, $L_c = 1.5d$ and $V_{av} = 2\text{m/sec}$ at different flow times

Figure 5.13 indicates the time histories of capsules velocities in an (RC) order at flow velocity 2m/sec. it has been clearly noticed that the rectangular capsule velocity is higher than the cylindrical capsule velocity. However, the rectangular capsule represents the second capsule in the order in the vertical pipeline. This due to the surface area of rectangular capsule that facing the flow direction is larger than the spherical capsule. Hence, the lift force affecting on the rectangular capsule is greater than the lift force on the cylindrical capsule.

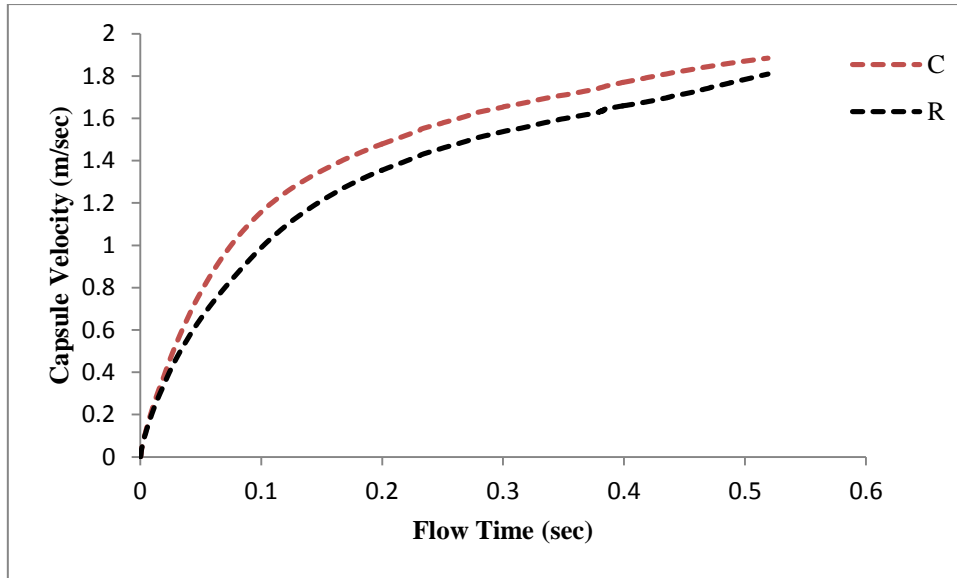


Figure 5.13 The effect of capsules in the (RC) order on the capsule velocity history

5.2 Simple Combination Analysis of Heavy Density Capsules Flow

As the capsules' weight is towards the direction of the earth's centre in a vertical pipe, the trajectory remains constant for both the capsules that are heavy-density and equal-density. Thereby, the flow structure across a vertical pipeline, conveying heavy-density capsules, resembles the flow structure for the equal-density capsules flow. Hence, the translational velocity dominates the capsules motion when contrasted to the rotational velocity.

5.2.1 Effect of the Position of the Capsule Shape in the SC order

Figure 5.14 depicts the distributions of the static gauge pressure and flow velocity magnitude in a hydraulic pipeline conveying a heavy-density spherical (S) and cylindrical (C) capsule of $k = 0.5$, $V_{av} = 2\text{m/sec}$ and $L_c = 1.5d$ respectively. It can be seen in this order of (SC) that the capsules with density equal to (1700kg/m^3) will collide with one another at 0.18 sec. The figure shows that both fields of the velocity and pressure are similar with the one noticed of the equal-density case with the same order of capsules in the pipe (figure 5.1).

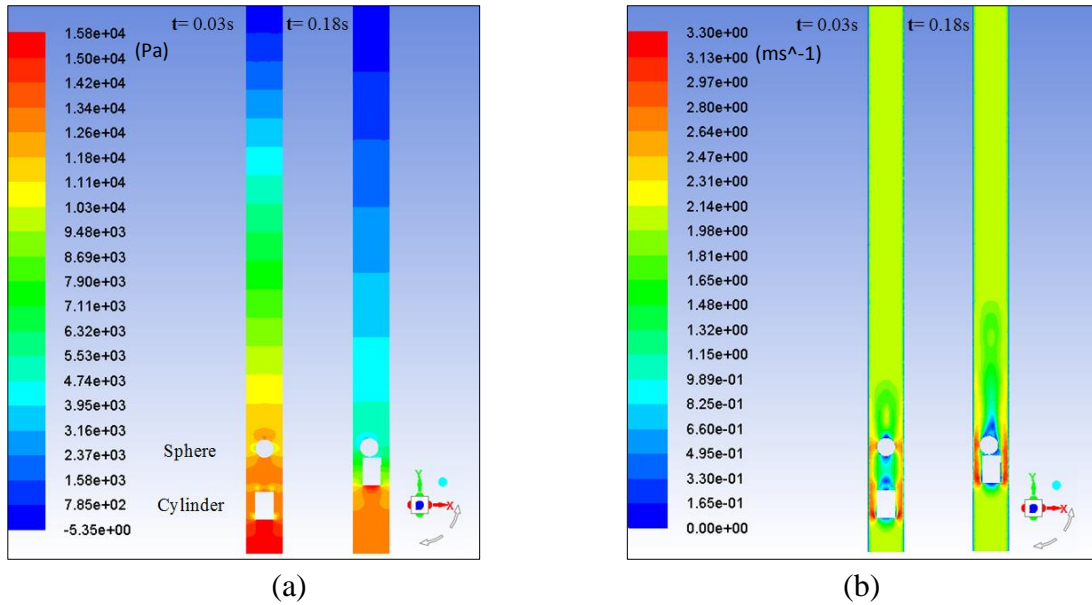


Figure 5.14 (a) Static gauge pressure and (b) Flow velocity magnitude variations for capsules in the (SC) order of $k = 0.5$, $L_c = 1.5d$ and $V_{av} = 2\text{m/sec}$ at different flow times

Figure 5.15 shows the history of the pressure drop owing to the existence of a spherical (S) and cylindrical (C) capsule in the (SC) order of two different capsules densities ($s = 1$ and 1.7) at a flow velocity of 2m/sec . The results indicate that the pressure drop for a heavy density capsule train ($s = 1.7$) is significantly higher than the pressure gradient of an equi-density capsule train ($s = 1$) by 1.5% . However, the pressure drop trend in the pipe is similar for two cases. The collision between the capsules can be clearly seen in the figure where the pressure drop increases abruptly.

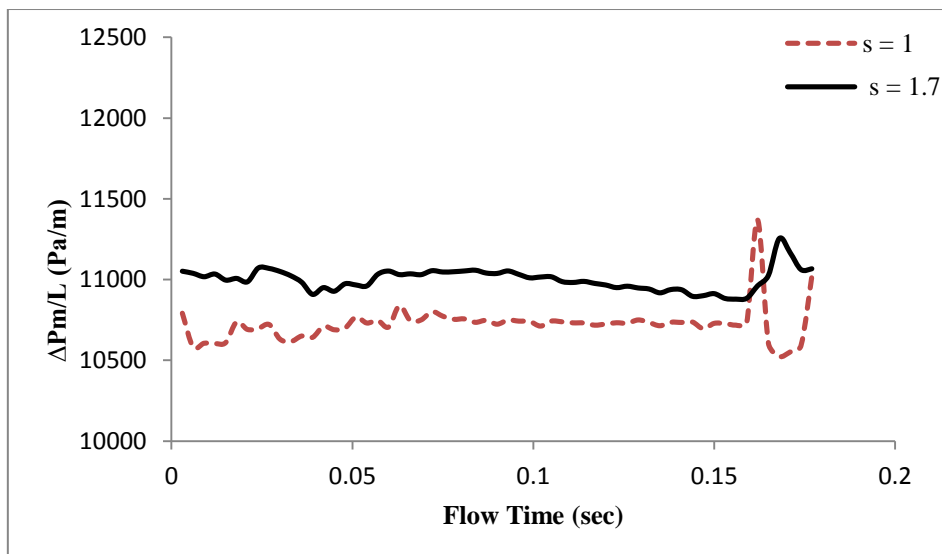


Figure 5.15 Variations in pressure drop, for two heavy density capsule flow in the (SC) order of $k = 0.5$, $L_c=1.5d$ and $V_{av} = 2\text{m/sec}$

Figure 5.16 depicts the time histories of the capsules velocity for spherical (S) and cylindrical (C) capsule in the (SC) order of two different capsules densities ($s = 1$ and 1.7) at flow velocity of 2m/sec. It can be obviously seen that the cylindrical capsule velocity is higher than the spherical capsule regardless if the capsule is heavy or equal density. On the other hand, it can be concluded that the capsule velocity decreases as the capsule density increases. Furthermore, The trend of capsules velocities is quite similar for heavy and equal capsules densities in this order of capsules in a pipe.

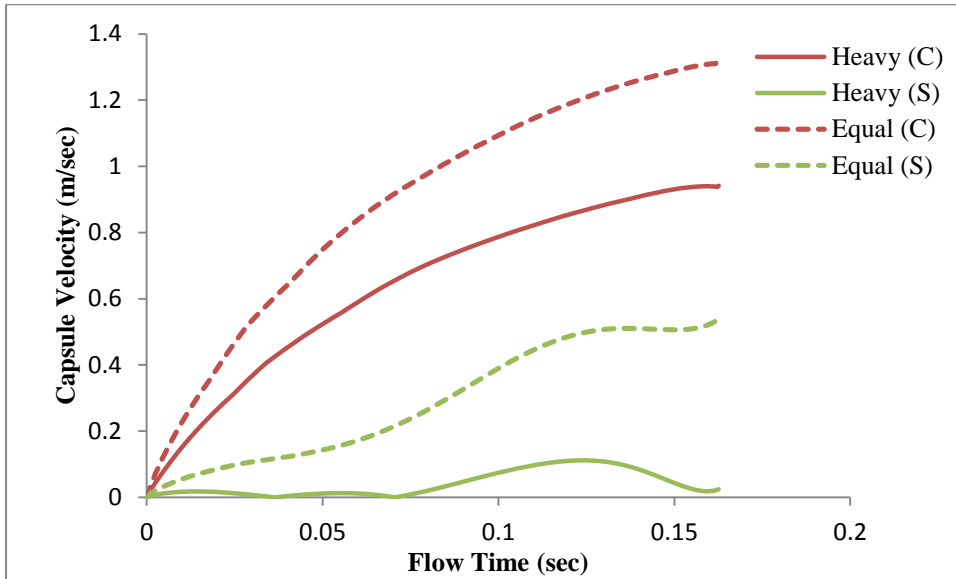


Figure 5.16 The effect of capsules in the (SC) order on the capsules velocities history

5.2.2 Effect of the Position of the Capsule Shape in the CS order

Figure 5.17 shows the static gauge pressure and flow velocity distribution in a hydraulic pipe carrying a heavy-density cylindrical (C) and spherical (S) capsule in a (CS) order of $k = 0.5$, $L_c = 1.5d$ and $V_{av} = 2m/sec$ respectively. It is evident in this order of (CS) that the capsule train does not collide with each other as compared with heavy-density capsules in the (SC) order. Therefore, the trend of the pressure distribution is different with what has observed in the order of (SC) at collision stage. Furthermore, the results show almost the same velocity distribution regardless the order of capsules between (CS) and (SC). However, the difference that has observed is the capsules behaviour and their location. Furthermore, the wake region downstream of the cylindrical capsule is larger than the wake region of the spherical capsule.

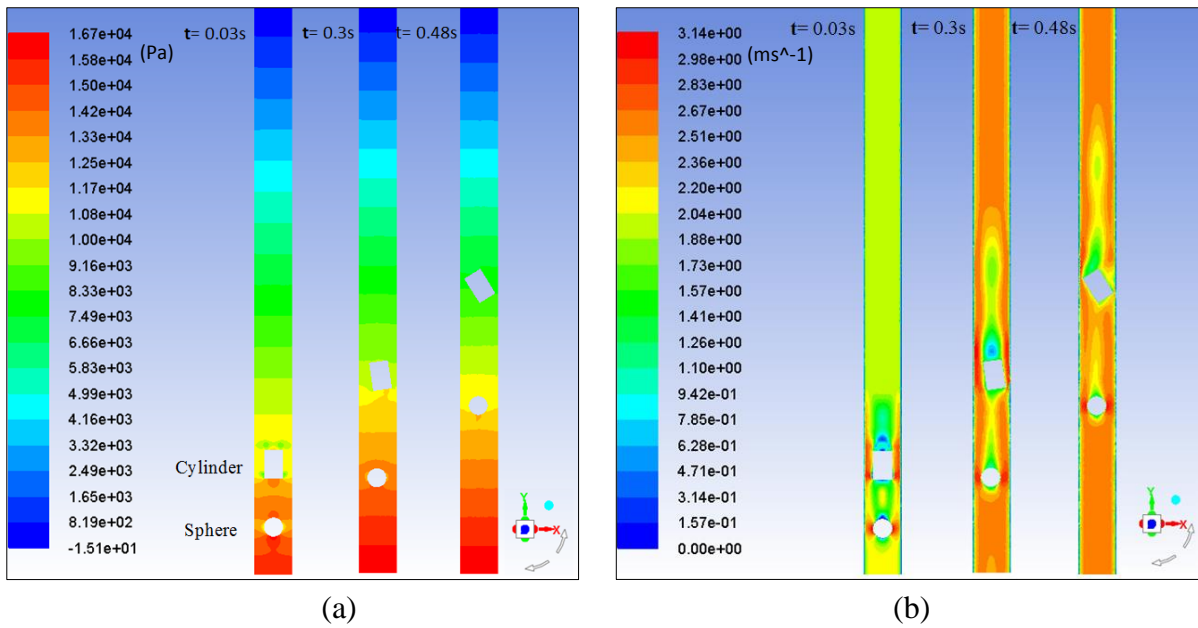


Figure 5.17 (a) Static gauge pressure and (b) Flow velocity magnitude variations for capsules in the (CS) order of $k = 0.5$, $L_c = 1.5d$ and $V_{av} = 2\text{m/sec}$ at different flow times

Figure 5.18 depicts the time histories of the capsules velocity for spherical (S) and cylindrical (C) capsule in the (CS) order of two different capsules densities ($\rho = 1$ and 1.7) at flow velocity of 2m/sec . It can be obviously seen that the equi-density capsules are higher than the heavy density capsules. On the other hand, it can be concluded that the capsule velocity decreases as the capsule density increases.

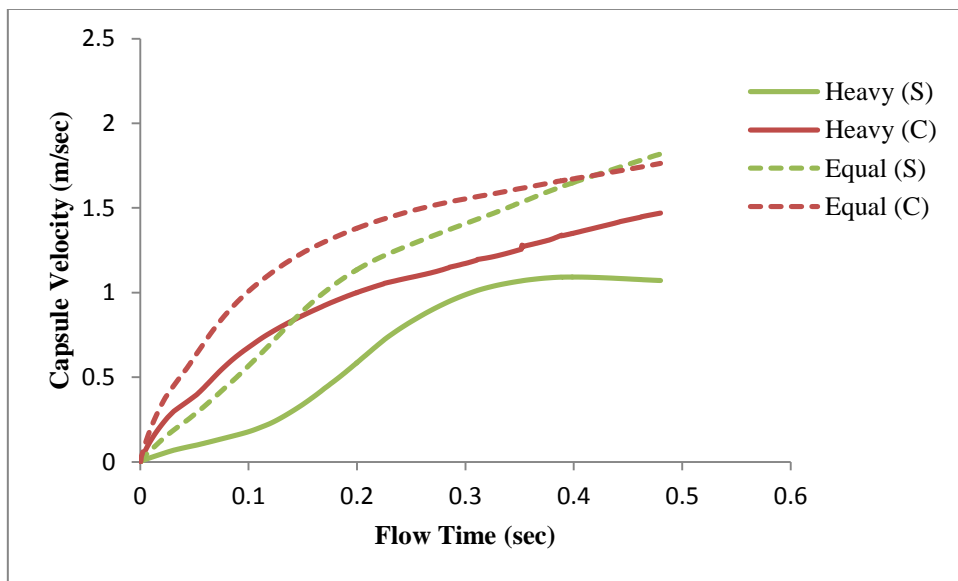


Figure 5.18 The effect of capsules in the (CS) order on the capsule velocity history

5.2.3 Effect of the Position of the Capsule Shape in the RS order

Figure 5.19 shows the static gauge pressure and flow velocity distribution in a hydraulic pipe carrying a heavy-density rectangular capsule (R) and spherical capsule (S) in a (RS) order of $k = 0.5$, $L_c = 1.5d$ and $V_{av} = 2\text{m/sec}$. It can be noticed that the pressure distribution trend seems to be the same as compared with the pressure field in the order (CS) (figure 5.17). The pressure at upstream location has decreased slightly by 0.3% during $t = 0.03\text{sec}$ as compared to the (CS) order at the same flow time. Furthermore, the wake region downstream of the rectangular capsule is larger than the wake region of the spherical capsule during the capsule train flow.

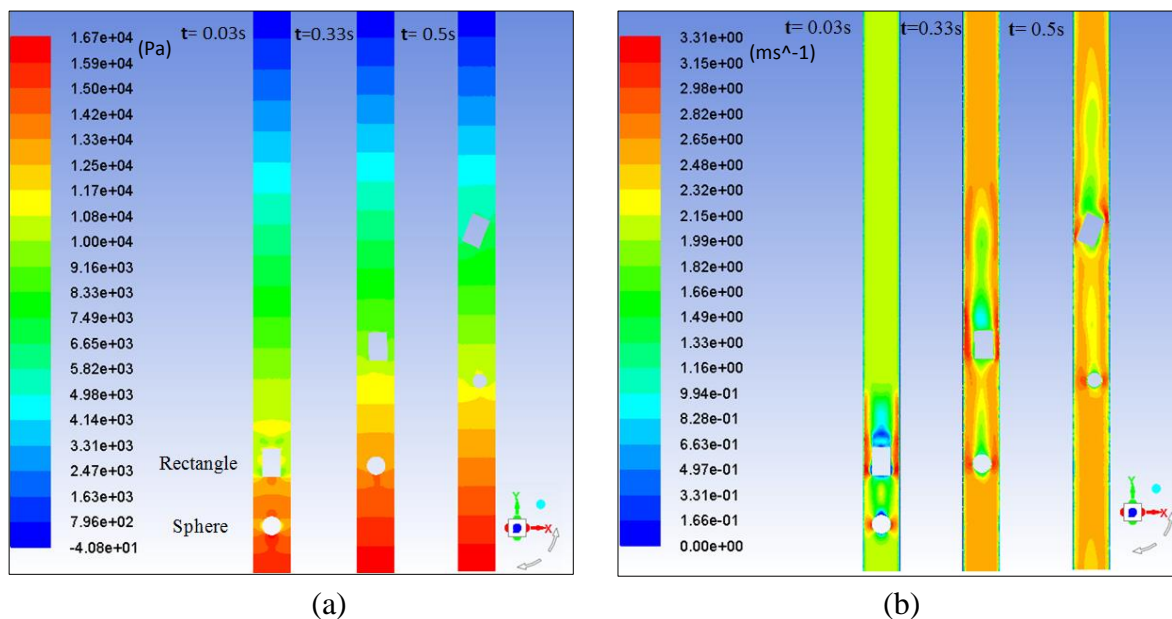


Figure 5.19 (a) Static gauge pressure and (b) Flow velocity magnitude variations for capsules in the (RS) order of $k = 0.5$, $L_c = 1.5d$ and $V_{av} = 2\text{m/sec}$ at different flow times

Figure 5.20 depicts the time histories of the capsules velocity for rectangular (R) and spherical (S) capsule in the (RS) order of two different capsules densities ($s = 1$ and 1.7) at flow velocity of 2m/sec . It can be obviously seen that the equi-density capsules are higher than the heavy density capsules. On the other hand, it can be concluded that the capsule velocity decreases as the capsule density increases.

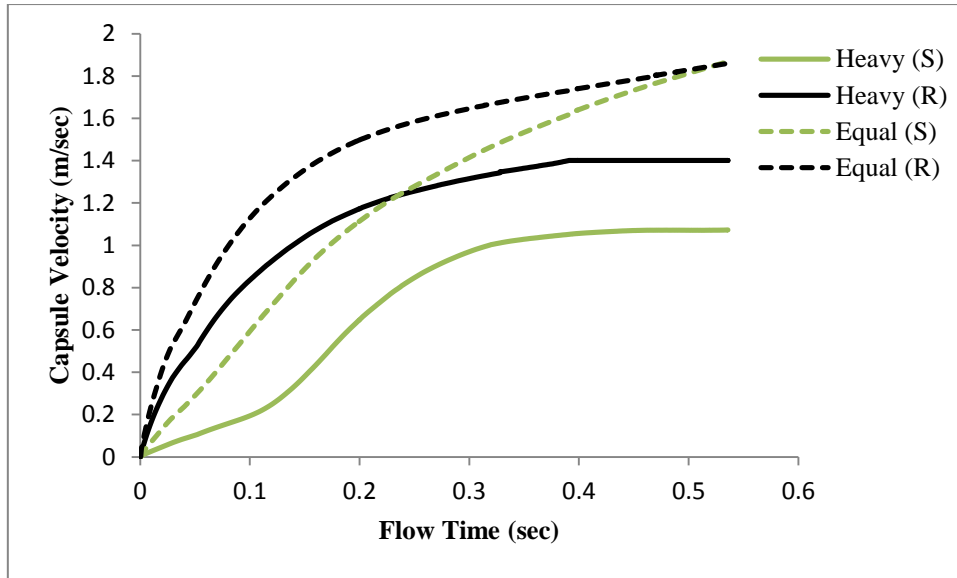


Figure 5.20 The effect of capsules in the (RS) order on capsule velocity history

5.2.4 Effect of the Position of the Capsule Shape in the SR order

Figure 5.21 depicts the static gauge pressure and flow velocity variations in a hydraulic pipe carrying a heavy density spherical (S) and rectangular (R) capsule in a (SR) order of $k = 0.5$, $L_c = 1.5d$ and $V_{av} = 2\text{m/sec}$. It can be seen in this order that the capsules will collide with one another at 0.18sec. As observed with the collision of capsules the trend of the pressure distribution has been changed. Consequently, the system of a mixed capsule shapes is unstable without precise position control. Furthermore, in figure 5.21(b) shows the velocity field distribution within a pipe is similar to the velocity field for the capsule train in the (SC) order (figure 5.14).

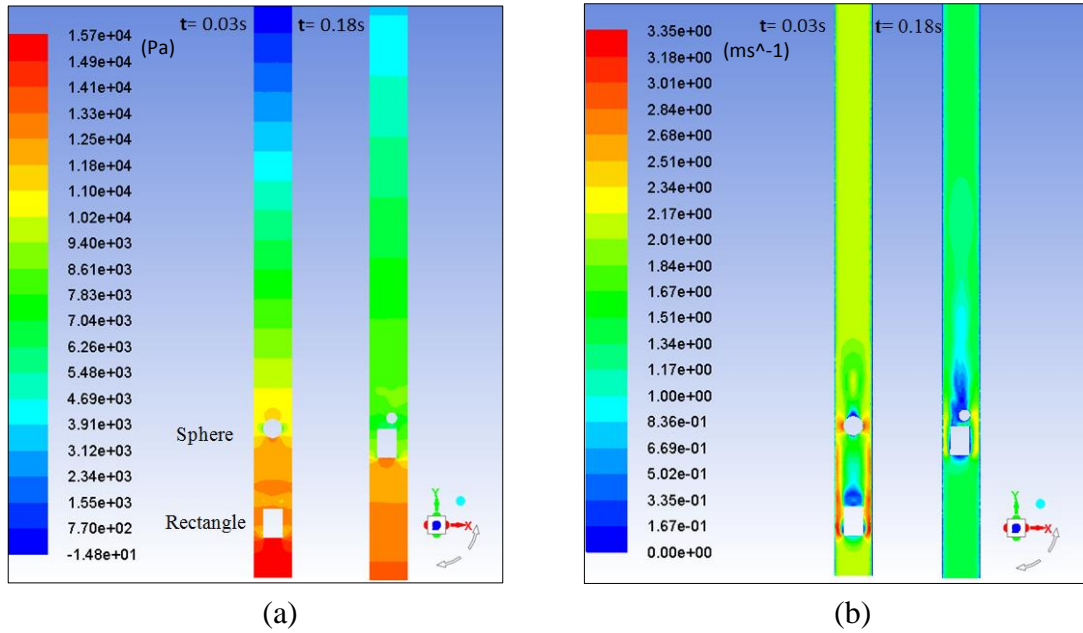


Figure 5.21 (a) Static gauge pressure and (b) Flow velocity magnitude variations for capsules in the (SR) order of $k = 0.5$, $L_c = 1.5d$ and $V_{av} = 2\text{m/sec}$ at different flow times

Figure 5.22 shows the time histories of the capsules velocity for spherical (S) and rectangular (R) capsule in the (SR) order of two different capsules densities ($s = 1$ and 1.7) at flow velocity of 2m/sec . It can be obviously seen that the rectangular capsule velocity is higher than the spherical capsule regardless if the capsule is heavy or equal density. On the other hand, it can be concluded that the capsule velocity decreases as the capsule density increases. Furthermore, the velocity of a heavy density spherical capsule at some points to be zero that means the capsule is traveling downward or stationary in a vertical pipe.

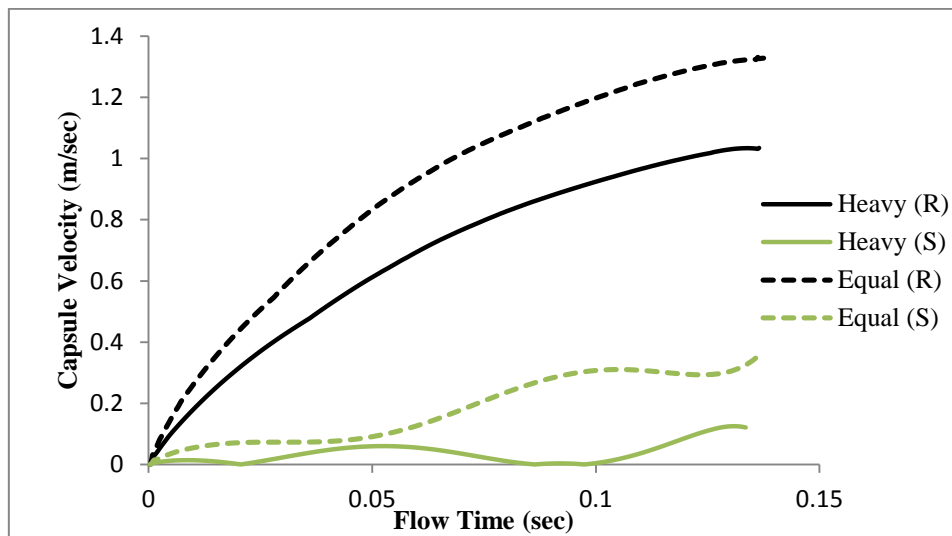


Figure 5.22 The effect of capsules in the (SR) order on the capsule velocity history

5.2.5 Effect of the Position of the Capsule Shape in the CR order

Figure 5.23 depicts the static gauge pressure and flow velocity distribution in a hydraulic pipe carrying a heavy density cylindrical (C) and rectangular (R) capsule of $k = 0.5$, $L_c = 1.5d$ and $V_{av} = 2\text{m/sec}$. It can be seen in this order of (CR) that the capsules will collide with one another during 0.24 sec. As observed with the collision of capsules the trend of the pressure distribution has been changed. Furthermore, as compared to heavy-density capsule train in a (SR) order, it can be seen that the velocity field is similar.

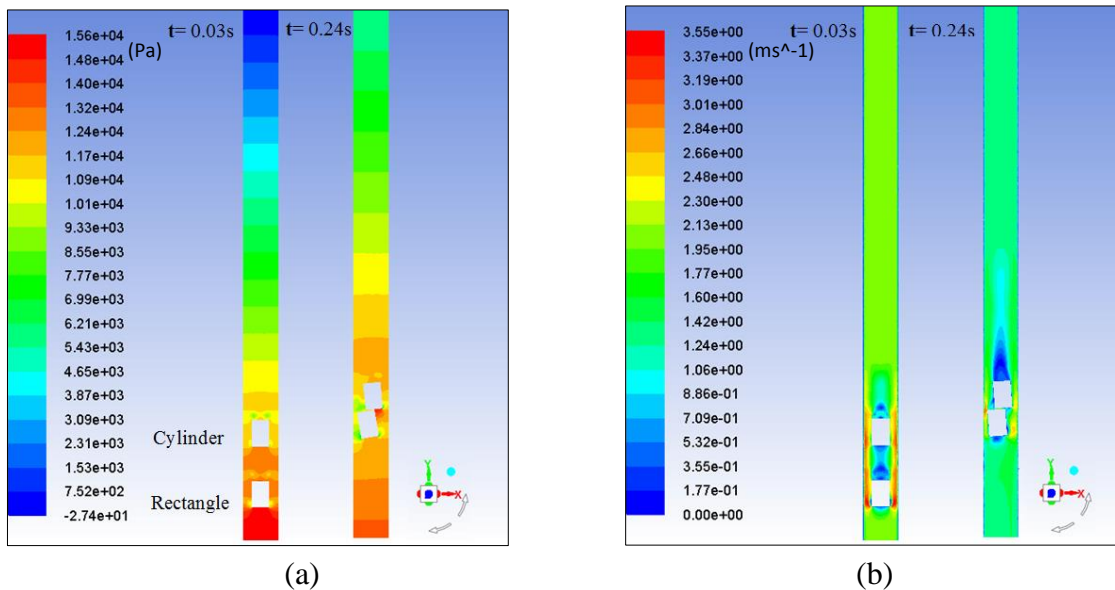


Figure 5.23 (a) Static gauge pressure and (b) Flow velocity magnitude variations for capsules in the (CR) order of $k = 0.5$, $L_c = 1.5d$ and $V_{av} = 2\text{m/sec}$ at different flow times

Figure 5.24 shows the time histories of the capsules velocity for cylindrical (C) and rectangular (R) capsule in the (CR) order of two different capsules densities ($s = 1$ and 1.7) at flow velocity of 2m/sec . It can be seen that the rectangular capsule velocity is higher than the cylindrical capsule regardless if the capsule is heavy or equal density. On the other hand, it can be concluded that the capsule velocity decreases as the capsule density increases. Furthermore, The trend of velocities distribution is quite similar for heavy and equal capsules densities in this order of capsules in a pipe.

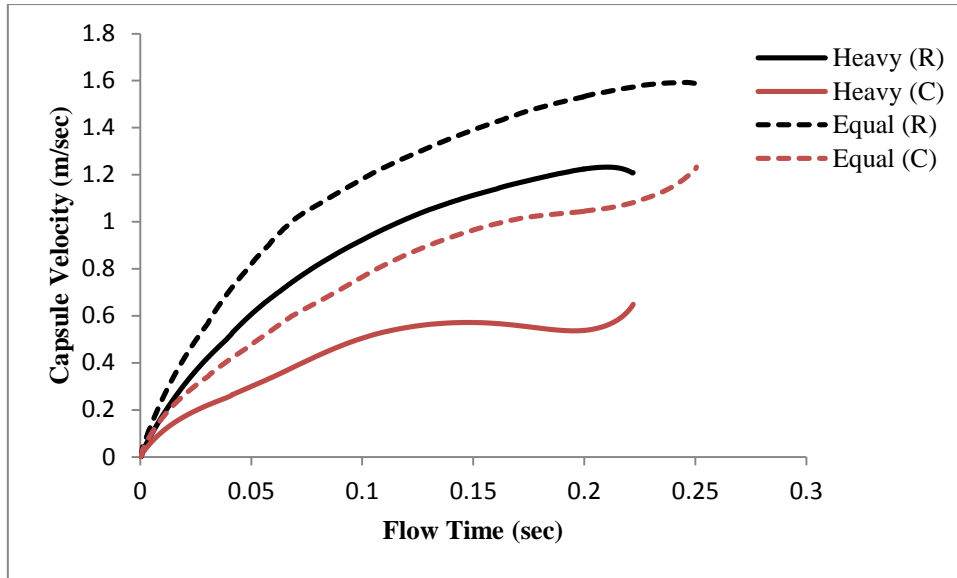


Figure 5.24 The effect of capsules in the (CR) order on the capsule velocity history

5.2.6 Effect of the Position of the Capsule Shape in the RC order

Figure 5.25 depicts the static gauge pressure and flow velocity distributions in a pipe carrying a heavy-density rectangular (R) and cylindrical (C) capsule in a (RC) order of $k = 0.5$, $L_c = 1.5d$ and $V_{av} = 2\text{m/sec}$. The trend of the pressure distribution is different as compared to a (CR) order due to the collision that is occurred in the (CR) order. It can be noted that the pressure in front of the capsule train at 0.03sec is 15962Pa, and then after the capsule train motion during 0.42sec the front pressure decreases by 32%. Moreover, the results show almost the same velocity distribution regardless the order of capsules between (RC) and (CR). However, the only difference observed is the capsules behaviour and their location. Furthermore, as shown in figure 5.25 (b) the wake region downstream of the capsule train is large, due to the shape and length of both of them during the capsule train flow.

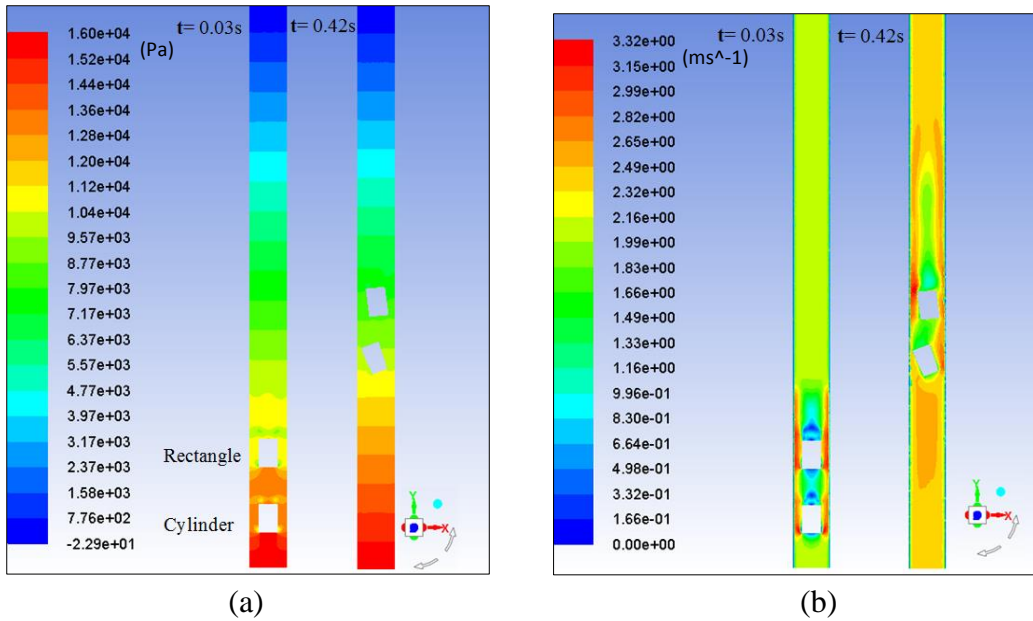


Figure 5.25 (a) Static gauge pressure and (b) Flow velocity magnitude variations for capsules in the (RC) order of $k = 0.5$, $L_c = 1.5d$ and $V_{av} = 2\text{m/sec}$ at different flow times

Figure 5.26 shows the time histories of the capsules velocity for rectangular (R) and cylindrical (C) capsule in the (CR) order of two different capsules densities ($s = 1$ and 1.7) at flow velocity of 2m/sec . It can be obviously seen that the equi-density capsules are higher than the heavy density capsules. On the other hand, it can be concluded that the capsule velocity decreases as the capsule density increases. The cylindrical capsule velocity is higher than the rectangular capsule velocity for both equal or heavy densities in this order.

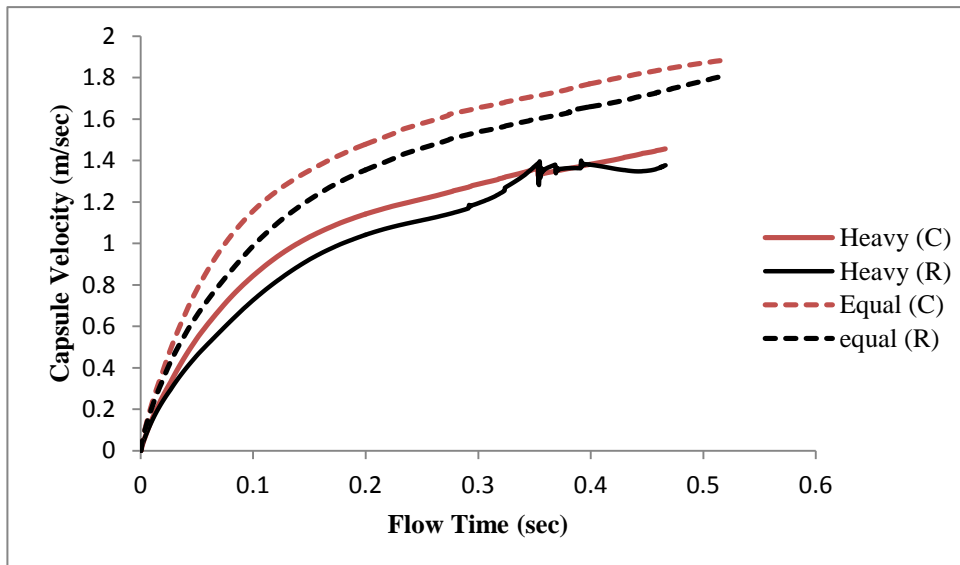


Figure 5.26 The effect of capsules in the (RC) order on the capsule velocity history

5.3 Complex Combination Analysis of an Equal Density Capsules Flow

The complex combination consists from three different shapes of the capsules (spherical, cylindrical and rectangular). As mentioned earlier, the initial spacing between the capsule is kept 2 times the diameter of the capsule. The effect of the order of capsule shapes on the flow field with keeping all other parameters constant are considered in this investigation.

5.3.1 Effect of the Position of the Capsule Shape in the SCR order

Figure 5.27 shows the distributions in the static gauge pressure and the flow velocity in a hydraulic pipe carrying spherical (S), cylindrical (C) and rectangular (R) capsules of $k = 0.5$, $L_c = 1.5d$ and $V_{av} = 2\text{m/sec}$ respectively. It can be seen in the order of (SCR) that the collision occurs in a capsule train between rectangular and cylindrical capsules at 0.45sec. Hence, the rectangular capsule cannot push a cylindrical capsule upwards. As observed with the collision of capsules the trend of the pressure distribution has been changed. Furthermore, it is observed in figure 5.27 (b), that the flow velocity magnitude in the annulus region for the rectangular and cylindrical capsules is higher than in the annulus region for the spherical capsule by 12% at 0.05sec.

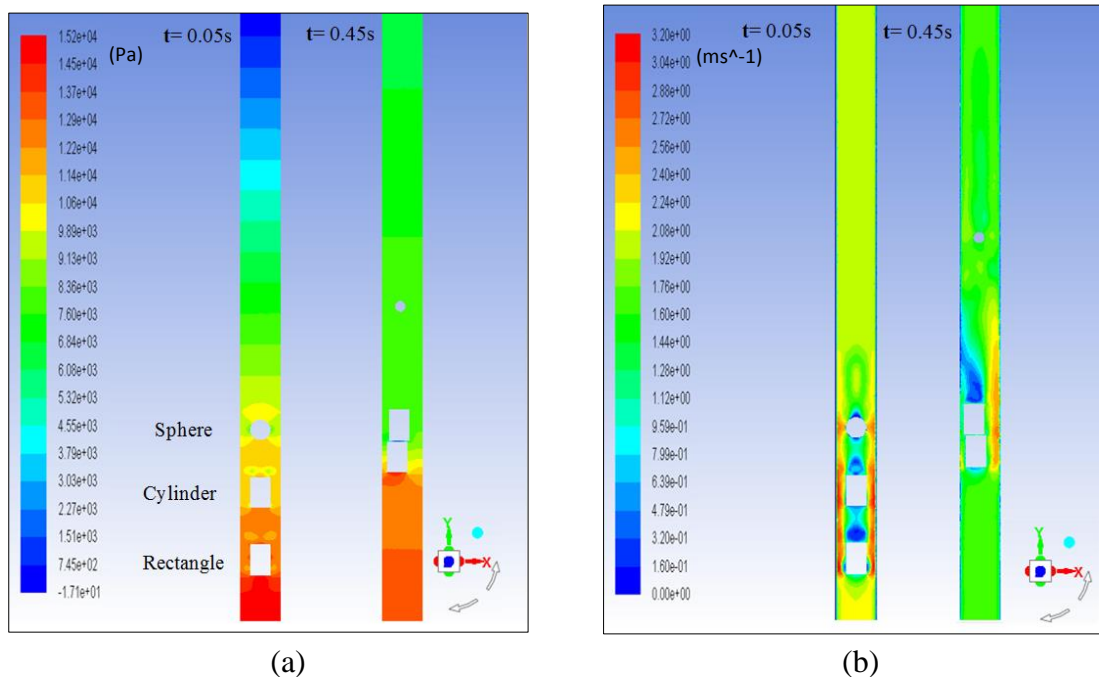


Figure 5.27 (a) Static gauge pressure and (b) Flow velocity magnitude variations for capsules in the (SCR) order of $k = 0.5$, $L_c = 1.5d$ and $V_{av} = 2\text{m/sec}$ at different flow times

Figure 5.28 illustrates the time histories of capsules velocities in a (SCR) order at flow velocity 2m/sec. It can be clearly observed that the rectangular capsule velocity is higher than the cylindrical and spherical capsule velocities. Hence, the rectangular capsule is travelling faster than the cylindrical and spherical capsules, however, their velocities are less than the water flow velocity due to the concentration of the solid phase inside the pipeline.

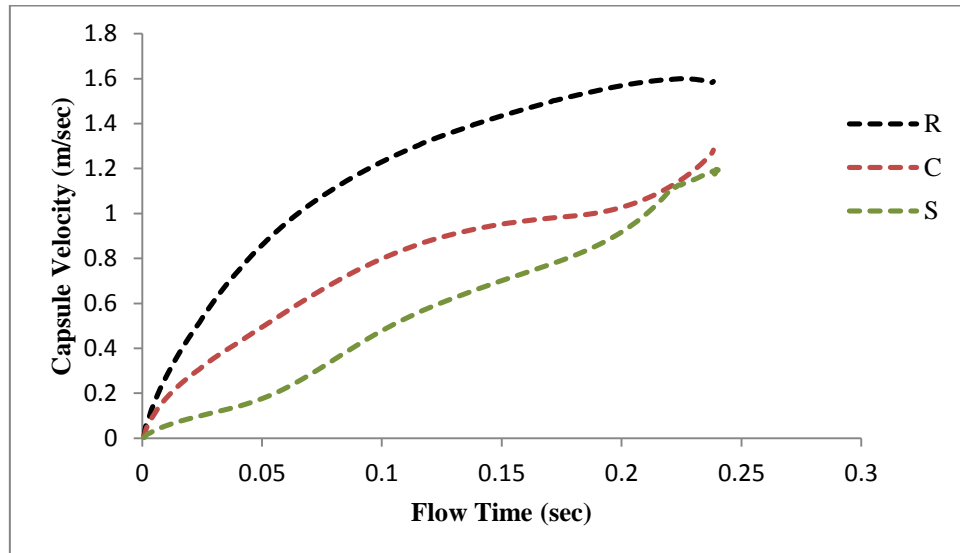


Figure 5.28 The effect of capsules in the (SCR) order on the capsule velocity history

5.3.2 Effect of the Position of the Capsule Shape in the SRC order

Figure 5.29 shows the static gauge pressure and flow velocity distribution in a hydraulic pipe carrying spherical (S), cylindrical (C) and rectangular (R) capsules of $k = 0.5$, $L_c = 1.5d$ and $V_{av} = 2\text{m/sec}$ respectively. It can be seen in this order of (SRC) that the collision occurs in a capsule train between the rectangular and spherical capsule during 0.3sec. As observed with the collision of capsules the trend of the pressure distribution has been changed. Furthermore, the velocity field distribution within the pipe is similar to the velocity field for the capsule train in the (SCR) order (figure 5.27) at the initial motion.

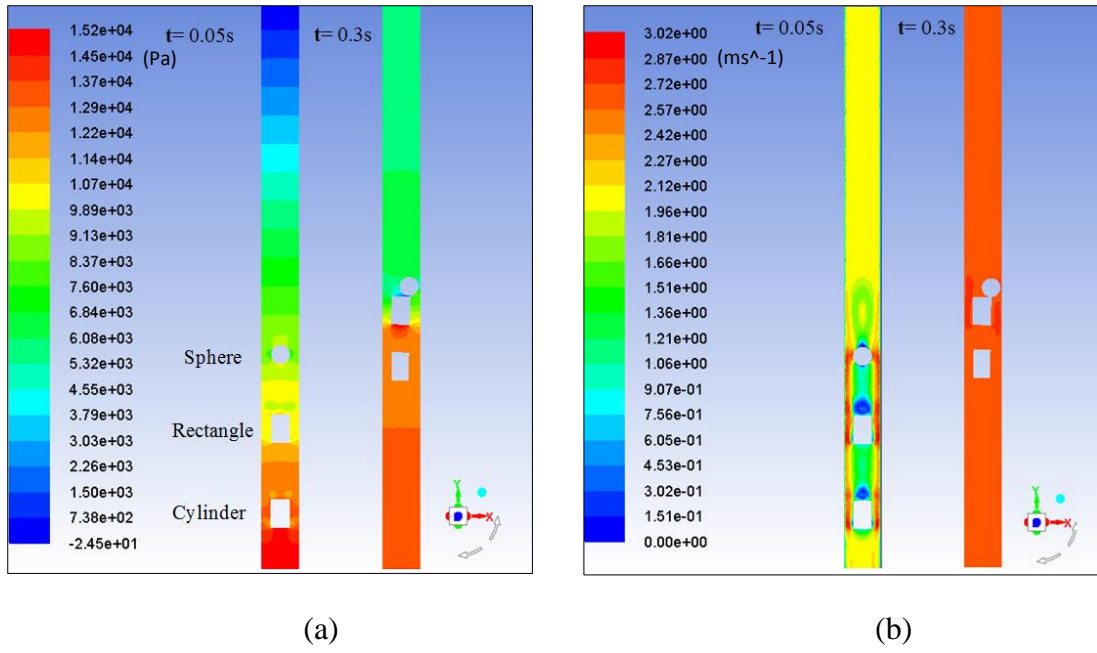


Figure 5.29 (a) Static gauge pressure and (b) Flow velocity magnitude variations for capsules in the (SRC) order of $k = 0.5$, $L_c = 1.5d$ and $V_{av} = 2\text{m/sec}$ at different flow times

Figure 5.30 shows the time histories of capsules velocities in an (SRC) order at flow velocity 2m/sec. It can be obviously seen that after the initial motion of the capsule train the cylindrical capsule velocity becomes higher than the rectangular capsule velocity whereas, the spherical capsule velocity is always smaller. However, all of them their velocities are less than the water flow velocity due to the concentration of the solid phase in the pipe.

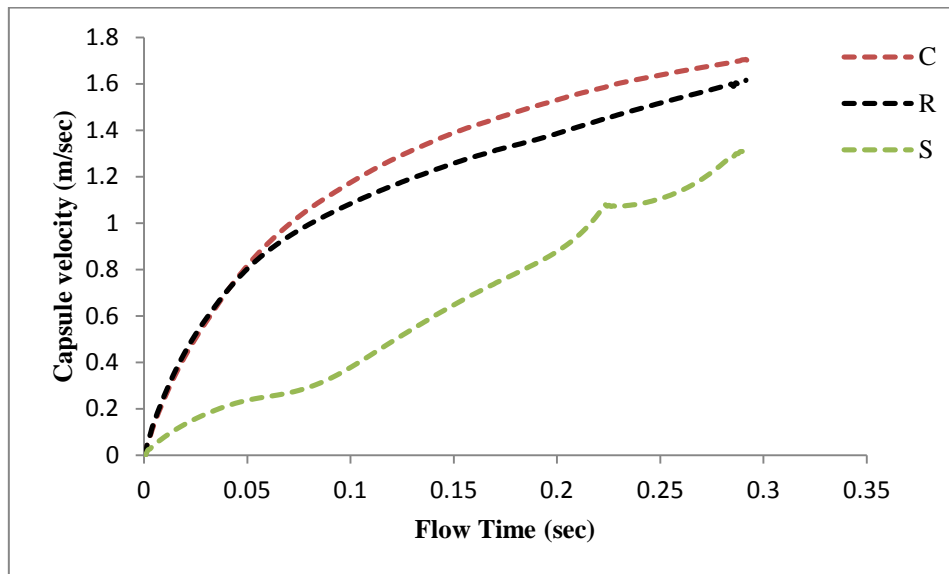


Figure 5.30 The effect of capsules in the (SRC) order on the capsules velocity history

5.3.3 Effect of the Position of the Capsule Shape in the RSC order

Figure 5.31 shows the static gauge pressure and flow velocity distribution in a hydraulic pipe carrying rectangular (R), cylindrical (C) and spherical (S) capsules of $k = 0.5$, $L_c=1.5d$ and $V_{av} = 2m/sec$ respectively. It can be seen in this order of (RSC) that the collision occurs in a capsule train between the cylindrical and spherical capsule during 0.25sec. As observed with the collision of capsules the trend of the pressure distribution has been changed. Furthermore, the velocity field resembles the one observed in a (SRC) order at $t = 0.05sec$ (figure 2.29). It is evident that a wake region downstream for each capsule shape different, where the larger one for the rectangular capsule then the cylindrical and spherical capsule respectively at 0.05sec.

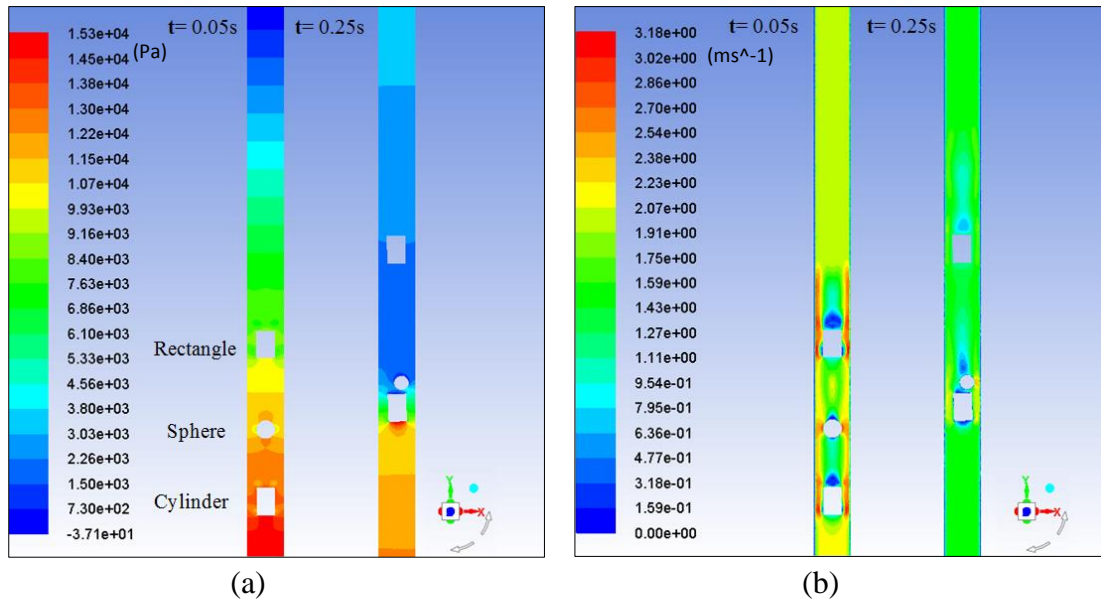


Figure 5.31 (a) Static gauge pressure and (b) Flow velocity magnitude variations for capsules in the (RSC) order of $k = 0.5$, $L_c = 1.5d$ and $V_{av} = 2m/sec$ at different flow times

Figure 5.32 shows the time histories of capsules velocities in a (RSC) order at flow velocity 2m/sec. the velocity profiles for both the cylindrical and rectangular capsule are identical to each other that indicate they travel by the same velocity. On the other hand, the spherical capsule travels by velocity less than them. The trend of velocity profiles is nearly as in case of the (SRC) order (figure 5.30).

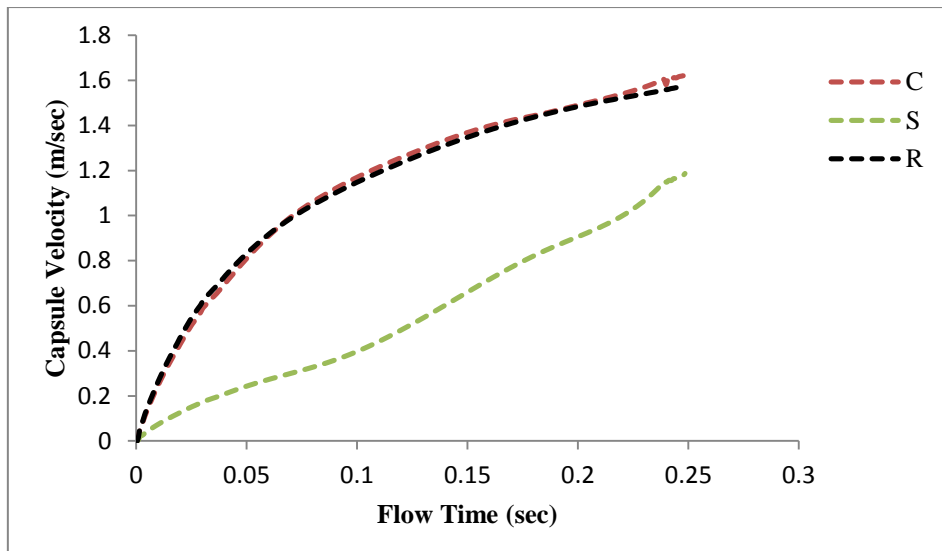


Figure 5.32 The effect of capsules in the (RSC) order on the capsule velocity history

5.3.4 Effect of the Position of the Capsule Shape in the RCS order

Figure 5.33 shows the static gauge pressure and flow velocity distribution in a hydraulic pipe carrying a rectangular (R), cylindrical (C) and spherical (S) capsules in a (RCS) order of $k = 0.5$, $L_c = 1.5d$ and $V_{av} = 2\text{m/sec}$. It is evident that the capsule train does not collide with each other as compared with the (RSC) order. Therefore, the trend of the pressure distribution is different with what has observed in the order of (RSC) at the collision stage. Furthermore, the results show almost the same velocity distribution as shown in case of the (RSC) order. However, the only difference observed is the capsule behaviour and its location.

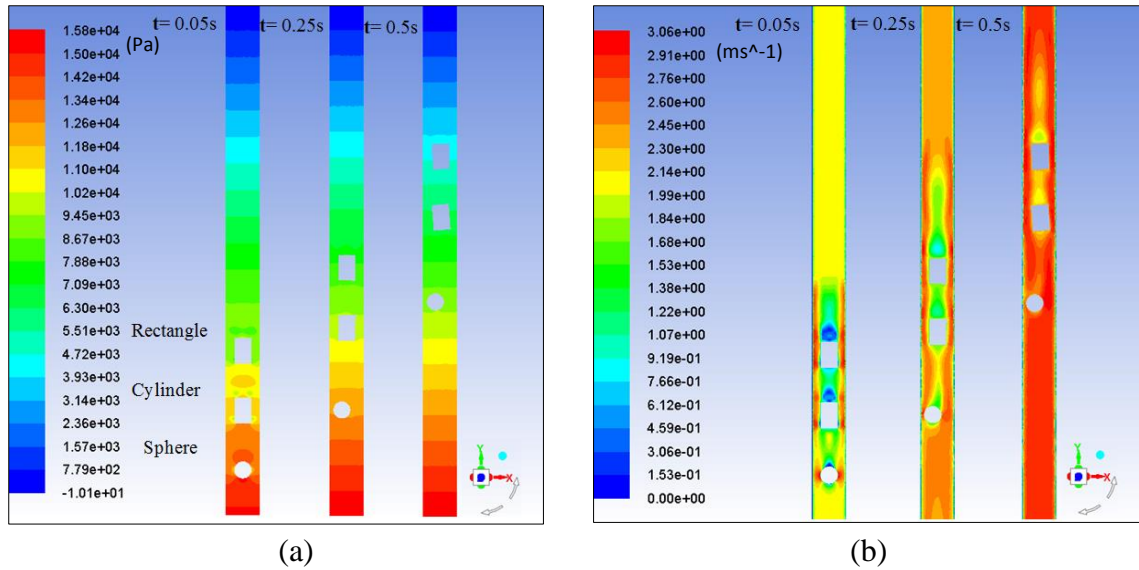


Figure 5.33 (a) Static gauge pressure and (b) Flow velocity magnitude variations for capsules in the (RCS) order of $k = 0.5$, $L_c = 1.5d$ and $V_{av} = 2m/sec$ at different flow times

Figure 5.34 shows the time histories of capsules velocities in an (RCS) order at flow velocity 2m/sec. the velocity profiles for both the cylindrical and rectangular capsule are identical to each other that indicate they travel by the same velocity. On the other hand, the spherical capsule travels by velocity less than them for a period of time then exceeds their velocities. The trend of velocity profiles is nearly as in case of the (RSC) order (fig 5.32).

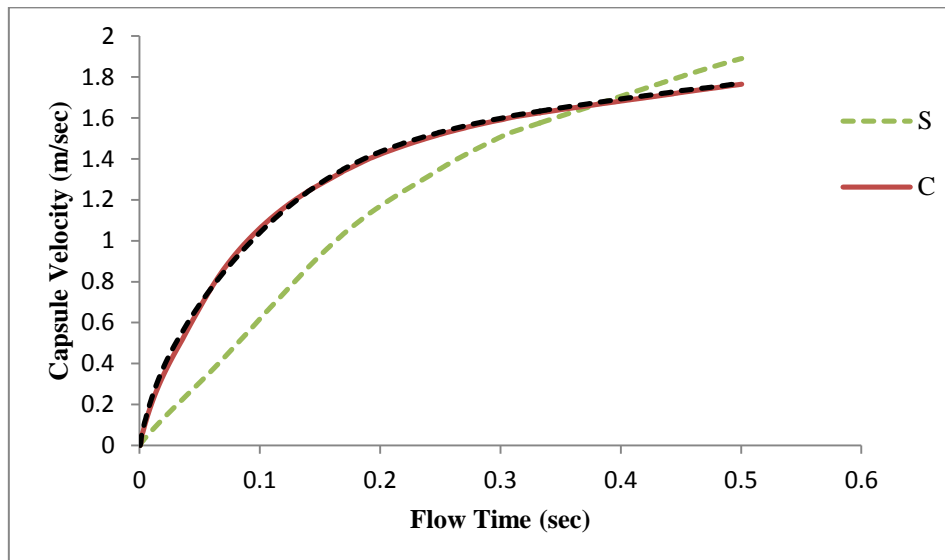


Figure 5.34 The effect of capsules in the (RCS) order on the capsule velocity history

5.3.5 Effect of the Position of the Capsule Shape in the CRS order

Figure 5.35 depicts the static gauge pressure and flow velocity distribution in a pipe carrying a cylindrical (C), rectangular (R) and spherical (S) capsules in an (CRS) order of $k = 0.5$, $L_c=1.5d$ and $V_{av} = 2m/sec$. It can be seen that the overall pressure and velocity distributions seem to be the same as compared with the (RCS) order in the previous section. However, the difference observed that the capsules flow time is shorter than the flow time in the (RCS) order.

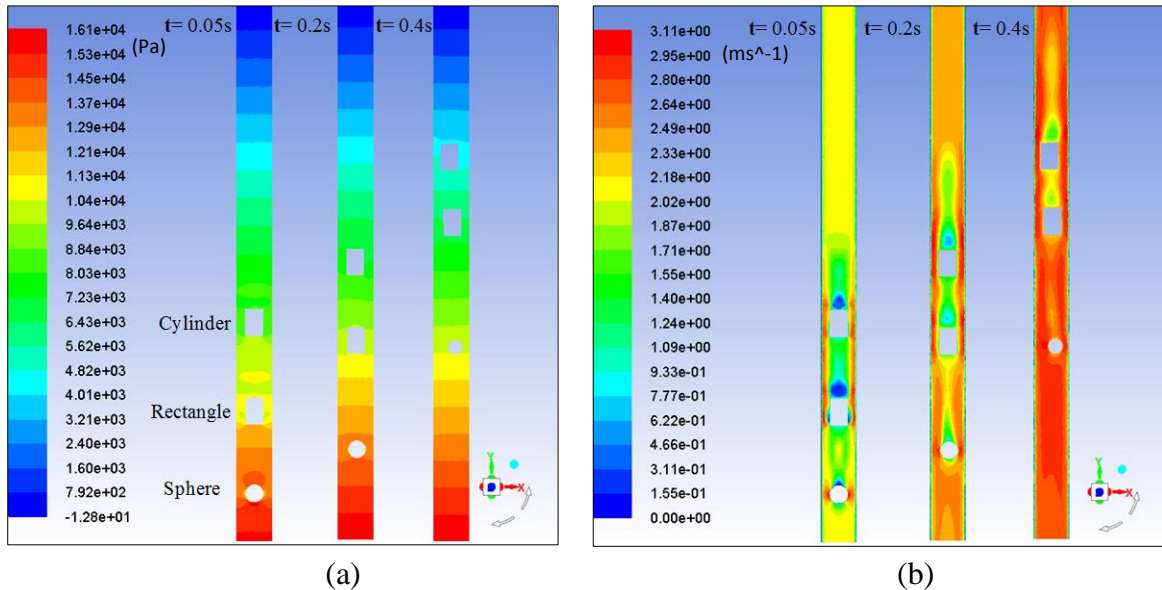


Figure 5.35 (a) Static gauge pressure and (b) Flow velocity magnitude variations for capsules in the (CRS) order of $k = 0.5$, $L_c = 1.5d$ and $V_{av} = 2m/sec$ at different flow times

Figure 5.36 illustrates the time histories of capsules velocities in an (CRS) order at flow velocity $2m/sec$. It can be obviously seen that the highest velocity in this order is the rectangular capsule. Hence, the rectangular capsule travels faster than the cylindrical and spherical capsule despite it is between other capsules. This is due to the cross section area of the rectangular capsule facing the flow direction is larger than the cylindrical and spherical capsule.

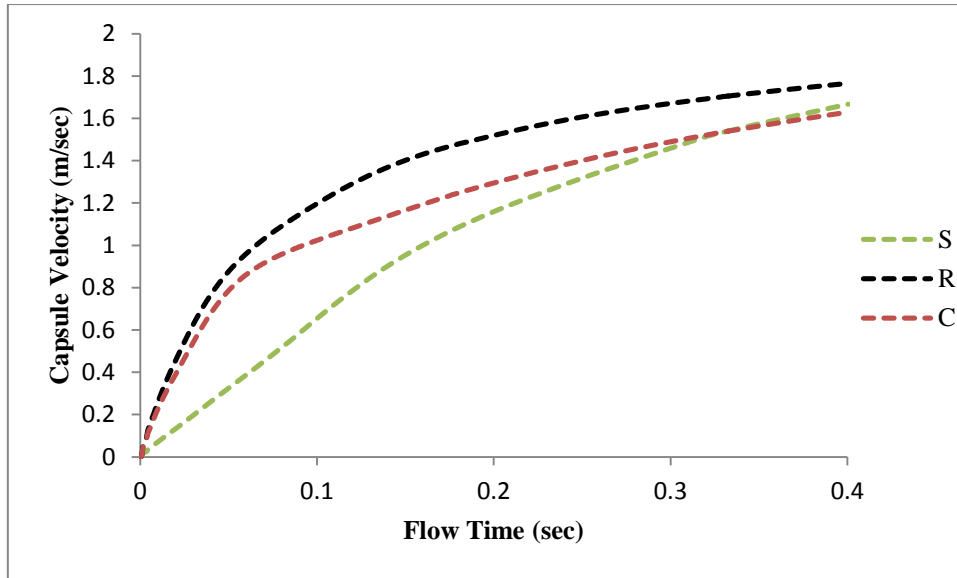


Figure 5.36 The effect of capsules in the (CRS) order on the capsule velocity history

5.3.6 Effect of the Position of the Capsule Shape in the CSR order

Figure 5.37 shows the static gauge pressure and flow velocity magnitude variations within a hydraulic pipeline carrying cylindrical (C), spherical (S) and rectangular (R) capsules of $k = 0.5$, $L_c = 1.5d$ and $V_{av} = 2\text{m/sec}$ respectively. It can be seen in this order of (CSR) that the collision occurs between the rectangular and spherical capsule during 0.2sec. The velocity and pressure fields resemble the one observed in case of (RSC) order in figure 5.31. It is evident that a wake region downstream for each capsule shape different, where the larger one for the rectangular capsule then the cylindrical and spherical capsule respectively at 0.05sec.

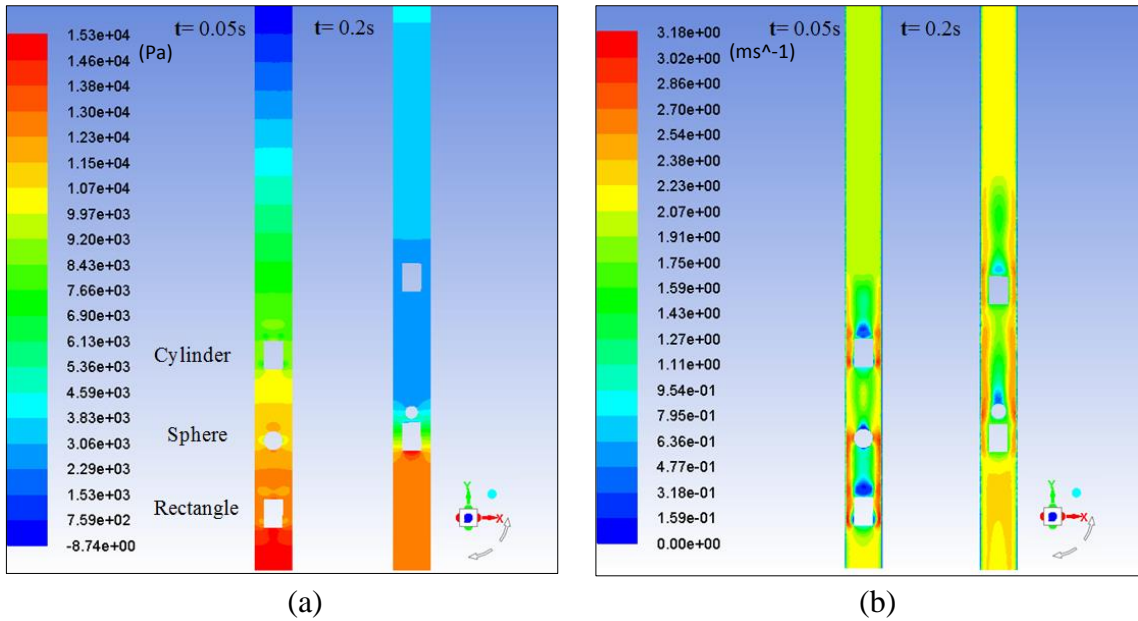


Figure 5.37 (a) Static gauge pressure and (b) Flow velocity magnitude variations for capsules in the (CSR) order of $k = 0.5$, $L_c = 1.5d$ and $V_{av} = 2\text{m/sec}$ at different flow times

Figure 5.38 illustrates the time histories of capsules velocities in an (CSR) order at flow velocity 2m/sec. It can be clearly seen that the rectangular capsule velocity is higher than the cylindrical and spherical capsule velocities. Hence, the rectangular capsule travelling faster than the cylindrical and spherical capsule. This due to the surface area of rectangular capsule that facing the flow direction is larger than the cylindrical and spherical capsule. It has been also observed that the trend of velocity profiles is different as in case of the (RSC) order (Figure 5.32).

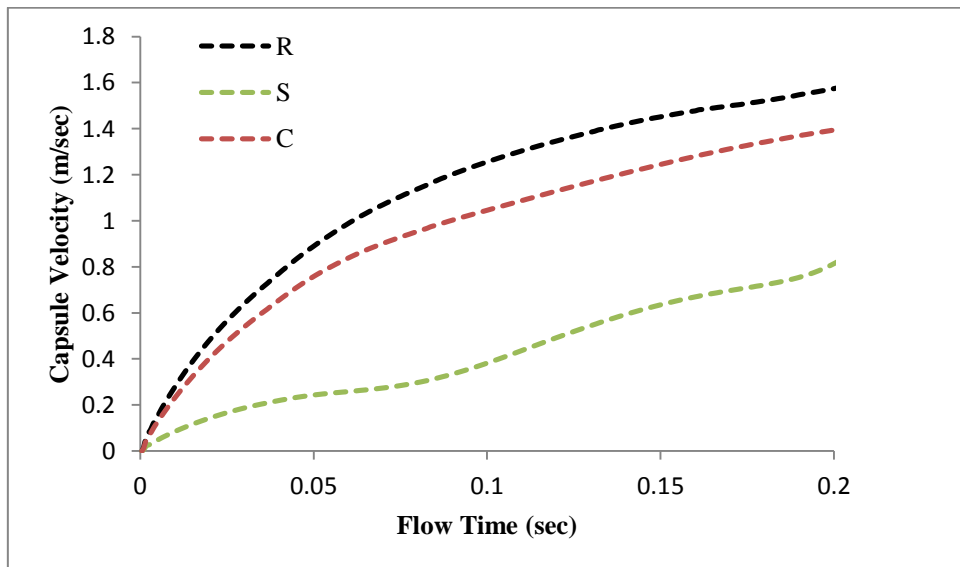


Figure 5.38 The effect of capsules in the (CSR) order on the capsule velocity history

5.4 Complex Combination Analysis of Heavy Density Capsules Flow

5.4.1 Effect of the Position of the Capsule Shape in the SCR order

Figure 5.39 depicts the local variations in the static gauge pressure and the flow velocity magnitude in a hydraulic pipe carrying heavy-density spherical (S), cylindrical (C) and rectangular (R) capsules of $k = 0.5$, $L_c = 1.5d$ and $V_{av} = 2\text{m/sec}$ respectively. The pressure at upstream location has increased by 6 % as compared to the upstream location for equi-density capsules for the same order of capsules at $t = 0.05\text{sec}$. Moreover, the results show almost the same velocity distribution regardless the density of capsules between equal or heavy density. However, the only difference observed is the capsules behaviour and their location as well as the flow time of capsules.

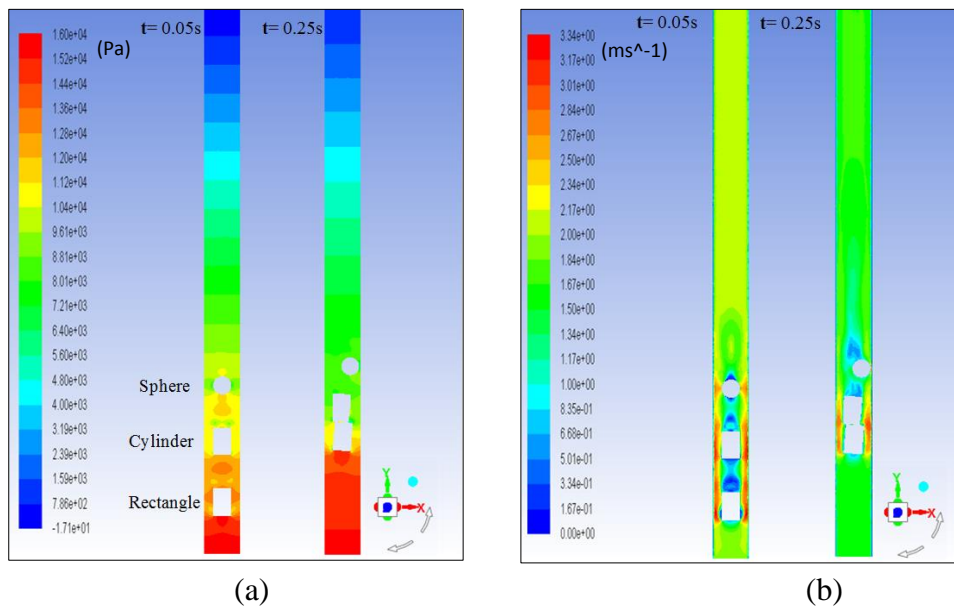


Figure 5.39 (a) Static gauge pressure and (b) Flow velocity magnitude variations for capsules in the (SCR) order of $k = 0.5$, $L_c = 1.5d$ and $V_{av} = 2\text{m/sec}$ at different flow times

Figure 5.40 depicts the time histories of the capsules velocity for the spherical capsule (S), cylindrical (C) and rectangular (R) capsule in the (SCR) order of two different densities at flow velocity of 2m/sec . It can be obviously seen that the rectangular capsule velocity is higher than the cylindrical and spherical capsule velocities regardless if the capsule is heavy or equal density. On the other hand, it can be concluded that the capsule velocity decreases as the capsule density increases. Furthermore, the velocity profiles are quite similar for heavy and equal capsules densities in this order of the capsules.

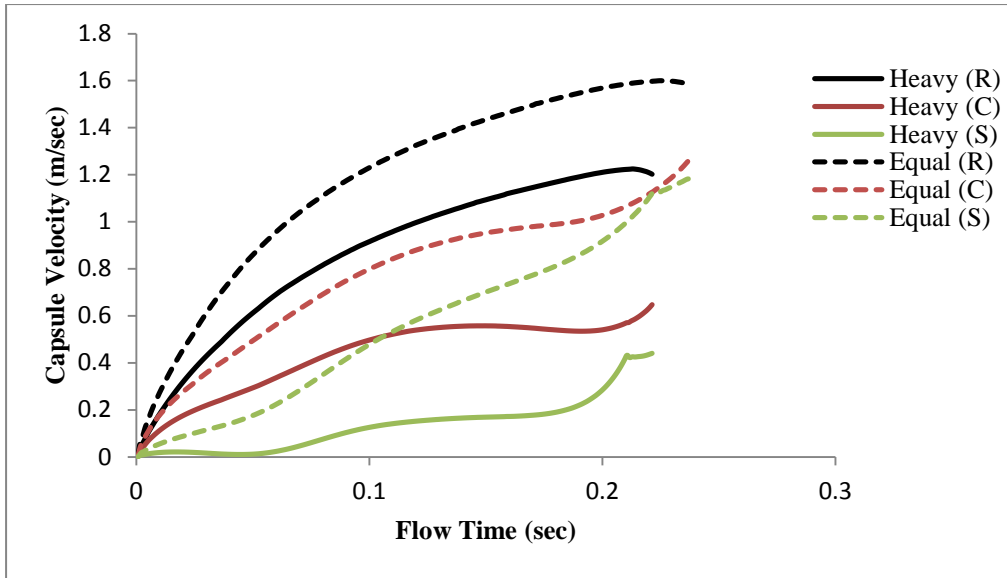


Figure 5.40 The effect of capsules in the (SCR) order on the capsule velocity history

5.4.2 Effect of the Position of the Capsule Shape in the SRC order

Figure 5.41 shows the local variations in the static gauge pressure and the flow velocity magnitude in a hydraulic pipe carrying heavy density spherical (S), rectangular (R) and cylindrical (C) capsule of $k = 0.5$, $L_c = 1.5d$ and $V_{av} = 2\text{m/sec}$. The pressure at upstream location has increased by 5% as compared to the upstream location for equi-density capsules for the same order of capsules during the initial motion. Furthermore, in figure 5.41(b) shows the velocity field distribution is similar to the velocity field for an equi-density capsule train for the same order of capsules.

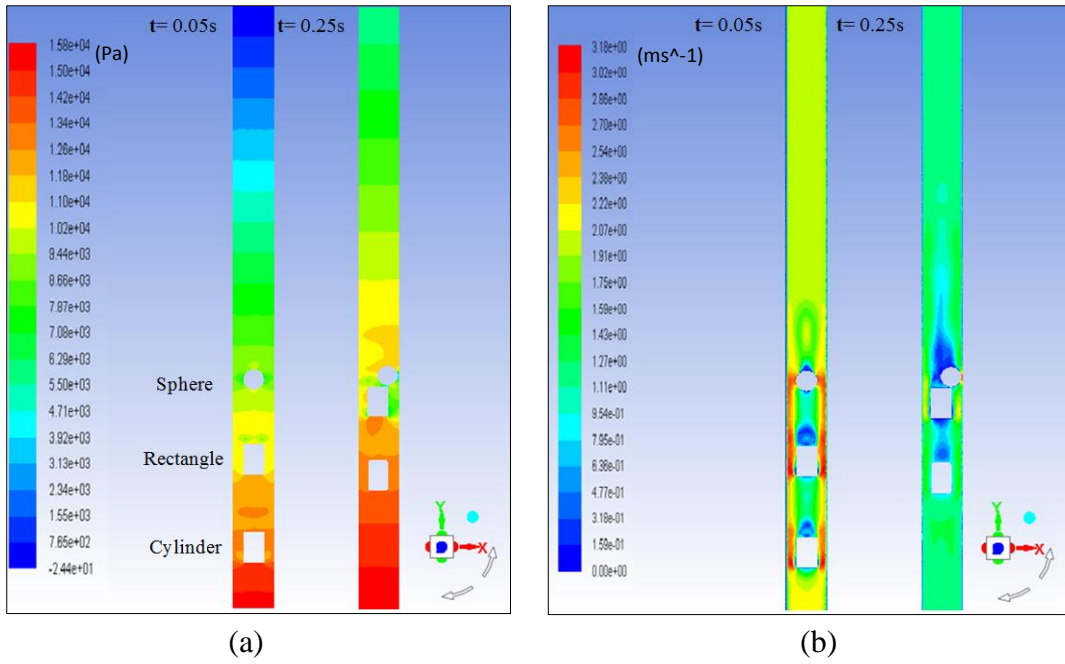


Figure 5.41 (a) Static gauge pressure and (b) Flow velocity magnitude variations for capsules in the (SRC) order of $k = 0.5$, $L_c = 1.5d$ and $V_{av} = 2\text{m/sec}$ at different flow times

Figure 5.42 depicts the time histories of the capsules velocity for the spherical (S), rectangular (R) and cylindrical (C) capsule in the (SRC) order of two different densities at flow velocity of 2m/sec. It can be noticed that the velocity profiles are quite similar for heavy and equal capsules densities in this order of the capsules. As it is observed in this order that the cylindrical capsule velocity is considerably higher than the other capsules velocity for both densities.

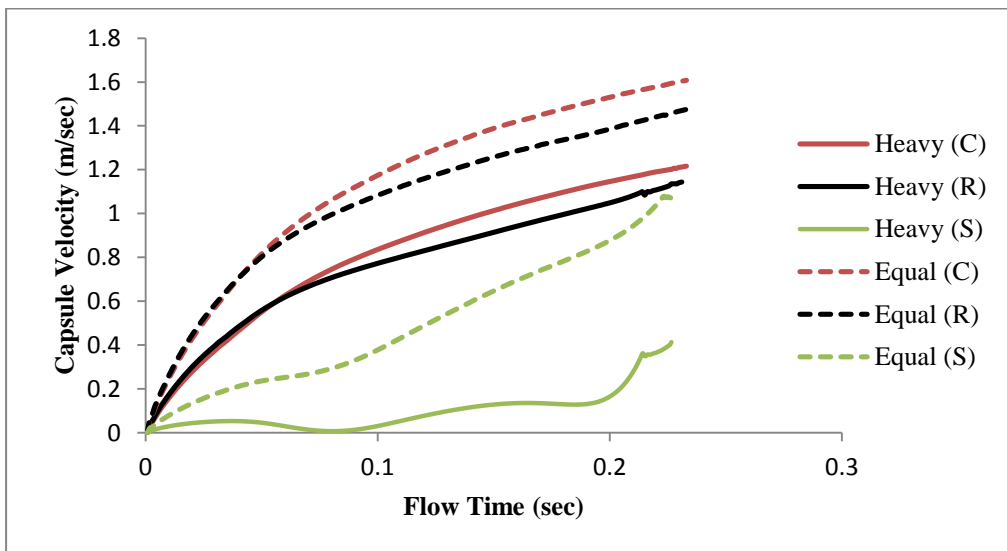


Figure 5.42 The effect of capsules in the (SRC) order on the capsule velocity history

5.4.3 Effect of the Position of the Capsule Shape in the RSC order

Figure 5.43 shows the local variations in the static gauge pressure and the flow velocity magnitude within a hydraulic pipe carrying a heavy density rectangular (R), spherical (S) and cylindrical capsules (C) of $k = 0.5$, $L_c = 1.5d$ and $V_{av} = 2\text{m/sec}$. The pressure at upstream location has increased by 4% as compared to the upstream location for equi-density capsules for the same order of capsules during the initial motion. The pressure and velocity fields resemble the one observed in the same order for the equal density in figure 5.31.

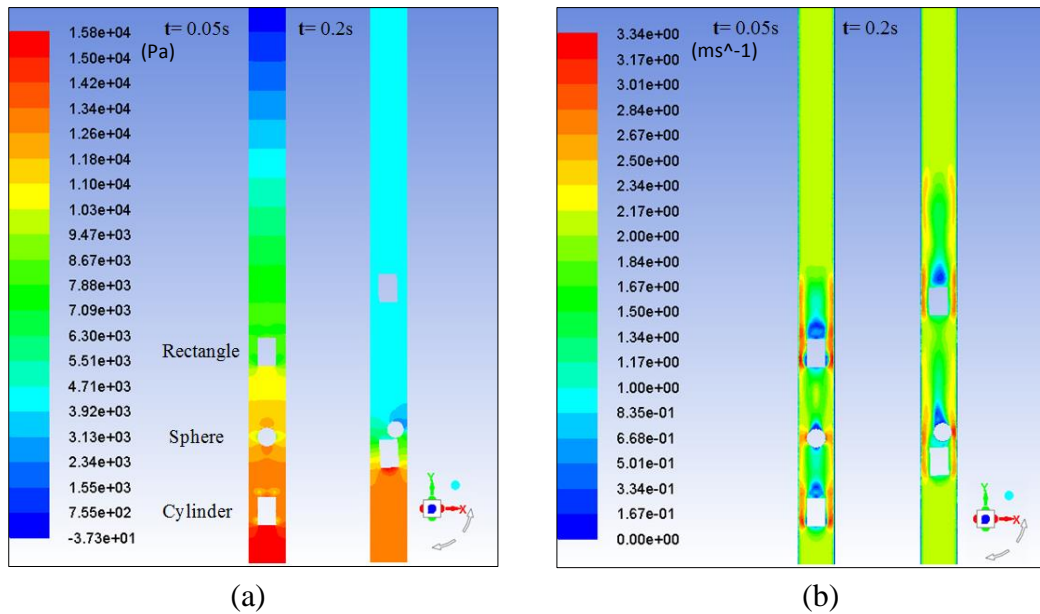


Figure 5.43 (a) Static gauge pressure and (b) Flow velocity magnitude variations for capsules in the (RSC) order of $k = 0.5$, $L_c = 1.5d$ and $V_{av} = 2\text{m/sec}$ at different flow times

Figure 5.44 depicts the time histories of the capsules velocity for the rectangular (R), spherical (S) and cylindrical capsules (C) in the (RSC) order of two different densities at flow velocity of 2m/sec. It can be observed that the velocity profiles are similar for heavy and equal capsules densities in this order of the capsules. Furthermore, it can be concluded that the capsules velocity decreases as the capsules density increases.

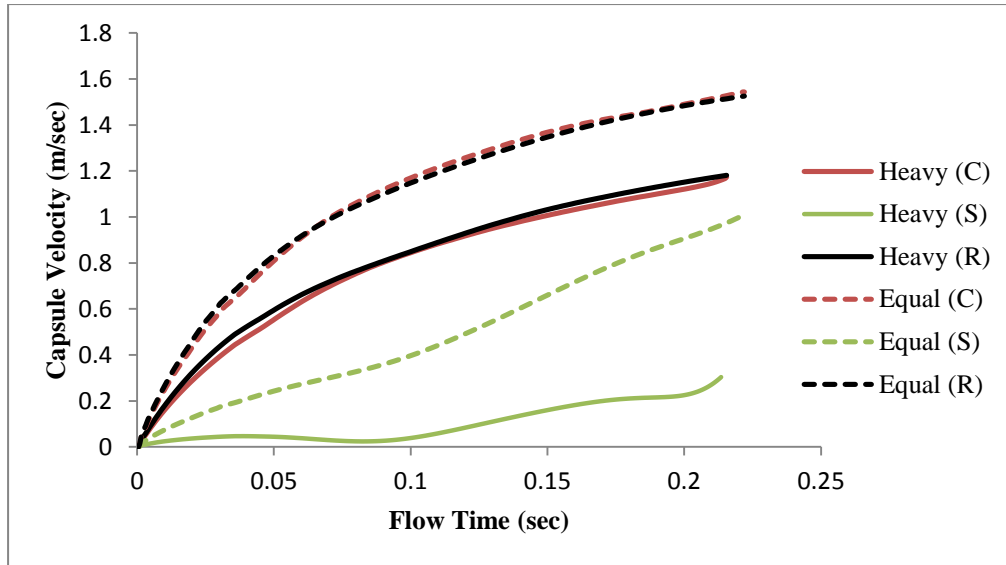


Figure 5.44 The effect of capsules in the (RSC) order on the capsule velocity history

5.4.4 Effect of the Position of the Capsule Shape in the RCS order

Figure 5.45 depicts the local variations in the static gauge pressure and the flow velocity magnitude in a hydraulic pipe carrying heavy density rectangular (R), cylindrical (C) and spherical (S) capsules of $k = 0.5$, $L_c = 1.5d$ and $V_{av} = 2\text{m/sec}$. The pressure at upstream location has increased by 8% as compared to the upstream location for equi-density capsules for the same order of capsules during the initial motion. Moreover, the results show almost the same velocity distribution regardless the density of capsules between equal or heavy density. It can be noticed that there is a large wake area downstream of the capsule train and also in-between the individual capsules in the train.

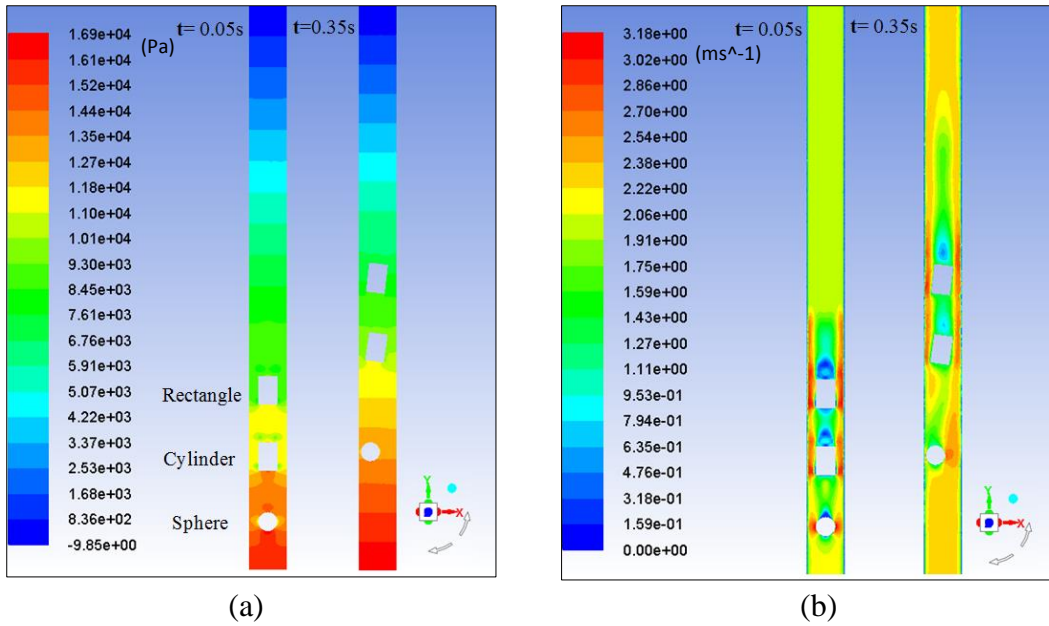


Figure 5.45 (a) Static gauge pressure and (b) Flow velocity magnitude variations for capsules in the (RCS) order of $k = 0.5$, $L_c = 1.5d$ and $V_{av} = 2\text{m/sec}$ at different flow times

Figure 5.46 depicts the time histories of the capsules velocity for rectangular (R), cylindrical (C) and spherical (S) capsules in the (RCS) order of two different densities at flow velocity of 2m/sec. It can be seen that the velocity of the equi-density capsules are higher than the heavy density capsules. On the other hand, it can be concluded that the capsules velocity decreases as the capsules density increases.

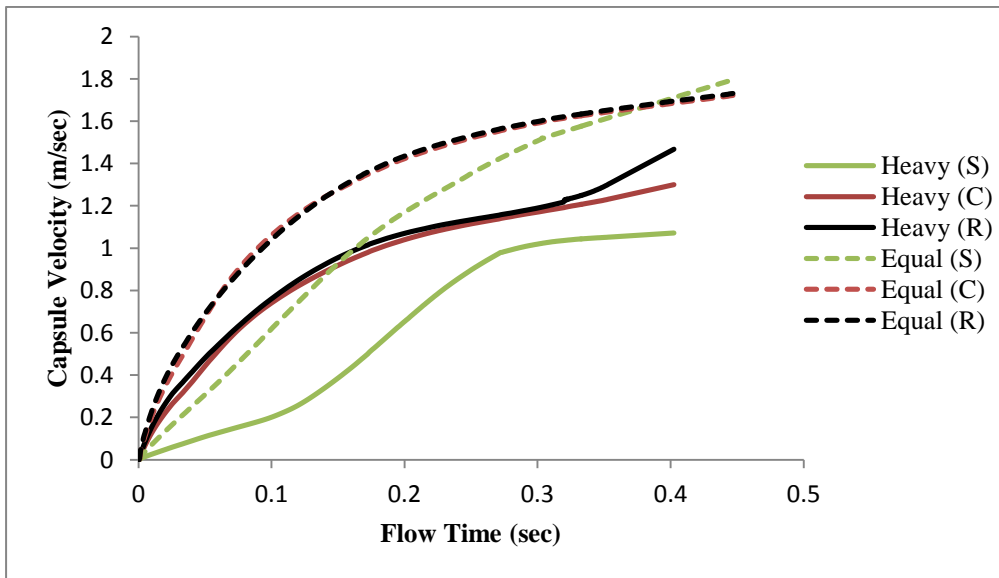


Figure 5.46 The effect of capsules in the (RCS) order on the capsule velocity history

5.4.5 Effect of the Position of the Capsule Shape in the CRS order

Figure 5.47 depicts the local variations in the static gauge pressure and the flow velocity in a hydraulic pipe carrying a heavy density cylindrical (C), rectangular (R) and spherical (S) capsules of $k = 0.5$, $L_c = 1.5d$ and $V_{av} = 2\text{m/sec}$. The pressure at upstream location has increased by 5% as compared to the upstream location for equi-density capsules for the same order of capsules during the initial motion ($t = 0.05\text{sec}$). Moreover, the results show almost the same velocity distribution regardless the density of capsules between equal or heavy density. However, it is observed that the flow time of the heavy density capsule train is longer than the equal density capsule train as in figure 35, under the same considerations.

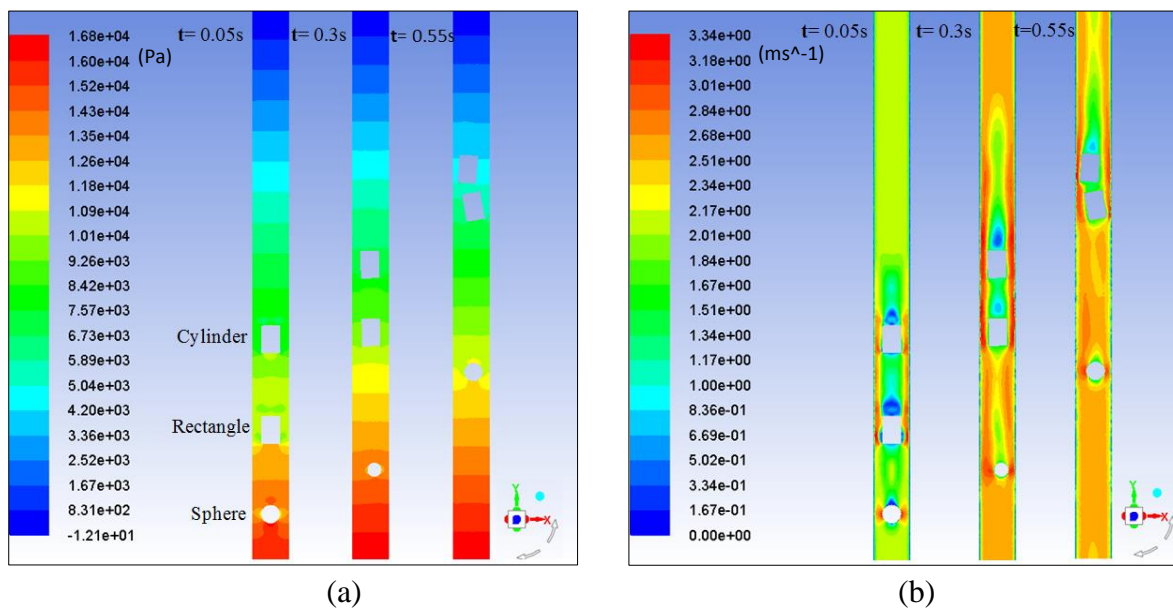


Figure 5.47 (a) Static gauge pressure and (b) Flow velocity magnitude variations for capsules in the (CRS) order of $k = 0.5$, $L_c = 1.5d$ and $V_{av} = 2\text{m/sec}$ at different flow times

Figure 5.48 depicts the time histories of the capsules velocity for the spherical (S), rectangular (R) and cylindrical (C) capsules in the (CRS) order of two different densities at flow velocity of 2m/sec . It can be seen that the velocity profiles along the test section are quite similar for heavy and equal capsules densities in this order of the capsules. Furthermore, it can be concluded that the capsules velocity decreases as the capsules density increases.

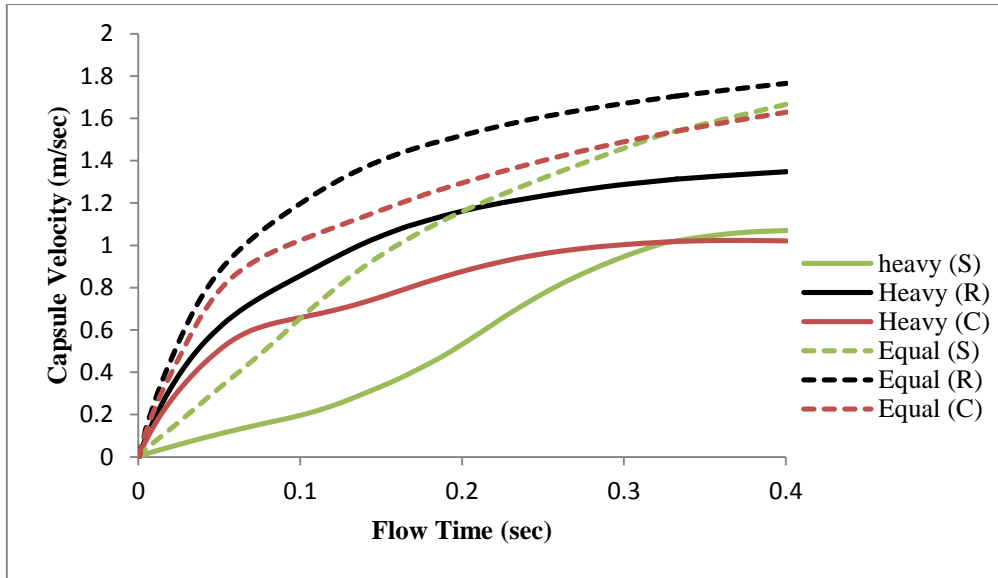


Figure 5.48 The effect of capsules in the (CRS) order on the capsule velocity history

5.4.6 Effect of the Position of the Capsule Shape in the CSR order

Figure 5.49 depicts the local variations in the static gauge pressure and the flow velocity magnitude in a hydraulic pipe carrying heavy density cylindrical (C) spherical (S) and rectangular (R) capsules of $k = 0.5$, $L_c = 1.5d$ and $V_{av} = 2\text{m/sec}$. The pressure at upstream location has increased by 4% as compared to the upstream location for equi-density capsules for the same order of capsules during the initial motion ($t = 0.05\text{sec}$). Moreover, the results show almost the same velocity distribution regardless the density of capsules. The heavy density capsule train provides more resistance to the flow and increasing the pressure drop.

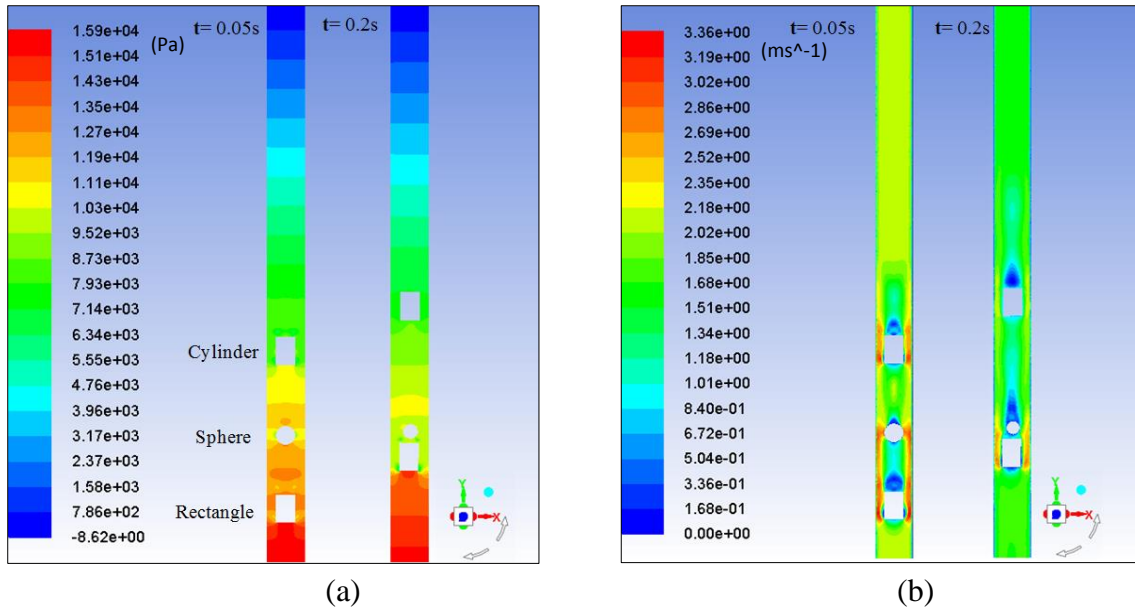


Figure 5.49 (a) Static gauge pressure and (b) Flow velocity magnitude variations for capsules in the (CSR) order of $k = 0.5$, $L_c = 1.5d$ and $V_{av} = 2\text{m/sec}$ at different flow times

Figure 5.50 depicts the time histories of the capsules velocity for the cylindrical (C), spherical (S) and rectangular (R) capsules in the (CSR) order of two different densities at flow velocity of 2m/sec. It can be observed that the velocity profiles are similar for heavy and equal capsules densities in this order of the capsules. Based on shape velocity of the capsule it observed that the rectangular faster than the cylindrical and spherical capsule respectively for both the densities. Furthermore, it can be concluded that the capsules velocity decreases as the capsules density increases.

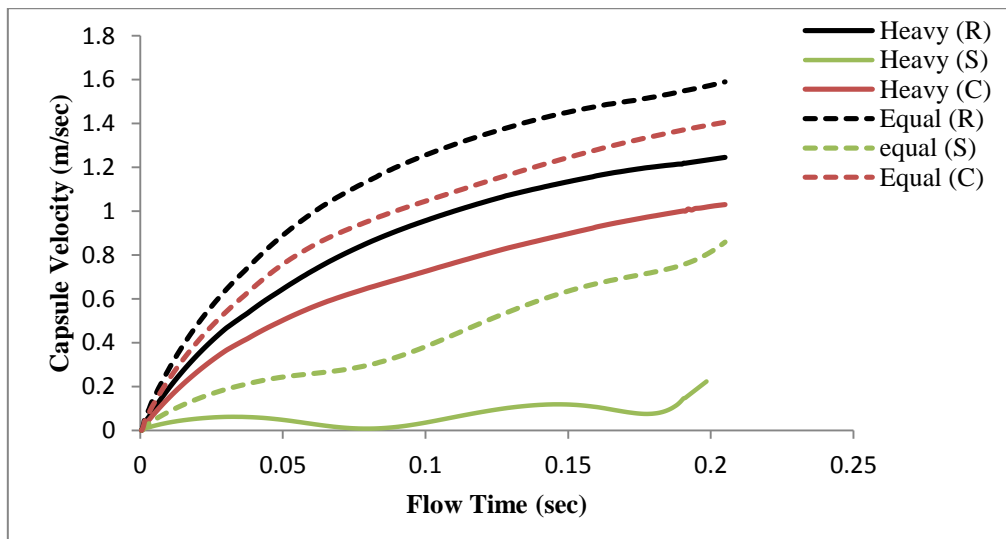


Figure 5.50 The effect of capsules in the (CSR) order on the capsule velocity history

5.5 Development of Novel Semi-Empirical Prediction Model

According to the results, which have been offered in this chapter from dynamic mesh simulations, a prediction model for the correction factor of mixed shapes of a capsules combination can be developed. The purpose of developing the correction factor is to compute the pressure drop accurately for mixed capsule shapes. Hence, the correction factor developed here needs to be used with the pressure drop prediction model developed in the previous chapter. All arrangements of capsules combination shapes included in the investigation have been involved in the formulation of the correction factor.

The analysis of multivariate regression has been used to obtain the coefficients; the semi-empirical correlation for the correction factor of mixed capsules shapes has been formulated. This factor can be linked to the capsule friction coefficient (f_c), developed in Chapter 4, in order to calculate the pressure drop for mixed shapes of a capsules combination.

$$C_f = \frac{10^{1.13} \left(\frac{Vol_c}{Vol_p} \right)^{0.63}}{(Cg)^{0.5}} \quad (5-1)$$

where Vol_c is the capsule volume, Vol_p is the pipe volume and Cg is the position of the capsule centre gravity within the vertical pipeline. The pressure drop for a single capsule shape flowing individually in the pipeline has been calculated in chapter 4, based on the capsule friction coefficient (f_c), developed in section 4.7.2.

The above equation and the pressure drop for a single capsule shape flow can hence be used to calculate the pressure drop for mixed shapes of capsules combination by the following expression:

$$\Delta P_{comb} = \frac{\sum \Delta P_{single}}{C_f} \quad (5-2)$$

where:

ΔP_{comb} : Pressure drop for a mixed shapes flow of a capsules combination in a pipeline

ΔP_{single} : Pressure drop for a single capsule shape flow within a pipeline

C_f : Correction factor

The following figure illustrates the accuracy of the developed equation for calculating correction factor. To determine the accuracy level of the equation, the calculated data from the equation is plotted versus the numerical data from CFD. According to the figure 5.51, the maximum difference between the predicted and calculated correction factor is 5%, and most of the points are well below that margin, which reveals excellent fitting of present model equation. Moreover, the prediction model established here can be utilised in the vertical HCPs design (for more details look to Chapter 6).

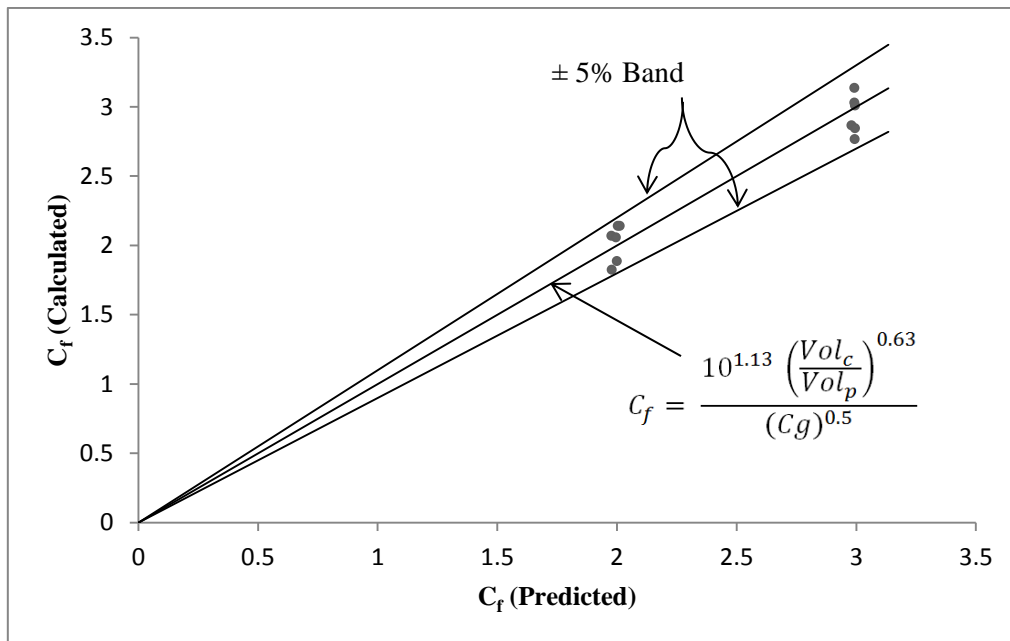


Figure 5.51 Correction factor for a mixed shapes flow of capsules

5.6 Summary

The main object of this chapter was to study the hydrodynamics of various shapes of capsules that flowing together. Moreover, it has been investigated the effect of a position order of a capsule shape in a capsule train, which affect the capsule train velocity and the change of pressure field. As a result of a simple and complex combination flow of basic capsule shapes, it was seen that some capsules in a mixed shapes system will collide with each other. Consequently, a mixed capsules system sometimes causes a blockage in the

vertical pipeline. Some important observations that have been observed during the numerical investigation are listed below.

- The change of capsule shape order lead to change in the pressure drop and the capsules velocity for a capsule train.
- The spherical capsule is considered the lowest velocity between the other shapes regardless the capsule order in a capsule train, whether is in a simple or complex combination flow of capsules.
- Increasing the density of the capsule increases the pressure drop and decreases the capsule velocity in a capsule train.

The prediction model was developed for the correction factor of the pressure drop of a capsules combination flow based on the capsules order in a pipeline. More details regarding the vertical HCPs design are provided in Chapter 6. Based on flow characteristics analysis, the next chapter includes the details regarding the optimal design of a vertical hydrilic capsule pipeline.

Chapter 6 - Optimisation Modelling

Optimisation of HCPs plays a vital role in the commercial acceptability of such pipelines. Based on the correlations have been developed regarding the capsules flow in vertical HCPs. The optimisation methodology proposed in this chapter has been developed for various geometric and flow conditions. The correlations developed in the current study, have been used to establish a methodology to determine the optimal vertical HCP design. The model of optimisation provided in this study is based on the least total cost.

6.1 Overview

As it was stated in the first Chapter that the foundation of this research is the hydraulic parameters that impact the way in which HCPs are designed. Thereby, the optimisation model that is established is also affected by the hydraulic design of HCPs. Pipeline designers are always looking towards optimisation to design pipelines based on different principles, such as least-cost of the pipeline, minimum energy consumption, etc. Same is true for hydraulic capsule pipelines as well. In view of this, the methodology of optimisation has been developed in the current research in relation to vertical hydraulic capsule pipes. The established methodology is depended on the least-cost principle; thereby, various costs involved in an HCP design have been taken into consideration and discussed in detail here. These costs comprise an HCP's manufacturing and operating costs. The present optimisation model utilises the Least-Cost Principle which asserts that an HCP's optimum design is one in which the overall pipeline cost is at a minimum and where the overall cost points to the total of the manufacturing and operating expenses.

6.2 Optimisation Process Theory

The design procedure for pipelines transporting capsules includes the determination of the pipeline diameter, where the total cost of an HCP should be the lowest cost. Then, minimising the overall cost based on the pipe diameter. The total cost of an HCP comprises of capsule and pipeline manufacturing costs as well as operating costs of the transport process.

$$C_{Total} = C_{Manufacturing} + C_{Operating} \quad (6-1)$$

The cost of manufacturing involves the manufacturing of the pipelines itself and the capsules to be transported. While the operating costs constitute the day-to-day operation of the pipeline system, and is also called as the cost of power consumed.

$$C_{Total} = C_{Pipe} + C_{Capsule} + C_{Power} \quad (6-2)$$

This process allows the designer to investigate all possible solutions of the system, thus decreasing practical applications, saving money and time.

6.3 Cost of Piping Material

The pipe cost is estimated per unit of pipe weight, which is presented by [68]:

$$C_{\text{Pipe}} = \pi D t_p \gamma_p C_2 L_p \quad (6-3)$$

where L_p is the total pipe length, t_p is pipe wall thickness. As reported by Davis et al [69] and Russel [70], the thickness of the pipe has been written as:

$$t_p = C_c D \quad (6-4)$$

where C_c refers to a proportionality constant dependent on diameter ranges of the pipeline and anticipated pressure.

6.4 Cost of the Capsules

The capsules costs can be calculated dependent on the capsule shape per unit weight of capsule material as following:

$$C_{\text{Capsules}} = (SA_c) t_c N \gamma_{\text{Cap}} C_3 \quad (6-5)$$

where SA_c is the surface area of the capsules, t_c is the capsule wall thickness, N is the capsules number within the pipe and γ_{cap} is the capsule specific weight. In order to compute the cost of the capsules in terms of their shape factors, a relationship has been developed between the surface area of the capsules and the shape factor, resulting in a modified equation for the cost of the capsules:

$$C_{\text{Capsules}} = 0.065 (\phi + 1)^{5.6} k^2 D^2 t_c N \gamma_{\text{Cap}} C_3 \quad (6-6)$$

6.5 Cost of Power Consumption

Energy requirements costs correspond to the costs included in pumping the carrier liquid and the capsules across the pipeline. The power consumption costs per unit watts are provided by:

$$C_{Power} = C_1 x P_W \quad (6-7)$$

where, P_W is the pipeline's power consumption. The power controls the chosen of the pumping unit for transporting the capsules across the vertical HCP. This pumping power is computed by [5]:

$$P_W = \frac{Q_m \times \Delta P_{Total}}{\eta} \quad (6-8)$$

where Q_m is mixture flow rate, ΔP_{Total} expresses on the total drop pressure due to transport the capsules across pipes whereas η expresses on the pumping efficiency. Liu [71] reports the equation to compute the mixture flow rate through a circular pipe as:

$$Q_m = \frac{\pi D^2}{4} V_{av} \quad (6-9)$$

The total pressure drop variation inside the straight vertical pipe can be calculated as follows:

$$\Delta P_{Total} = f_w \frac{L_p}{D} \frac{\rho_w V_{av}^2}{2} + f_c \frac{L_p}{D} \frac{\rho_w V_{av}^2}{2} + \rho_w g \Delta h \quad (6-10)$$

The term f_w in the above equation indicates the friction coefficient due to water alone, which can be can be estimated by the Moody's Chart [67] as:

$$f_w = 0.0055 + \frac{0.55}{Re_w^{\frac{1}{3}}} \quad (6-11)$$

A semi-empirical formulation for the friction coefficient of the capsule f_c has been developed for any capsule shape in chapter 4. This relation is to be used in the optimisation model in order to predict the total pressure drop across the HCP.

6.6 Solid Throughput

Hydraulic capsule pipelines are designed for particular solid throughput requirements; hence, the solid throughput (in m³/sec) is an input to the optimisation model being developed here. The *solid* throughput can be expressed as:

$$\text{Solid Throughput } (Q_c) = \text{Volume of a capsule} \times \frac{\text{Number of capsules in the train}}{\text{Time taken to travel unit length}}$$

Hence:

$$Q_c = 0.02 (0.25\phi + 1)^{4.82} k^2 D^2 L_c N \frac{V_c}{L} \quad (6-12)$$

6.7 Total Cost of the Optimal Pipeline

For the optimum diameter of pipe, total cost must be a minimum, where the pipeline total cost can be computed from Eq (6-1). The main cost of operating a pipeline is the cost of energy consumed by pumps that are pushing the water with capsules upward the pipeline. The work associated with operating a pump and the manufacturing cost of pipe and capsules are interrelated by the diameter of the pipe. Therefore, designing a pipe with the appropriate diameter is crucial to the optimisation of the pipeline. The optimal diameter can be obtained by taking the first derivative of the total cost with respect to the pipe diameter and equating it to zero [72]:

6.8 The Optimisation Model Implementation

Design optimisation of HCPs is quite important in order to the commercial viability of transportation system. The following section of this chapter comprises the process to select the optimised model. In order to run the optimisation model following steps should be followed, which are given below:

1. Assume a value of D where k and d are a function of D .
2. The the pipeline length is known from the essential information of the capsules injection and evacuations sites.
3. Specify capsule density s will be directly calculated.
4. Specify L_c , t_c , C_1 , C_2 , C_3 , C_c , η and the material properties of the pipe (already determined).
5. Compute the cost of pipe and the capsules.
6. Compute V_c and V_{av} hence Re_w and Re_c are directly calculated.
7. Q_m is computed using Eq (6-9) and Q_w is directly calculated as Q_c is known.
8. Calculate friction coefficients for both water and the capsules addition to the elevation pressure. Thereby, the total pressure drop can be directly computed.
9. Compute the power requirement for the system using Eq (6-8) and the cost of power using Eq (6-7).
10. Compute the overall cost of the pipeline.
11. Repeating the steps mentioned above for different diameters values till such value is reached that is the minimum total cost of the pipelines.

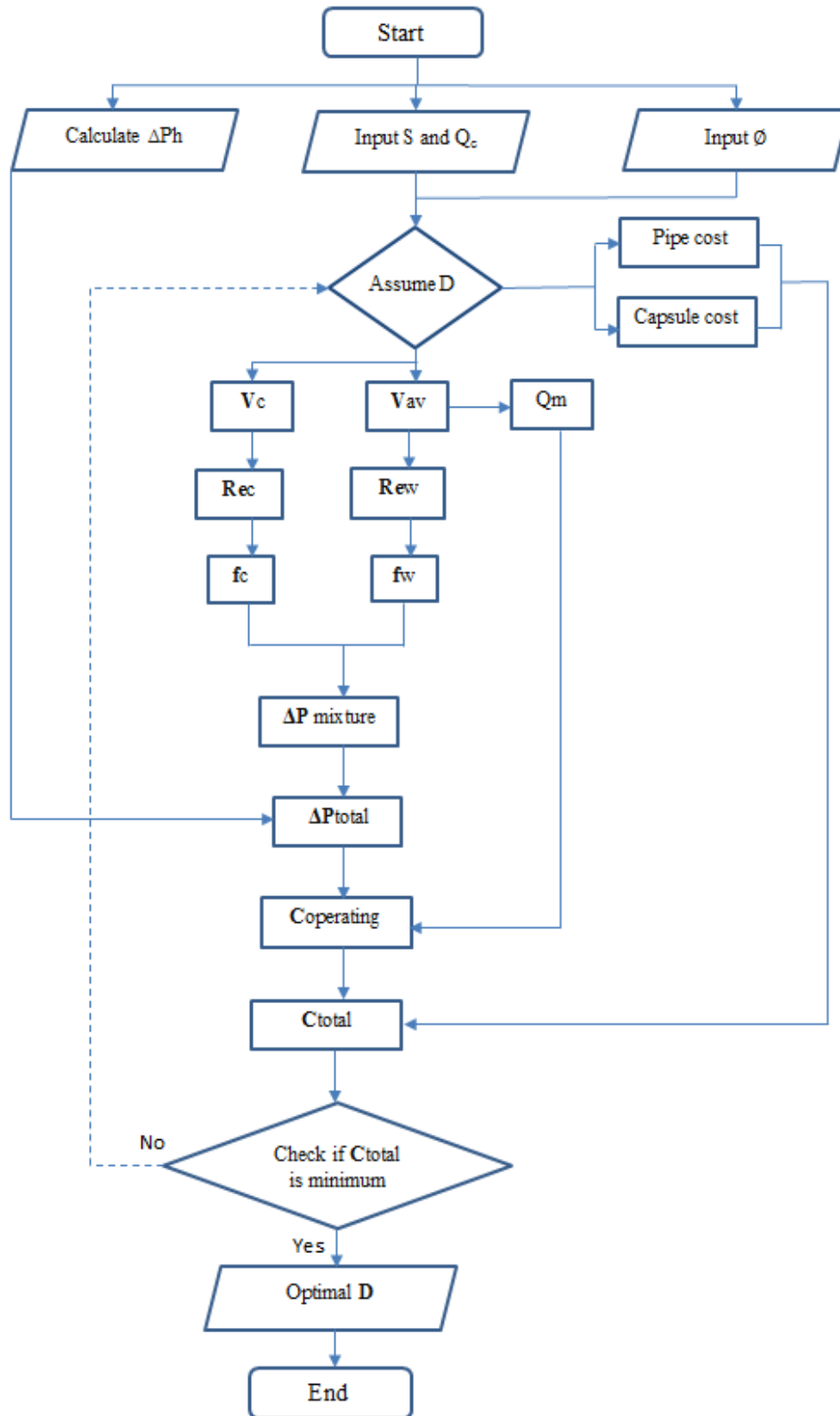


Figure 6.1 Flow chart of the optimisation model

6.9 Design Example of Vertical HCP

This section will illustrate the procedure and the steps to understand the optimisation methodology and how can this be utilised in the design process. In this application, polypropylene needs to be transported from the sea bed to the upper deck, 100m up, in the form of spherical capsules of $\varnothing = 4$ and $k = 0.5$, across a steel pipeline. The required throughput is $0.003\text{m}^3/\text{sec}$. It is required to determine the optimal diameter of the pipeline and the pumping power, which can deliver the required throughput at a lower cost.

Solution: Based on the current market, the values of various constants are:

$$C_1 = 1.4 \qquad C_2 = 1.1 \qquad C_3 = 0.95 \qquad C_c = 0.01$$

The density of Polypropylene is equal to that of water. Based on the above-mentioned HCP design optimisation steps for the transport of capsules, different costs involved and the required pumping power are indicated in table 6-1.

Table 6-1 Variations in Various Costs versus Pipeline Diameter

D (m)	P (kW)	C_{Manufacturing} (£)	C_{Power} (£)	C_{Total} (£)
0.15	82.17	6153	115047	121200
0.16	80.8	7013	113121	120134
0.17	79.76	7932	111662	119594
0.18	78.95	8908	110531	119439
0.19	78.31	9943	109639	119582
0.20	77.80	11036	108921	119958
0.21	77.38	12190	108336	120526
0.22	77.04	13401	107853	121254

According to the results obtained in table 6-1 it can be noticed that the optimum diameter of pipe is 0.18m for the case under consideration as its total cost is minimum. The power of the desired pumping unit, corresponding to the optimum diameter of the pipeline, is 78.95kW.

Figure 6.2 also shows an analysis of the results in table 6.1 of changes in operating and manufacturing costs as a function of the diameter of the pipeline. It can observe that as the diameter of the pipeline increases, the cost of manufacturing increases. This is because in the reality the pipelines of larger diameters cost more than pipelines that have comparatively smaller diameters. Moreover, with the increased diameter of the pipeline, the operating cost declines. This is because of the fact that, as the diameter of the pipeline is increased for the same solid throughput, this leads to the flow velocity decline inside the pipeline. The cost of operating is connected to a proportional relation to the flow velocity; thereby, the increase in the internal diameter of the pipeline reduces the cost of operating of the HCP.

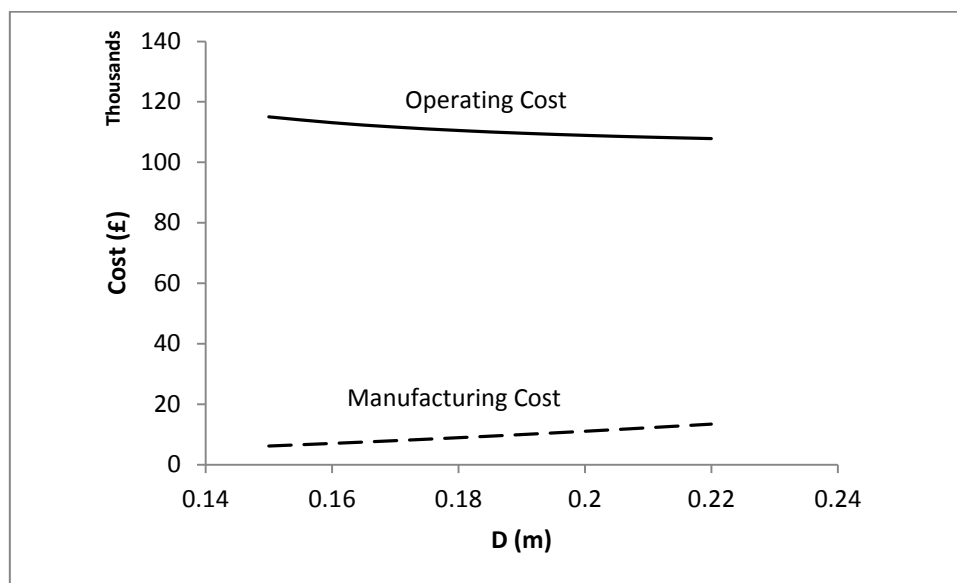


Figure 6.2 Variations in manufacturing and operating costs versus pipeline diameter

Figure 6.3 indicates the variations of the power of the desired pumping and the total cost at varied pipe diameters. It is observed that as the diameter of the pipe increases, the power of the desired pumping declines. Moreover, as the diameter of the pipe increases, the total cost of the pipe first reduces and then rises afterwards. The total cost of the pipeline is the sum of operating and manufacturing costs in the opposite directions compared to the diameter of the pipe, thereby, the combination of these costs presents the curve of the overall cost. The diameter of the pipeline corresponding to the minimum of the total cost is the optimum diameter of the vertical pipeline.

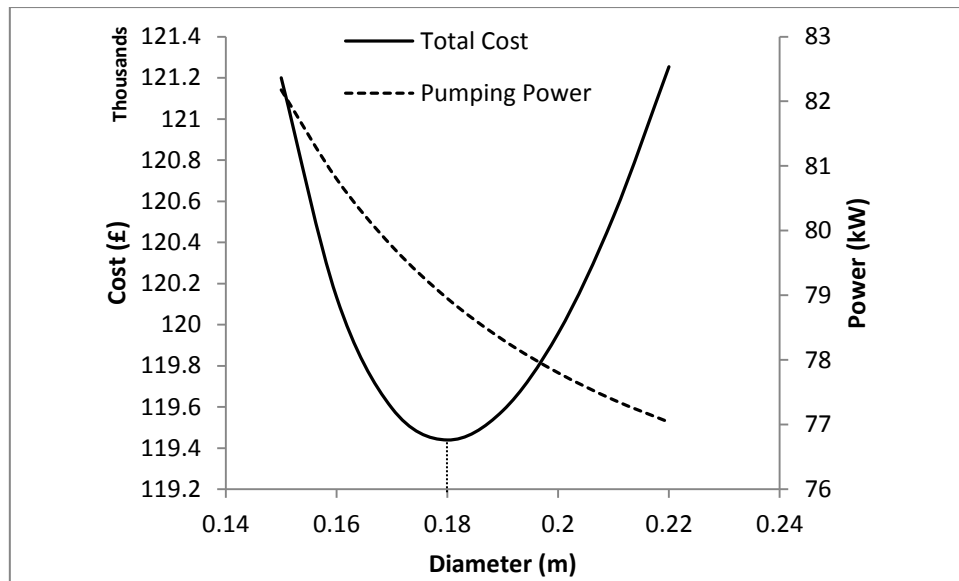


Figure 6.3 The total cost and pumping power versus pipeline diameter

6.9.1 Effect of Cylindrical Capsule Shape

For sake to analyse the impact of the capsule shape on the design of the pipeline, the above example is resolved for cylindrical shapes of capsules of $\varnothing = 6$, despite whole other parameters are kept the same. Table 6.2 provides the findings of the design of cylindrical capsules pipeline.

Table 6-2 Variations in Various Costs versus Pipeline Diameter

D (m)	P (kW)	C_{Manufacturing} (£)	C_{Power} (£)	C_{Total} (£)
0.08	31.694	1791	44371	46162
0.09	29.639	2280	41495	43775
0.1	28.386	2832	39741	42573
0.11	27.569	3447	38597	42044
0.12	27.007	4127	37810	41937
0.13	26.603	4873	37245	42118
0.14	26.304	5685	36825	42510
0.15	26.075	6564	36505	43069
0.16	25.896	7512	36255	43767

From the results shown in table 6.2, it is observed that the optimum diameter of the pipeline for the cylindrical capsules flow is 0.12 m, which is less than the flow rate of the spherical capsules in the pipeline. The shape factor of the cylindrical capsule is greater than the shape factor of a spherical capsule in the same considerations. Thereby, it is evident that as the shape factor increases, the pipe optimum diameter also decreases, with a decrease in total cost of the pipeline. .

6.9.2 Effect of Rectangular Capsule Shape

The designers of the pipelines are constantly searching for the best options to design a specific throughput pipeline. Thus, the above example is resolved once more employing rectangular capsules of $\phi = 7.63$, , despite whole parameters have been kept the same.

Table 6.3 provides the findings of the design of rectangular capsules pipeline.

Table 6-3 Variations in Various Costs Variations versus Pipeline Diameter

D (m)	P (kW)	C_{Manufacturing} (£)	C_{Power} (£)	C_{Total} (£)
0.05	18.946	715	26524	27240
0.06	15.862	1045	22206	23251
0.07	14.413	1441	20178	21619
0.08	13.623	1908	19072	20980
0.09	13.146	2447	18404	20850
0.1	12.835	3061	17969	21030
0.11	12.621	3752	17669	21421
0.12	12.467	4523	17454	21977
0.13	12.353	5375	17294	22669

As shown in table 6.3 it can be noticed that the pipeline optimum diameter for rectangular capsules transport is 0.09m, which is less than for flowing of cylindrical and spherical

capsules in the pipeline. The shape factor of rectangular capsules is greater than for cylindrical and spherical capsules.

The same trends in the different costs are observed for different shape factors of the capsules. Hence, a comparison of only the optimal pipeline diameter for different shape factors is presented in table 6-4. It can be clearly seen that the shape factor is inversely proportional with the optimal diameter of the pipeline; hence, increase in shape factor decreases the pipeline's optimal diameter, and then, the pipeline's total cost.

Table 6-4 Effect of the Shape Factor of the Capsules on the Optimal Pipeline Diameter and the Total Cost of the Pipeline

Capsule Shape (-)	Shape Factor (-)	Optimal Diameter (m)	Total Cost (£)
Spherical	4	0.18	119439
Cylindrical	6	0.12	41937
Rectangular	7.63	0.09	20850

In order to further analyse the usefulness of the design optimisation methodology developed in this chapter, a vast band of the parameters concerned is considered. This has led to the development of a performance chart for HCPs with different shaped capsules (having different shape factors), and different solid throughput requirements. The variations in the optimum pipeline diameter as a function of the solid throughput, and the shape factor of the capsules are depicted in figure 6.4. It can be clearly seen that as the shape factor increases, the optimal pipeline diameter decreases at any solid throughput.

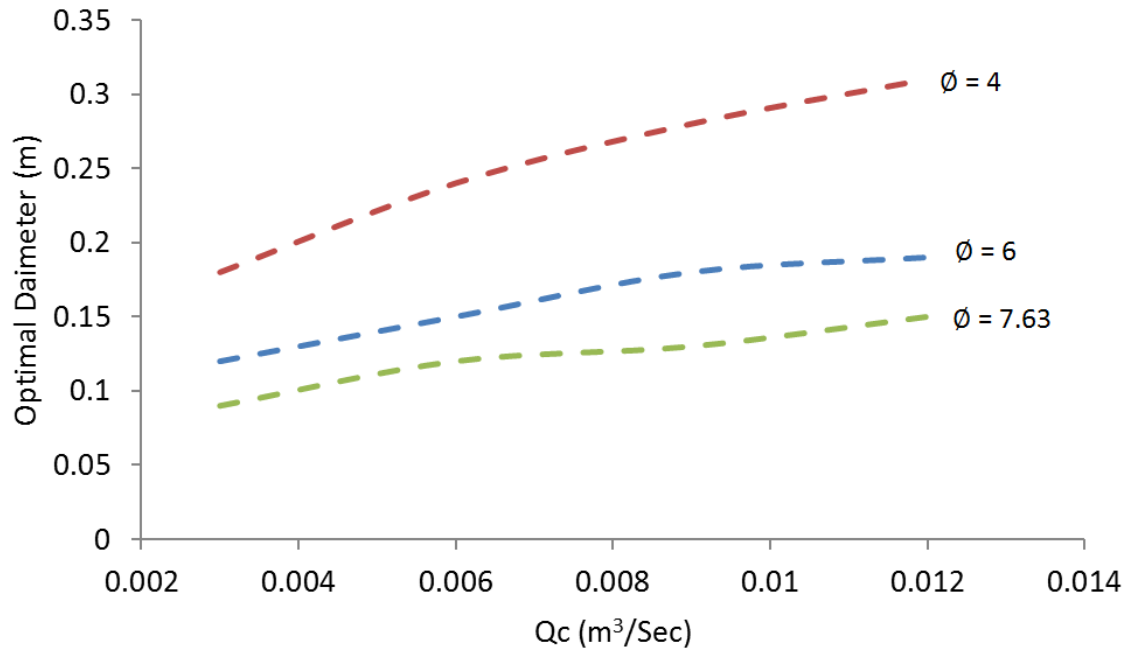


Figure 6.4 Effect of the solid throughput required and the shape factor of the capsules on the optimal diameter

6.10 Effect of Mixed Capsules Shapes

Cylindrical (C) and spherical (S) capsules, made from polypropylene, need to be conveyed from the sea bed to the upper deck, 100m up, in the form of a combination in CS order. The capsules have $L_c = 1d$ and $k = 0.5$, and need to be transported inside a steel pipeline. The required solid throughput is $0.02\text{m}^3/\text{sec}$. It is required to determine the optimum diameter of the pipeline and the pumping power needed for this purpose.

Solution: Based on the current market, the values of various constants are:

$$C_1 = 1.4 \qquad C_2 = 1.1 \qquad C_3 = 0.95 \qquad C_c = 0.01$$

Based on the aforementioned HCP optimisation steps for the transport of capsules, different costs involved and the required pumping power are summed up in table 6.5.

Table 6-5 Variations in Transportation Costs versus Pipeline Diameter in the CS order

D (m)	P (kW)	C_{Manufacturing} (£)	C_{Power} (£)	C_{Total} (£)
0.13	81.99	6966	114788	121754
0.14	78.44	8299	109820	118119
0.15	75.68	9780	105953	115733
0.16	73.49	11415	102884	114299
0.17	71.72	13211	100407	113618
0.18	70.27	15175	98378	113553
0.19	69.07	17313	96696	114009
0.20	68.06	19633	95285	114919
0.21	67.21	22141	94092	116233
0.22	66.48	24844	93072	117916

It can be seen in table 6.5 that as increasing in the pipeline diameter, the manufacturing cost increased. This is because of the fact that pipelines of smaller diameters are cheaper than pipelines with comparatively larger diameters. Moreover, with the increased diameter of the pipeline, the cost of operating reduces. This because the truth that the same solid productivity for the same increase in diameter of the pipeline reduces the flow velocity inside the pipe. The cost of operating has a relation proportional to the flow velocity. Thus, increasing the diameter of the pipeline reduces the cost of operating the pipeline.

These trends have been plotted in figure 6.5, for the costs only. It can be observed that the increase in the manufacturing cost is not directly proportional to the decrease in the cost of power. Hence, the total cost is seen to first decrease up to a certain value of the diameter of the pipeline, and then it increases. Thereby, the effect of the cost of power is dominant on the total cost at lower pipeline diameters, while the manufacturing cost is dominant at larger diameters. Due to this shift in the cost dominance from the manufacturing and power costs,

the total cost curve shows a local minimum at the point where this shift occurs. The corresponding pipeline diameter is the pipeline's optimal diameter, for that particular solid throughout required, based on the least-cost principle. It can be noted that a pipe with a diameter of 18 cm is optimum for the transport of capsules in an CS order and $k = 0.5$. The corresponding total cost and the required power of the pumping unit are £113553 and 70.27kW.

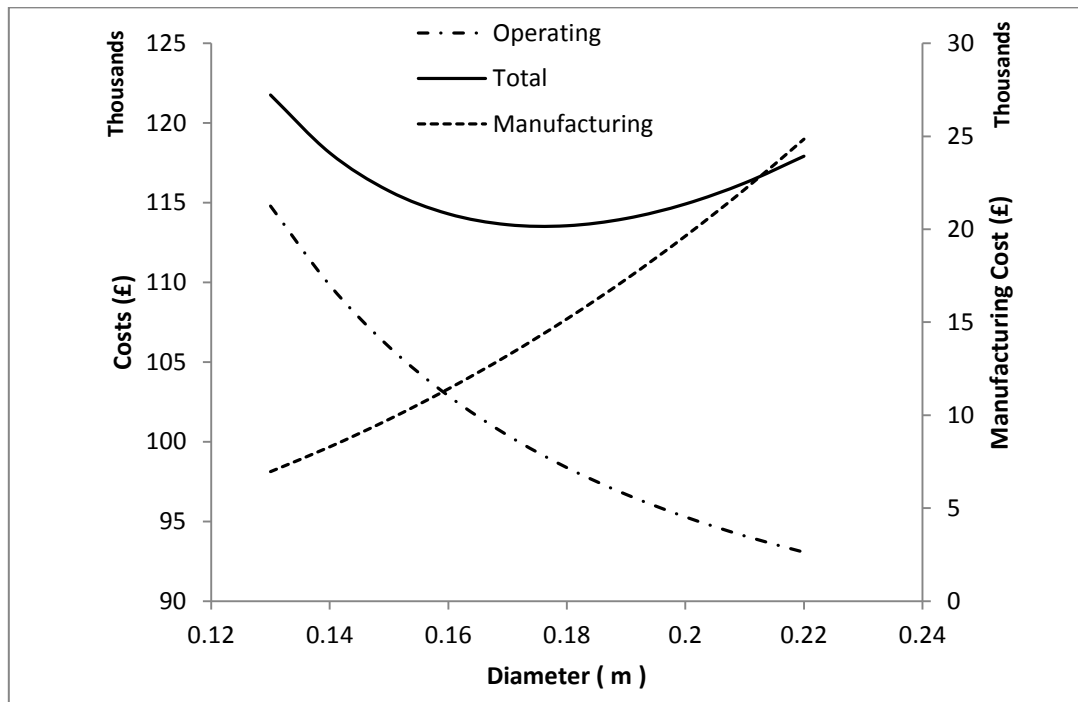


Figure 6.5 Variations in the different costs of the pipeline versus pipeline diameter for the transport of capsules in a CS order

6.10.1 Effect of the Capsules order of Mixed Shapes

For sake to examine the impact of the capsule shape on the design of the optimal pipeline, the above example is resolved once more using the capsules combination in the opposite order of the previous order, keeping all other parameters. Hence, the capsules combination becomes in an SC order instead of the CS order. Table 6.6 depicted the results of differences in the pumping capacity and the diameter of the pipeline versus the different costs of the pipeline.

Table 6-6 Variations in Transportation Costs versus Pipeline Diameter in the SC order

D (m)	P (kW)	C_{Manufacturing} (£)	C_{Power} (£)	C_{Total} (£)
0.13	92.26	6966	129170	136136
0.14	88.01	8299	123204	131503
0.15	84.68	9780	118560	128339
0.16	82.05	11415	114872	126287
0.17	79.92	13211	111895	125106
0.18	78.18	15175	109456	124631
0.19	76.74	17313	107434	124747
0.20	75.52	19633	105738	125372
0.21	74.50	22141	104303	126444
0.22	73.62	24844	103077	127921

As indicated in table 6.6 it is clearly observed in this order the optimum diameter of the pipe is 0.18m, which considered the same as depicted in the CS order for flowed capsules through the pipelines. Moreover, the pumping consumed power that needs for the optimum pipeline diameter is 78.18kW, which was 70.27kW for CS order. It can be seen that the manufacturing cost has remained the same as for the flow in the CS order. This is because the same capsules shapes and pipe have been used in both cases where the only difference is the capsules order in the pipeline.

Figure 6.6 illustrates the variations of the operating cost and total cost for the flow of the SC order and CS order in the vertical pipeline. From the figure, it is observed that the pipeline overall cost for the flow of SC order is considerably higher in comparison with the flow of CS order. Moreover, in the transportation pipeline, the cost of operating for the flow of SC order is greater in comparison with the flow of CS order. The reason beyond these trends is identical as above-mentioned, SC order leads to a greater pipeline pressure drop.

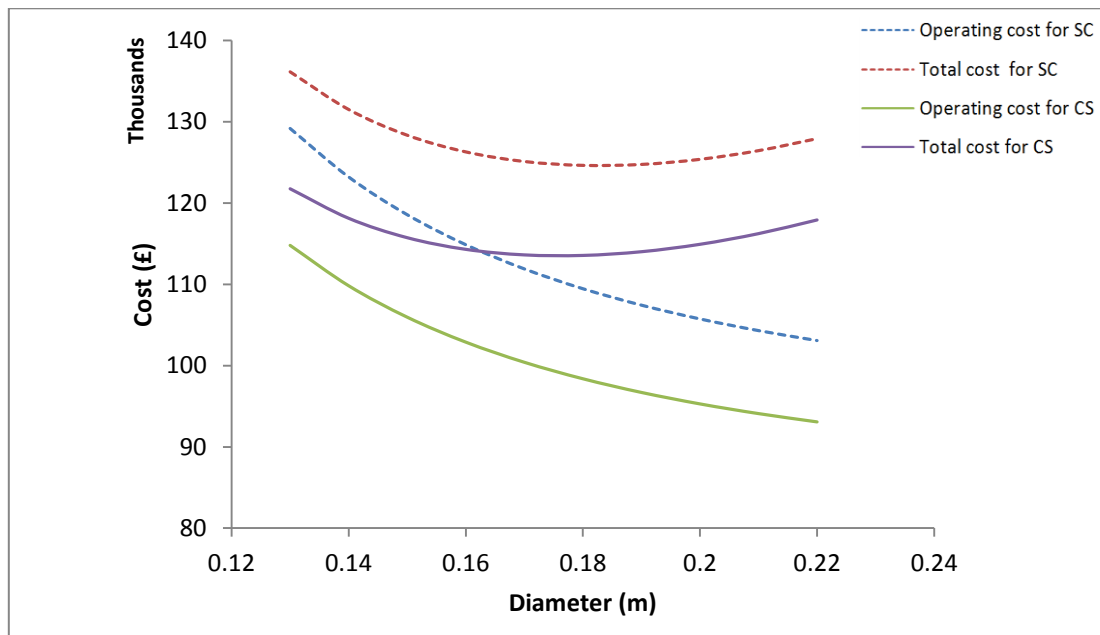


Figure 6.6 Comparison of different costs of the pipeline for the SC and CS order

It is evident in this chapter that the design examples provided reveal that the methodology of optimisation considers user-friendly in this research presented. Moreover, these practical examples have been included to demonstrate the usage and effectiveness of this optimisation model. Hence, this optimisation model can be applied to commercial applications.

6.11 Summary

The methodology has been proposed to determine the optimal size of vertical pipelines transporting different shaped capsules for practical applications. The optimal size of the pipeline has been identified for the minimum total cost. Based on the parametric investigations, the following outcomes are:

- ◆ The increase in the diameter of the pipe leads to decrease the pumping energy needed for the pipeline

- ◆ The manufacturing cost of the pipeline increases with the increase in the diameter of pipeline
- ◆ The pipeline's operating costs reduce with the increase in the pipeline diameters
- ◆ The pipeline total cost decreases initially and then increases with increase in the diameter of the pipe
- ◆ Increase the capsule shape factor decreases the optimal pipeline diameter
- ◆ Change in the order of capsule shapes in the pipeline does not change the optimal pipeline diameter, but change the required power of the pumping and the total cost

Furthermore, based on the results of the numerical analysis that carried out in Chapter 4 and 5. An optimisation approach has been proposed in this Chapter for vertical hydraulic capsule pipelines.

Chapter 7 - Conclusions

The flow of capsules of various shapes has been numerically simulated within vertical hydraulic capsule pipelines. This chapter concludes the thesis with a summary of the achievements, conclusions and contributions of this study. In this regards, this chapter will draw conclusions from the current study. At the end, recommendations for the future work are made for the continuation of this scientific investigation.

7.1 Research Problem Synopsis

The cargo transportation within containers (capsules) across pipeline considers as a modern manner of transporting goods. Consequently, this method is earning further significance around worldwide for reasons, such as the rise the cost of the fuel as well as the fossil fuels depletion. Furthermore, most of these studies that were conducted on capsule transport across pipelines are based on either practical experiments or analytical methods, which lack an accurate analysis on the complicated behaviour for the flow structure inside these types of transporting pipes. Recently, with the appearance of super-computers and advanced computerised applications, it has become possible to analyse the flow map and capsule trajectory motion across these pipelines under varying configurations.

According to the published literature, presented in chapter two, a group of aims of research objectives were identified, which formulate the field of the present study. These objectives were established for the sake of predicting the flow behaviour transporting capsules in vertical pipelines more accurately.

A summary of the primary thesis aims is presented along with the main achievements this study has attained as follows.

7.2 Research Aims and Main Achievements

The primary aims of this research that specified through an extensive review of the literature in this scope are presented below with a summary of how these goals can be achieved.

Research Aim # 1: Flow diagnostics in off-shore HCPs transporting basic capsule shapes under different operating conditions

Achievement # 1: In this thesis CFD has been used to provide an exhaustive investigation on the flow analysis of vertical pipes carrying different capsules shapes, and proposes prediction models for the capsule velocity and pressure reduction for such pipelines. Dynamic mesh technique with six degrees of freedom modelling has been used in order to move the capsules in full freedom. This technique is utilised to captures the transient flow phenomena arising

during a capsule interaction with the fluid motion and then offers a practical conception for these implementations.

The numerical model has been validated with available experimental data from published literature and it has shown good performance results. In this regards, numerical model can be used for further investigation with different configurations. Thus, a computational investigation about the flow of spherical, cylindrical and rectangular capsules under different geometric and flow considerations has also been presented. For the sake of covering a wide domain of investigations, the flow of these capsule shapes has been computationally simulated for various average flow velocities, capsule diameter, capsule length, capsule density and concentration of capsules.

The results obtained from the CFD simulations of the flow structure, the pressure and velocity fields at different flow times for transporting different capsules shapes have been analysed critically, in terms of quantity and quality. Qualitative analysis has been used to show the pressure and velocity contours in the capsule conveying pipeline, whereas the quantitative analyse has been conducted respectively to illustrate the pressure drop and capsule velocity inside the pipeline. The findings provided show an obvious description of the behaviour of the flow inside the pipeline and the impact of the capsule's existence on the structure of the flow and the pressure variation inside the pipeline. Furthermore, the motion of capsule can be monitored in a pipeline and the time that needs to arrive at its destination. While pipeline designers benefit from pipeline's pressure drop considerations for their design, the current study has used values of the pressure drop for different states under research to formulate semi-experimental relationships, which is predicting the capsule velocity and pressure reduction for any capsule shape in a vertical pipeline. The first main achievement of this study is the development of the relationships for the capsule velocity and pressure drop, which comprises the impacts of various geometrical parameters for conveying capsules in pipes. Furthermore, it can be demonstrated that these semi-empirical prediction models have a reasonable precision depending on the numerical findings.

Research Aim # 2: Flow diagnostics in off-shore HCPs transporting a combination of basic capsule shapes under different operating conditions

Achievement # 2: Due to limitations identified in the literature review a thorough study of mixed shapes of capsules has been carried out across vertical pipelines. In this work, a simple and complex combination of basic capsule shapes with a different order in a pipeline has been investigated numerically using CFD. The transient impacts were precisely caught from these simulations using techniques of sophisticated modelling like Dynamic Mesh with six-degree of freedom. In this technique, the capsule motion physically moves with fluid flow, and hence it affects the flow characteristics.

The effects of mixed capsules shapes on flow characteristics were also investigated, which is a main achievement of this study. Furthermore, a simple and complex combination flow of the heavy density and equal density capsules have been presented.

According to the elaborated numerical investigations regarding the fields of the velocity and the pressure in transporting mixed capsules have been analysed in terms of quantitatively and qualitatively. It has been depicted that the velocity and pressure differences in the capsules combination depend on the capsules order. Based on the findings by CFD simulations, the prediction model for the mixed capsules shapes has been established utilising sophisticated statistical tools. This model has been developed for the correction factor as a function of the pressure drop of a capsules combination flow based on the capsules order in a pipeline. This semi-empirical prediction model has also been given a reasonable accuracy.

Research Aim # 3: Development of an efficient optimisation model for predicting the optimal size of Off-Shore HCPs

Achievement # 3: The methodology of optimisation displayed here benefits from the semi-empirical relationships developed, based on the concept of least-cost, which is simple to utilise and can be depended upon. In this approach, semi-experimental relationships have been developed for anticipating of the pressure drop and capsule velocity for any capsule

shape within vertical pipelines. The models developed are unique in this study in the meaning that the parameters such as the shape of the capsules, density, size and flow velocity that affect the capsules transportation have been included in a vertical hydraulic capsule pipeline, which consider one of the significant accomplishments for this research.

In this study, the inputs to the model that has been established for optimum design including the shape factor, solid throughput and specific gravity. all other required parameters necessary for the HCP designing were calculated mathematically. The methodology of optimisation developed can as well precisely calculates the needed pumping power for this system, besides providing with the optimal diameter of the pipeline. Furthermore, this prediction model presents related parameters such as the capsule velocity, average flow velocity and mixture flow rate across the pipe. Thereby, this methodology that used is powerful and can be confidently employed in designing a vertical HCP system for different capsules.

7.3 Thesis Conclusions

An inclusive investigation has been conducted supporting the existed literature related to the capsules flow in vertical pipelines. Novel additions have also been done with an aim of developing the present conception of the process of design, operational characteristics, the effects related to the geometry and methodology of optimisation for the capsules transportation across vertical pipelines. In the following section, the main conclusions that have been summarized from each aspect of this study are presented.

- **Analyse the effect of the spherical capsule shape on flow characteristics of HCPs under transient conditions.**

This work conducted investigations concerning the shape of the spherical capsule, which include the effects of average flow velocity, capsule size, capsule density and capsule concentration on the flow characteristics. From the investigation, it can be deduced that the increase in average flow velocities leads to increase the pressure drop inside pipelines in comparison with the flow in low velocities. The capsules that have greater diameters lead to a

pressure drop in pipelines in comparison with capsules flow that has smaller diameters. Furthermore, heavy-density capsules lead to increase the pressure drop inside the pipeline in comparison with an equal density capsules flow. From the side of a capsules concentration, it may be deduced that increasing in the capsules concentration causes an increase in the pressure drop and decrease the capsule train velocity in the pipeline. The findings offered in this investigation with respect to the spherical capsules flow in pipelines is of important significance for designers of vertical pipelines as the model of the prediction that developed for the friction coefficient depends on this type of capsules; where it can be utilised in the optimisation and designing of the vertical HCP.

- **Investigate the effect of the cylindrical capsule shape on flow characteristics of HCPs under transient conditions.**

Through the investigations with respect to the shape of the cylindrical capsule that encompass the impacts of average flow velocity, capsule size, capsule length, capsule density and capsule concentration on the flow characteristics, conducted in this research. In comparison with the flow in low velocities, it can be deduced that the increase in average flow velocities leads to increase the pressure drop inside pipelines. The impacts of cylindrical capsules with greater diameters lead to a drop in pressure in pipelines when contrasted to the cylindrical capsules flow of smaller diameter capsules. It has also been noted that cylindrical capsules with longer lengths lead to an increased pressure drop. Moreover, the fact that cylindrical capsules with heavy density lead to a greater pressure drop has been deduced, when compared with the flow of equi-density cylindrical capsules in pipes. From the aspect of a capsules concentration, it can be deduced that the increased concentration of capsules leads to a greater pressure drop and decrease the capsule train velocity in the pipeline. The cylindrical shape of the capsule has an obvious impact on the flow characteristics. The results provided in this study with respect to the cylindrical capsules flow within pipelines, has major significance for designers of vertical pipelines as the prediction model devised for the coefficient of friction depend on this type of capsules, where it can be utilised in the optimisation of vertical HCPs.

- **Evaluate the effect of the rectangular capsule shape on flow characteristics of HCPs under transient conditions.**

From the investigations performed on the shape of the rectangular capsule, which include the effects of average flow velocity, capsule diameter, capsule length, capsule density and capsule concentration on the flow characteristics in vertical pipelines. It can be deduced from those investigations that the increased flow velocities lead to increase the pipelines' pressure drop in comparison with the flow in low velocities. The effects of rectangular capsules with greater diameters lead to an increase in pressure reduction across the pipeline when contrasted to the capsules flows with smaller diameters. It has also been noted that the rectangular capsules with longer lengths cause an increase in the pressure drop. Moreover, the fact that rectangular capsules with heavy density lead to a greater pressure drop has been deduced, when compared with the flow of equal density rectangular capsules that flowing across pipelines. From the side of a rectangular capsules concentration, the increase in the capsules concentration leads to a greater drop in the pressure and decrease the capsule train velocity in the pipeline. The rectangular shape of the capsule has a clear effect on the flow characteristics. The outcomes exhibited in this investigation in regards to the rectangular capsules flows inside pipes is of extraordinary significance for designers of vertical pipeline as the predictive model formulated for the friction coefficient rely upon this type of capsules, where it can be utilised in the optimisation of a vertical HCPs.

- **Development of a novel mathematical formulation to calculate the shape factor for any capsule shape**

The shape factor has been defined to reflect the variations in the shapes of the capsules. The shape factor formulation used in the literature is only appropriate for spherical and cylindrical shapes, where the shape factor for the cylindrical and rectangular shape gives the same factor. Hence, a novel formulation for shape factor in this study has been developed to distinguish between a wide range of capsule shapes.

- **Development of prediction models for the capsule velocity and friction coefficient in vertical hydraulic capsule pipelines.**

Through the numerical findings have been obtained throughout this research, and after examining the effects of different geometric and flow linked variables, semi-experimental correlations have been established for the capsule velocity and friction coefficient for any capsule shape. Multiple variable regression approach was utilized to estimate the impacts of different parameters on the velocity and friction coefficient of the capsule. In addition, for sake of designing capsule pipelines, the equations of the drop in pressure have been formulated based on the developed models.

- **Investigate the effect of the simple combination of capsules of basic shapes on the flow characteristics under transient conditions**

Numerical investigations have been performed to show the impact of a simple combination of capsules on the pipeline's pressure drop as well the structure of the flow, where this combination consists of two different shapes of capsules. In terms of the structure of the flow is interested, further capsules within a pipe reduce the pipeline's effective flow region. This presents the flow with more resistance and thereby, reducing the capsule train velocity and increasing the pressure drop. Furthermore, in a simple combination case of heavy-density capsules, the capsule velocity significantly reduces because of the gravitational effects. This impact reinforces the shear layers surrounding the capsules and subsequently results in the pressure drop in the pipe growing. The impact of the simple combination of the capsules shapes within HCPs was formulated to develop the pressure drop's prediction model.

- **Investigate the effect of the complex combination of capsules of various shapes on the flow characteristics under transient conditions**

Through the investigations relating to the impact of a complex combination of capsules on the pressure gradient and flow structure inside the pipeline, where this combination consists of three different shapes of capsules Furthermore, increasing the capsules number inside a

pipeline decrease the flow region, generating greater resistance to the flow across these pipelines. and thus decrease the capsule train velocity and increasing the pressure drop. Furthermore, in a complex combination case of the heavy-density capsule, as result to the gravitational effect the capsules velocity reduces significantly. This impact enhances boundary layers in the circumference of the capsule, increasing the pipeline's pressure drop. The impacts of the complex combination of the various capsule shapes were formulated inside vertical HCPs to develop a predictive model for the pressure drop.

- **Estimate the order effect of mixed shapes of capsules on flow characteristics under transient conditions**

Numerical investigations have been performed to show the impact of the shape order of capsules on the pressure reduction and the structure of the flow inside the pipeline. Through this investigation, it can be concluded that the change of capsule shape order leads to change in the pressure drop and the capsules velocity for a capsule train. In terms of the importance of the flow structure, an order of a capsule shape in a pipeline can generate collision between the capsules, providing greater resistance to flow and thus making the pressure drop is higher. That is attributed to the capsule shape in a capsule train that is traveling faster than another shape. The order effect of the capsule shapes has been formulated inside HCPs to develop a predictive model for the pressure drop that deals with a combination of mixed capsules shapes in pipelines.

- **Development of an optimisation model for vertical capsule pipelines based on the Least-Cost Principle**

On the basis of semi-experimental correlations, which have been developed in the current study, an optimisation methodology for a vertical hydraulic capsule pipeline system has been developed. This methodology has been proposed to specify the optimum size of vertical pipelines conveying various shapes of the capsules. Moreover, with regard to such pipelines, it can be noted that in the case of fixed solid throughput and shape factor, increase in the

pipeline's diameter increases the costs of manufacturing. This is due to the fact that a greater pipe's diameter in addition to capsules is more costly than smaller pipe's diameters. On the other hand, as the pumping power needed for the system is a pressure drop function inside the pipeline, any increase in the diameter of the pipeline corresponds to a pumping power reduction and subsequently a reduction in a pipeline's operational cost. Thereby, the pipeline's total cost initially reduces and subsequently increases as the increased pipeline's diameter, for a fixed shape factor and solid throughput. The diameter of the pipeline with the minimum overall cost represents the optimal pipeline diameter. A design chart has also been presented which can be easily used to design vertical HCPs.

7.4 Thesis Contributions

The following section presents a summary of the main contributions of this thesis where the novelties of this research are described:

Contribution # 1:

The first main contribution of this research is represented in a comprehensive investigation on the characteristics of global and local flow in a vertical pipeline carrying various shapes of capsules. The existing literature regarding the distribution of the pressure drop and capsule velocity within vertical pipelines are extremely limited. Thereby, a Computational Fluid Dynamics solver was employed to conduct large-scale investigations on the distribution of the pressure drop and capsule velocity within vertical HCPs. Parameters effects on flow characteristics like average flow velocity, capsule shape capsule diameter, capsule density and capsule length have been considered. Moreover, novel prediction models of the capsule velocity and pressure drop have been developed as a function of the shape factor. The prediction models have been developed through data from the extensive numerical investigations. Hence, these models consider a novel contribution to the scientific knowledge, which can be employed in designing a hydraulic vertical capsule pipeline for any capsule shape and density for particular applications.

Contribution # 2:

The unique contribution of this research is a comprehensive investigation on the characteristics of global and local flow on a flow of mixed capsules shapes in vertical pipelines. The available literature does not include any study on a combination of various capsules shapes within pipelines. In this research, CFD solver has enabled the author to conduct this novel investigation. In this case also, the pressure and velocity distributions have been investigated based on the impact of the order of the capsule shape and the capsules density inside the vertical pipeline. Moreover, a novel factor has been developed to link it with prediction models that have been developed for transporting basic capsule shapes. This can be used to calculate the pressure drop for a combination of different capsule shapes with various arrangements. Hence, this prediction model is a novel contribution to the knowledge base that can be used to design vertical hydraulic capsules pipeline in transporting a mixed capsule shapes for various arrangements and densities.

Contribution # 3:

According to studies available in the literature, the design methodology of capsule pipelines depends on numerous design parameters. In this study, a design methodology for a vertical capsule pipelines system has been developed based on the shape factor. This methodology has been proposed to specify the optimal size of a vertical pipeline conveying different shapes of capsules based on the given capsule shape factor, throughput and density. The optimal size of the pipeline has been identified for the minimum total cost. The design methodology involved models for operating costs in addition to the cost of pipelines and capsules. Moreover, this methodology is user-friendly, coherent and reliable to provide a pipeline's optimal size corresponding to the minimum overall cost comprised in the process.

7.5 Future Work

This thesis represents a stepping-stone to further research in this field, for sake to fill in the gaps of knowledge that have been determined in the literature. The design, operation and optimisation of vertical pipelines transporting capsules have been undertaken in the present research. Based on the investigations that have been performed, it has become clear in this particular area that there is a vast possibility for further studies and investigations. The followings are some suggestions for future studies.

- ◆ CFD investigations can be performed on the flow of capsules with specific gravity less than 1 in the pipelines based on the techniques used in this study. These capsules are specifically appropriate in off-shore applications, where the freight must be conveyed from a low altitude position to a high altitude position. In this state, the capsules with low densities will have little influence on the pressure reduction and the capsules behaviour in the vertical pipeline, due to buoyancy forces. Moreover, investigations on the capsules flow in the slanted pipes can be carried out. The motion of capsule in both directions can also be investigated, such as capsules propagating down slanted or vertical pipelines instead of just only being travelled vertically upwards.
- ◆ Numerical investigations can be conducted on the flow through bends and horizontal sections transporting a combination of mixed capsule shapes to predict the pressure drop. These investigations are based on the transient flow for the mixed capsules shapes.
- ◆ A hydrodynamic investigation on the effects of complicated shapes as well as solidities rate of the capsules within the HCPs can be carried out for further analysis. This will include the unsteady analysis of the flow, and the findings can be compared with those presented in this study for optimisation purposes.

References

1. LIU, H. and J. WU. Economic feasibility of using hydraulic capsule pipeline to transport grain in the midwest of the United States. in *Freight Pipelines: Proceedings of the 6th International Symposium on Freight Pipelines*. 1990. Taylor & Francis.
2. KDD, W. Can A Capsule Pipeline System Compete With Truck, Rail, and Barge in Shipping Agricultural Products? in *Freight Pipelines: Proceedings of the 6th International Symposium on Freight Pipelines*. 1990. CRC Press.
3. Subramanya, K., Pipeline transportation technology: An overview. *Current Science*, 1998: p. 824-826.
4. Mole Solutions, L., Aggregate Strategic Research Programme Project 05: Assess the feasibility of using pipelines to transport aggregates in England. 2010.
5. Govier, G.W. and K. Aziz, *The flow of complex mixtures in pipes*. 2nd ed ed. 2008, Society of Petroleum Engineers.
6. Carter, J. and K. Troyano-Cuturi, Capsule Pipelines for Aggregate Transport. *QUARRY MANAGEMENT*, 2010. **37**(3).
7. Kosugi, S. A capsule pipeline system for limestone transportation. in *4th International Conference on Bulk Materials, Storage, Handling and Transportation: 7th International Symposium on Freight Pipelines; Preprints of Papers*. 1992. Institution of Engineers, Australia.
8. Montgomery, B., S. Fairfax, and B. Smith. Capsule pipeline transport using an electromagnetic drive. in *Cement Industry Technical Conference, IEEE-IAS/PCA 2001*. 2001. IEEE.
9. Maseles, J.S. and M.S. Rennells, *Portfolio: Thomas R. Marrero*. 2017.
10. Shaughnessy, E.J., I.M. Katz, and J.P. Schaffer, *Introduction to fluid mechanics*. Vol. 8. 2005: Oxford University Press New York.
11. Asim, T., *Computational Fluid Dynamics based Diagnostics and Optimal Design of Hydraulic Capsule Pipelines*. 2013, University of Huddersfield.
12. Ellis, H.S., An Experimental Investigation of the Transport by Water of Single Cylindrical and Spherical Capsules with Density Equal to that of the Water. *The Canadian Journal of Chemical Engineering*, 1964. **42**(1): p. 1 – 8.

13. Ulusarslan, D. and I. Teke, An experimental investigation of the capsule velocity, concentration rate and the spacing between the capsules for spherical capsule train flow in a horizontal circular pipe. *Powder technology*, 2005. **159**(1): p. 27-34.
14. Kruyer, J., P. Redberger, and H. Ellis, The pipeline flow of capsules. Part 9. *Journal of Fluid Mechanics*, 1967. **30**(3): p. 513-531.
15. Hwang, L., D. Wood, and D. Kao, Capsule hoist system for vertical transport of coal and other mineral solids. *The Canadian Journal of Chemical Engineering*, 1981. **59**(3): p. 317-324.
16. Charles, M.E., The pipeline flow of capsules: Part 2: Theoretical analysis of the concentric flow of cylindrical forms. *The Canadian Journal of Chemical Engineering*, 1963. **41**(2): p. 46-51.
17. Round, G. and L. Bolt, An experimental investigation of the transport in oil of single, denser-than-oil, spherical and cylindrical capsules. *The Canadian Journal of Chemical Engineering*, 1965. **43**(4): p. 197-205.
18. Mishra, R., V. Agarwal, and R. Mathur. Empirical Relations for Spherical Capsules of Various Densities. in *In the Proceedings of the 19th National Conference on Fluid Mechanics and Fluid Power*. 1992. Bombay.
19. Agarwal, V., M. Singh, and R. Mathur, Empirical relation for the effect of the shape of the capsules and the nose shape on the velocity ratio of heavy density capsules in a hydraulic pipeline. *Proceedings of the Institution of Mechanical Engineers, Part E: Journal of Process Mechanical Engineering*, 2001. **215**(2): p. 147-155.
20. Mathur, R.R. and C.R. Agarwal. Transport Velocity of Equal Density Spherical Capsules in Pipeline. in *In the Proceedings of the 4th Asian Congress of Fluid Mechanics*. 1989. Hongkong.
21. Feng, J., P. Huang, and D. Joseph, Dynamic simulation of the motion of capsules in pipelines. *Journal of Fluid Mechanics*, 1995. **286**: p. 201-227.
22. Tomita, Y., M. Yamamoto, and K. Funatsu, Motion of a single capsule in a hydraulic pipeline. *Journal of Fluid Mechanics*, 1986. **171**: p. 495-508.
23. Tomita, Y., et al., Unsteady analysis of hydraulic capsule transport in a straight horizontal pipeline. *Freight Pipelines*, Hemisphere Publishing Corp., New York, 1990: p. 273-278.
24. Lenau, C. and M. El-Bayya, Unsteady flow in hydraulic capsule pipeline. *Journal of engineering mechanics*, 1996. **122**(12): p. 1168-1173.

25. Ulusarslan, D., Analysis of the Pressure Gradients According to Capsule Flow Mechanism. *Particle & Particle Systems Characterization*, 2012. **29**(3): p. 167-177.
26. Chow, K.K., An experimental study of the hydrodynamic transport of spherical and cylindrical capsules in a vertical pipeline. 1979.
27. Tsuji, Y., et al., Fundamental Investigation of the Capsule Transport: 2nd Rep. Wake of a capsule and the effect of interaction between two capsules on the drag. *Bulletin of JSME*, 1984. **27**(225): p. 468-474.
28. Hammoud, A.H. and M. Khalil. Upward and Downward Inclination Hydraulic Capsule Pipeline. in *Eighth International Congress of Fluid Dynamics & Propulsion*. 2006.
29. Tachibana, M., Basic Studies on Hydraulic Capsule Transportation: Part 2. Balance and Startup of Cylindrical Capsule in Rising Flow of Inclined Pipeline. *Bulletin of JSME*, 1983. **26**(220): p. 1735-1743.
30. Latto, B. and K. Chow, Hydrodynamic transport of cylindrical capsules in a vertical pipeline. *The Canadian Journal of Chemical Engineering*, 1982. **60**(6): p. 713-722.
31. OHASHI, A. and K. YANAIDA, The Fluid Mechanics of Capsule Pipelines: 1st Report, Analysis of the Required Pressure Drop for Hydraulic and Pneumatic Capsules. *Bulletin of JSME*, 1986. **29**(252): p. 1719-1725.
32. Yanaida, K. and M. Tanaka, Drag coefficient of a capsule inside a vertical angular pipe. *Powder technology*, 1997. **94**(3): p. 239-243.
33. Bartosik, A. and C. Shook, Prediction of vertical liquid solid pipe flow using measured concentration distribution. *Particulate science and technology*, 1995. **13**(2): p. 85-104.
34. Swamee, P.K., Capsule-hoist system for vertical transport of minerals. *Journal of transportation engineering*, 1999. **125**(6): p. 560-563.
35. Khalil, M.F., et al., Turbulent flow around single concentric long capsule in a pipe. *Applied Mathematical Modelling*, 2010. **34**(8): p. 2000-2017.
36. Asim, T. and R. Mishra, Optimal design of hydraulic capsule pipelines transporting spherical capsules. *The Canadian Journal of Chemical Engineering*, 2016. **94**(5): p. 966-979.
37. Asim, T., et al., Development of a design methodology for hydraulic pipelines carrying rectangular capsules. *International Journal of Pressure Vessels and Piping*, 2016. **146**: p. 111-128.

38. Swamee, P.K., Design of sediment-transporting pipeline. *Journal of Hydraulic Engineering*, 1995. **121**(1): p. 72-76.
39. Polderman, H., Design Rules for Hydraulic Capsule Transport-Systems. *Journal of Pipelines*, 1982. **3**(2): p. 123-136.
40. Assadollahbaik, M. and H. Liu, Optimum design of electromagnetic pump for capsule pipelines. *Journal of Pipelines*, 1986. **5**(3): p. 157-169.
41. Agarwal, V. and R. Mishra, Optimal design of a multi-stage capsule handling multi-phase pipeline. *International journal of pressure vessels and piping*, 1998. **75**(1): p. 27-35.
42. Colebrook, C.F., et al., Correspondence. *Turbulent Flow In Pipes, With Particular Reference To The Transition Region Between The Smooth And Rough Pipe Laws.(Includes Plates)*. *Journal of the Institution of Civil engineers*, 1939. **12**(8): p. 393-422.
43. Sha, Y. and X. Zhao. Optimization design of the hydraulic pipeline based on the principle of saving energy sources. in *Power and Energy Engineering Conference (APPEEC), 2010 Asia-Pacific*. 2010. IEEE.
44. Asim, T., et al., Optimisation of a Capsule Transporting Pipeline Carrying Spherical Capsules. 2011.
45. Asim, T., et al., Optimal sizing and life-cycle cost modelling of pipelines transporting multi-sized solid-liquid mixtures. *International Journal of Pressure Vessels and Piping*, 2014. **113**: p. 40-48.
46. Asim, T. and R. Mishra, Computational fluid dynamics based optimal design of hydraulic capsule pipelines transporting cylindrical capsules. *Powder Technology*, 2016. **295**: p. 180-201.
47. Versteeg, H.K. and W. Malalasekera, *An introduction to computational fluid dynamics: the finite volume method*. 2007: Pearson Education.
48. Lomax, H., T.H. Pulliam, and D.W. Zingg, *Fundamentals of computational fluid dynamics*. 2013: Springer Science & Business Media.
49. Ferziger, J.H. and M. Peric, *Computational methods for fluid dynamics*. 2012: Springer Science & Business Media.
50. Wesseling, P., *Principles of computational fluid dynamics*. Vol. 29. 2009: Springer Science & Business Media.

51. Anderson, J.D. and J. Wendt, Computational fluid dynamics. Vol. 206. 1995: Springer.
52. Cebeci, T., Computational fluid dynamics for engineers: from panel to navier-stokes methods with computer programs. 2005: Springer Science & Business Media.
53. Cebeci, T., et al., Computational fluid dynamics for engineers. 2005: Springer Berlin Heidelberg.
54. Barth, T.J. and D.C. Jespersen, The design and application of upwind schemes on unstructured meshes. 1989.
55. Menter, F.R., Two-equation eddy-viscosity turbulence models for engineering applications. AIAA journal, 1994. **32**(8): p. 1598-1605.
56. Munson, B.R., Fundamentals of fluid mechanics. 4th ed. 2002: John Wiley & Sons, Inc.
57. Salim, S.M. and S. Cheah. Wall Y strategy for dealing with wall-bounded turbulent flows. in Proceedings of the international multiconference of engineers and computer scientists. 2009. Hong Kong.
58. Gerasimov, A., Modeling turbulent flows with fluent. Ansys Inc, Sheffield, UK, 2006.
59. Khalil, M.F., et al., Prediction of lift and drag coefficients on stationary capsule in pipeline. CFD Letters, 2009. **1**(1): p. 15-28.
60. Fluent, A., 12.0 User's Guide, 2009. Fluent Inc., New Hampshire.[Links].
61. ANSYS, I., ANSYS Fluent Tutorial Guide. 2015
62. ANSYS, I., ANSYS FLUENT Theory Guide: Release 14.0. 2011, Ansys Inc Canonsburg^ ePA PA.
63. Fluent, I., FLUENT 6.3 user's guide. Fluent documentation, 2006.
64. Fluent, A., 12.0/12.1 Documentation. Users Guide Manual, Ansys Inc, 2009.
65. Fluent, A., Release 15," ANSYS FLUENT UDF Manual," ANSYS. 2013, Inc.
66. Fluent, A., Fluent 6.3 Documentation. Fluent Inc., Lebanon, NH, 2006.
67. Moody, L.F., Friction factors for pipe flow. Trans Asme, 1944. **66**: p. 671-684.
68. Chermisinoff, P.N. and S.I. Cheng, Civil Engineering Practice. 1988, Lancaster, P. A., U.S.A: Technomies Publishing Co.

69. Davis, C.V. and K.E. Sorensen, Handbook of applied hydraulics 3rd ed. 1969, New York: McGraw-Hill.
70. Russel, G., Hydraulics, Holt, Rinehart and Winston. 5th ed. 1963, U.S.A.
71. Liu, H. Hydraulic behaviors of coal log flow in pipe. in 4th International Conference on Bulk Materials, Storage, Handling and Transportation: 7th International Symposium on Freight Pipelines; Preprints of Papers. 1992. Institution of Engineers, Australia.
72. Carroll, L. and R.W. Hudkins, Advanced Pipeline Design.
73. Blazek, J., Computational fluid dynamics: principles and applications. 2015: Butterworth-Heinemann.

Appendices

A-1: Computational Fluid Dynamics

➤ Numerical Analysis using CFD

The primary aim of computational fluid dynamics is to numerically solve the partial differential equations that govern fluid flows. CFD calculations are based upon the fundamental governing equations of fluid dynamics the conservation of mass, momentum and energy equations. These equations combine to form the Navier-Stokes equations. The equations describing fluid flow are solved iteratively so residuals appear. The residual is the imbalance of the conservation equation for a general variable summed over all the computational cells. They are a measure of error in the discretised equations, summed over all control volumes and are a guide to convergence. For the analysis purpose, the fluid is considered to be a continuum. The behaviour of the fluid is described in terms of macroscopic properties such as velocity, pressure, density, etc.

➤ Mass Conservation

The equation is derived from the principle that the mass of fluid elements is always conserved regardless of their operating conditions. The continuity equation considers correct for incompressible and compressible flows but in the latter case, the fluid density is considered to be constant as shown in Equation below.

$$\text{Div } V = 0 \quad (\text{A-1.1})$$

$$\frac{\partial u}{\partial x} + \frac{\partial v}{\partial y} + \frac{\partial w}{\partial z} = 0 \quad (\text{A-1.2})$$

This equation for three-dimensional continuity mass conservation at a point, which is valid for incompressible flows [73].

➤ Momentum Conservation

The conservation of momentum is originally expressed in Newton's second law. Such as the velocity, momentum is a vector quantity as well as a magnitude. Momentum is also a conserved quality, meaning that for a closed system, the total momentum will not change as long as there is no external force. Newton's second law also states that the rate of momentum change of a fluid particle equals the sum of the forces on the particle. We can differentiate the rate of momentum change for x, y and z direction. The momentum equation is expressed in respect to the pressure and viscous stresses affecting on a particle in the fluid as:

$$\rho g_x + \frac{\partial \sigma_{xx}}{\partial x} + \frac{\partial \tau_{yx}}{\partial y} + \frac{\partial \tau_{zx}}{\partial z} = \rho \left(\frac{\partial u}{\partial t} + u \frac{\partial u}{\partial x} + v \frac{\partial u}{\partial y} + w \frac{\partial u}{\partial z} \right) \quad (\text{A-1.3})$$

The y and z –directions can be written as follows:

$$\rho g_y + \frac{\partial \tau_{xy}}{\partial x} + \frac{\partial \sigma_{yy}}{\partial y} + \frac{\partial \tau_{zy}}{\partial z} = \rho \left(\frac{\partial v}{\partial t} + u \frac{\partial v}{\partial x} + v \frac{\partial v}{\partial y} + w \frac{\partial v}{\partial z} \right) \quad (\text{A-1.4})$$

$$\rho g_z + \frac{\partial \tau_{xz}}{\partial x} + \frac{\partial \tau_{yz}}{\partial y} + \frac{\partial \sigma_{zz}}{\partial z} = \rho \left(\frac{\partial w}{\partial t} + u \frac{\partial w}{\partial x} + v \frac{\partial w}{\partial y} + w \frac{\partial w}{\partial z} \right) \quad (\text{A-1.5})$$

➤ Energy Equation

“The energy equation is based on the first law of thermodynamics that states the rate of change of energy of a fluid particle is equal to the rate of heat addition to the fluid particle and the rate of work done on the particle” [48].

The equation can be written as;

$$\frac{DE}{Dt} = -div(p\mathbf{u}) + \left[\begin{array}{l} \frac{\partial(u\tau_{xx})}{\partial x} + \frac{\partial(u\tau_{yx})}{\partial y} + \frac{\partial(u\tau_{zx})}{\partial z} + \frac{\partial(v\tau_{xy})}{\partial x} \\ + \frac{\partial(v\tau_{yy})}{\partial y} + \frac{\partial(v\tau_{zy})}{\partial z} + \frac{\partial(w\tau_{xz})}{\partial x} + \frac{\partial(w\tau_{yz})}{\partial y} + \frac{\partial(w\tau_{zz})}{\partial z} \end{array} \right] + div(k \text{ grad } T) + S_E \quad (\text{A-1.6})$$

➤ **Equations of State**

The motion of a fluid in three dimensions is described by a system of five partial differential equations, i.e. mass conservation, x, y and z momentum equations and energy equation. Among the unknowns are four thermodynamic variables, i.e. density, pressure, temperature and internal energy. Relationships between the thermodynamic variables can be obtained through the assumption of thermodynamic equilibrium.

The fluid velocities may be large, but they are usually small enough that, even though properties of a fluid particle change rapidly from place to place, the fluid can thermodynamically adjust itself to new conditions so quickly that the changes are effectively instantaneous. Thus, the fluid always remains in thermodynamic equilibrium. The only exceptions are certain flows with strong shockwaves, but even some of those are often well enough approximated by equilibrium assumptions. The state of a substance in thermodynamic equilibrium can be described by means of just two state variables. Equations of state relate the other variables to the two state variables, i.e. density and temperature. The equations of state are:

$$p = p(\rho, T) \quad (\text{A-1.7})$$

$$i = i(\rho, T) \quad (\text{A-1.8})$$

A-2: Mass and Moment of Inertia for a Capsule Shape

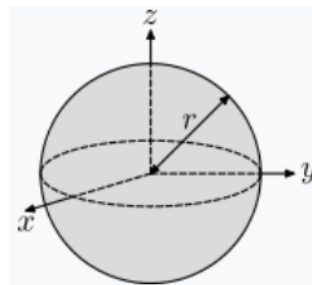
- The mass and moment of inertia are to be calculated for a solid sphere of radius r .

Calculating the mass (m):

Mass of the cylinder (m) = Volume \times Density, volume of the cylinder, $V = \frac{4}{3}\pi r^3$

Calculating the moments of inertia (I):

$$\mathbf{I} = \begin{bmatrix} \frac{2}{5}mr^2 & 0 & 0 \\ 0 & \frac{2}{5}mr^2 & 0 \\ 0 & 0 & \frac{2}{5}mr^2 \end{bmatrix}$$



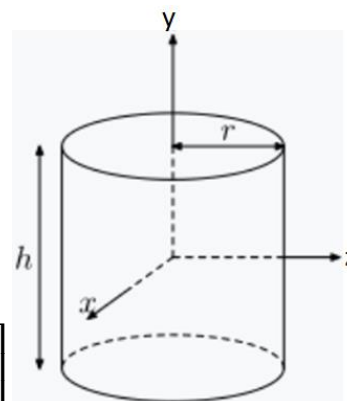
- The mass and moment of inertia are to be calculated for a solid cylinder of radius r .

Calculating the mass:

Mass of the cylinder (m) = Volume \times Density, volume the cylinder, $V = \pi r^2 h$

Calculating the moments of inertia (I):

$$\mathbf{I} = \begin{bmatrix} \frac{1}{12}m(3r^2 + h^2) & 0 & 0 \\ 0 & \frac{1}{2}mr^2 & 0 \\ 0 & 0 & \frac{1}{12}m(3r^2 + h^2) \end{bmatrix}$$



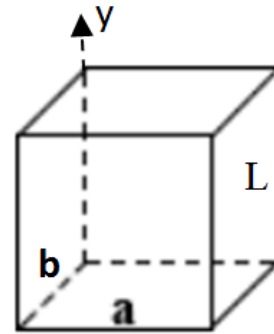
- The mass and moment of inertia are to be calculated for a solid cuboid of width a , height b , depth L .

Calculating the mass:

Mass of the cylinder (m) = \times Density , volume the cuboid, $V = abL$

Calculating the moments of inertia (I):

$$\mathbf{I} = \begin{bmatrix} \frac{1}{12}m(a^2 + L^2) & 0 & 0 \\ 0 & \frac{1}{12}m(a^2 + b^2) & 0 \\ 0 & 0 & \frac{1}{12}m(b^2 + L^2) \end{bmatrix}$$



A-3: UDF Used in ANSYS FLUENT

This is the user define function (UDF) used in Fluent to define the motion of the capsules due to the flow. It is used when the movement of the rigid body is determined by the forces of the flow. The following is the UDF transcript for two cylindrical capsules.

```
#include "udf.h"

/*****
User Inputs - Cylindrical Capsule1
*****/

#define MASS 0.097948375 /*Mass*/
#define IXX 0.000035710345052 /*moment of inertia*/
#define IYY 0.000030608867187
#define IZZ 0.000035710345052
#define IXY 0.0
#define IXZ 0.0
#define IYZ 0.0

#define ID_capsule1 8

real f_glob1[ND_ND];
real m_glob1[ND_ND];
real cg1[ND_ND],theta_y;
int flag1;

/*****
SDOF property UDF for a moving body
*****/

DEFINE_SDOF_PROPERTIES(capsule1_motion, prop, dt, time, dtime)
{
    int i;
    real x_cg[ND_ND];
    Domain *domain;
    Thread *t1;
    # if !RP_NODE

    FILE *fp = NULL;
    char filename[]="udf_motion_history_capsule1.txt";
    if ((fp = fopen(filename, "a+"))==NULL)
        Message("\n Warning: Unable to open %s for writing\n", filename);
    else
    {
```

```

    Message("\n Writing motion history to %s...",filename);

}

# endif

domain = Get_Domain(1);
t1= Lookup_Thread(domain,ID_capsule1);

prop[SDOF_MASS]    = MASS;
prop[SDOF_IXX]    = IXX;
prop[SDOF_IYY]    = IYY;
prop[SDOF_IZZ]    = IZZ;
prop[SDOF_IXY]    = IXY;
prop[SDOF_IXZ]    = IXZ;
prop[SDOF_IYZ]    = IYZ;

prop[SDOF_ZERO_ROT_X] = FALSE;
prop[SDOF_ZERO_ROT_Z] = FALSE;
prop[SDOF_ZERO_ROT_Y] = FALSE;

for (i = 0; i < ND_ND; i++)
{
    x_cg[i] = DT_CG(dt)[i];
}

Compute_Force_And_Moment (domain, t1, x_cg, f_glob1, m_glob1, TRUE);

theta_y= -DT_THETA(dt)[1];

# if !RP_NODE

if (flag1!=1)
{
    flag1=1;
    fprintf(fp,"Time cg_x cg_y cg_z theta_x theta_y theta_z vel_x    vel_y  vel_z
        omega_x omega_y omega_z force_x    force_y force_z moment_x moment_y
moment_z \n");
}

fprintf(fp, "%g %g %g %g %g %g    %g    %g    %g %g %g %g %g %g
    %g %g %g %g %g \n", time,x_cg[0],x_cg[1],x_cg[2], DT_THETA(dt)[0]*180/3.14,
DT_THETA(dt)[1]*180/3.14, DT_THETA(dt)[2]*180/3.14, DT_VEL_CG(dt)[0],
DT_VEL_CG(dt)[1], DT_VEL_CG(dt)[2],DT_OMEGA_CG(dt)[0], DT_OMEGA_CG(dt)[1],
DT_OMEGA_CG(dt)[2], f_glob1[0],f_glob1[1],f_glob1[2],m_glob1[0],m_glob1[1],m_glob1[2]);
fclose(fp);

```

```

# endif

}

/*****
User Inputs - Cylindrical Capsule2
*****/

#define MASS 0.097948375 /*Mass*/
#define IXX 0.000035710345052 /*moment of inertia*/
#define IYY 0.000030608867187
#define IZZ 0.000035710345052
#define IXY 0.0
#define IXZ 0.0
#define IYZ 0.0

#define ID_capsule2 9

real f_glob1[ND_ND];
real m_glob1[ND_ND];
real cg1[ND_ND],theta_y;
int flag1;

/*****
SDOF property UDF for a moving body
*****/

DEFINE_SDOF_PROPERTIES(capsule2_motion, prop, dt, time, dtime)
{
    int i;
    real x_cg[ND_ND];
    Domain *domain;
    Thread *t1;
    # if !RP_NODE

    FILE *fp = NULL;
    char filename[]="udf_motion_history_capsule2.txt";
    if ((fp = fopen(filename, "a+"))==NULL)
        Message("\n Warning: Unable to open %s for writing\n", filename);
    else
    {
        Message("\n Writing motion history to %s...",filename);
    }

    # endif
}

```

```

domain = Get_Domain(1);
t1= Lookup_Thread(domain,ID_capsule2);

prop[SDOF_MASS]    = MASS;
prop[SDOF_IXX]    = IXX;
prop[SDOF_IYY]    = IYY;
prop[SDOF_IZZ]    = IZZ;
prop[SDOF_IXY]    = IXY;
prop[SDOF_IXZ]    = IXZ;
prop[SDOF_IYZ]    = IYZ;

prop[SDOF_ZERO_ROT_X] = FALSE;
prop[SDOF_ZERO_ROT_Z] = FALSE;
prop[SDOF_ZERO_ROT_Y] = FALSE;

for (i = 0; i < ND_ND; i++)
{
    x_cg[i] = DT_CG(dt)[i];
}

Compute_Force_And_Moment (domain, t1, x_cg, f_glob1, m_glob1, TRUE);

theta_y= -DT_THETA(dt)[1];

# if !RP_NODE

if (flag1!=1)
{
    flag1=1;
    fprintf(fp,"Time cg_x cg_y cg_z theta_x theta_y theta_z vel_x    vel_y  vel_z
        omega_x omega_y omega_z force_x    force_y force_z moment_x moment_y
moment_z \n");
}

fprintf(fp, "%g %g %g %g %g %g    %g    %g    %g %g %g %g %g %g
    %g %g %g %g %g \n", time,x_cg[0],x_cg[1],x_cg[2], DT_THETA(dt)[0]*180/3.14,
DT_THETA(dt)[1]*180/3.14, DT_THETA(dt)[2]*180/3.14, DT_VEL_CG(dt)[0],
DT_VEL_CG(dt)[1], DT_VEL_CG(dt)[2],DT_OMEGA_CG(dt)[0], DT_OMEGA_CG(dt)[1],
DT_OMEGA_CG(dt)[2], f_glob1[0],f_glob1[1],f_glob1[2],m_glob1[0],m_glob1[1],m_glob1[2]);
    fclose(fp);
# endif

}

```

```

/*****
Contact detection properties
*****/

DEFINE_CONTACT(contact_props, dt, contacts)
{
  Objp *o;
  face_t face;
  Thread *thread;
  Domain *domain = NULL;
  Dynamic_Thread *ndt = NULL;

  int tid, nid, n_faces;

  real v0dotn1, v1dotn0;
  real nc_mag, norm0_mag, norm1_mag;

  real N3V_VEC (vel_rel);
  real N3V_VEC (nc), N3V_VEC (nctmp);
  real N3V_VEC (xc), N3V_VEC (xctmp);
  real N3V_VEC (vel0), N3V_VEC (omega0), N3V_VEC (theta0), N3V_VEC (norm0);
  real N3V_VEC (vel1), N3V_VEC (omega1), N3V_VEC (theta1), N3V_VEC (norm1);

  if (!Data_Valid_P())
  {
    return;
  }

  /* Define a common contact point / plane */
  N3V_S (nc, =, 0.0);
  N3V_S (xc, =, 0.0);

  /* Fetch current thread ID */
  tid = THREAD_ID (DT_THREAD (dt));

  nid = -1;
  n_faces = 0;

  loop (o, contacts)
  {
    face = O_F (o);
    thread = O_F_THREAD (o);

    /* Skip faces on current thread */
    if (THREAD_ID (thread) == tid)
    {
      continue;
    }

    /* Note ID for posterity */

```

```

if (nid == -1)
{
    nid = THREAD_ID (thread);
}

/* Initialize to zero */
N3V_S (nctmp, =, 0.0);
N3V_S (xctmp, =, 0.0);

F_AREA (nctmp, face, thread);
F_CENTROID (xctmp, face, thread);

# if DEBUG
{
    Message0
    (
        "\nFace:: %d (%d): Area: (%f %f %f) Centre: (%f %f %f)",
        face, THREAD_ID (thread),
        nctmp[0], nctmp[1], nctmp[2],
        xctmp[0], xctmp[1], xctmp[2]
    );
}
# endif

/**
 * Negative sum because wall normals
 * point out of the fluid domain
 */
N3V_V (nc, -=, nctmp);
N3V_V (xc, +=, xctmp);

n_faces++;
}

# if RP_NODE
{
    /* Reduce in parallel */
    nid = PRF_GIHIGH1 (nid);
    n_faces = PRF_GISUM1 (n_faces);

    PRF_GRSUM3 (nc[0], nc[1], nc[2]);
    PRF_GRSUM3 (xc[0], xc[1], xc[2]);
}
# endif

if (n_faces > 0)
{
    nc_mag = N3V_MAG (nc) + REAL_MIN;

    N3V_S (nc, /=, nc_mag);
    N3V_S (xc, /=, n_faces);
}

```

```

    }
else
    {
        return;
    }

Message
(
    "\nContact:: tid: %d nid: %d n_faces: %d "
    "Point: (%f %f %f) Normal: (%f %f %f)",
    tid, nid, n_faces,
    xc[0], xc[1], xc[2],
    nc[0], nc[1], nc[2]
);

/* Fetch thread for opposite body */
domain = THREAD_DOMAIN (DT_THREAD (dt));
thread = Lookup_Thread (domain, nid);

if (NULLP (thread))
    {
        Message ("\nWarning: No thread for nid: %d ", nid);

        return;
    }
else
    {
        ndt = THREAD_DT (thread);
    }

/* Fetch body parameters */
SDOF_Get_Motion (dt, vel0, omega0, theta0);

/* Compute difference vectors and normalize */
N3V_VV (norm0, =, xc, -, DT_CG (dt));
norm0_mag = N3V_MAG (norm0) + REAL_MIN;
N3V_S (norm0, /=, norm0_mag);

if (NULLP (ndt))
    {
        /* Stationary body / wall. Use contact normal */
        N3V_V (norm1, =, nc);

        /* Compute relative velocity */
        N3V_S (vel1, =, 0.0);
        N3V_V (vel_rel, =, vel0);
    }
else
    {
        /* Fetch body parameters */
        SDOF_Get_Motion (ndt, vel1, omega1, theta1);
    }

```

```

/* Compute relative velocity */
N3V_VV (vel_rel, =, vel0, -, vel1);

/* Compute difference vectors and normalize */
N3V_VV (norm1, =, xc, -, DT_CG (ndt));
norm1_mag = N3V_MAG (norm1) + REAL_MIN;
N3V_S (norm1, /=, norm1_mag);

/* Check if velocity needs to be reversed */
if (N3V_DOT (vel_rel, nc) < 0.0)
{
  /* Reflect velocity across the normal */
  v1dotn0 = 2.0 * N3V_DOT (vel1, norm0);

  N3V_S (norm0, *=, v1dotn0);
  N3V_V (vel1, -=, norm0);

  /* Override body velocity */
  SDOF_Overwrite_Motion (ndt, vel1, omeg1, theta1);
}

/* Check if velocity needs to be reversed */
if (N3V_DOT (vel_rel, nc) < 0.0)
{
  /* Reflect velocity across the normal */
  v0dotn1 = 2.0 * N3V_DOT (vel0, norm1);

  N3V_S (norm1, *=, v0dotn1);
  N3V_V (vel0, -=, norm1);

  /* Override body velocity */
  SDOF_Overwrite_Motion (dt, vel0, omega0, theta0);
}

Message
(
  "\ncontact_props: Updated :: vel0 = (%f %f %f) vel1 = (%f %f %f)",
  vel0[0], vel0[1], vel0[2], vel1[0], vel1[1], vel1[2]
);
}

```

A-4: Capsule Velocities

Table A-3.1 Velocities of Equi-Density Spherical Capsules in a Vertical Pipeline

N/Lp	k	Vav (m/sec)	Vc (m/sec)
1	0.4	4	4.07956
	0.5	2	2.15342
		4	4.03615
	0.6	2	2.14373
		4	4.02784
	2	0.5	2

Table A-3.2 Velocities of Heavy-Density Spherical Capsules in a Vertical Pipeline

N/Lp	k	Vav (m/sec)	Vc (m/sec)
1	0.5	2	1.15968
		4	3.79936
	0.6	2	1.30889
2	0.4	2	1.16368
	0.5	2	1.03312
	0.5	4	3.79936
	0.6	2	1.30889

Table A-3.3 Velocities of Equi-Density Cylindrical Capsules in a Vertical Pipeline

N/Lp	k	Lc (m)	Vav (m/sec)	Vc (m/sec)
1	0.4	1.5 * d	4	4.10133
	0.5	1 * d	2	2.14016
		1 * d	4	4.08214
		1.5 * d	2	2.01215
	0.6	1 * d	2	2.13217
		1.5 * d	4	4.0321
2	0.4	1.5 * d	2	2.09315
	0.5	1 * d	2	2.14016

Table A-3.4 Velocities of Heavy-Density Cylindrical Capsules in a Vertical Pipeline

N/Lp	k	Lc (m)	Vav (m/sec)	Vc (m/sec)
1	0.5	1 * d	2	1.54357
		1 * d	4	3.65993
		1.5 * d	2	1.43445
	0.6	1 * d	2	1.56799
2	0.5	1 * d	2	1.54357
	0.5	1 * d	4	3.65993
	0.6	1.5 * d	2	1.68302

Table A-3.5 Velocities of Equi-Density Rectangular Capsules in a Vertical Pipeline

N/Lp	k	Lc (m)	Vav (m/sec)	Vc (m/sec)
1	0.5	1 * d	2	2.06977
		1 * d	4	4.16613
		1.5 * d	2	2.06021
	0.6	1 * d	2	2.02171
2	0.4	1 * d	2	2.0481
	0.5	1 * d	2	2.06977
	0.5	1.5 * d	4	4.01507
	0.6	1 * d	2	2.07104

Table A-3.6 Velocities of Heavy-Density Rectangular Capsules in a Vertical Pipeline

N/Lp	k	Lc (m)	Vav (m/sec)	Vc (m/sec)
1	0.4	1 * d	4	3.75863
	0.5	1 * d	2	1.57746
		1 * d	4	3.55241
		1.5 * d	2	1.48363
	0.6	1 * d	2	1.63589
	0.6	1 * d	4	3.34038
2	0.5	1 * d	2	1.57746

A-5: Pressure Drop in Vertical HCPs

Table A-4.1 Pressure Drop variations in a Vertical Pipe carrying Equal-Density Spherical Capsules

N/Lp	k	S.G	Vav (m/sec)	ΔPm/Lp (Pa/m)
1	0.4	1	4	11563
	0.5	1	2	10721
		1	4	11584
	0.6	1	2	10749
		1	4	11642
2	0.5	1	2	10755

Table A-4.2 Pressure Drop variations in a Vertical Pipe carrying Heavy-Density Spherical Capsules

N/Lp	k	S.G	Vav (m/sec)	ΔPm/Lp (Pa/m)
1	0.5	1.7	2	10792.75
		1.7	4	11680.3
	0.6	1.7	2	10862.88
2	0.4	1.7	2	10778.74
2	0.5	1.7	2	10872.3
		1.7	4	11777.26
2	0.6	1.7	2	10992.33

Table A-4.3 Pressure Drop variations in a Vertical Pipe carrying Equi-Density Cylindrical Capsules

N/Lp	S.G	k	Lc (m)	Vav (m/sec)	$\Delta Pm/Lp$ (Pa/m)
1	1	0.4	1.5 * d	4	11541.94
		0.5	1 * d	2	10711.78
			1.5 * d	2	10728.78
			1 * d	4	11521.17
		0.6	1 * d	2	10722.95
			1.5 * d	4	11657.27
2	1	0.4	1.5 * d	2	10718.63
		0.5	1 * d	2	10750

Table A-4.4 Pressure Drop variations in a Vertical Pipe carrying Heavy-Density Cylindrical Capsules

N/Lp	S.G	k	Lc (m)	Vav (m/sec)	$\Delta Pm/Lp$ (Pa/m)
1	1.7	0.5	1 * d	2	10792.31
			1.5 * d	2	10841.91
			1 * d	4	11671.28
		0.6	1 * d	2	10902.71
2	1.7	0.5	1 * d	2	10949.44
			1 * d	4	12045.11
		0.6	1.5 * d	2	11503.65

Table A-4.5 Pressure Drop variations in a Vertical Pipe carrying Equi-Density Rectangular Capsules

N/Lp	S.G	k	Lc (m)	Vav (m/sec)	ΔPm/Lp (Pa/m)
1	1	0.5	1 * d	2	10724.16
			1.5 * d	2	10740.7
			1 * d	4	11418.58
		0.6	1 * d	2	10732.15
2	1	0.4	1* d	2	10734.4
		0.5	1 * d	2	10739.77
			1.5 * d	4	11552.78
		0.6	1 * d	2	10811.46

Table A-4.6 Pressure Drop variations in a Vertical Pipe carrying Heavy-Density Rectangular Capsules

N/Lp	S.G	k	Lc (m)	Vav (m/sec)	ΔPm/Lp (Pa/m)
1	1.7	0.4	1 * d	4	11713.03
		0.5	1 * d	2	10848.22
			1.5 * d	2	10927.01
			1 * d	4	11774.84
		0.6	1 * d	2	10994
		0.6	1 * d	4	11954.65
2	1.7	0.5	1 * d	2	10985.92

A-6: Pressure Drop for Capsules Combination

Order of capsules	ΔP_m (Pa) Equal density capsules	ΔP_m (Pa) Heavy density capsules
Spherical Cylindrical	10719	10964
Cylindrical Spherical	10845	11000
Cylindrical Rectangular	10708	11090
Rectangular Cylindrical	10665	11225
Spherical Rectangular	10746	11027
Rectangular Spherical	10846	11132
Spherical Cylindrical Rectangular	10748	11245
Cylindrical Spherical Rectangular	10747	11275
Cylindrical Rectangular Spherical	10744	11278
Spherical Rectangular Cylindrical	10797	11232
Rectangular Spherical Cylindrical	10753	11286
Rectangular Cylindrical Spherical	10755	11322

A-7: Expressions for Capsule Velocities, Friction Coefficient and Correction Factor in Vertical HCPs

Relationships $\frac{V_c}{V_{av}}$, f_c and C_f Expressions

Holdup
Expression
$$\frac{V_c}{V_{av}} = \frac{(1.76 \phi^{0.0514})}{(s + 1)^{0.9}}$$

Friction
Coefficient
Expression
$$f_c = \frac{\left(10^{6.17} \phi^{0.567} \left(N * \frac{Lc}{L} \right)^{0.43} k^{1.767} \right)}{Re_c^{1.398} (s + 1)^{0.5}}$$

Correction
Factor
Expression
$$C_f = \frac{10^{1.13} \left(\frac{Vol_c}{Vol_p} \right)^{0.63}}{(Cg)^{0.5}}$$
